RADC-TDR-62-274, Vol II
Final Report

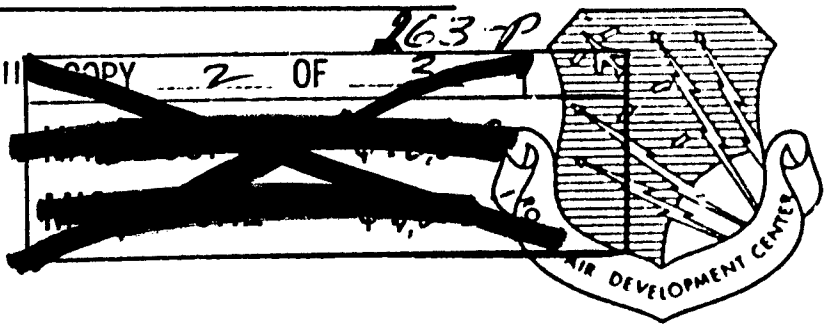

ADVANCED NOMOGRAPHY

NOMOGRAPHIC ELECTRONIC COMPUTATION

Volume II

TECHNICAL DOCUMENTARY REPORT NO. RADC-TDR-62-274

June 1964

Information Processing Branch
Rome Air Development Center
Research and Technology Division
Air Force Systems Command
Griffiss Air Force Base, New York

Project No. 5581, Task No. 558109

(Prepared under Contract AF30(602)-2411, by Douglas P. Adams, Department of Mechanical Engineering, Massachusetts Institute of Technology, Cambridge, Massachusetts.)

FOREWORD

The contents of this volume represent the application of modern technological developments in electronics, mechanics and other fields to the body of mathematics known as nomography. It also represents the application of nomography to the electronics area. Volume I described the field of nomography and prepared the subject for this application. The reader will do well to familiarize himself with the contents of that volume which, to the best knowledge of the author, is not readily available elsewhere. The various techniques which give the subject greater scope and especially greater flexibility, such as central projection and extension to more than two dimensions, etc., should be carefully kept in mind when reading Volume II. Remarks on these matters will be made through reference to Volume I.

This volume will be limited to discussions primarily of "NOEL I", the first "nomographic electronic" machine to be built. Occasional reference may be made to the potentialities of further developments which this work has disclosed but, in general, these must await a later presentation.

All of the work performed on the NOEL computer was completed or started in the Engineering Projects Laboratory at Massachusetts Institute of Technology under Contract AF30(602)-2411 with the United States Air Force, Rome Air Development Center, Rome, New York. Much of the text has been derived from consultations and discussions with students at M. I. T. who were working on thesis or course work problems. The names of those to whom the author is chiefly indebted appear below. Their respective projects are listed among the references at the end of the report.

William H. Broadley
John B. Cohen
Douglas E. Dancis
Chong-Jin Lee
Yeong-Suei Low
Philip D. Marcus
Richard F. McRay
Richard S. Orr
Howard E. Pollack
John H. Wasserlein
Harold Weiss Bara
Jerry P. Skelton

AIR FORCE, GOODWAY PRINTING CO., PHILADELPHIA, PA., 8/31/64, 318

Key Words: Nomographs; Graphical Techniques

ABSTRACT

This report shows how Nomography and Electronics can be combined to achieve Nomographic Electronic Computation. An electronic computer (identified as NOEL I for Nomographic Electronic) was designed and constructed to perform nomographic computation. Throughout the effort the choice of hardware and system configuration was evaluated in terms of expected performance figures and system cost. The report describes many approaches taken and alludes to others which were not tried due to time and funding limitations. The results obtained indicate that the concept of electronic nomography is feasible and further work is outlined which will extend the range of applicability.

PUBLICATION REVIEW

This report has been reviewed and is approved. For further technical information on this project, contact Mr. Denis Maynard, EMIID, x71170.

Approved: FRANK J. TOMAINI
Chief, Information Processing Branch

WILLIAM H. HARRIS
MAJOR, U. S. AIR FORCE

Approved: ROBERT J. QUINN, JR.
Colonel, USAF
Chief, Intel and Info Processing Div.

FOR THE COMMANDER:
IRVING J. GABELMAN
Chief, Advanced Studies Group

TABLE OF CONTENTS

TABLE OF CONTENTS (Continued)

TABLE OF CONTENTS (Continued)

TABLE OF CONTENTS (Continued)

TABLE OF CONTENTS (Continued)

TABLE OF CONTENTS (Continued)

NOMOGRAPHIC ELECTRONIC COMPUTATION

CHAPTER 1

THE NATURE OF GRAPHICS

The ability to deal effectively with quantities which vary in a definite way and to convey information about them requires the ability to express this variation in a way subject to common interpretation. That is, if functional behavior is to be used, it must first be represented. A common way to do this is by mathematical symbolizing, as

$$y^2 = 2x + 5 \qquad (1\text{-}1)$$

where the symbols and their arrangement convey, through a memory code learned by lifelong practice, just what the mutual variation of the variables is. This may be called algebraic or analytic representation of the mutual variation between the variables x and y and is probably a sufficient example to characterize, for our purposes, all such representations. The graph shown in Figure 1-1 also gives a representation of this same relationship, although in a totally different way, relying merely upon intuitive appreciation of size; that is, an intuitive counting or evaluation technique, where the size of the unit has been indicated. The counting need not be explicit in order to convey the variation usefully. It will be exact only to the degree of care exercised and cannot have an accuracy requiring closer estimation or measurement than is supportable by the reading power at hand, the thickness of the line, and similar effects. This can be called a graphical representation of the mutual variation between the variables x and y.

> These two processes of representation are inherently and intrinsically different. The one is based on a memory code of identifications and operations that can be quite involved; the other is based upon the intuitive evaluation of the magnitudes of geometric elements. The ability to count may be helpful to the latter representation, though it does not appear to be essential to rough evaluations.

It will be important to note later certain processes of representation which are of a somewhat hybrid form, and to appreciate just how strongly they partake of one or the other of these two basic processes.

In Figure 1-2, a simple correspondence has been established between the curved lines and the straight lines which permits a common intuitive interpretation.

On agreement between users, the four parallel lines are assumed to be four parallel planes seen on edge—an intuitive conception. Each of the curves can, on agreement, be regarded as the intersection between an irregular space surface and the particular plane which has been attached to it by a dotted line. The unit of both parts of the drawing can be regarded as the same, and of any natural size. The interpretation of the surface then is quantitatively usable with results unique within certain bounds. No numerical values have been used here—this is a purely graphical representation.

In Figure 1-3 are seen parallel strings of bit marks. These consist solely of small, perfectly rectangular areas, but some definition has been lost in reproduction. A possible use of such a pattern would be to find optimum correlation of portions of its bit patterns with a second set of codified bit patterns representing some encoded word or message. For practical use, the parallel strings are mapped into concentric circular strings of the bit marks and the correlation with the second set of bit marks is found after or during rotation of the disc on which the former appear. Using photographic reduction on fine-grained film, a density of 5000 characters per linear inch is achieved, which yields an operating area density of 25,000,000 bits per square inch. With this graphical tool, IBM has achieved a practical translating technique for several languages, including Russian. The circular string of bit marks is a language dictionary and the optimum electronic correlation between the encoded words and the dictionary words identifies the particular words. A purer and a more elegant use of modern graphics would be hard to imagine.

In Figure 1-4, there are two columns of parallel marks starting from a common level. If ability to count up the columns is assumed, the values of the counts achieved at the same level can be said to represent the functional behavior of two variables. Limitation of accuracy is a characteristic of any one representation, but it should be noted that expanding the scale of the representation by putting in more bit marks will bring a higher degree of accuracy.

These ways of representing functional behavior are entirely non-algebraic. We call them graphical techniques and believe they can serve as foundation material for advanced devices.

I. It is possible to represent many types of functional behavior through the relative distribution of marks in space.

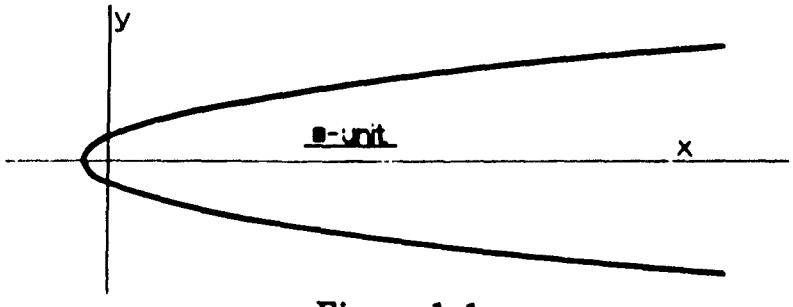

Figure 1-1.

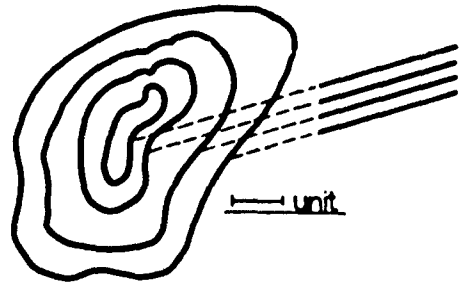

Figure 1-2.

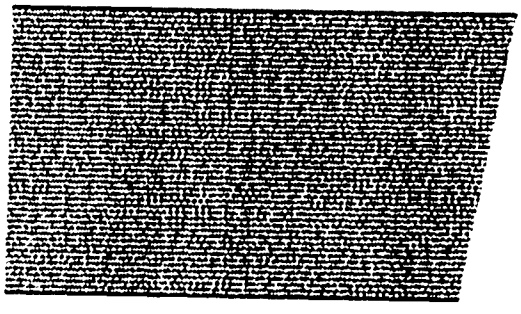

Figure 1-3.

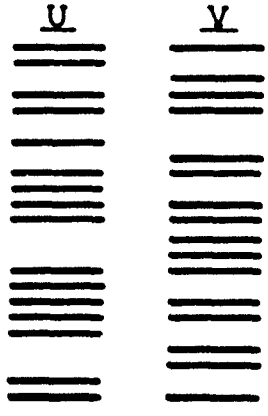

Figure 1-4.

We wish next to discuss the superposition of the numbering system upon this purely graphical framework. This represents an additional step which, as we shall use it, is often a matter of convenience and never removes the underlying character of the graphical process, which is the quantitative interpreting of the relative placement of the marks in quantitative space.

In Figure 1-5, a grid of numbered lines aids in evaluating the functional relationship seen in Figure 1-1. The reader should convince himself that the presence of the lines does nothing for the diagram that could not have been achieved without them except to use a memory code of numbers to speed up the arrival of a closer answer. Figure 1-2 has had attached to part of it certain numbers (Figure 1-6) which permit the elimination of the set of parallel lines, but there is no intrinsic difference in the use or contribution of the diagram. Figure 1-6 is an ordinary topographic map.

In Figure 1-7, numerical values have been attached to marks similar to those of Figure 1-4 to yield numerically readable scales. Such a scale does not differ intrinsically from those of Figure 1-4 although marks no longer carry the same value in different parts of the scale.

In Figure 1-8, projective diagrams are shown, using central, parallel and orthographic projection. The notion of projection is a purely graphical one and carries the full implication of space representation without the slightest reference to a number system.

In Figure 1-9, numerical values have been attached to an ordinary orthographic projection diagram which lend precision to the shapes and sizes shown there originally but do not change the basic interpretation.

In Figure 1-10, still another familiar type of drawing is seen in the alignment diagram, roughly called the nomogram. Here the value of abstract algebra is clearly manifested since it tells if and how a function of three variables can be arranged in scales of those variables such that a straight line cutting the three scales does so at values which satisfy the original relationship for which these scales were contrived. The representation of this behavior is then made graphical, as in the figure. The ease of drawing a straight line has always made this type of diagram a popular graphical one where three-figure accuracy would suffice.

There is a large number of constructions well-known to Euclidean and projective geometrists expressing other special relations in similar ways which the graphical method is well-adapted to exploit.

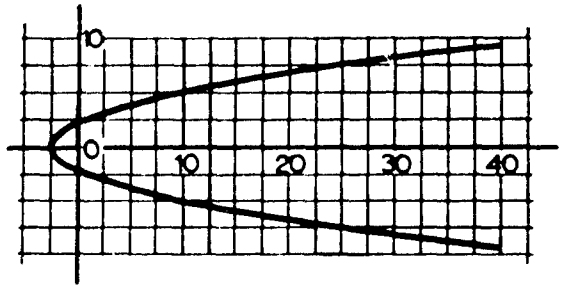

Figure 1-5.

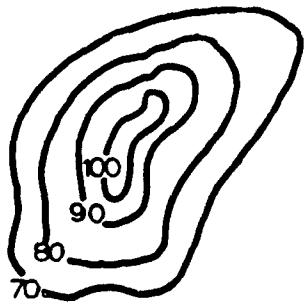

Figure 1-6.

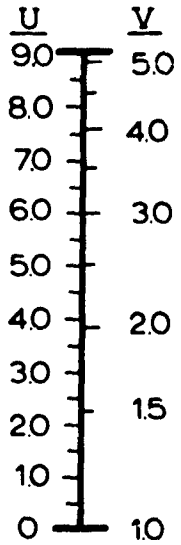

Figure 1-7.

We now have discussed a sufficient number of graphical diagrams and looked into their foundation requirements and procedures so that we can define what we mean by a graphical procedure. We propose to broaden the preceding statement I. by the addition of the word "encoded", referring to "encoded marks", which permits us to associate with a figure's points, lines or curves, numerical values in a fashion similar to the examples just cited. The underlying properties and usage of the diagram remain graphical. They retain the strength and weaknesses of the graphical technique.

> II. It is possible to represent many types of functional behavior by the relative distribution of plane or numerically encoded marks in space. Such a representation will be called a graphical representation.

It should be noted in Figure 1-9 that in the practical machining of the pieces described, the tolerances specified are absolutely necessary for the finished article to lie within this accuracy. It will never achieve the perfection of the round figures inasmuch as the technique for reducing it to size and of measuring its size has to be accomplished by use of or comparison with a graphical scale of limited accuracy. The field of measurement turns out to be graphical itself. We live by a system of perfect, conceptual entities but within a universe of uncertainties and probabilities. The algebraic system of perfect numbers is an abstraction useful in its limited domain but attachable to the world of reality only through channels involving instrumentation or measurement. Ours is a graphical world—a world of physical experience, employment of the physical senses and evaluations by graphical instruments. The daily use of the algebraic system for practical purposes requires that a problem first have a perfect model made of it to which the abstract system of numbers can attach. Such a representation must then in turn be interpreted, as in the dimensioning case above, in terms of the realities of the operating world in which human beings are living, through graphical instrumentation.

In Figure 1-9, we saw an application of graphical representation which has come to be called engineering drawing. An enormous amount of this type of representation is required to keep up with our volume of national invention, design and manufacture. Descriptive geometry has become associated with it and the two subjects to their detriment are inextricably caught in the rising standards of achievement universally sought by our colleges. *There has been failure to realize that the two subjects constitute only a tiny portion of the large service area of modern graphics.* If, however, we thoroughly understand the large field and its potentialities, the remedies for the lesser troubles of engineering drawing and descriptive geometry reveal themselves in proper perspective.

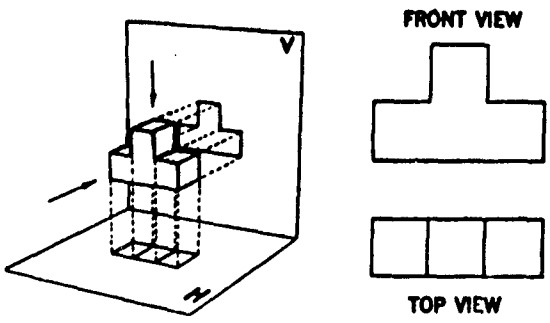

Figure 1-8a. "Descriptive Geometry" - Watts and Rule

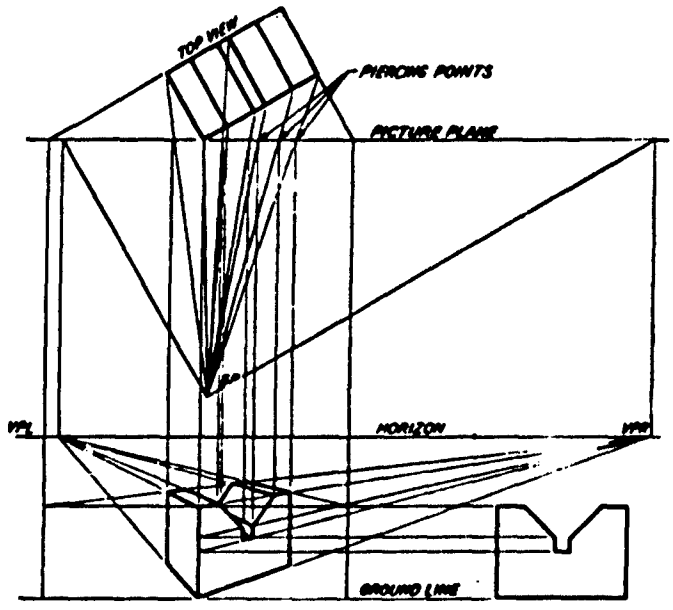

Figure 1-8b. "Graphics for Engineers" - Luzadder

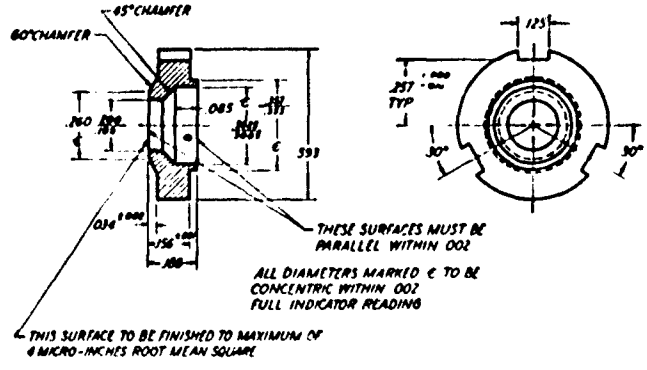

Figure 1-9. "Graphics for Engineers" - Luzadder

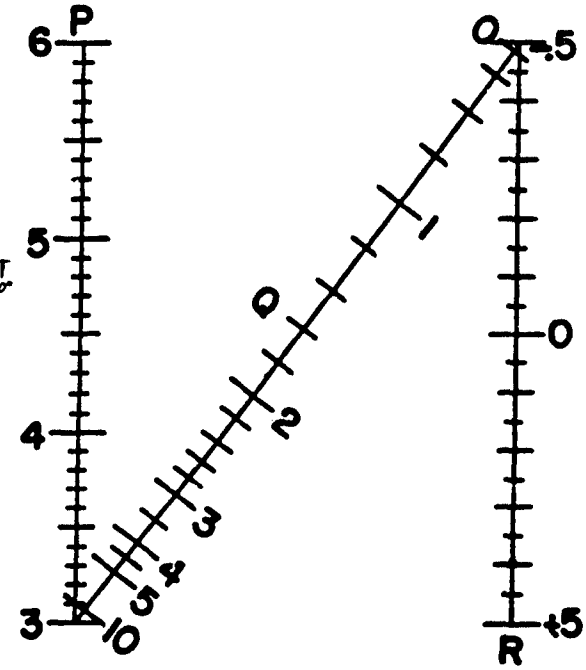

$$(P-3)Q^2 = 8R+4$$

Figure 1-10. "Elements of Nomography" - D. P. Adams

CHAPTER 2

COMPUTATION ORGANIZATION

We shall now show how the definition of graphics developed in the preceding chapter can be coupled with mathematical theory and modern engineering techniques to yield an effective research device—in this case a computer with certain desirable properties. The breadth of the definition as given in Chapter 1 suggests the strong likelihood of other applications of a similar nature and the advisability of further attention to this field. One purpose at this time is to show the natural association of the definition with numerous elements of modern research and development.

A. ORGANIZED VS GENERALIZED COMPUTATION

The extended or even the simple computation shows some degree of what might be called serial organization which means merely the sequential ordering or arrangement of intermediate tasks to carry out and evaluate the given relationship. Groups of machines or portions of a given computing machine could conceivably be mutually time-scheduled to carry through what might be called, in contrast to the word "serial", a form of "parallel" organization of computation. A third even more significant mode of organization would arise if the entire computation task itself could be materially altered and a simpler task undertaken, the result of which could be correlated with the answer value. When the answer to the simpler task was known, it would uniquely imply the answer to the original task.

If the advantages of organization of a computation are not to be lost, a degree of specialization of computer purpose to carry out the task will inevitably accompany and be somewhat proportional to the degree of organization present. This specialization may or may not be made a rigid and permanent feature of a computing machine. The battle between general and special purpose computers must ponder the advantages of the computation organization and the computer organization, weighing the advantages of the former with the restrictions imposed by the latter.

> If a computation organization is sufficiently powerful and has some generality of application, it may warrant the creation and maintenance of a machine commensurately specialized to effectuate its limited task with maximum efficiency.

The computer specialization may well show up in the creation of one or more permanent memory patterns and the development of specialized circuits for carrying through rapidly and repeatedly a certain key computation. A major technique of specialization turns out to be fast repetition—repeated because it can be made fast and made fast because it is going to be many times repeated.

The storing of a quantity $X_U(U)$, correlated through the value of U for quick retrieval, may present a substantial savings in time over the serial computation of X_U. Note that it may be advantageous to correlate through U a pair, a triplet, a quadruplet, etc. $X_U(U)$, $Y_U(U)$, $Z_U(U)$, $T_U(U)$, all retrievable by reference to the value of U. Conceivably the retrieval could be in parallel, that is time shared, or simultaneously.

B. CORRELATION PAIRING

In organizing a computation, we have observed that an appealing and certainly logical notion would be to replace the particular equation or relation by a simpler one by some relationship not in itself too arduous; for instance, a multiplication can be reduced to a simpler addition by logarithms. If the need for the computation is to be made rapidly many times, say a thousand times a second, the ease of the second correlated-relation need not be emphasized quite as much, provided means are found for quick access and evaluation. As an example, (without reference to logarithms) the multiplication $U \cdot V = W$ can be reduced to a common linear relation between the components of three PAIRS in those variables in the following way. We correlate:

$$\begin{aligned} &\text{with U, a pair of functions of U: } (U_1, U_2) = (O, uU);\ u = \text{constant} \\ &\text{with W, a pair of functions of W: } (W_1, W_2) = (G, wW);\ w = \text{constant} \\ &\text{with V, a pair of functions of V: } (V_1, V_2) = (G/(1 - \tfrac{w}{u} V), O) \end{aligned} \qquad (2\text{-}1)$$

The linear relationship is then clear in the sense that the three component pairs satisfy it, namely the linear relationship:

$$\frac{W_2 - V_2}{W_1 - V_1} = \frac{U_2 - V_2}{U_1 - V_1} . \qquad (2\text{-}2)$$

This is valid, inasmuch as $\dfrac{wW - 0}{G - \dfrac{G}{1 - \frac{w}{u}V}} = \dfrac{uU - 0}{0 - \dfrac{G}{1 - \frac{w}{u}V}}$ (2-2a)

yields

$$U \cdot V = W. \tag{2-2b}$$

Figure 2-1 shows the nomogram with u = 1/2, w = 2.

Note that the linear relationship (2-2) expresses the original equation (2-2b), even with these values included. We note that this is the same as saying that α and β exist such that the common linear relation holds between the three pairs:

$$\begin{aligned} \alpha U_1 + \beta U_2 + 1 &= 0 \\ \alpha V_1 + \beta V_2 + 1 &= 0 \\ \alpha W_1 + \beta W_2 + 1 &= 0 \ . \end{aligned} \tag{2-3}$$

This is the same relation as (2-2).

C. GEOMETRIC INTERPRETATION OF THE CORRELATION RELATIONSHIP

These relations can be phrased in geometric form as follows: Let an equation or relationship

$$F(U,V,W) = 0 \tag{2-4}$$

be such that it is possible to correlate each variable with a pair of functions of that variable

$$\begin{aligned} &U: (U_1, U_2) \\ &V: (V_1, V_2) \\ &W: (W_1, W_2) \end{aligned} \tag{2-5}$$

where for any triple of values of U_o, V_o, W_o satisfying (2-4) it is found that α, β exist such that (2-3) always holds. Then since (2-3) is a set of three, linear, nonhomogeneous, equations in two unknowns (α, β), for their compatibility it

must be true, with a minor exception, that

$$\begin{vmatrix} U_1 & U_2 & 1 \\ V_1 & V_2 & 1 \\ W_1 & W_2 & 1 \end{vmatrix} = 0 \quad . \qquad (2\text{-}6)$$

Note that equations (2-6), (2-3) and (2-2) are identical.

A direct geometric interpretation of this is immediately seen to be

IF THE CORRELATED PAIRS (U_1, U_2), (V_1, V_2), (W_1, W_2) ARE INTERPRETED AS THREE PAIRS OF CARTESIAN COORDINATES, THEN FOR ANY THREE ANSWER-VALUES U_o, V_o, W_o, THESE THREE POINTS MUST LIE ON A STRAIGHT LINE IN THAT COORDINATE FRAMEWORK. THE COMPATIBILITY OF EQUATIONS (2-3) REQUIRES THE IDENTITY OF EQUATIONS (2-2), (2-3), AND (2-6) WITH (2-4). THE NOMOGRAPHIC PROPERTY OF AN EQUATION (2-4) IS CUSTOMARILY EXPRESSED IN THE FORM (2-2), (2-3), OR ESPECIALLY (2-6). SOLUTION CAN THEN BE EFFECTED BY DRAWING A STRAIGHT LINE, THAT IS, FINDING AND APPLYING α AND β, (WHICH IS THE LINE OF EQUATION (2-2)).

D. THE CONVENTIONAL ROLE OF THE NOMOGRAPHIC PROPERTY

The plotting of Cartesian coordinates under the correlation (2-5) for each member of a triple U_o, V_o, W_o satisfying (2-4), is a writing in a memory. It is not hard to do and gives rise to three curves parametric in the three variables U, V and W. If U_o and V_o are specified, the value of W_o satisfying (2-4) will be found by drawing a straight line through the former two and noting point W_o where it cuts the W-curve, on the graphical plot just referred to.

IT IS THUS SEEN THAT THE NATURAL LOGICAL COMPUTATION ORGANIZATION USING PAIRS ENVISAGED ABOVE IS SIMPLY THE PROCESS OF MAKING AN ALIGNMENT CHART OR NOMOGRAM FOR THE EQUATION IN QUESTION. THE CORRELATION IS RECORDED ON PAGE MEMORY BY PLOTTING THE PARAMETRIC CURVES (2-5), WHENCE IT IS EASILY RETRIEVED BY VISUAL MEANS. THE "SIMPLER RELATIONSHIP" IN THE NEW ORGANIZATION OF THE COMPUTATION IS, IN THIS CASE, A STRAIGHT LINE CONNECTING VALUES U_o, V_o. IT IS CARRIED OUT WITH A STRAIGHT-EDGE, AND ITS INTERSECTION AT W_o WITH THE W-SCALE, THE ANSWER VALUE, IS NOTED BY EYE.

OTHER LOGICAL ORGANIZATIONS OF COMPUTATION ARE POSSIBLE WITH THE CORRESPONDING CORRELATING RELATION IDENTIFIED AND GRAPHICALLY EXPRESSED. THE GEOMETRIC FORM OF THE SIMPLER RELATIONSHIP, THE ANSWER-LOCUS, CAN VARY WIDELY, SUCH AS BEING A CIRCLE OF FIXED RADIUS, OF FIXED CENTER, OR VARIABLE CENTER AND RADIUS, A PARABOLA OF FIXED ORIENTATION, OF GENERAL ORIENTATION, A GENERAL CONIC, A GENERAL POLYNOMIAL FORM. SUCH NOMOGRAPHIC DEVELOPMENTS ARE NOT WELL-KNOWN IN THIS COUNTRY BUT HAVE BEEN STUDIED SOMEWHAT ABROAD. WE SHALL LIMIT OURSELVES TO THE STRAIGHT LINE ANSWER LOCUS IN THIS PAPER.

For instance: the condition that four points $P_1(X_1, Y_1)$, $P_2(X_2, Y_2)$, $P_3(X_3, Y_3)$, $P_4(X_4, Y_4)$ lie on a circle can be written:

$$\begin{aligned} X_1^2 + Y_1^2 + \alpha X_1 + \beta Y_1 + \gamma &= 0 \\ X_2^2 + Y_2^2 + \alpha X_2 + \beta Y_2 + \gamma &= 0 \\ X_3^2 + Y_3^2 + \alpha X_3 + \beta Y_3 + \gamma &= 0 \\ X_4^2 + Y_4^2 + \alpha X_4 + \beta Y_4 + \gamma &= 0 \end{aligned} \qquad (2\text{-}7)$$

The compatibility of these equations (2-7) means that α, β, γ do exist such that

$$X^2 + Y^2 + \alpha X + \beta Y + \gamma = 0 \ . \qquad (2\text{-}8)$$

$P_1 \ldots P_4$ lie on (2-8) and that, with a minor exception,

$$\begin{vmatrix} X_1^2 + Y_1^2 & X_1 & Y_1 & 1 \\ X_2^2 + Y_2^2 & X_2 & Y_2 & 1 \\ X_3^2 + Y_3^2 & X_3 & Y_3 & 1 \\ X_4^2 + Y_4^2 & X_4 & Y_4 & 1 \end{vmatrix} = 0 \ . \qquad (2\text{-}9)$$

If we have

$$F(U,V,R,S) = \begin{vmatrix} U^2 & U & 0 & 1 \\ V^2 & -V & 0 & 1 \\ R^2 & 0 & R & 1 \\ S^2 & 0 & -S & 1 \end{vmatrix} = 0 \ . \qquad (2\text{-}10)$$

Using U, V, R, S, we can correlate the pairs as follows and express (2-9) in the form (2-10):

$$\begin{aligned} X_1 &= X_U(U) = U; \quad Y_1 = Y_U(U) = 0 \\ X_2 &= X_V(V) = -V; \quad Y_2 = Y_V(V) = 0 \\ X_3 &= X_R(R) = 0; \quad Y_3 = Y_R(R) = R \\ X_4 &= X_S(S) = 0; \quad Y_4 = Y_S(S) = -S \ . \end{aligned} \qquad (2\text{-}11)$$

Then nomographically plotting (2-11), we have Figure 2-2. In this figure, one has position-storage of the pairs of (2-11) correlated through the values of U, V, R, S, and must utilize an answer locus of form (2-8). A circle through known values of U, V, and S cuts R at the answer to (2-10), which is

$$(U \cdot V - R \cdot S)\ (U + V)\ (R + S) = 0 \qquad (2\text{-}10a)$$

$$U \cdot V = R \cdot S \quad U \neq -V \quad R \neq -S$$

In this, (2-8) is scarcely an easier form to deal with than (2-10a), except that pre-storage of correlated positions in Figure 2-2 and the availability of a many-circled template make graphical use of Figure 2-2 fast and easy.

The specific procedure developed up to now in Figures 2-1 and 2-2 has been based upon two totally distinct steps: first, the graphical storage of such a correlation as (2-11); and second, the nomographic relationship. In the graphical step, there is a correlation or reference between physical position and variable value. Graphical plotting is a form of memory writing of this reference whence value can be retrieved by eye. In the nomographic step, we have acquired a new, simpler relationship (2-3) between these physical positions. From now on we must restrict ourselves to a subgroup of functions $F(U, V, W) = 0$

such that the common relationship between the elements of each pair, like the straight line in (2-3) and the circle of (2-8), actually exists and is truly simpler in computational form than the original relationship F(U,V,W) = 0. The simpler computation is then carried out. The advantages deriving from purely graphical procedures and from nomographic procedures will both receive attention.

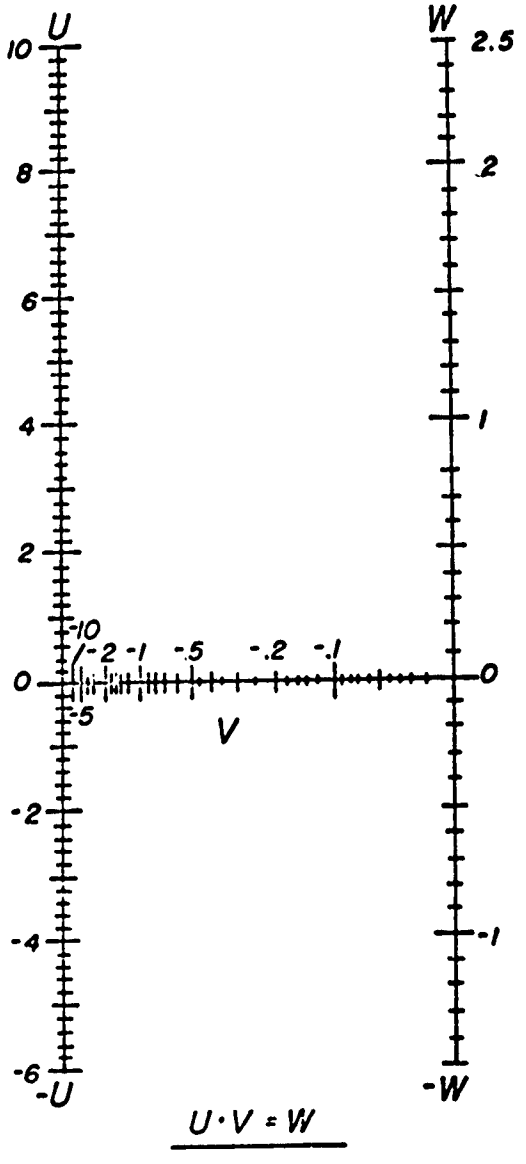

Figure 2-1.

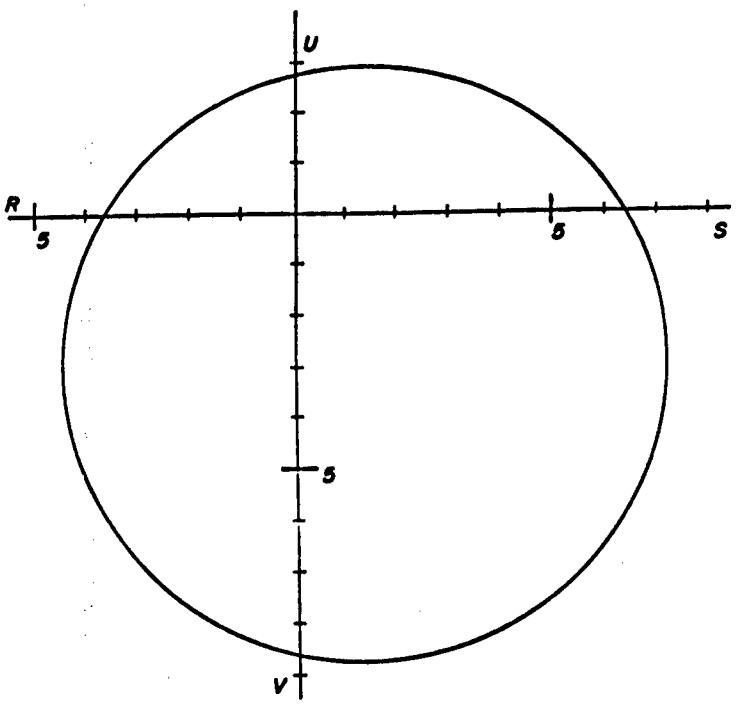

$$\underline{R \cdot S = U \cdot V} \qquad \begin{matrix} (3.7 \times 6.4) + (2.7 \times 8.7) \\ 23.5 \qquad 23.7 \end{matrix}$$

Figure 2-2.

CHAPTER 3

THE COUNTABLE BIT MEMORY GENERAL PLAN—AUTOMATIC CORRELATION

A. CORRELATION BY COUNTABLE BIT

In the nomogram, the value of a variable has been correlated with a pair of Cartesian coordinates, as in (2-1), (2-5), and (2-11). A convenient permanent memory for this correlation is the page where, unfortunately, a human operator is required first, to search this memory and, second, to effectuate the subsequent computation by drawing the straight line. We seek the automation of these steps.

Following the nomographic steps outline, we later substitute for our page-memory coordinate-pairs a written memory of countable bits, Figure 3-1, whose cumulative counts are correlated as earlier described: U with the pair $(U_1, U_2,) \equiv (U_x, U_y) \equiv (X_U, Y_U)$ etc. by vertical juxtaposition of the reading heads.

> Cumulative counts at the same level in three columns, Figure 3-1, will then always automatically represent correlated values of those quantities. The secondary computation — the calculation carrying through the collineation — we propose to do by circuitry which shall carry through a simple linear relation between the counts now stored from the columns.

B. AN EXAMPLE

A simplified but revealing version of what we propose to do is seen in Figure 3-2. A relation F(U, V, W) = 0 is assumed to have the nomographic form at lower left, so that the equation of alignment between the coordinate pairs correlated with values as described earlier is the one shown below it. The film strip shows schematically the vertical columns of countable bits for quantities $U = U_Y (\equiv Y_1)$, $V = V_Y (\equiv Y_2)$ and finally $W_X = X_3$, $W_Y = Y_3$ and W. Note that U_X and V_X remain constant in value. Hence they do not require any columns in this computation for their representation, and so are not shown.

As the film moves, the pulses created in the reading heads from reading the bit patterns enter the BPC's (Binary Pulse Counters) as indicated. At an input value V_0, BPC1 is saturated and opens the switch S2 to prevent further Y_2

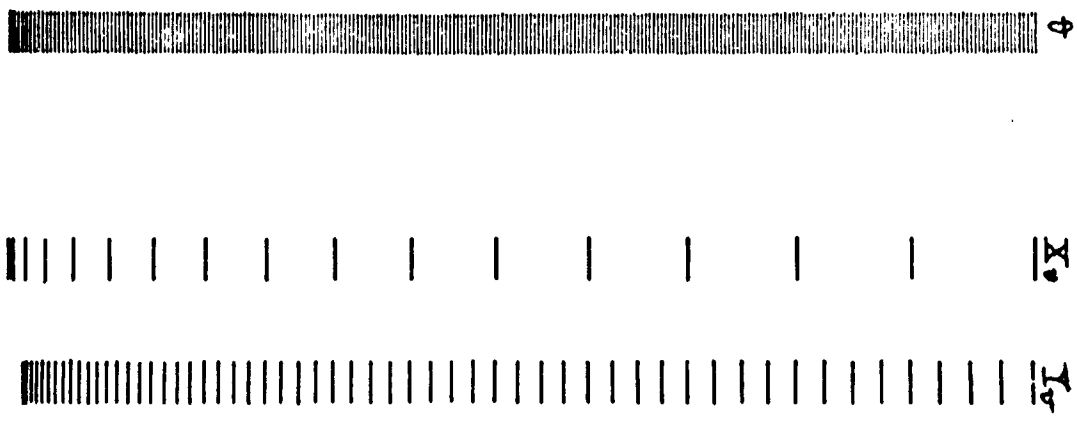

Figure 3-1.

counts from entering BPC2 and also drops the Y_2 count into ACC6. Similarly for U and Y_1, the REVERSIBLE COUNTER acquires a count ($-Y_1$) during the first phase of reading, and the final count in ACC6 is $Y_2 - Y_1$. Y_2 and Y_1 can be read as a single Y column rather than as the double column shown here. This is a <u>parallel</u> organization and computation.

During the second phase of film passage, commonly called the second pass, the <u>FIRST</u> W_x-Pulse clears BPC2 and drops ACC6 into it, leaving $Y_2 - Y_1$ in BPC2. Each <u>successive</u> W_x-Pulse drops BPC2 into ACC6, building up X_3 ($Y_2 - Y_1$) there. A COMPARISON COUNTER 7 now detects when ACC6 = X_3 ($Y_2 - Y_1$) equals REVERSIBLE COUNTER 5 = $G(Y_3 - Y_1)$ and at that moment opens the gate on BPC4 trapping answer W. Many of these processes are clearly parallel in the sense of organization of the computation.

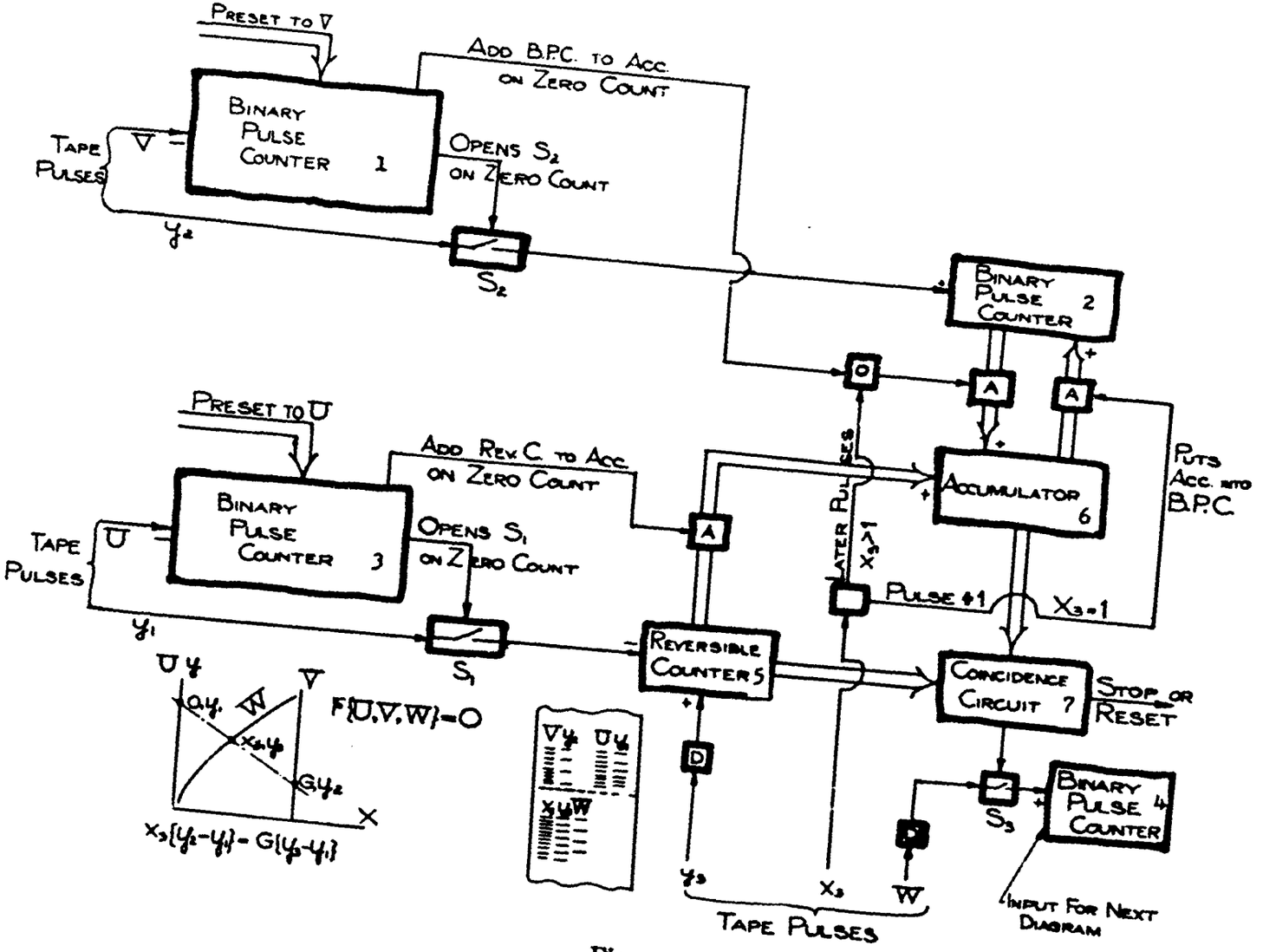
PRESET TO V
ADD B.P.C. TO ACC. ON ZERO COUNT
BINARY PULSE COUNTER 1
TAPE PULSES
V
OPENS S2 ON ZERO COUNT
y2
S2
BINARY PULSE COUNTER 2
PRESET TO U
ADD REV. C. TO ACC. ON ZERO COUNT
BINARY PULSE COUNTER 3
TAPE PULSES
U
OPENS S1 ON ZERO COUNT
y1
S1
ACCUMULATOR 6
PUTS ACC. INTO B.P.C.
LATER PULSES
X3>1
PULSE #1
X3-1
REVERSIBLE COUNTER 5
COINCIDENCE CIRCUIT 7
STOP OR RESET
S3
BINARY PULSE COUNTER 4
INPUT FOR NEXT DIAGRAM
F(U,V,W)=0
X3{y2-y1}-G{y2-y1}
y3
X3
W
TAPE PULSES

Figure 3-2.

C. PROBLEMS AND PROMISE; PLAN OF THIS PAPER

On the basis of the concepts of correlation and techniques of parallel-organized computation we have presented, we shall be concerned first, with details of the form and the automatic writing of large numbers of bits - how to compute where they belong and physically write them there - a programming problem; second, with several quite different methods for reading the bits and all the problems these imply from diffraction to vibration; third, with logic modules for counting and computing the relationship between pairs, corresponding to equation (2-3), and fourth, with some potentialities of this technique and evaluation of its promise. These may not fit perfectly into a tight, logical presentation but their interrelationships and import will be clear.

CHAPTER 4

MEMORY, ITS FORM AND WRITING

A. GENERAL BIT PATTERN DECISIONS

The preceding description of bit patterns immediately creates numerous alternatives in writing techniques. A bit pattern will tend to be uniform, that is regularly spaced, if the nomographic scale it is representing is uniform, or will tend to diverge or converge correspondingly. Each bit adds a certain power of 2 to the accumulated sum of the column. To avoid the disparity in bit-separation at the top and bottom of Y_U, Figure 3-1, bit placement should appropriately be halved or doubled in frequency, hence in value, in an attempt to keep bit spacing more constant, as well as keeping it somewhat the same across columns. Such an event will require a signal, described later as a "scale-factor signal."

It would be possible to have the bit marks of various columns rather evenly spaced and consistently "out of step" as in Figure 3-1, or alternatively, to have a "bit-or-no-bit" technique whereby bits appeared or were omitted only on grid lines at even raster intervals. The latter has seemed the easier way to date.

Other considerations have recommended that memory be written on 35mm film in six columns at about 50 bits per inch, half black, half white. The use of double- or triple-width bits for scale-factor "signalling" has actually been abandoned though corresponding signals have been retained which can conveniently be referred to by these suggestive names.

The bit's presence or absence according to the scheme just adopted is computed by 709/7090 and is written into film memory by being photographed on an oscilloscope on the output as described later. The technique appears to be reliable but is now being replaced because of non-uniform illumination of the face of the scope.

B. FUNCTIONAL REPRESENTATION BY DIGITAL INCREMENTATION

NOMAG I

NOMAG I is a 709 program which was completed during the summer of 1961. Its purpose was twofold:

1. To determine the feasibility of producing input data film for the computer by using the oscilloscope facility of the 7090.

2. To develop the mathematical relations and computational considerations necessary for the realization of such a program.

We found that the techniques developed were quite efficient and the film produced was of a quality sufficiently promising for our purposes. We have been able to use some of the film patterns for some time in the testing of some aspects of our optical systems.

NOMAG II

NOMAG II is a 7090 program which is currently being written at the Engineering Projects Laboratory. This program differs from NOMAG I in that it is not a feasibility study, but a program to produce film to be used in unaltered form by the computer. We did not, however, find it necessary to change any of the basic mathematical considerations of NOMAG I.

At this point we shall consider the following problem. We are given x(t), y(t), real-valued, analytic functions of a parameter t. We may think of x and y as coordinates of the real plane. We desire to produce a digital bit pattern on film or piece of paper which will represent x(t) and y(t). The exact "sense", or way of working, of the representation can be best described in stages. We start with an example.

In Figure 4-1 suppose that the reading device is initially (before any action) in position A and the three counters are set to zero. Assume that the functional relation to be represented by the columns of countable bits is $x(t) = t/2$ and $y(t) = \sqrt{t}$. We shall let the increment t, the "parameter-increment" or "clock-increment," be 1. Let x be the instantaneous number of bits in the x counter, (do not confuse with x(t)) and y be the instantaneous number of bits in the y counter (do not confuse with y(t)). For example when the reading head is in position C (Figure 4-1) we have $t = 2$, $x(t) = 1$, $x = 1$, $y(t) = 1$ and $y = 1$. At any instant let us assume that x must not differ from x(t) by more than 1 (the "x-increment") and a similar position B (Figure 4-1) that $t = 16$, $x = 8$, $x(t) = 8$, and $y = 4$, $y(t) = 4$.

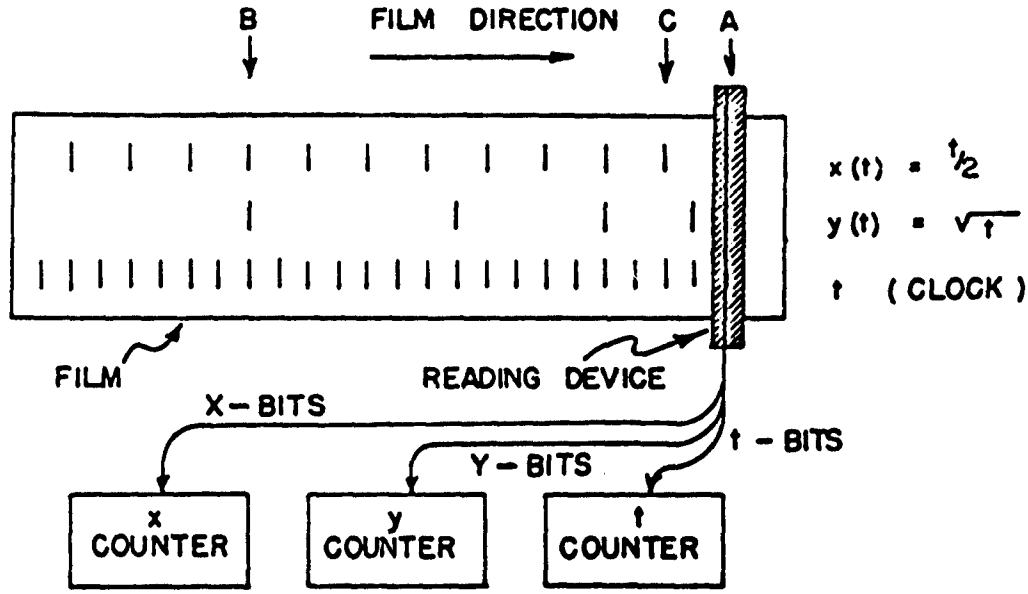

Figure 4-1. Example of Digital Incrementation

In our particular scheme here, there can be no bits between clock pulses. For every "clock pulse" or "t-bit" there is either a coordinate bit ("x-bit", "y-bit") or a blank.

Figure 4-1 involves even quantities and computations. This is rarely the case in practice, so a suitable algorithm must be found for the representation of functional behavior.

Figure 4-2 shows a very simple algorithm, suggestive of what we shall use later, which will produce the film of Figure 4-3 for $x(t) = t/2$, $y(t) = \sqrt{t}$ and $dt = 1$. We suggest that the reader verify by examination of Figure 4-3 that x and x(t) differ by no more than $dx = 1$ at any instant and that y and y(t) are similarly related.

Figure 4-3 indicates how the increments and values from the algorithm of Figure 4-2 create the suitable pattern. At first it will seem rough but if the increment dy is reduced, it will even out. This scheme does not yet include provisions for scale factor changes.

Some of the additional considerations in the practical realization of the process of digital incrementation are:

- Counter initialization
- Scale-factor initialization

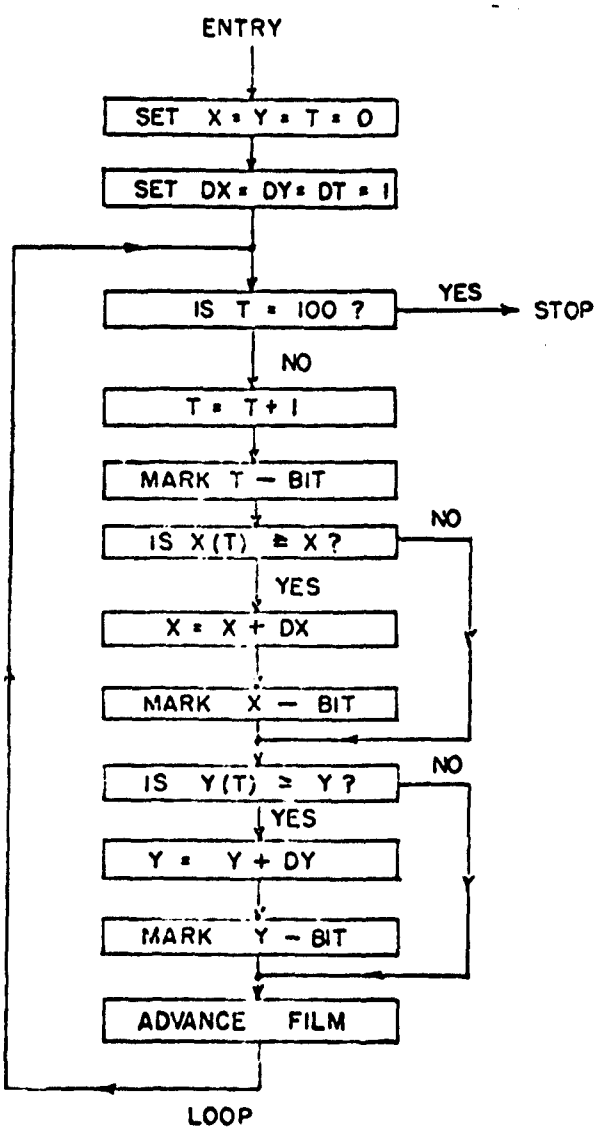

Figure 4-2. Block Diagram of Simple Program

- **Provision for both increasing and decreasing scale-factors.**

In processing film for the computer, an additional complexity is encountered. A nomogram function is of the form:

$$x(u) = f_1(u)$$

$$y(u) = f_2(u) \qquad (4\text{-}1)$$

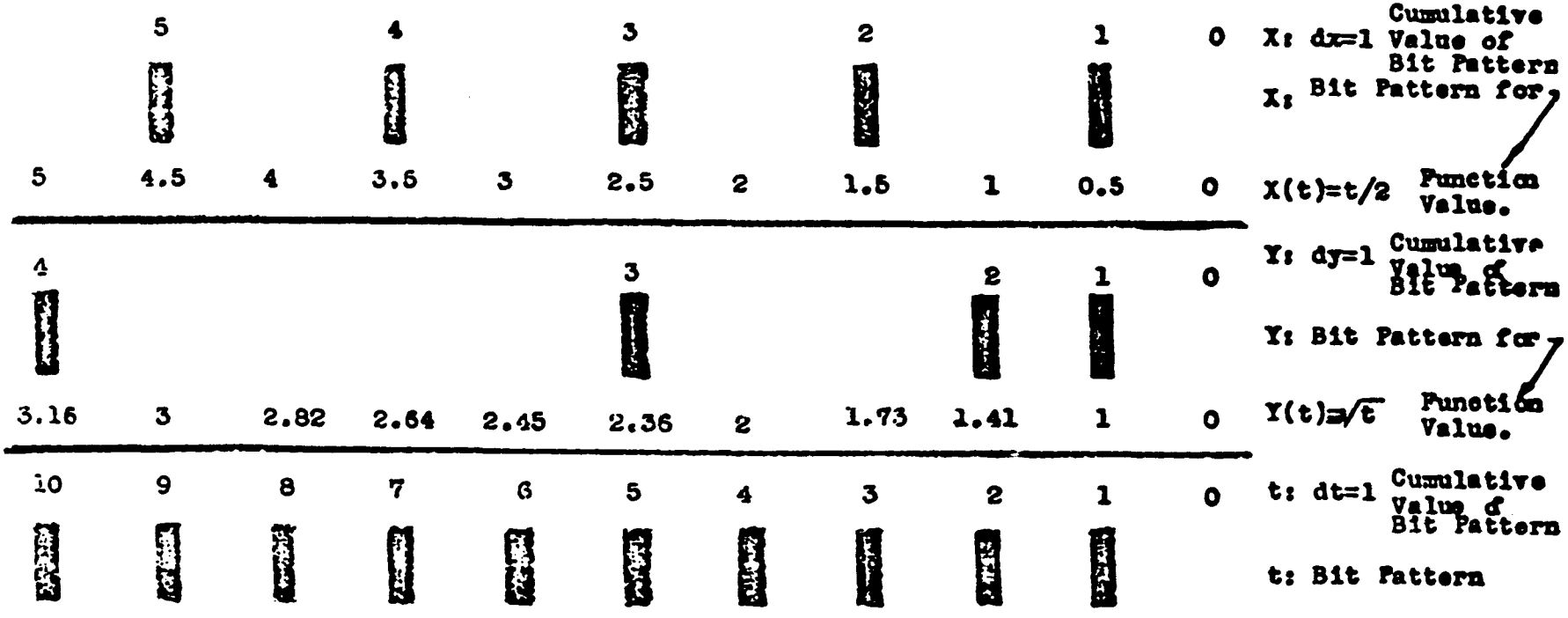

Figure 4-3.

This figure shows the accrual of values in the cumulative style of bit counting that characterizes the nomographic style of computing. It demonstrates that it is possible in both cases, that is for both Y and X, to lay down a regular clock pattern (t) and increase Y and X by a uniform amount each time and yet have the cumulative value of Y and X differ from a specific function of t, Y(t) or X(t), by less than this uniform amount. The increments of t, Y and X are at all times 1.

Where x and y are the coordinates, u is the parameter and f_1, f_2 are analytic functions of u. In the computer, y is used somewhat as the "clock" or parameter. Thus the functions must be computed so that u is given explicitly in term of y, using y as independent variable:

$$u(y) = g_1(y)$$

$$f_1(u) = x(u)$$

$$x(y) = f_1(g_1(y)) \qquad (4\text{-}2)$$

Since it is, in general, not possible to obtain g_1 and f_1 explicitly from (4-1) and (4-2), we have developed the "bit, no-bit" and scale-factor criteria in an indirect fashion.

The "u-bit criterion," i.e., whether or not to print or omit a u-bit, now becomes specifically:

$$y(u) - y_r < 0 \qquad \text{criterion } (B) \qquad (4\text{-}3)$$

Generally speaking, if the inequality (4-3) holds in the 7090 computation at any point, a u-bit is placed on film at the level in question. If not, it is omitted, unless (4-4) renders (4-3) inapplicable.

The u scale-factor is determined by

$$dy < |\, y(u + du) - y(u) \,| \leq 2dy \quad y > 0 \qquad \text{criterion } (A) \qquad (4\text{-}4)$$

If the double inequality (4-4) is satisfied, du is left unchanged. If not, du is raised or lowered by a factor of 2.

The x-bit criterion is, assuming all x positive

$$x(u) - x_r < 0 \qquad (4\text{-}5)$$

If (4-5) holds, an x-bit is placed on film (Compare (4-5) with (4-3)).

The x-scale-factor is determined by

$$\frac{dx}{2} < \frac{|\, x(u + du) - x(u) \,|\, dy}{|\, y(u + du) - y(u) \,|} \leq dx \qquad (4\text{-}6)$$

The complexity in (4-6) is necessary to prevent a y scale-factor change from causing an unwanted x scale-factor change. If (4-6) is satisfied, dx remains the same. If not, it is changed by a power of 2.

The tape convention of the computer is: (See schematic Figure 4-4.)

1. Single pulse implies single bit.

2. Double pulse implies single bit and increase of scale factor for succeeding bits.

3. Triple pulse implies bit and decrease of scale factor for succeeding bits.

An application of criteria (A) and (B) can be watched in detail in Tables 4-1a, 4-1b, and Figure 4-5. Figure 4-6 shows the order of agreement of cumulative bit values and theoretical values of the function for small increments of the independent variable.

Many other schemes for placing bit marks in columns to represent functional behavior are possible.

C. PROGRAM STRUCTURE AND WRITING

Let us now examine the structure of the program. It is composed of two sections: PASS 1 and PASS 2. On PASS 1 all the computations for the U and V scales are made, whereas PASS 2 (by scanning and identification) computes W. This is necessary because of the way in which NOEL I finds the correct W values. It first writes identification on the film, and then puts on some control pulses for the machine operation. It then calls SEQ(A), which through the use of several subsequences does all the computation involved in getting the initial scale factors and other pertinent data for the variables. In SEQ(B) and SEQ(C) these values are put on film in the appropriate bit patterns, so that NOEL can read them in. SEQ(D) does the work of putting the bits representing the U and V counting on film. It calls subsequences which check the bit and scale factor criteria, and depending upon their results, goes to routines BIT, (UP, or DOWN,) which add the appropriate increment and, if necessary, alter the scale factor. This is the bulk of PASS 1. After more control pulses are put on film, PASS 2 which consists of SEQ(E), SEQ(F), SEQ(G), and SEQ(H) begin. These do the same things for the W scale as PASS 1 does for U and V. After the W information is on film, control pulses and more identification close the film.

The computer film to be produced by NOMAG II contains in sequence the following (See Figure 4-4):

1. Control and clearing pulses
2. Counter initialization
3. Control pulses
4. Scale factor initialization (u and v)
5. Control pulses
6. Pass 1 digital incrementation
7. Control pulses
8. Scale factor initialization
9. Control pulses
10. Pass 2 digital incrementation
11. Control pulses
12. Parameter transformation

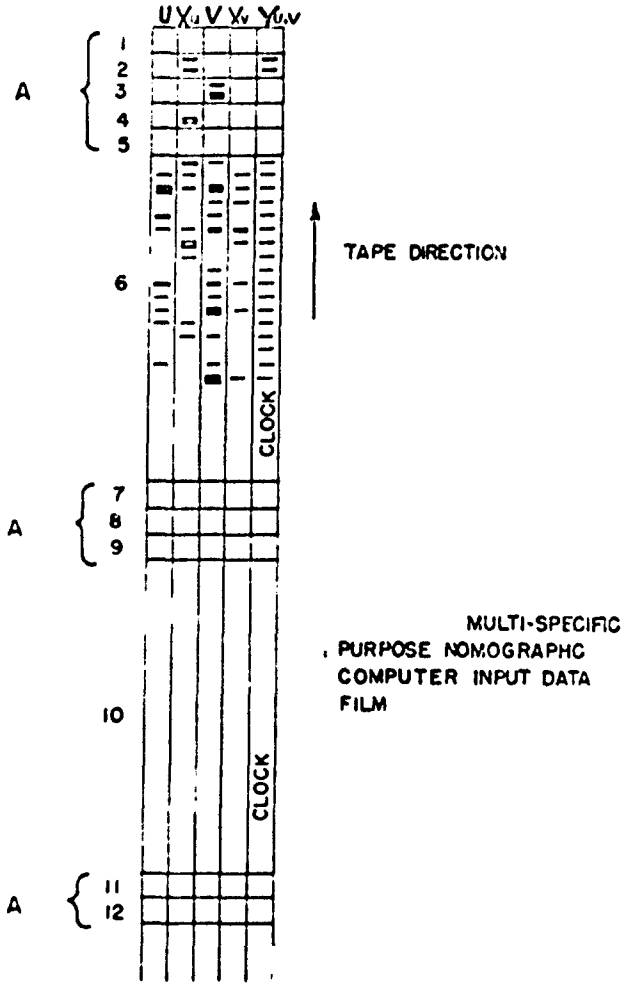

Figure 4-4.

TABLE 4-1a

DETERMINATION OF A U-SCALE BIT PATTERN $F(U,V,W,) \equiv \begin{vmatrix} X_1 & \sqrt{u} & 1 \\ X_2 & Y_2 & 1 \\ X_3 & Y_3 & 1 \end{vmatrix} = 0$

Functional Relation	$y = \sqrt{u}$	$y = \sqrt{u}$	$y = \sqrt{u}$	$y = \sqrt{u}$
Threshold Values Just below bit-line y_r, u	$y_r = 0$, $u = 0$	$y_r = 1$, $u = 0$	$y_r = 2$, $u = 2$	$y_r = 3$, $u = 4$
Increments dy, du	dy = 1, du = 2	dy = 1, du = 2	dy = 1, du = 2	dy = 1, du = 4
Independent Variable Incremented, Current u + du, u	u+du = 2, u = 0	u+du = 2, u = 0	u+du = 4, u = 2	u+du = 8, u = 4
① Criterion: $dy < y(u+du)-y(u) \leq 2dy$ Retain du, Apply ⑧ | Change du, Ignore ⑧,	$1 < \sqrt{2}-0 \leq 2$ 1.414 Retain du Apply ⑧	$1 < \sqrt{2}-0 \leq 2$ 1.414 Retain du Apply ⑧	$1 < \sqrt{4}-\sqrt{2} \leq 2$ 2 - 1.4 = .6 Change du Ignore ⑧	$1 < \sqrt{8}-\sqrt{4} \leq 2$ 2.8 -2 = .8 Change du Ignore ⑧
② Criterion: $y(u) - y_r < 0$ Insert, Omit u-bit u-terminal = ?	0 - 0 0 NO! Omit u bit u-terminal = 0	0 - 1 0 YES! Insert u-bit u-terminal = 2	Insert double-bit From ① u-terminal = 4	Insert double-bit From ① u-terminal = 8
Insert y-bit Evaluate Terminal y_r = next threshold y_r	$y_r = 1$	$y_r = 2$	$y_r = 3$	$y_r = 4$
Record Value of Increment du halfway between bits	---- du = 2	------- du = 2	------ du = 4	----- du = 8

TABLE 4-1b

DETERMINATION OF A U-SCALE BIT PATTERN $F(U,V,W,) \equiv \begin{vmatrix} X_1 & \sqrt{u} & 1 \\ X_2 & Y_2 & 1 \\ X_3 & Y_3 & 1 \end{vmatrix} = 0$

Functional Relation	$y = \sqrt{u}$	$y = \sqrt{u}$	$y = \sqrt{u}$	$y = \sqrt{u}$
Threshold Values Just Below bit-line y_r, u	$y_r = 4$; u = 8	$y_r = 5$; u = 16	$y_r = 6$; u = 24	$y_r = 7$; u = 40
Increments: dy (fixed); du	dy = 1; du = 8	dy = 1; du = 8	dy = 1; du = 16	dy = 1; du = 16
Independent Variable Incremented, Current u + du, u	u + du = 16; u = 8	u + du = 24; u = 16	u + du = 40; u = 24	u + du = 56; u = 40
(A) Criterion: $dy < y(u+du)-y(u) \leq 2dy$ Retain du, Apply (B); Change du, Ignore (B)	$1 < \sqrt{16} - \sqrt{8} \leq 2$ $4 - 2.8$ 1.2 Retain du Apply (B)	$1 < 4.9 - 4 \leq 2$ $.9$ Change du Ignore (B)	$1 < 6.3 - 4.9 \leq 2$ 1.4 Retain du Apply (B)	$1 < 7.4 - 6.3 \leq 2$ 1.1 Retain du Apply (B)
(B) Criterion: $y(u) - y_r$ 0 Insert, Omit u-bit u-terminal = ?	$\sqrt{8} - 4 < 0$ $2.8 - 4$ Insert u-bit u-terminal = 16	Insert double-bit From (A) u-terminal = 24	$\sqrt{24} - 6 < 0$ $4.9 - 6$ Insert u-bit u-terminal = 40	$6.3 - 7 < 0$ Insert u-bit u-terminal = 56
Insert y-bit y_r terminal = ? = next threshold y_r	$y_r = 5$	$y_r = 6$	$y_r = 7$	$y_r = 8$
Record value of increment du halfway between bits	--- du = 8	--- du = 16	--- du = 16	--- du = 16

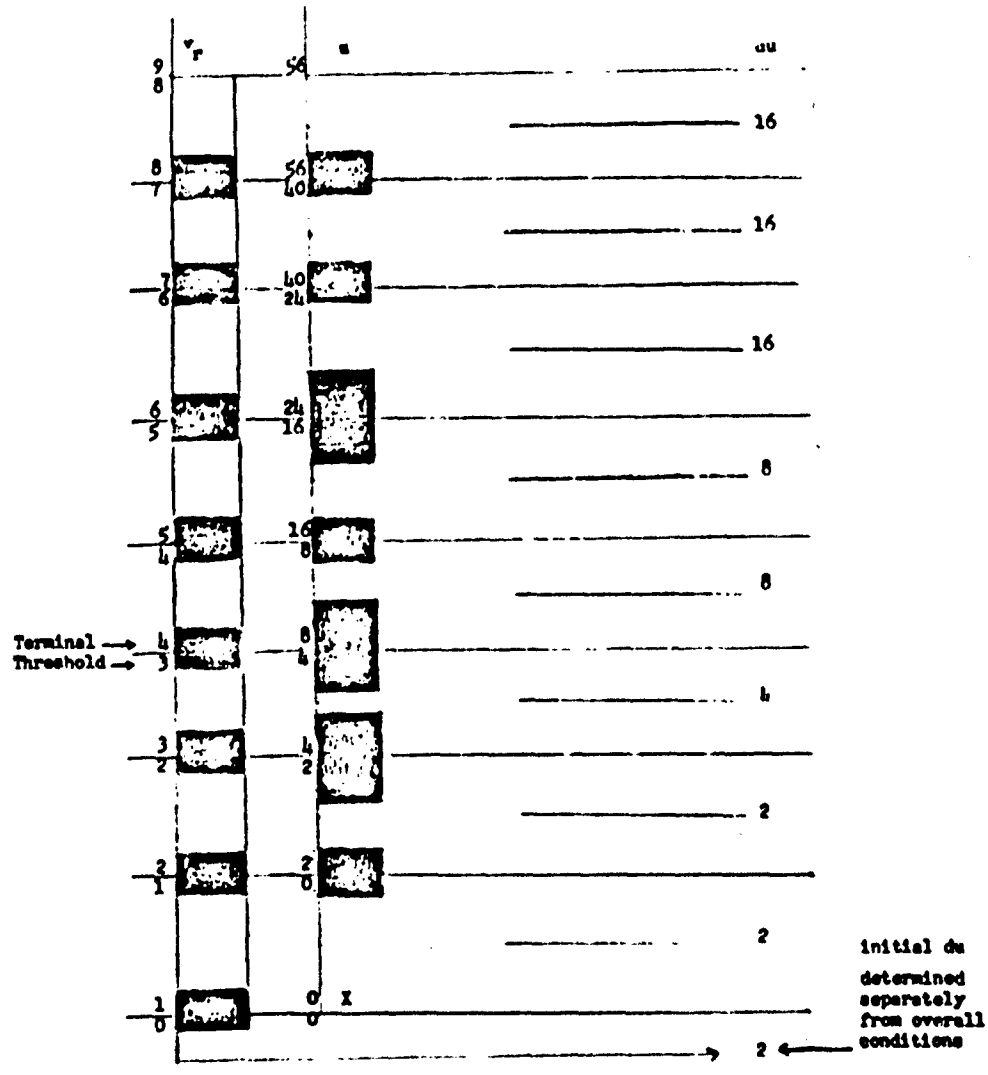

Figure 4-5.

Nothing has been said thus far about the film writing process. One of the NOMAG routines is called FILM, and it has entry points S1, S2, S3, S4, S5, D1, ... D5, T1, ... T5, ST1 ... ST5. Each of these is an entry to a section that writes a single, (double, triple, or special triple) pulse in the appropriate column 1-J. A sixth column, column 6, has not been shown in Figure 4-4, but contains the true clock track. These routines display appropriate dot configuration on the scope track, and are photographed. The x and y coordinates of the dots are stored in a block of storage and are called when needed.

Between sequences on the film, control pulses are interspersed to signify the end of one and the beginning of the next, and to clear the necessary counters.

SCALE OF HEAT EXCHANGE NOMOGRAM

$$U = Y^2$$

$$DY = \frac{15}{2\ 10} = 0.0146$$

Y	U(Y)	U
0.60	0.36	0.36
1.04	1.08	1.07
1.48	2.19	2.17
2.06	4.27	4.23
2.50	6.27	6.23
3.09	9.55	9.48
3.53	12.46	12.43
3.97	15.76	15.72
4.56	20.75	20.86
5.00	24.95	24.86
5.53	31.15	31.11
6.02	36.25	36.11
6.61	43.65	43.61
7.05	49.64	49.61
7.49	56.03	55.86
8.07	65.15	65.11
8.51	72.43	72.36
8.95	80.11	80.11
9.53	90.94	91.11
10.12	102.47	102.61
10.56	111.55	111.61
11.00	121.02	121.11
11.59	134.27	134.17
12.03	144.63	144.67
12.47	155.40	155.17
13.05	170.35	170.11
13.49	182.01	182.11
14.51	210.73	210.61
14.96	223.67	223.61

Figure 4-6.

All the above is with reference to film representation of the nomogram. To produce tape, for example, the scheme is the same, and only the writing routines need be changed. The tape units for the 7090 have six columns of data, so this is readily convertible to our demands. All that is necessary is a routine with the same entry points as FILM which will write the equivalent bit patterns on tape. Similarly, paper tape may be written from binary cards punched in the appropriate fashion. Routines to cover all these cases are now being developed.

There is quite a bit that can be done with the system currently available. It can handle virtually all kinds of 3-variable nomograms, the restrictions being that the slopes of the scales in the X-Y plane be positive (monotone

increasing coordinates). Using central projection this geometry can almost always be achieved.

Future plans call for the construction of a NOEL II, capable of solving general equations. In conjunction with this will be used new tape and drum units with 256 tracks to handle the necessary information. The programming techniques will be similar, although for certain types a method has been found which will be based upon a new solution algorithm. This procedure uses graphical techniques but does not employ alignment diagram techniques and hence is not limited by them.

D. A DISC MEMORY WRITING METHOD

1. Purpose of the Method

We wish to develop a device for placing digital data in the form of rectangular spots on a photographic emulsion on a transparent disc, hereafter referred to as "printing" of a "memory."

The memory must be suitable for a high-speed scanning system using the moving storage principle, as employed in the nomographic electronic computation system referred to earlier in this chapter.

The method used must have a potential capability for high-speed printing of high density storage patterns; however, this requirement is not of immediate importance.

Because of the size of the bits (400 bit positions per inch) and the velocity at which they are scanned (eventually at about 1,000,000 per second) accuracy in the alignment of the bit pattern, the optical system, the light source, and the photocells is of crucial importance.

The proposed memory is then an outgrowth of an existing memory produced by taking a series of photographs of a pattern of information as displayed on a cathode-ray tube. This early type of display was composed of parallel rows of binary bits exhibited in a series of pictures. The resulting photographic memory pattern (Figure 4-7) was mounted in such a way that it became part of a cylinder (Figure 4-8). Scanning, described later, was accomplished by spinning this cylinder past a light source and a series of photocells (moving memory) or by one of several moving reader techniques.[7] It is thus readily apparent that the optical path is greatly simplified by using a rotating disc-type storage system where each word is on a radial line of the disc. Figure 4-9 shows the system.

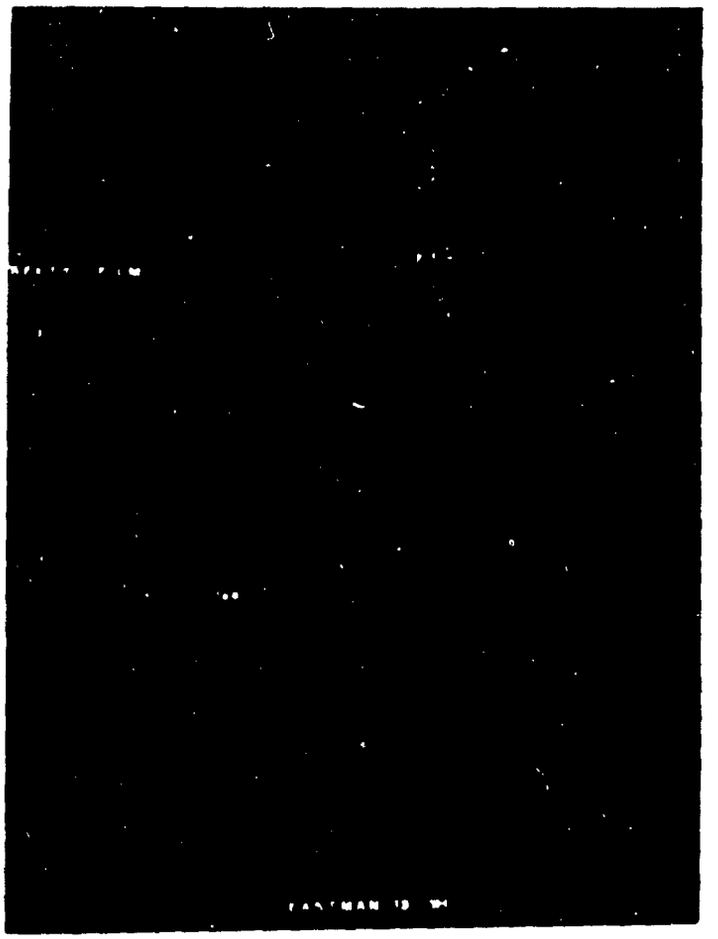

Figure 4-7. Present Memory Pattern

2. The Disc-Type Memory Pattern

The memory pattern to be printed was established after an investigation of the complete computation system. The pattern would be printed on a photographic plate six inches in diameter. The six channels necessary for the present nomographic electronic computation system would be printed near the outside edge of the plate.

Each channel should have a capacity of 6000 binary bit positions for 1% accuracy of computation. A density of 350 to 400 bit positions per inch would easily meet this requirement. The bits within each word must be accurately aligned to eliminate the possibility of scanning errors.

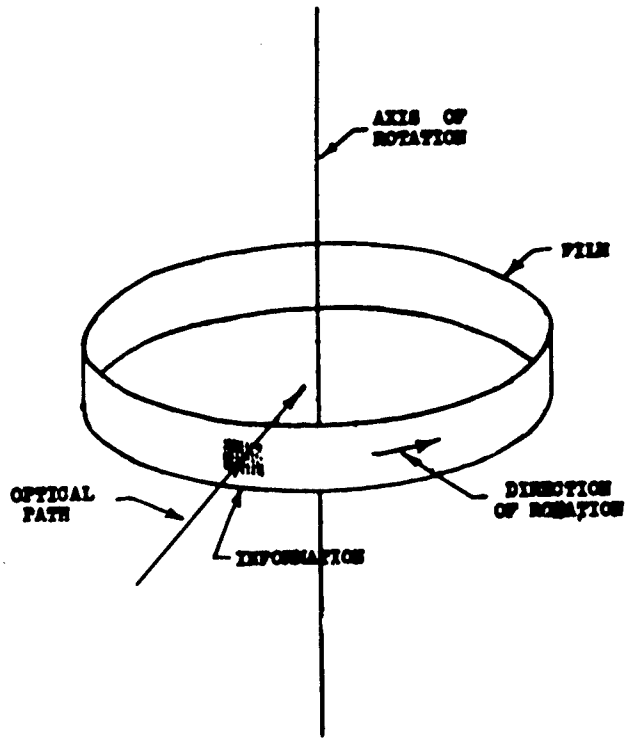

Figure 4-8. Early Scanning System

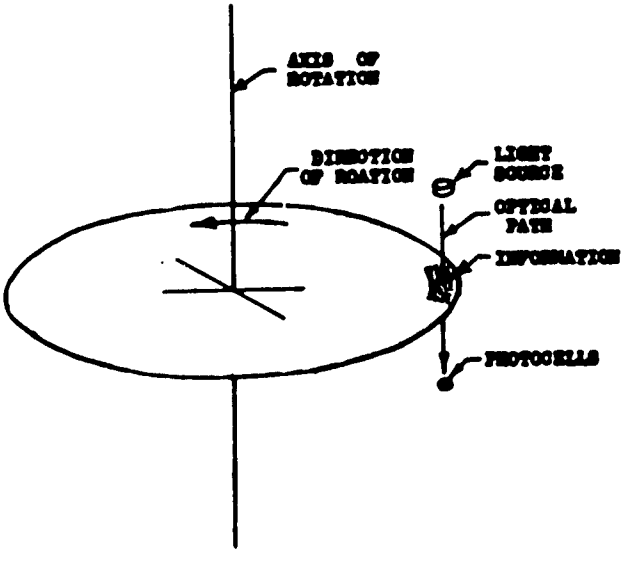

Figure 4-9. New Scanning System

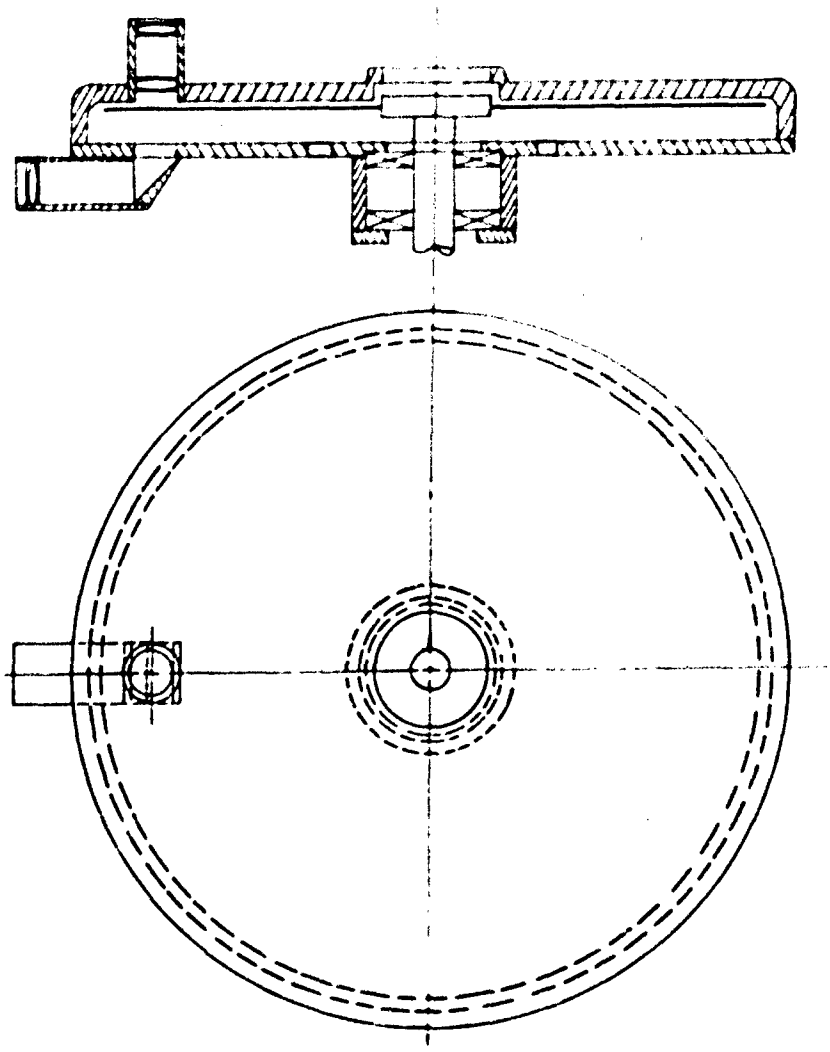

Figure 4-9a. Disc Scanning System

The scanning system counts the bits in each channel. For this reason a space is left between each word in the memory pattern. The memory pattern is shown in Figure 4-10.

3. Past Investigations of Printing Methods. (The contributions of these to the proposed system will be apparent.)

a. Blake's Apparatus

Ernest Blake [8] produced a memory pattern by photographing an array of lights with a press camera. After each exposure the shutter was recocked,

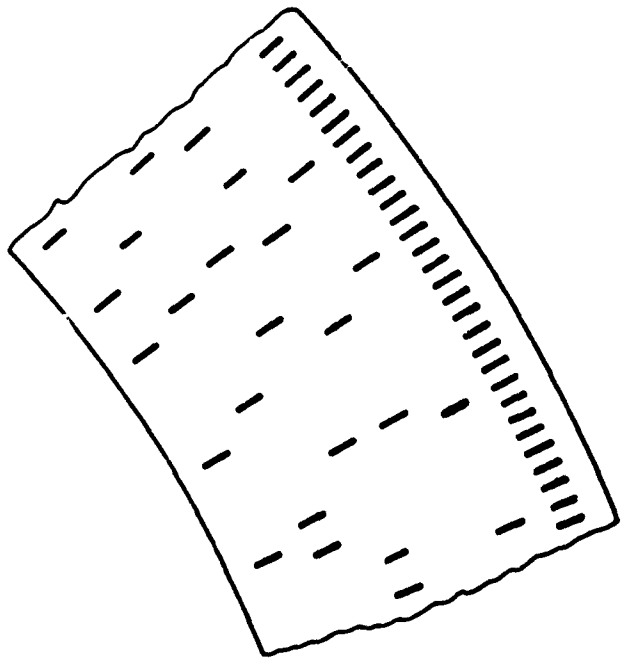

Figure 4-10. The Memory Pattern

the binary information in the array was changed by repositioning the switches for each channel, and the position of the array was changed by moving it a short distance. Each exposure produced one binary word. The light for each channel was produced by a penlight bulb and was transmitted by a lucite light pipe to the surface where the array was being photographed.

Each binary word required 15 seconds to record. Problems were encountered with penlight bulb and shutter life.

b. Cathode-Ray Tube Techniques

This is presently being done rather successfully and was described earlier. A picture produced by this method is shown in Figure 4-7. The method, however, is only usable in memories where the information is in a parallel array. The method is not readily adaptable to a disc pattern memory.

The method also is not accurate enough for some current and numerous future demands of a photographic memory storage.

c. Linear Shift Technique

The linear translation method of pattern printing is merely a refinement of Blake's method as proposed by William G. Dosse [15]. Dossé used a fluorescent tube in a light-tight box. Solenoid-operated shutters were placed on top of the fluorescent tube.

The input to the pattern printer actuated the solenoids to position the shutter to either an open or closed position. The fluorescent light behind these shutters was then flashed to expose the film.

The array was again moved as in Blake's apparatus, and a new word was photographed.

This method is quite slow, requiring two seconds to record one binary word. Even if sufficient illumination were available for rapidly exposing the film, mechanical limitations on shutter actuation would limit speeds to five or ten words per second.

d. Rotating Mirror Preparation

Dossé has printed bits with a Sylvania Glow Modulator tube (R1131C). A pulse of 1/40,000 of a second duration was recorded. The bits are distributed on the photographic emulsion by a rotating mirror. The system employs a timing track and photo-tube to position the bits being printed. Several pictures are available of the patterns produced. [15].

e. Summary

Present methods which have produced an acceptable photographic memory pattern are very slow. The method using Glow Modulator Tubes has an acceptable speed (2.5×10^{-5} sec.). However, the apparatus is very complicated and the results have not been good.

4. Techniques of Printing a Photographic Memory

In the early design stages of the proposed printer, several methods were considered and eventually discarded. A description of several of the more plausible of these ideas follows, including a description of the idea eventually used. Pro and con arguments for each of the ideas are discussed and reasons are given for the final choice of the best apparent method.

a. Punched Mask

This printer would utilize a group of punches that would produce the binary word. A hole would be a "1", and the lack of a hole would be a "0" or vice versa. After each word was punched, the disc would be rotated and then the next word could be punched.

This punched disc would then be used as a mask. If the punched disc were white, it could be placed on a black sheet and photographed The resulting negative could then be photographically reproduced to the desired size.

There are several objections to this system. First, printing speed would be limited to about 50 rasters per second, and then it would still have to be photographed. Secondly, the punching system would be very expensive and difficult to build. The third disadvantage is that the disc would have to be rotated with intermittent motion.

b. Typing

This system would be similar to the punched mask system, except that the bit would be typed instead of punched. The system was discarded for the same reasons that the punched mask system was discarded. It might be better, however, than the punched mask system, because the disc could be rotated at a uniform speed while the printing operation was performed. The finished disc would still have to be photographically reproduced to the appropriate size.

c. Flash Tube Printing

This system utilizes the pulse of light from a flash tube to print directly on a photographic emulsion. Each flash tube illuminates one rectangular opening, in an array of openings which forms a binary word. The light leaving these openings would be focused with a lens on the photographic emulsion which is moved at a rate such that the bits will be properly spaced.

This system was chosen because the pulse of light from the flash tube is only 3×10^{-6} seconds or less (10 times faster than glow modulator tubes) and is of very high intensity.

Other very important advantages will be discussed later.

5. Flash Tube Printing

Flash tube printing of a photographic memory pattern is accomplished by taking a picture of a changing pattern of lights, while the film is being moved (Figure 4-11).

In this chapter the basic components of the printing system are discussed in regard to design, use, results, and possible improvements.

a. Film Rotation Mechanism

The logic inputs available for our experimental work limited the printing rate to 50 cps. At these speeds the primary rotational problem is to maintain a uniform velocity.

A large flywheel was used which was driven by a 1 rpm motor with a 1-inch diameter rubber wheel running on the outside edge of the flywheel (Figures 4-12 and 4-13). This gave a velocity of approximately 3 inches per minute.

The proper rate of rotation was established by the printing frequency and the geometry of the memory pattern. The film velocity where the printing operation is being performed is given by

$$V = (d_G + d_B)\ f = \frac{f}{D}$$

where

d_G = the distance between bits

d_B = the bit width

f = the printing frequency

D = the density of bits.

In the memory patterns exhibited, the velocity, frequency, and density respectively are:

for memory patterns (1000), (1001) and (1011) (Figures 4-19, 4-20, 4-21)
f = 1200 cpm D = 400/in. V = 3 in./min

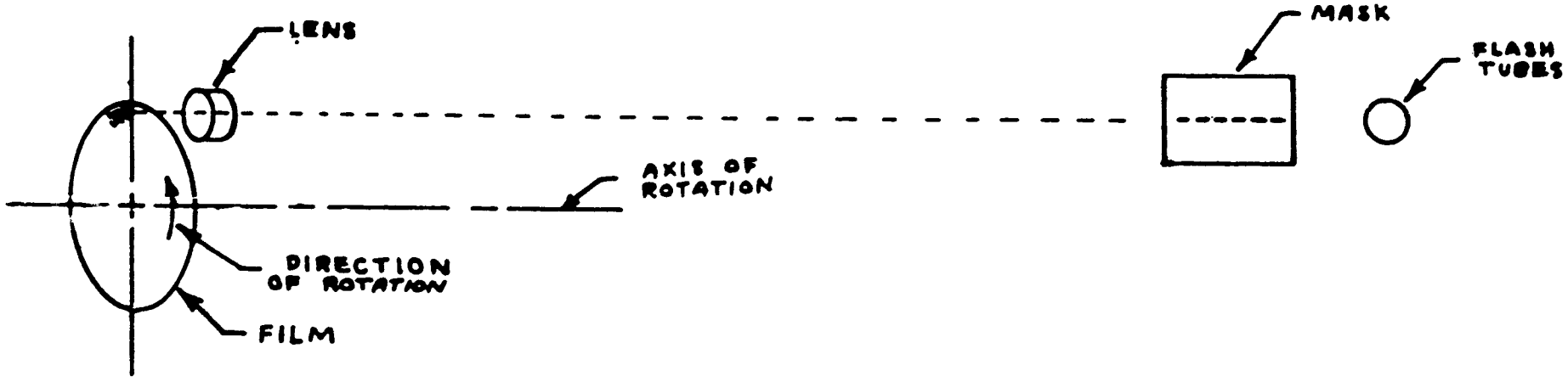

Figure 4-11. Flash Tube System of Printing

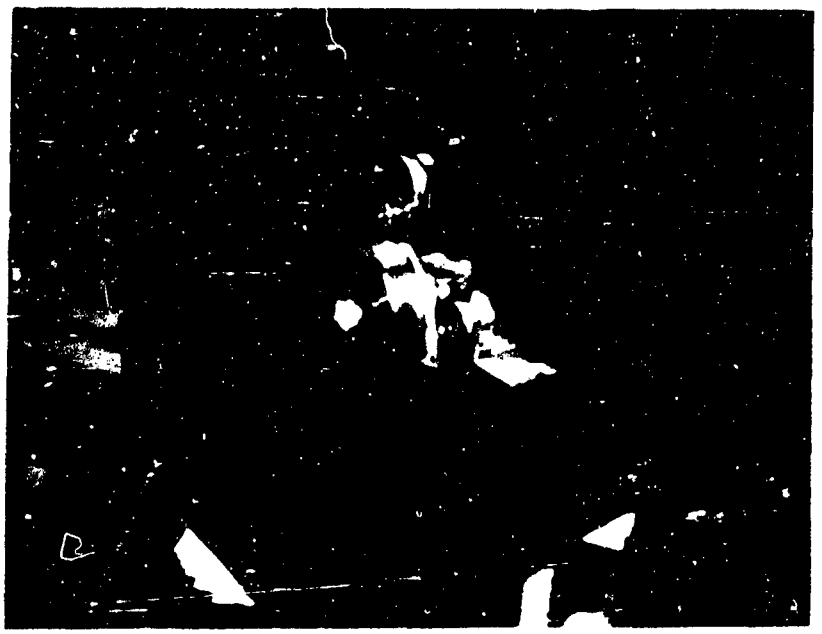

Figure 4-12. Film Rotation Mechanism and Lens Syste n

Figure 4-13. Close-Up Picture of Film Rotation Mechanism and Lens System

for memory patterns (1101) (Figure 4-22)
f = 3000 cpm D = 1000/in. V = 3 in./min

The film rotation mechanism as used in the experimental work was not uniform. A repeating pattern of irregularity appears in all photographs, but it is not clear at this time which, if any, of the irregularities would be damaging.

b. Flashing Light Apparatus

Flash tubes, which provide the light to expose the photographic emulsion, are arranged behind the word pattern mask and are triggered according to the input logic from a paper tape reader.

In the experimental work the "Strobotac" unit manufactured by General Radio Company was used to fire the flash tube. The entire Strobotac was placed within the flash tube chamber (Figure 4-14).

c. Word Pattern Mask

The light from each flash tube is used to illuminate a rectangular hole in the large word-pattern mask. This mask contains six such openings, one for each channel of the memory pattern. The six openings in the mask form a complete word in the memory each time the lights flash.

The masks used in the experimental work were cut from aluminum foil. The cutting operation was performed by hand with a razor blade. Although these masks worked quite well, they would not be accurate enough to be used in producing a memory pattern that would be used in the computation system. The same material could be used if accurately cut to the desired shape.

In some pictures of the memory patterns, a ground glass was placed on the aluminum foil mask with the aluminum foil on the ground side. This had the effect of further diffusing the light to produce more uniform bits. Memory pattern (1011), (Figure 4-12), was produced by this means.

d. Flash Tube Chambers

The flash tube chambers were designed such that the only optical path between the flash tube and the film was one of multiple reflections from diffusing

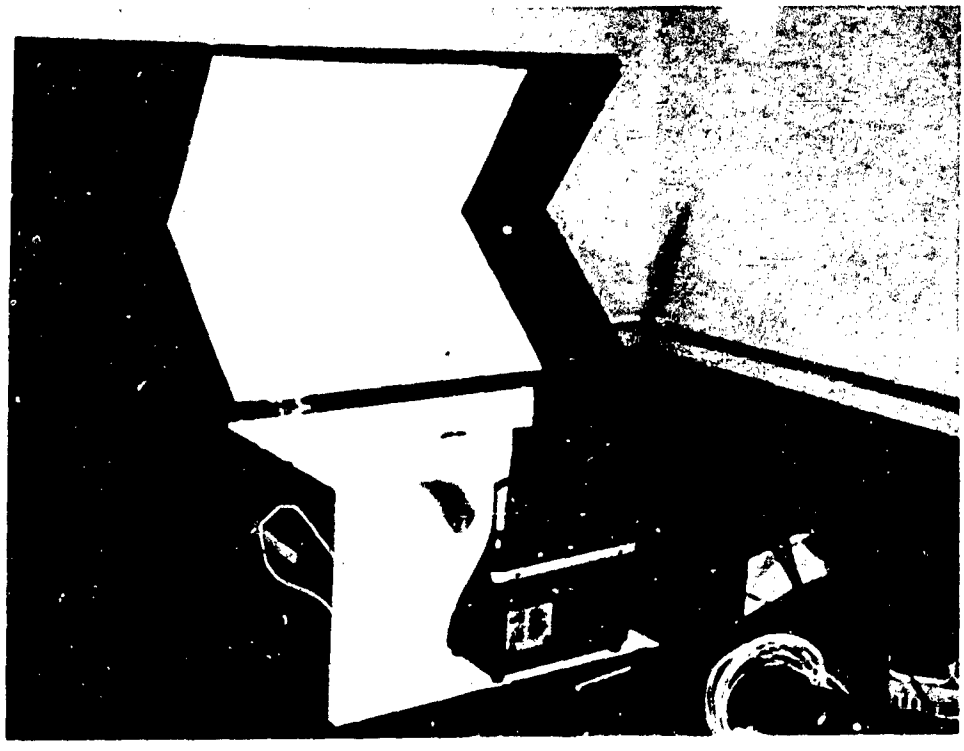

Figure 4-14. Flashing Light Apparatus

surfaces. The goal in the design of the flash tube chamber was to have maximum diffusivity to produce a uniform light intensity over the area of the rectangular opening. This avoids nonuniform bits caused by a small, high intensity, moving light source.

High intensity is also desirable, as it would allow smaller aperture openings which would make focusing less critical. High reflectance of the diffusing surface would be most desirable in producing a high light intensity.

The flash tube chamber is much like a black body, because of the small hole leading into the large cavity. To prove that the light emitted from the flash tube did not chiefly travel directly to the mask, a piece of tin foil was placed between the source and the mask. The foil actually cast a shadow on the mask. Memory pattern (1001), (Figure 4-20), was produced by this means.

e. Flash Tube Characteristics

The flash tubes used for this experimental work are part of the "Strobotac" unit manufactured by General Radio Company. These tubes have a flash

duration of 0.8, 1.2, and 3.0 microseconds, for high-, medium- and low-speed ranges respectively, as measured at 1/3 of peak intensity.

External triggering is usually possible at frequencies as high as 750 cps. The Strobotac can be triggered with a 6-volt peak-to-peak signal.

Peak light intensity is a minimum of 0.21, 1.2, and 4.2 million-beam candlepower on high-, medium-, and low-speed ranges respectively[34].

f. Input Logic

The pictures of the memory patterns in this chapter were produced by using the continual flashing of the Strobotac. These pictures contain no information, but were taken to prove the feasibility of the rest of the printing system.

A Strobotac can be fired as desired from an external signal. A punched tape reader (Figure 4-15) was used for input logic in order to print a binary memory pattern. This unit reads punched tape at the rate of 20 cps.

The paper tape reader was used solely because of availability. Even in the experimental stages a 400 cps reader would have been desirable.

g. Switching Circuit

The purpose of the switching circuit is to insure alignment of the bits within each word of the memory pattern. The signals from each of the channels of the tape reader might not occur at the same time.

To avoid any possibility of misalignment, a circuit (Figure 4-17) was designed such that the binary input "set" an "and" gate for each channel, and then the signal from the timing channel, which is delayed, completes the "and" gate for all binary "1" channels, and they subsequently trigger the proper flash tubes.

The finished switching circuit is shown in Figure 4-16, and will be used when printing the binary memory pattern.

h. Lens Systems and Focusing

Two lens systems were tried in the apparatus; however, all pictures were taken with the first. The lens mounting was designed such that the lenses were interchangeable.

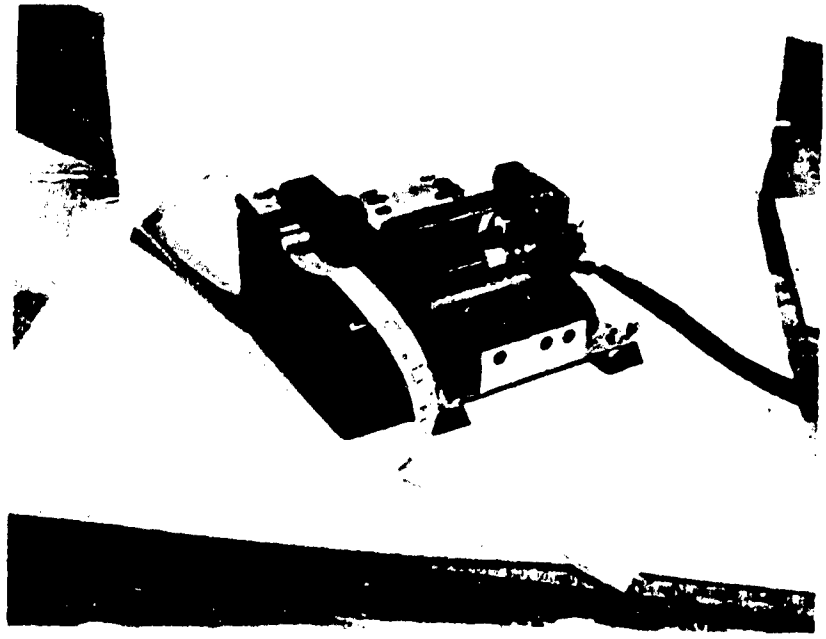

Figure 4-15. Tape Reader Used as Logic Input

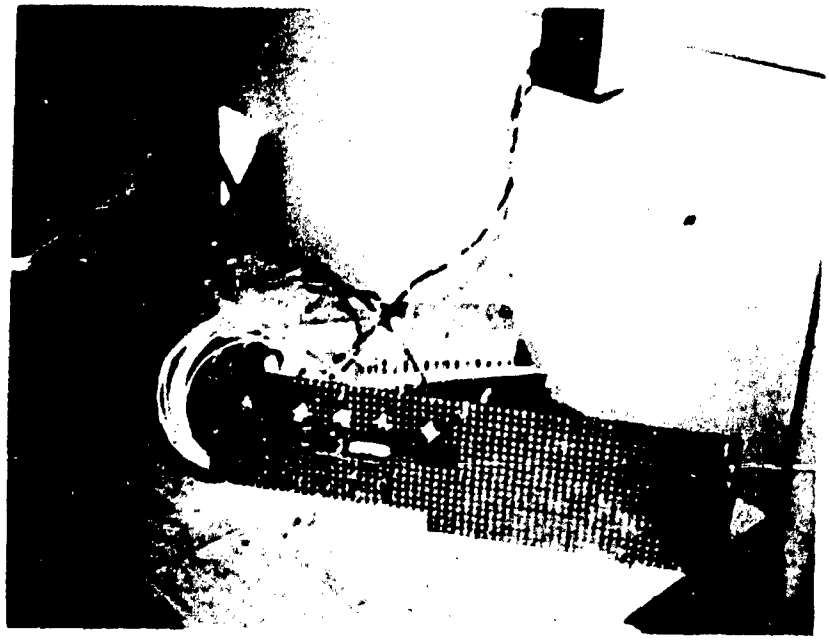

Figure 4-16. Switching Circuit

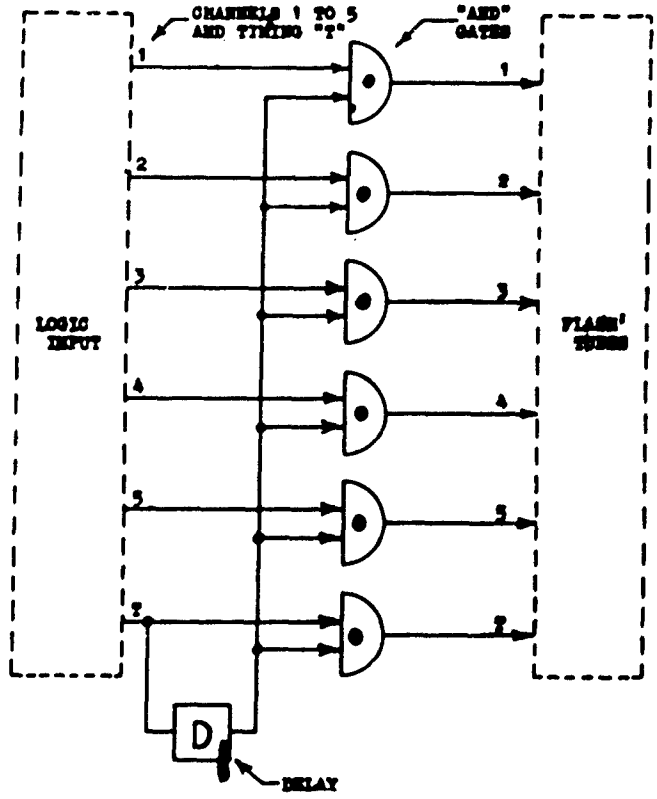

Figure 4-17. Circuit Logic

Lens #1. From a 35mm Nikon S-2 Camera. It is a Carl Zeiss Jena (Germany), Sonnar 1:2, f. 2.0, 50mm lens.

Lens #2. A wide angle lens from a 35mm camera. It is a Som Berthiot (Paris) Angulor 1:3.3, f.2.8, 28mm lens.

Focusing was accomplished by observing the image as it appeared on a ground glass. The surface of this glass was positioned where the film would be in the actual operation and was held by the same mechanism, (Figures 4-12 and 4-13).

Focusing is very difficult because of the extremely small size (.001 by .005 in.) of the bits. To improve the focus, a binocular microscope (40 power) was focused on the surface of the ground glass, (Figure 4-18). This helped considerably; however, it was not used for any of the pictures included in this report.

Further improvement could be realized by using a 300-power microscope with an extremely fine ground glass to focus on.

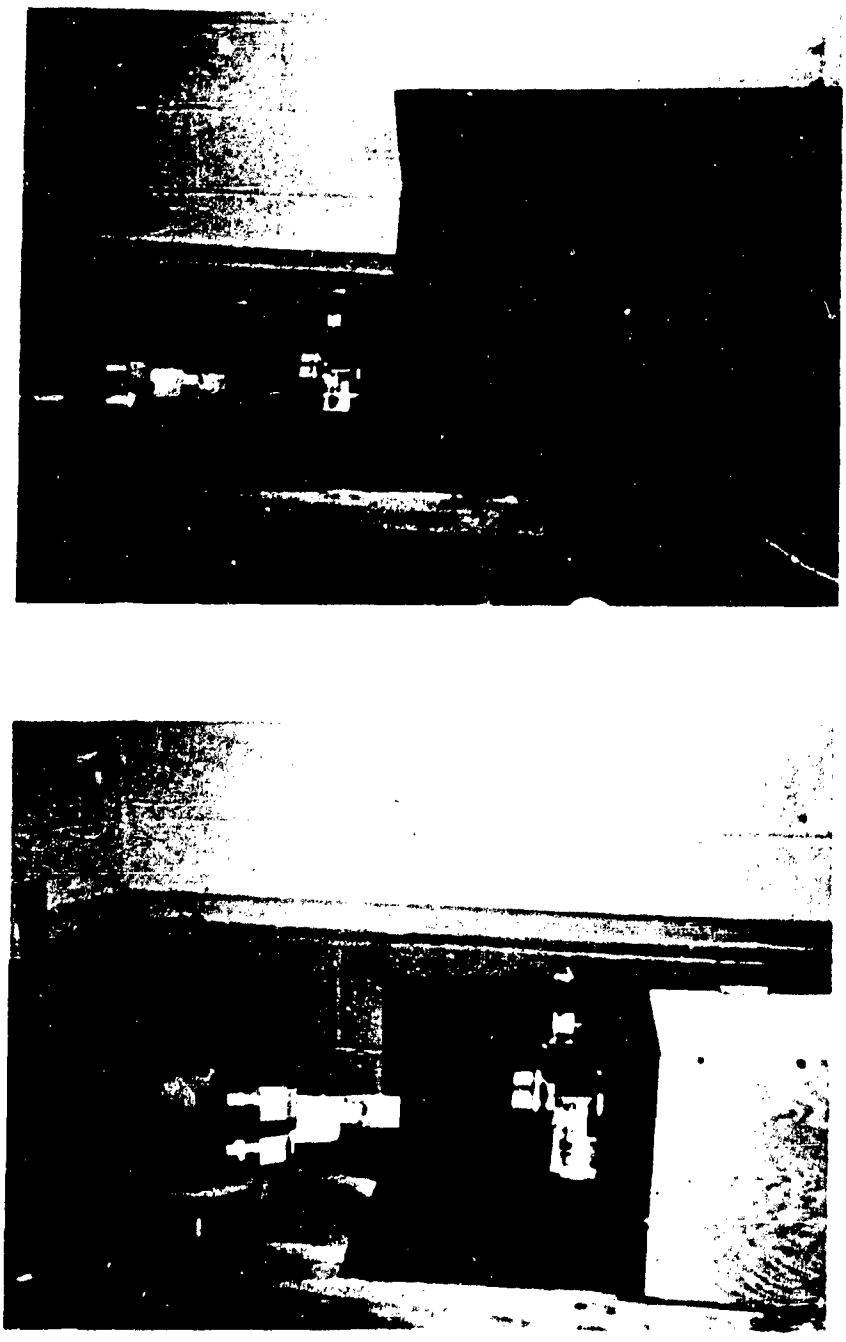

Figure 4-18. Use of a Microscope to Aid in Focusing

i. Film

"Panatomic X", a professional grade cut film was used for all experimental work included in this report. The film was processed in Kodak D-76 Developer.

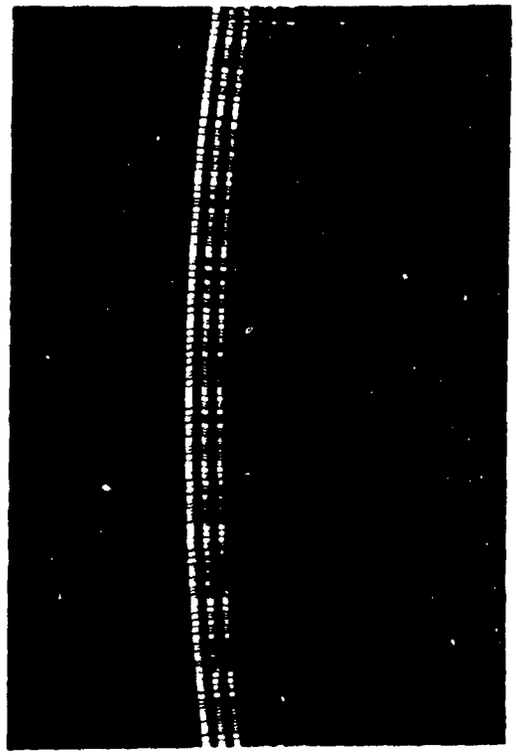

Figure 4-19. Memory Pattern (1000), 16X, Flash Tube Out of Optical Path

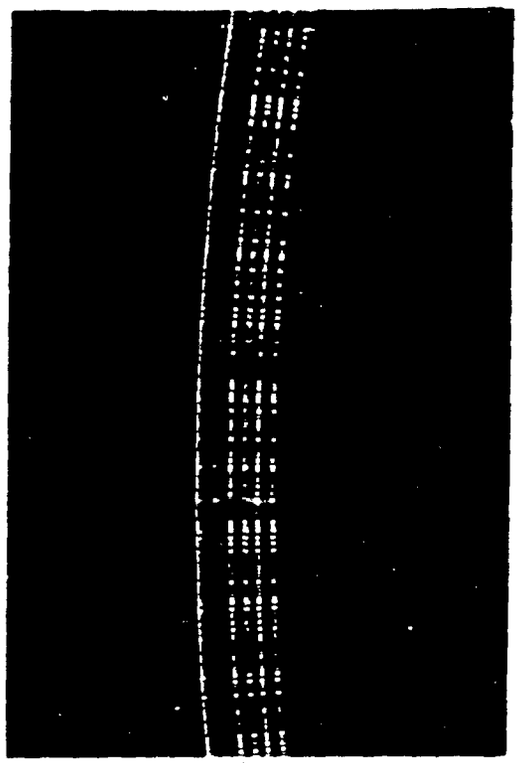

Figure 4-20. Memory Pattern (1001), 16X, Foil Between Flash Tube and Mask

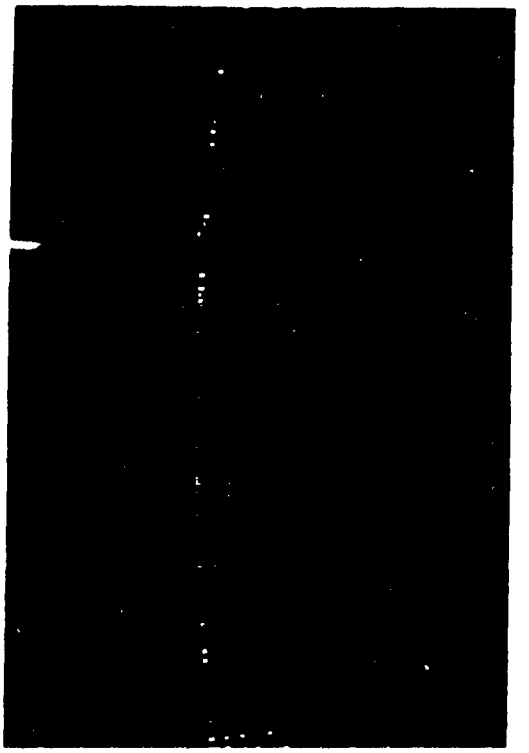

Figure 4-21. Memory Pattern (1011), 16X, Ground Glass On Tin Foil Mask

Figure 4-22. Memory Pattern (1101), 16X, One-Thousand Lines Per Inch

"Panatomic X" is not a good film for work of this type. Film improvement should substantially improve results.

In the flash tube method of printing, light intensity is not a problem; and for this reason a high resolution, high contrast, reasonably slow emulsion on a glass plate would be best. The glass plate would have to be cut into a 6-inch diameter circle and a 1-inch diameter hole would have to be cut into the center of it.

Cut film, 3-1/4" x 4-1/4", was used in the experimental work, because of convenience and cost. The entire disc is not needed unless the memory pattern will actually be used in the computation system.

The use of a good film, properly processed, would yield a significant improvement.

6. Conclusions. (Some are worthy of note)

Good quality memory patterns were printed by light pulses of less than 3×10^{-6} seconds duration. This was accomplished with simple apparatus which contained only one lens system. The same apparatus would be capable of printing 500-700 words per second if a capable input system was available. Construction of the printer is simplified because the flash tube can be placed anywhere within the flash tube chamber.

7. Applications for High-Speed Printing

a. Blur Limitations

The flash tube memory pattern printing system has a fundamental blur limitation for uniform film rotation velocities. The limitation is not applicable when the film is rotated with an intermittent motion at the printing frequency.

This limitation results in an upper velocity limit for a given density because of increased blur at high speeds. To produce sharp uniform bits a maximum of about 2% blur could be tolerated. With a 2% blur the maximum frequency and velocity is given by

$$f_M = \frac{0.02}{(FD)}$$

$$V_M = \frac{0.02}{(FD)\ \ (D)}$$

where (FD) is the light flash duration and D is the printing density.

With a 3-microsecond flash duration the maximum frequency is 6600 words per second. This maximum frequency is a fundamental limitation of the system (with 2% blur and uniform rotation).

This frequency would allow printing of the entire memory in less than one second.

b. Multiple Light Rotation

The flash tubes used in this experimental work cannot be successfully fired at rates much above 700 cps. Because the design of the system does not use the image of the source, it is possible to "rotate" flash tubes.

The flash tube chamber would contain as many as 10 flash tubes. The signal to fire the flash tube would be distributed between the 10 flash tubes within the chamber. Speeds of 7000 cps would then be possible.

c. Adaptability to Different Pattern Forms

The flash tube memory pattern printing system can be used in printing several different geometry patterns. The only modification would have to be in the film moving mechanisms. A film translation mechanism would make the present system capable of printing parallel memory patterns.

d. Increased Density

Increased densities are possible by improving the film, processing, and focusing. Uniformity in the rotational velocity of the film rotating mechanism is essential in making uniform high density memory patterns.

E. 7090 WRITING

This has been discussed to a considerable extent in Section C (this chapter) and needs little elucidation here. No other form of writing a cylindrical memory has been tried. A disadvantage of the system (seldom interfering with the uses to which the 7090 scope is customarily put) is that a turbid form of film and development resulted when optimum use of the phosphors was employed at our particular laboratory. This never interfered with normal use, but when employed for bit writing, as earlier described, yielded nonuniform illumination over the face of the scope. Further processing invariably accentuated this nonuniformity and gave rise to serious trouble with pulse strength uniformity, not only as between different columns of bits, but especially on moving along a given column.

CHAPTER 5

READING BIT MEMORIES. SEVERAL RETRIEVAL DEVICES

A. TYPES OF READING DEVICES

Magnetic drum writing and reading is probably the most practical procedure available for our purposes at this time, but may eventually have to yield for speed and economy to some of the other types described here.

For present purposes, reading devices can utilize a wide variety of retrieval systems such as magnetic drum reading, optical-mechanical reading, a figure spot scanner reading, delay-line pulse reading, optical-magnetic reading, a slot-feeder or punched-tape reading system and others with varying efficiencies depending upon what speed, accuracy, economy, etc. is desired. We consider only optical mechanical reading devices here since this was a natural and average one from several points of view and illustrates a great many useful aspects of the general problem.

Within the optical-mechanical reading group there can be retrieval techniques using fixed or moving memory, fixed or moving optics, or combinations of these and, depending upon purpose and design, having certain advantages and disadvantages.

B. IMAGE METHOD DATA RETRIEVAL SYSTEMS - CYLINDER (DRUM) AND DISC SCANNERS

1. Introduction

Photographic-optical scanning systems can, in general, be classified according to the type of memory; fixed or moving, and optical scanning method; reflection, shadow, or image, etc. The scanning machine of A. D. Thumin [50] is a fixed memory shadow method scanning unit where the shadow of a fixed film is flashed across the phototransducers. The unit mentioned by D. P. Adams, (Machine Design, Sept., 1961)[2], is of the fixed memory reflection category where the light to be read is reflected from silvered bits onto the phototransducer. Both of these methods, however, are definitely limited with regard to bit density and generally make poor use of the storage potential available from photographic media.

To date, the best results have been obtained from the image scanning method whether using fixed or moving memories. Consequently, the scanning machines described herein are based on the image method, one with a moving memory and one with a fixed memory. A third machine, the rotating disc is mentioned since a machine of that type is presently being constructed. It is not, however, a main part of the thesis.

The scanning rate of a photographic-optical scanning machine is determined entirely by the relative speed of the reader to the film memory and the density of the film memory. Therefore, a higher scanning rate can be achieved by increasing the relative speed, storage density, or both. However, it is quite understandable that for all mechanical devices it is very difficult to increase many-fold a rotating speed which is originally at a few thousand rpm without adding sophisticated devices to eliminate the problems as vibration, lubrication, stress concentration, etc. But to reduce photographic data to a smaller size is frequently a simple job today. Then, by using a powerful light source and proper optical unit, this reduced data can be easily magnified and scanned.

The drum or cylinder scanner[30] has been designed to make use of the very high density storage capacity available from modern photographic storage media. For this scanner, it is necessary that the original IBM 7090 film be reduced to a field height of equal to or less than one-half inch, corresponding to film linear bit densities of 120 lines per inch or greater. Storage capacity, because of the construction of the cylinder, is limited to 15 inches of film, corresponding to a minimum capacity of 1800 bits per track. This machine, while used to investigate photo-optical scanning problems in general, also served as a back-up device for the dove scanner, since one of its most prominent assets is extreme reliability.

The dove scanner [30], on the other hand, was designed as a low density high rate device, being capable of scanning field heights from one to one-half inch, although experimental data is given for other films outside this design range. Prior to the inception of the dove project, it was decided, after consideration of NOEL I's capabilities, that the storage capacity should be on the order of 1000 to 2000 bits per track with a scanning rate of up to 10,000 passes per minute. Systems other than the dove method could have been chosen to meet these requirements. The author felt, however, that any system selected should have growth potential sufficient to make it a serious contender for any optical scanning application. The dove system as designed for the NOEL Project, is only the beginning; variations of the system can easily be made to triple the present scanning rate, and with ingenuity to triple that.

2. The Moving Memory Drum or Cylinder Scanner

The basic optical principle of the drum or cylinder scanner is the same as a projection lantern. Refer to Figures 5-1, 5-2, and 5-3 for the discussion of scanner operation. The light source is mounted above and to the left of the drum. The light from the arc lamp, after being collimated by the lens set, is given a parallel displacement by the prism set and passed through the film memory. A projection lens mounted in the photomultiplier box magnifies the film image, and through variable length optical path projects the image of the memory onto a slot of variable width in front of the photomultipliers. Behind the slot are small right angle prisms, called reflectors, used to deflect the image of each track onto the corresponding multiplier; slot width is varied according to the size film used in the scanner in order that only one bit at a time per track be projected onto the transducer.

The entire scanner contains essentially three major units:

- Sending unit,
- Receiving unit and
- Rate control unit.

Details of most of the apparatus will be given in the following sections. The components of the electronic units common to both scanners will be given later.

3. Sending Unit

a. Condensing Lens

The condensing lens set is situated so that the light spot on the memory storage, 10 inches distant, will be large enough to cover the whole field. The lens set contains two lenses which give an equivalent focal length of 1.25 inches and is located 2 inches from the light source, causing the light beam to have a divergent angle of approximately 20°.

b. Cooling Blower

The purpose of the cooling fan is to transfer the heat accumulated by the arc-lamp. Based on the temperature of the arc-lamp, we can calculate the flow rate of the cooling blower by the method of force convection heat transfer

over a cylinder. The surface heat transfer coefficient h is approximately:(43)

$$h = 0.25 \left(\frac{\Delta T}{D}\right)^{1/4} \qquad (5\text{-}1)$$

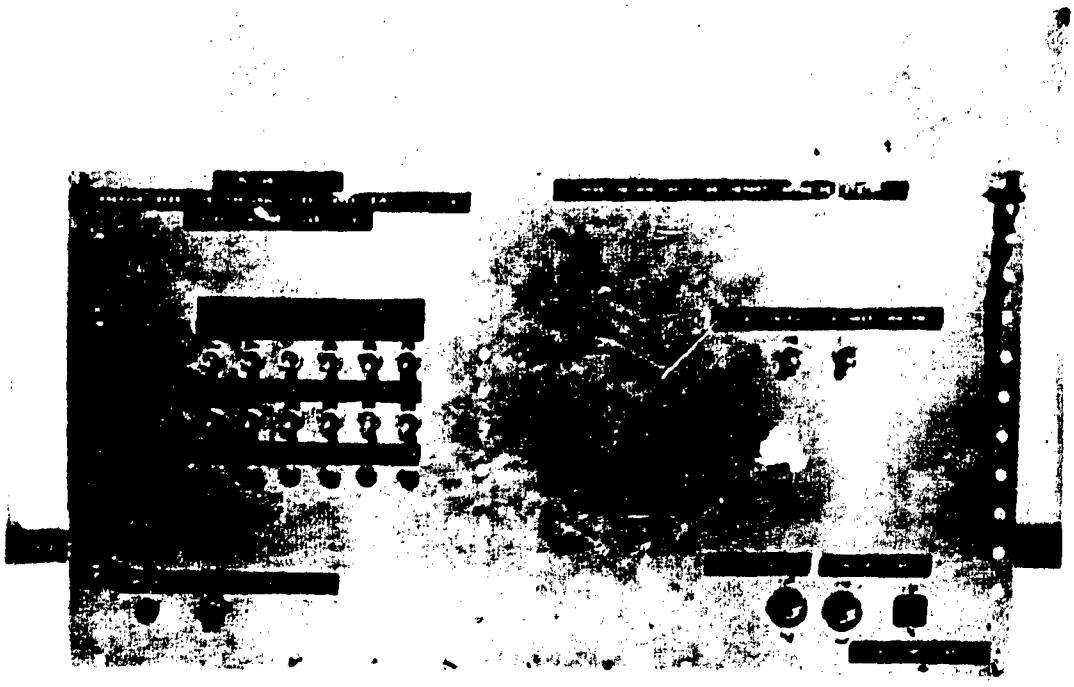

Figure 5-1. Control Panel of Drum Scanner

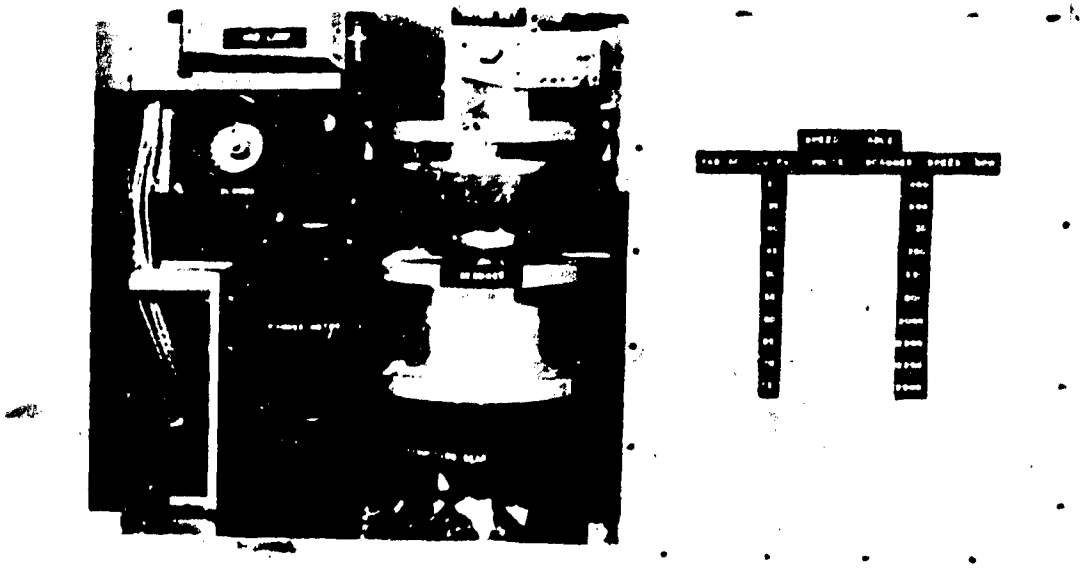

Figure 5-2. Rear View of Drum Scanner: Light Source and Scanning Drum. The Projecting Lens and Photomultiplier Tubes are Contained Inside The Right Black Chamber as Shown in Picture

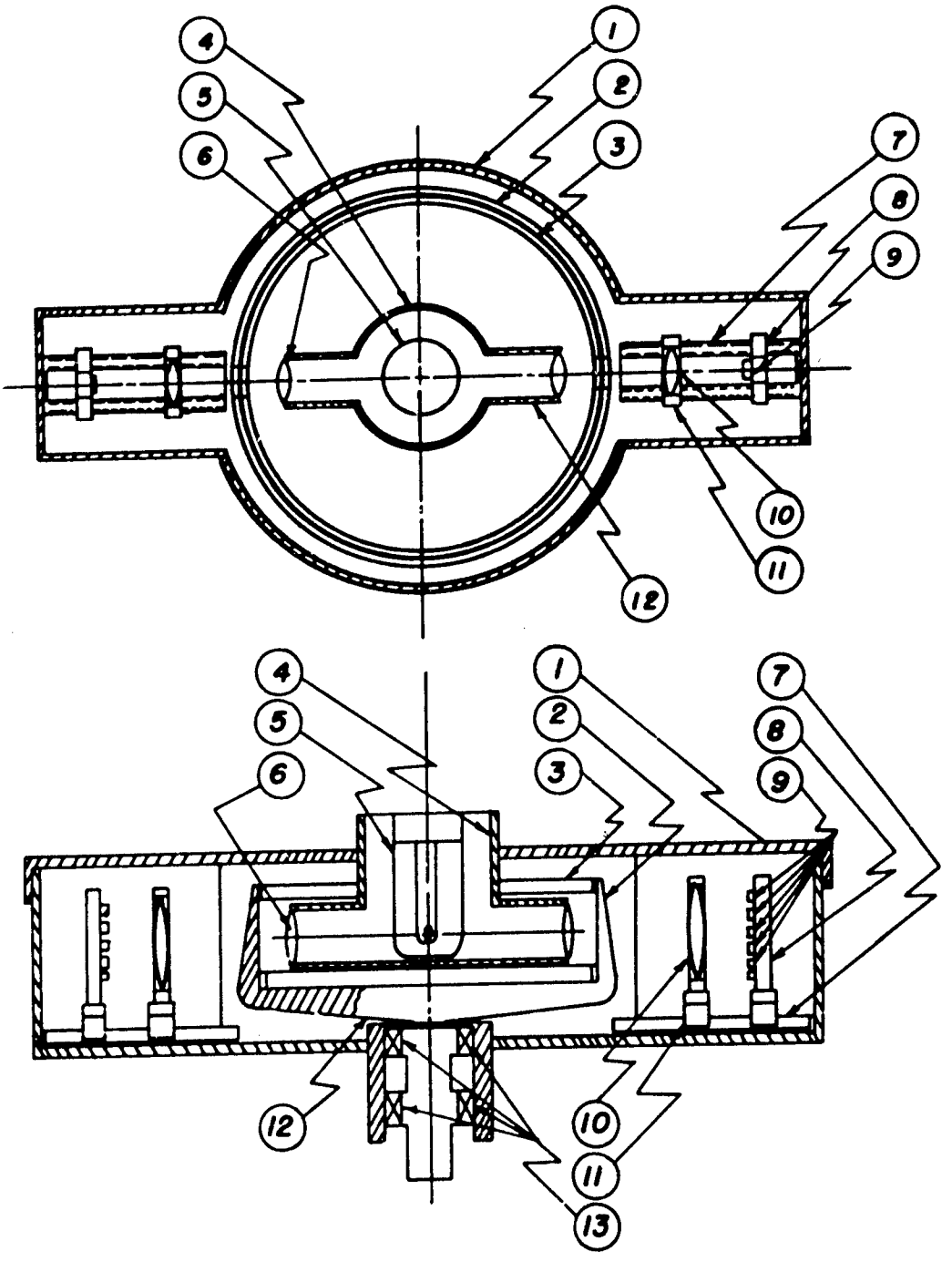

1. CASING
2. ROTATING DISK
3. FILM HOLDER
4. LIGHT SOURCE HOUSING
5. LIGHT SOURCE
6. LENS L_1
7. GUIDE
8. PHOTODIODE HOLDER
9. PHOTODIODE
10. LENS L_2
11. LENS HOLDER
12. ARM
13. BEARINGS

Figure 5-2a.

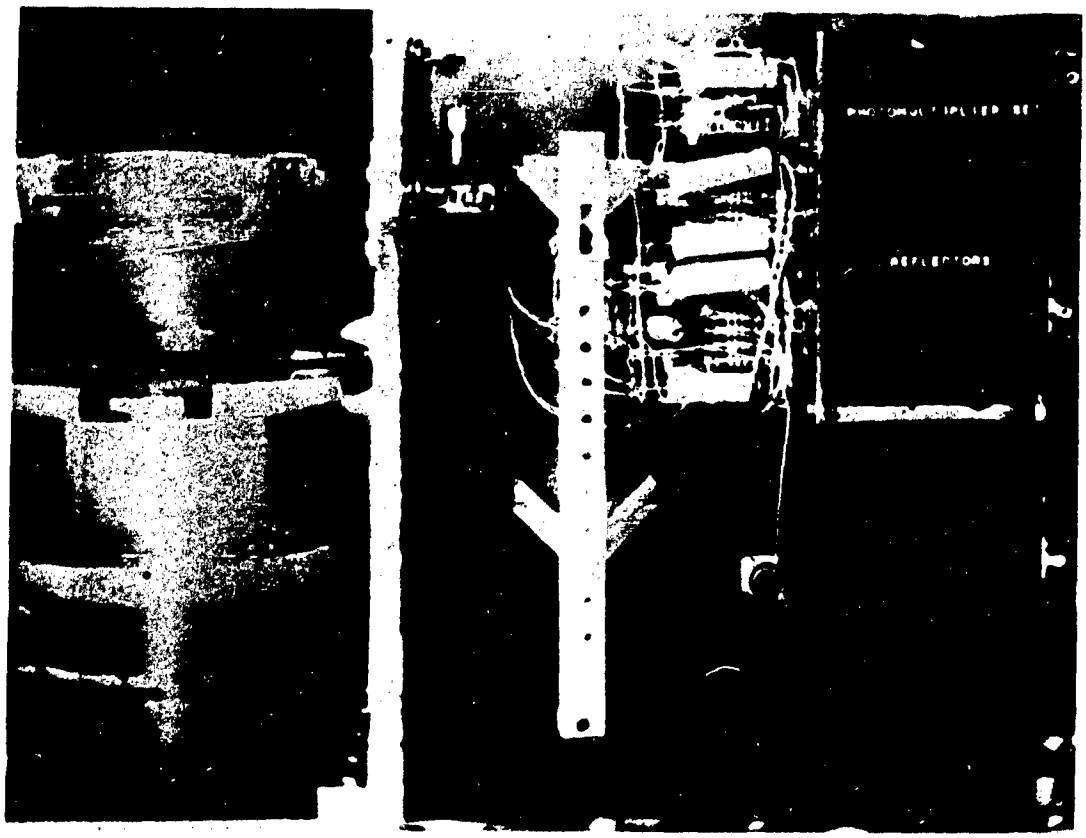

Figure 5-3. Projecting Lens, Light Deflector II, and Photomultiplier Tubes With Their Circuits. The Apparatus Is Contained In The Black Chamber.

where ΔT is the temperature difference between the tube surface and the incoming air, and D is the diameter of the tube. The temperature difference between the tube surface and incoming air $T_s - T_i$ is about 300°F. The diameter of the arc-lamp is 1-1/8 inches. Therefore:

$$h = 0.25 \left[\frac{300}{\frac{9}{8x12}} \right]^{1/4} = 1.9 \text{ BTU/ft}^2 \text{ hr°F} \qquad (5\text{-}2)$$

The flow rate is then determined by

$$V \rho C_p (T_e - T_i) = h \pi DL \left(T_s - \frac{T_e + T_i}{2} \right)$$

where

V = volumetric flow rate

T = temperature

T_e = exit air temperature

ρ = density of air at mean air temperature $T_m = \frac{T_i + T_e}{2}$

C_p = specific heat of air

L = length of lamp

D = diameter of lamp

Solving for V, we get

$$V = \frac{h \pi DL \left[T_s - \frac{1}{2}\left(T_e + T_i\right)\right]}{\rho C_p \left(T_e - T_i\right)} \qquad (5\text{-}3)$$

In the case of air flow temperature difference, $T_e - T_i = 10°F$, the values of ρ and C_p will be 0.0763 lbm/ft^3 and 0.240 BTU/lbm°F respectively corresponding to $T_m = 75°F$. The lamp surface temperature T_s is found to be 355°F from (Figure 5-52). Substituting the values: $T_i = 70°F$, $L = \frac{1}{4}$ ft., $D = \frac{9}{8x12}$ ft., $h = 1.9$ BTU/ft^{2}hr°F, we get:

$$V = 14.5 \text{ cu. ft./min.} \qquad (5\text{-}4)$$

The Model 8433 blower used in the scanner is made by Ripley Company. It has a volumetric flow rate of 17 cu. ft./min; the driving motor has a power output of 17 watts at 115VAC input and 2800 rpm. Continuous operation is allowed. The blower, inside a high impact phenolic housing, has a wheel diameter of 2 inches and an outlet of 1-7/16 x 1-19/32 inches. The blower unit with the light source is shown in Figure 5-4.

c. Prism Set

The prism set is made of two 38 x 38 x 54 mm right angle ditto and silvered prisms. Each prism is mounted on an adjustable shaft as shown in Figure 5-5. The center-to-center distance is 4 inches. The function of this deflector is to give the light rays a parallel displacement.

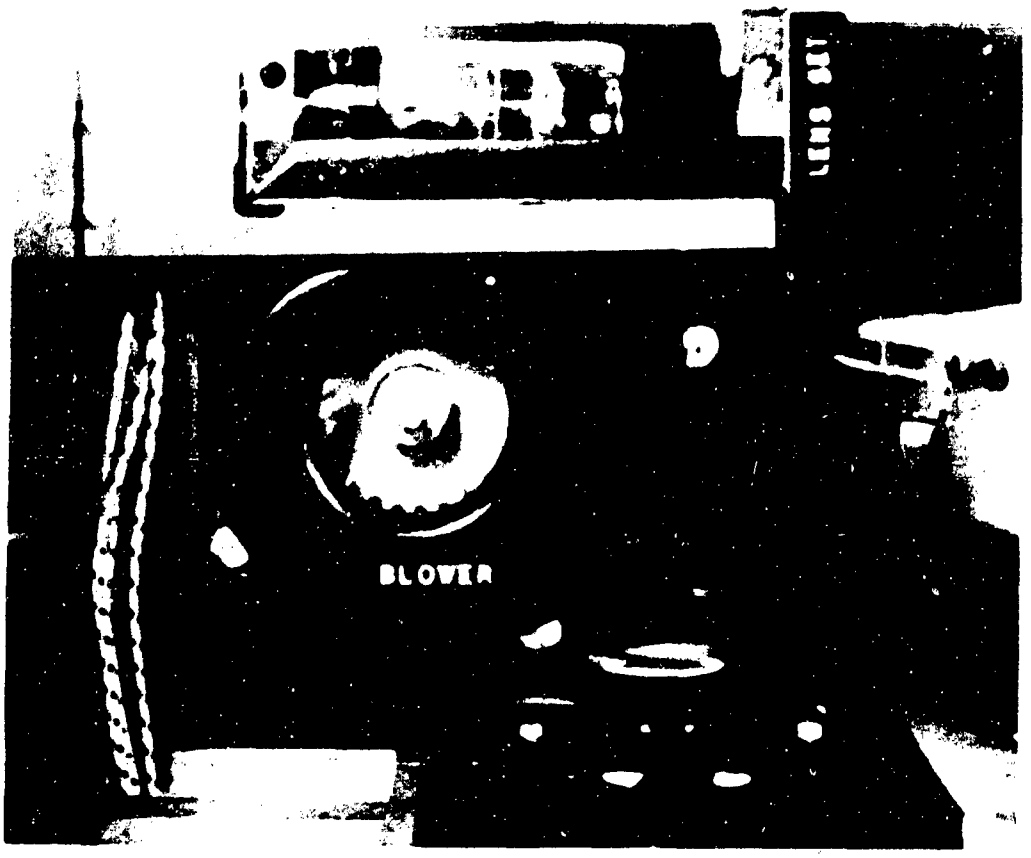

Figure 5-4. Light Source Unit. View Shows the Condensing Lens Set And The Cooling Blower. The Blower Motor Is Located Directly Behind The Blower But Not Shown In Picture.

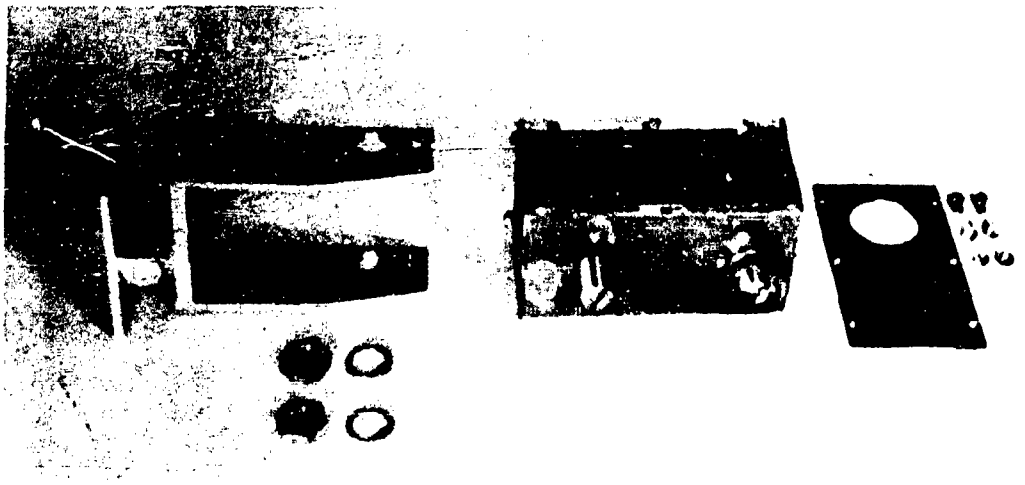

Figure 5-5. Prism Set Unit. Contains Two Right Angle Prisms As Shown In The Rectangular Box. Axes Of Prisms Are Adjustable From Outside.

4. Receiving Unit

a. Projecting Lens

The projecting lens is one important piece of apparatus in all optical scanners. Its magnification power brings the reduced bit image back to a larger size which then can be read by the photomultiplier tubes. The preferred lens magnification power is determined by the physical size of the photomultiplier tube, the size of the small right angle prism used to deflect each track to its respective multiplier and the slot. The size of the slot, however, is limited by the interference effect. Since each reflector has a dimension of 11/32 inches in diameter, the total height of the image should be at least 6 x 11/32 = 2-1/16 inches, plus space for adjustment purposes. Then the minimum magnification power of the lens is the field height of the image divided by the field height of the memory storage.

The coated, double convex projecting lens used in the drum scanner has a diameter and focal length of 17 mm; the lens position is adjustable, being mounted inside a hollow tubing which slides inside a housing as shown in the left-hand part of Figure 5-6.

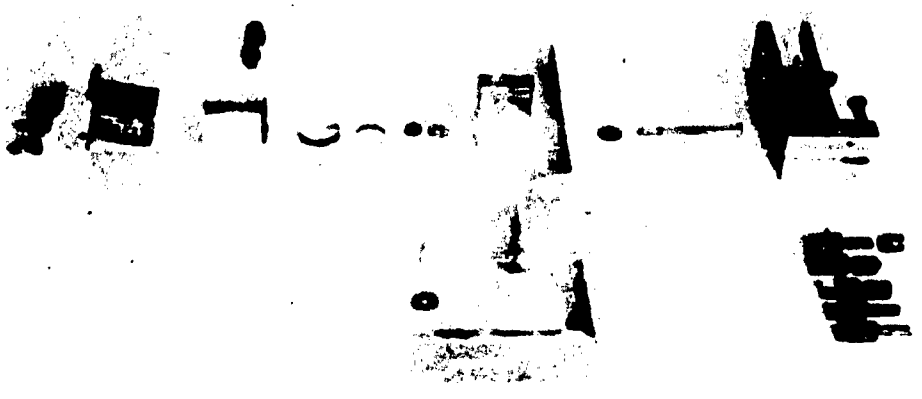

Figure 5-6. Major Optical Components Of Drum Scanner. From Left To Right They Include: Projecting Lens; Light Deflector II; Selecting Slot And Six Reflectors, Each With A Small Right Angle Prism

b. Path Deflector

The installation of this deflector is made in order to facilitate different magnifications without changing the physical distance between the projecting lens and phototubes, thus making it possible to handle memory storages of

different densities. This deflector is made of four 3.5 x 25 x 35 mm front surface reflecting mirrors mounted on the faces of a 90° wedge and a 90° adjustable V groove as shown in Figure 5-6.

c. Reflector

The reflector contains six 6 x 6 x 8 mm right angle prisms, each mounted on a holder which can be moved along a vertical slot of the clamp as shown in Figure 5-6. The reflector gives a 90° angle change in the light path and separates the bits of different tracks to their respective photomultiplier tubes.

d. Photomultiplier Tube Array

Six photomultiplier tubes have been arranged into two rows as illustrated in Figure 5-7. Between the two rows of photomultiplier tubes, the slot and reflectors are situated. The distance between rows is 2.5 inches; the distance between tubes of the same row is 1.5 inches. The photomultiplier tube array is covered by a black plastic cover when it is in operation.

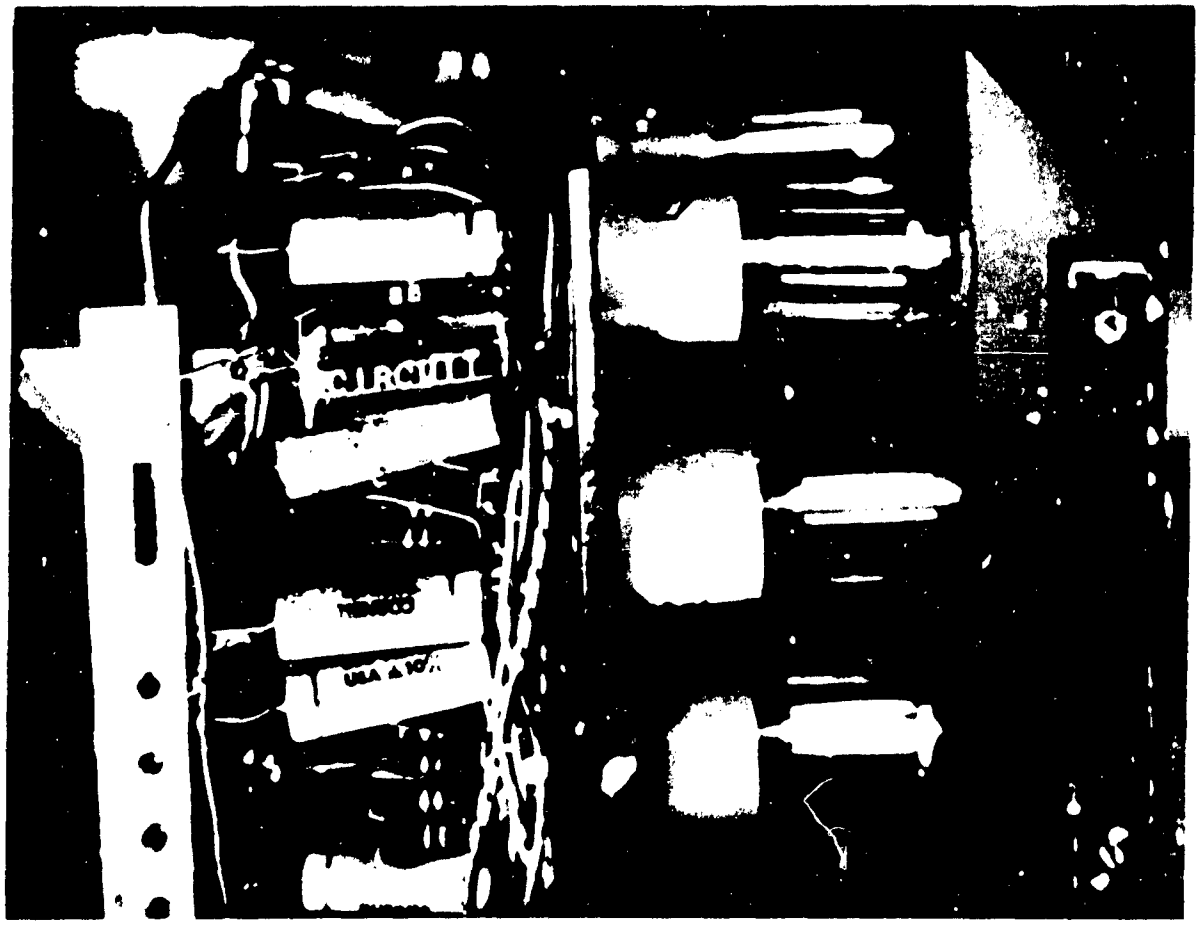

Figure 5-7. Photomultiplier Unit And Its Circuitry. The Reflector And Slot Unit Is Mounted Between The Two Arrays Of The Photomultipliers.

5. Rate Control Unit

a. Rotating Drum

The drum is constructed of steel and designed to rotate at 2500 rpm. The drum contains a disc with four vertically extended legs onto which a cylindrical film holder is attached, the shaft of which is mounted with two wide face bearings inside a housing as shown in Figure 5-8. The stress analysis of such a rotating disc of variable thickness can be carried out in the following manner: the governing differential equation can be obtained by balancing the forces acting on a small element of the disc [14], given as:

$$\frac{d}{dr}(trs_r) - t S_t + t \rho w^2 r^2 = 0 \qquad (5\text{-}5)$$

where

t = thickness of the disc

r = radius of the disc

S_t = tangential stress

S_r = radial stress

ρ = density of the material

w = rotating speed

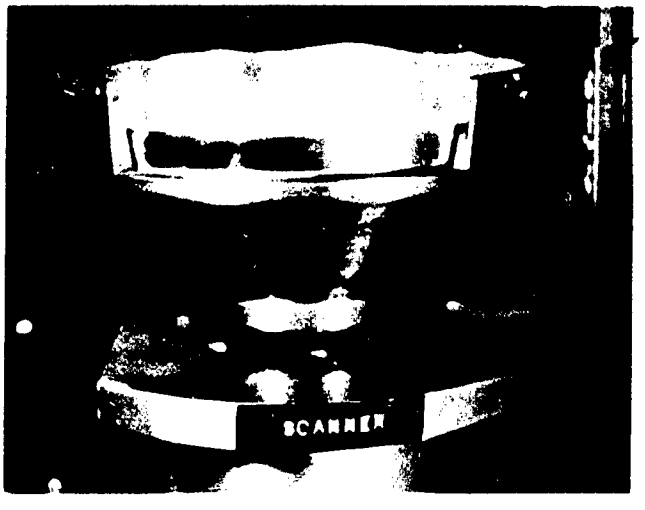

Figure 5-8. Scanning Drum. The Film Holder Is Mounted On Its Four Supporting Legs. Two Wide Face Bearings Are Contained Inside Its Housing.

With the u representing radial deformation, we have

$$\frac{du}{dr} = \frac{1}{E} (S_r - \mu S_t) \tag{5-6}$$

$$\frac{u}{r} = \frac{1}{E} (S_t - \mu S_r) \tag{5-7}$$

where μ is Poisson's ratio and E is the modulus of elasticity.

By differentiating equation (5-7) and eliminating u from equations (5-6) and (5-7), after simplification, we get:

$$\frac{d}{dr} (S_t) - \mu \frac{d}{dr} (S_r) + \frac{1+\mu}{r} (S_t - S_r) = 0 \tag{5-8}$$

From equations (5-5) and (5-8) we can solve for S_r in the final form

$$r^2 \frac{d^2}{dr^2} (trS_r) + r \frac{d}{dr} (trS_r) - (trS_r)$$

$$- \frac{r}{t} \frac{dt}{dr} \left[r \frac{d}{dr} (trS_r) - \mu (trS_r) \right] + (3+\mu) \rho w^2 r^3 t = 0 \tag{5-9}$$

The solution to differential equation (5-9) was found by Stodola that the thickness t can be assumed as the following function of r:

$$t = \frac{ti}{(r/r_i)^q} \tag{5-10}$$

where t_o is the thickness at the root of the disc and q is any positive number. The equation (5-9) can be reduced by substituting (5-10).

$$r^2 \frac{d^2}{dr^2} (trS_r) + r(i + \mu q) \frac{d}{dr} (trS_r) - (1 + \mu q) (trS_r)$$

$$+ (3+\mu) \rho w^2 r^3 t = 0 \tag{5-11}$$

The general solution of equation (5-11) is then

$$trS = C_1 r^{n_1} + C_2 r^{n_2} - \frac{(3+\mu)}{8-(3+\mu)q} \rho w^2 r^3 t \qquad (5\text{-}12)$$

where

$$\begin{matrix} n_1 \\ n_2 \end{matrix} = -\frac{q}{2} \pm \sqrt{\frac{q^2}{4} + \mu q + 1} \qquad (5\text{-}13)$$

The disc of the drum scanner has an outer radius r_o of 3 inches and a root radius r_i of 3/4 inches. The root thickness t_o is 3/4 inches and the rim thickness is 1/4 inches, the variation being linear.

Therefore, q can be calculated as

$$q = \frac{\ln \frac{t_o}{t_i}}{\ln \frac{r_o}{r_i}} = \frac{\ln 3}{\ln 4} = +0.8 \qquad (5\text{-}14)$$

By assuming $\mu = 0.3$, we get

$$n_1 = 0.78 \text{ and } n_2 = -1.58 \qquad (5\text{-}15)$$

Substituting equations (5-10), (5-13) and (5-15) into (5-12), we get

$$S_r = C_1 r^{0.78} + C_2 \frac{1}{r^{1.58}} 0.62 e w^2 r^2 \qquad (5\text{-}16)$$

$$S_t = \frac{r dS_r}{dr} + e w^2 r^2 \qquad (5\text{-}17)$$

The constants C_1 and C_2 may be obtained by applying the proper boundary conditions. For example, the stresses of the disc model for a shrink fit at 2500 rpm will be $S_t = 2600$ psi, $S_r = 1000$ psi when the radius of the disc is 3 inches and the disc is fixed at 3/4 inches from the center.

It is quite obvious that the disc thickness has been overdesigned for the purpose of having an increased disc inertia which would stabilize the rotating speed.

b. Film Holder

The film holder is made up of a metal inner cylinder and a Plexiglas outer cylinder with the film memory situated in between as illustrated in Figure 5-9. The metal cylinder is 3/4 inches in height with four 1/2-inch wide slots along its wall. The Plexiglas outer cylinder is of the same height, and has a 6-inch outside diameter with a thickness of 1/8 inch. The entire assembly is mounted on the rotating disc and held in place with the top ring shown in the right-hand part of the picture, the ring being screwed to the four vertically extended legs on the rotating disc.

c. Reduction Gear Unit

The reduction gear unit offers a four-to-one reduction and contains four spur gears, as shown in Figure 5-10. The two small gears are made of fabric-Nylon material so that the motor vibrations and gear noise are minimized. Two of the gears have a 3-inch pitch diameter, 32 pitch, and 3/16-inch face; the remaining two have a 1.5-inch pitch diameter, 32 pitch, and 3/16-inch face. Since a 2500 rpm motor was not found in the commercial product line, a reduction gear unit was a necessary part of the scanner.

6. Disc Scanner

The concept of using a rotating film disc has long been recognized as desirable but not developed for NOEL I as there was no machine available which could lay the data peripherally along the film disc. However, such a machine is now under construction. The proposed disc scanner has a sending and a receiving unit essentially similar to the drum scanner, the only difference being the form of data storage.

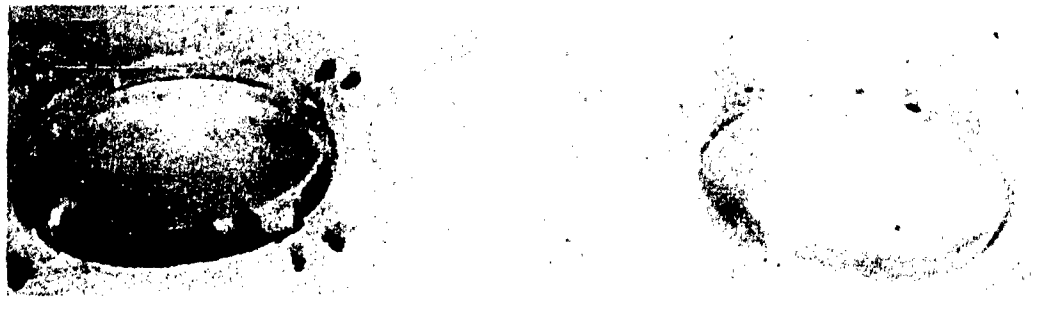

Figure 5-9. Film Holder. View Shows the Inside Metal Ring, The Outside Plexiglas Ring and the Fastening Ring.

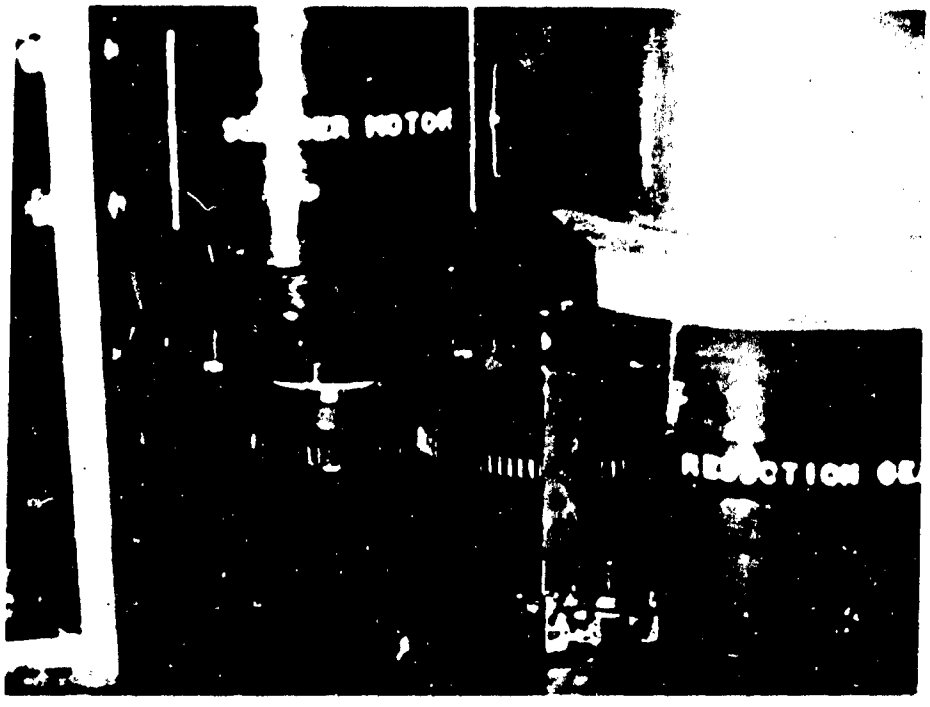

Figure 5-10. Reduction Gear Unit With the Scanning Drum Motor. Smaller Gear at the Left is Made of Fabric-Nylon Material

7. Rotating Disc-Stress Problem

The disc of the scanner is essentially a film disc clamped on a shaft which is driven directly by a motor through a flexible coupling. The stress analysis of such a rotating device is solved by assuming: First, the strain of the shaft is negligible. This is usually true if the material of the shaft is much stronger than that of the disc. This means that at the inside diameter of the film disc clasped by the shaft, the strains are zero. Second, stress and strain along the axis direction of the shaft are negligible.

We first simplify our model in Figure 5-11 by considering only the disc portion and imagining that the center part of it is made of a different material, which will not be deformed during the rotation. Our final model will then become a plain annulus as shown in the bottom diagram of Figure 5-11.

Suppose the radius of the disc is r_o and the radius of the clasping shaft is r_i. The disc rotates at an angular speed w. Then for a small element $rdrd\theta$ with unit thickness as shown in Figure 5-12, the forces acting on it under the second assumption will be simply $S_t\, dr$ in the tangential direction and $S_r\, rd\theta$ and $\left[S_r + \frac{dSr}{dr}\, dr\right] rd\theta$ in the radial direction plus the force due to rotation,

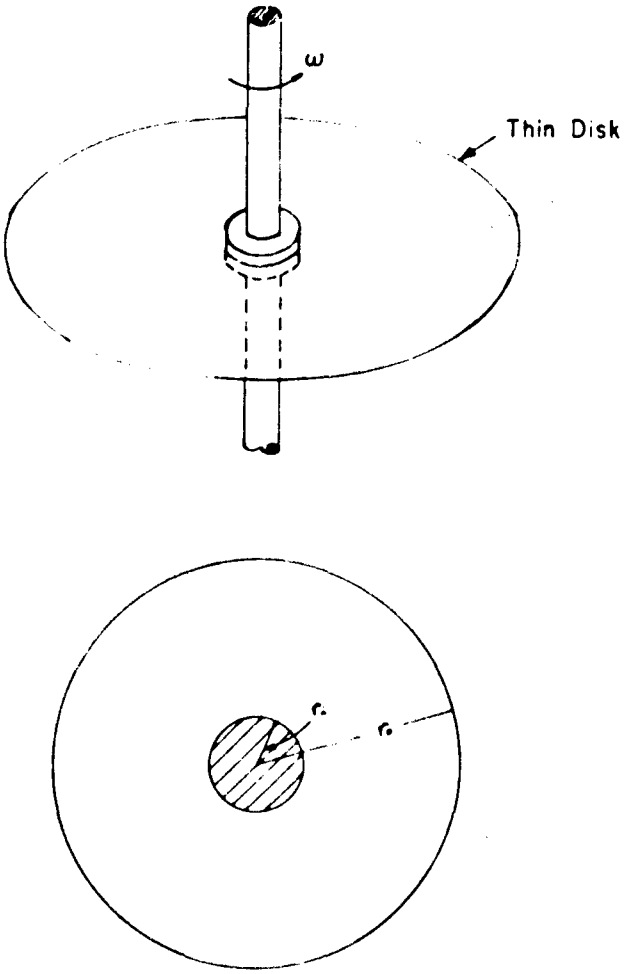

Figure 5-11.

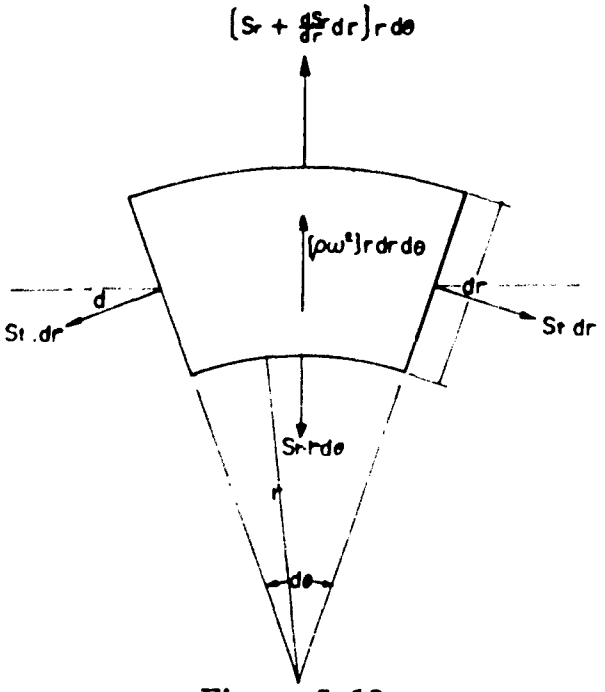

Figure 5-12.

e rdrdθ rw^2. By D'Alambert's principle this dynamic problem can be convected into a static problem by adding the centripetal force in an outward direction.

Then, by equilibrium of forces in radial direction[14], we get

$$\frac{d}{dr}(rS_r) + ew^2r^2 - S_t = 0 \qquad (5\text{-}18)$$

By Hooke's Law we have

$$\epsilon_r = \frac{1}{E}(S_r - \mu S_t) \qquad (5\text{-}19)$$

$$\epsilon_t = \frac{1}{E}(S_t - \mu S_r) \qquad (5\text{-}20)$$

where ϵ = strain; E = modulus of elongation; and μ = Poisson's ratio. By using the relation of displacement u and strains ϵ_r, ϵ_t:

$$\epsilon_r = \frac{du}{dr}, \quad \epsilon_t = \frac{u}{r} \qquad (6)$$

Then equation (5-19) and (5-20) become

$$\frac{du}{dr} = \frac{1}{E}(S_r - \mu S_t) \qquad (5\text{-}21)$$

$$\frac{u}{r} = \frac{1}{E}(S_t - \mu S_r) \qquad (5\text{-}22)$$

differentiate, equation (5-22) with respect to r and solve it with equation (5-21) we get:

$$(rS_r)' - S_r' + \frac{1+\mu}{r}(S_t - S_r) = 0 \qquad (5\text{-}23)$$

where S_t' and S_r' are the first order derivatives of S_t, S_r with respect to r.

From equation (5-18)

$$S_t = (rS_r)' + \rho w^2 r^2 \qquad (5\text{-}24)$$

$$S_t' = (rS_r)'' + 2\rho w^2 r \qquad (5\text{-}25)$$

Substitute equations (5-24) and (5-25) into equation (5-18). After clarification we get

$$(rS_r)'' - \frac{u}{r}\left[(rS_r)' - S_r\right] + \frac{1+\mu}{r}\left[(rS_r)' - S_r + \rho w^2 r^2\right] + 2\rho w^2 r = 0 \qquad (5\text{-}26)$$

Expand terms in parenthesis and multiply each term by r^2, we get after simplification:

$$r^2(rS_r)'' + r(rS_r)' - rS_r + (3+\mu)\rho w^2 r^3 = 0 \qquad (5\text{-}27)$$

Equation (5-27) is a linear differential equation of the second order. It can be solved by superposition method. The general solution of equation (5-27) is of the form

$$(rS_r) = r^n \qquad (5\text{-}28)$$

Put equation (5-28) into equation (5-27) with the last term equal to zero and we get

$$\left[n(n-1) + (n-1)\right] r^n = 0$$

since

$$r^n \neq 0, \quad n = \pm 1$$

the particular solution of equation (5-27) is then

$$rS_r = -\frac{3+\mu}{8}\rho w^2 r^3$$

Final solution of equation (5-27) is then

$$S_r = C_1 + C_2\frac{1}{r} - \frac{3+\mu}{8}\rho w^2 r^2 \qquad (5\text{-}29)$$

From equations (5-24) and (5-29) we get

$$S_t = C_1 - C_2\frac{1}{r} - \frac{1+3\mu}{8}\rho w^2 r^2 \qquad (5\text{-}30)$$

with the boundary conditions as follows

$$r = r_o \quad , \quad S_r = 0$$

$$r = r_i \quad , \quad S_t = \mu S_r$$

we get

$$C_1 = \frac{3+\mu}{8} \rho w^2 r_o^2 - \frac{\rho w^2}{8 r_o^2} \left[\frac{(1-\mu)(3+\mu) r_o^2 - (1-\mu^2) r_i^2}{\frac{1-\mu}{r_o^2} + \frac{1+\mu}{r_i^2}} \right]$$

$$C_2 = \frac{\rho w^2}{8} \left[\frac{(1-\mu)(3+\mu) r_o^2 - (1-\mu^2) r_i^2}{\frac{1-\mu}{r_o^2} + \frac{1+\mu}{r_i^2}} \right]$$

The numerical solution of S_r and S_t has been obtained from equations (5-29) and (5-30) by the use of the IBM 7090 computer. The results are for r_o = 3 inches. Poisson's ratio varies from 0.1 to 0.5, r_i varies from 0.05 r_o to 0.5 r_o. The density of film made of cellulose acetate is 2.44 $\frac{\text{lb. sec}^2 (9)}{\text{ft.}^4}$. The angular velocity w is $\approx$ 1500 rad/sec or 14,300 rpm.

Some of the results have been plotted in Figures 5-13, 5-14, and 5-15 with ordinate expressed in dimensionless R ($= \frac{r}{r_o}$) and abscissa is expressed in S_t or S_r.

A particular point of interest is that within the range of $0.25 \leq \mu \leq 0.35$, RI may be selected arbitrarily within the range of $0.1 \leq RI \leq 0.3$. The maximum error in radial stress S_r resulting from this selection will be less than 3.3%. Even for a wide range of RI, from 0.1 to 0.4, the maximum error is only 5%. This means for industrial materials (most of the materials have a μ value within 0.25 to 0.35), the radial stress of the rotation disc is not very sensitive to the variation of RI ($= \frac{r_i}{r_o}$) for range $0.1 \leq RI \leq 0.3$.

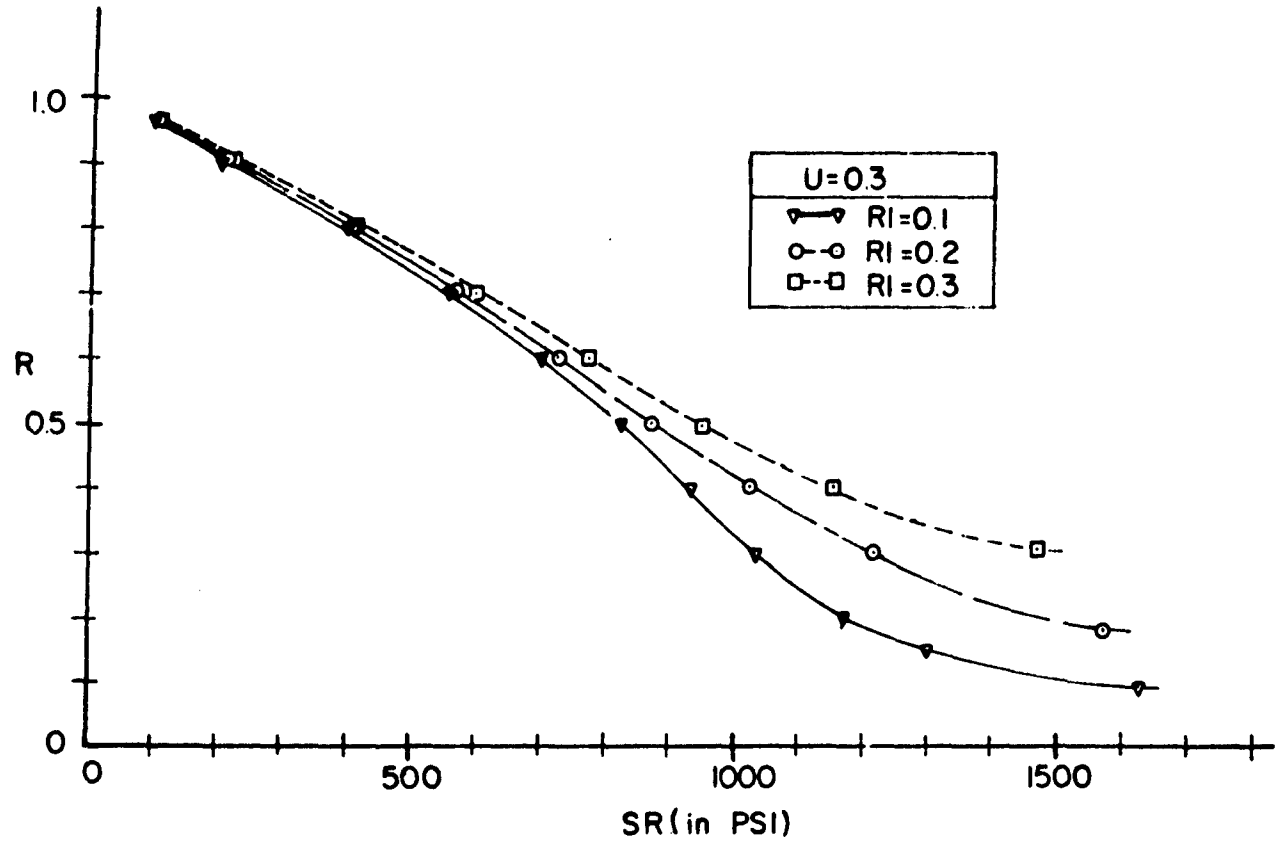

Figure 5-13.

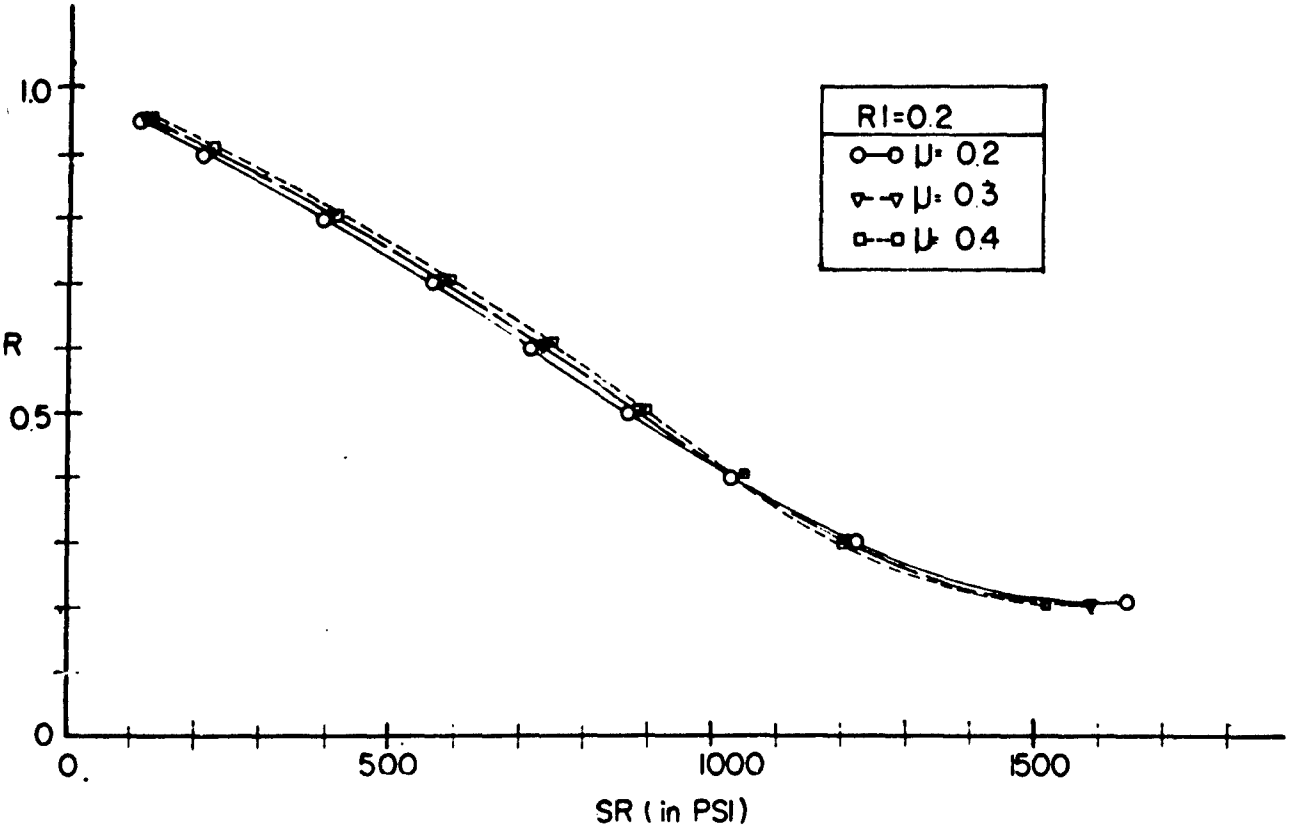

Figure 5-14.

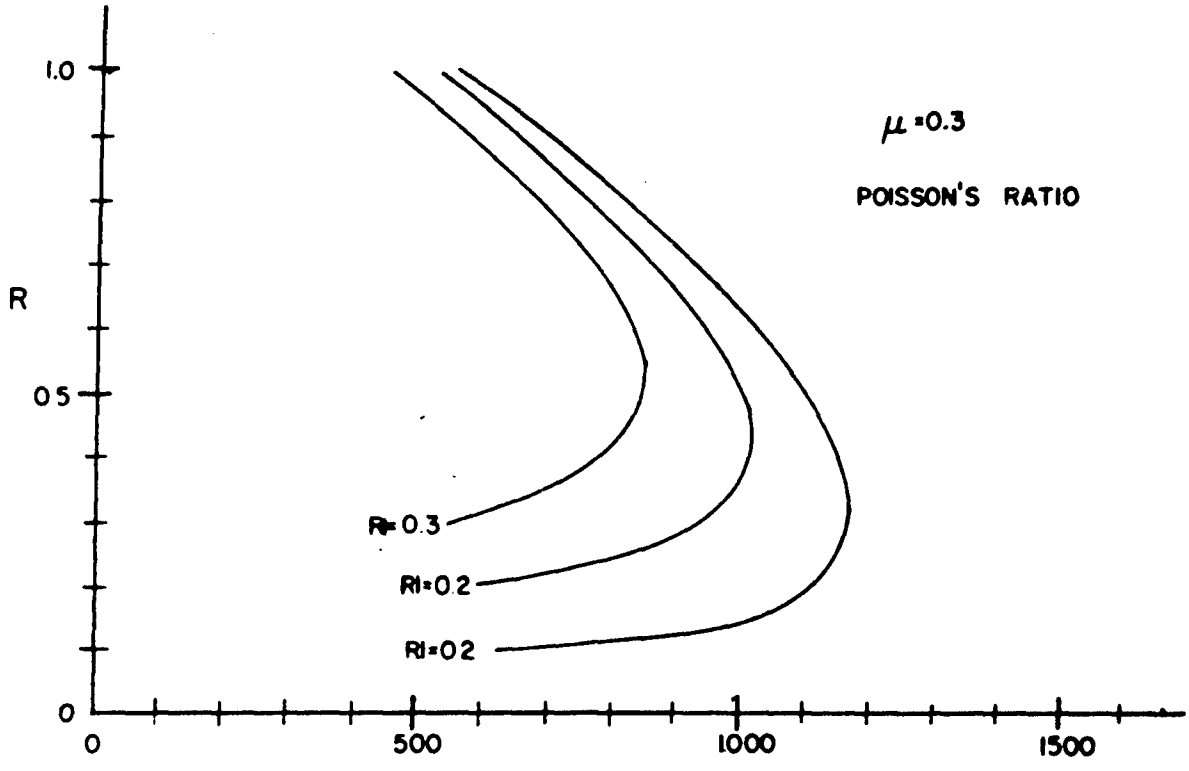

Figure 5-15.

Poisson's ratio for ordinary cellulose acetate or Estar base film, however, are still unknown properties. But a value of 0.48 was obtained for cellulose nitrate film by the Experimental Division of the Eastman Kodak Company many years ago; J. M. Calhoun[11] suggested that a value in this neighborhood should be reasonable. The maximum stresses corresponding to a value of $\mu = 0.48$ and RI = 0.2 would be about 1600 psi for a radial stress S_r and 1000 psi for a tensile stress S_t at a rotating speed of w = 1500 rad/sec. Corresponding to these stresses the elongation is negligible for an Estar base film[11] and is only 1% for an acetate butyrate base film.

8. Stabilization of the Rotating Disc

The vibration phenomena is the most unfavorable characteristic of any photo-optical scanner. In the disc scanner, however, it is an even greater task to eliminate any vibrational disturbances associated with the high-speed rotation of such a thin film disc. In order to do this, air flows should be induced into both sides of the disc chamber near the center position of the shaft. By the centrifugal effect, the air flows will stabilize the pressure distribution on both sides of the disc when the air flows radially outward. Such an arrangement is known as the Bernoulli Disc. In addition, if permanent magnetic material is coated along the outer edge on both sides of the disc with the

magnetic pole of opposite polarity mounted on the upper and lower chamber wall, the repulsive magnetic forces act as positive springs of high stiffness, limiting the amplitude of the disc vibration.

C. DOVE PRISM DATA RETRIEVAL SYSTEM

1. Introduction

The dove system[30] is of the fixed-field, moving-reader type where the moving image of a stationary film is flashed across a bank of photomultiplier tubes. The field is cylindrical, the scanning head rotating about the axis and projecting the image of the field down the axis in a manner to be explained shortly.

The concept of center line scanning as illustrated in Figure 5-16 has one advantage which makes it worth considering and one disadvantage which is usually sufficient to designate the system as unfeasible for more than one track of information. To its credit is the fact that the rotating mirror can be made quite small, resulting in very high rotational speeds or fast data retrieval. As noted by the figure, the rotation of the scanning head causes the projected field not only to translate with a speed $\vec{V} = \vec{w} \times \vec{r}$ but also to rotate at an angular speed $\vec{w}$, since image and object lines are always co-planer. If just the center track is to be read, a circular aperture could be placed before the image on the center line just before a transducer. The images of the bits in other tracks would sweep out a locus of points such that their loci are concentric annuli, a display pattern which is difficult to decipher.

One possible system would be to project the image onto a rotating slotted plate such that only the part of the image being read could pass through, the light passing through being gathered by annuli of bonded optical fibers leading to phototransducers. The system is feasible but expensive; therefore it was dropped. An obvious answer would be to remove the rotational component from the motion of the field, leaving only the translational aspect. This may be done with a dove prism.

The basic property of the dove prism which makes it applicable to reversing rotation is illustrated in Figure 5-17. Light rays A and B entering the prism in the plane x' - z' are refracted downward to the lower surface S where they make a total internal reflection. Since the rays are parallel, all incidence, refraction, and reflection angles are congruent for both rays. Therefore, ray B entering the prism below A emerges above it and vice versa; this does not happen in the y' - x' plane. Hence, the net effect for an image projected, through a dove prism is an inversion in one plane about the axis C-D which is parallel to the y' direction, as illustrated in Figure 5-18.

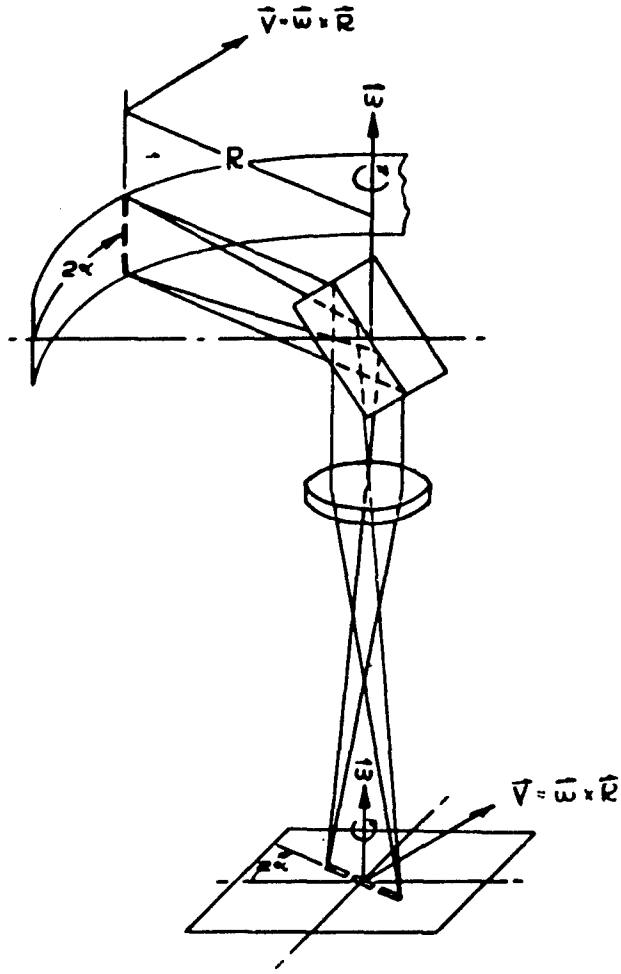

Figure 5-16. Center Line Scanning

Figure 5-19 illustrates how this prism can rotate an image to any desired orientation. Solid lines represent the actual object as seen without the prism, while dotted lines are the object as seen through the prism. Letting the z' axis make an arbitrary angle α with the z axis, while x' and x remain parallel, causes the image to rotate through an angle 2 α as shown. If the object has one axis of symmetry, as do the bits on the film memory, the image appears identical to the object, with the exception of having been rotated by angle 2 α, a point illustrated by Figure 5-20.

Assume that the rotating translating image in the lower part of Figure 5-16 and reproduced in Figure 5-21 is the image to be read. For $\vec{w} = 0$, it becomes evident, referring to Figure 5-20, that a dove prism oriented at angle α as shown, will bring the image back to a desired orientation, and will do so continuously for $\vec{w}$ non-zero if α dove $\vec{w}/2$. The rotational component can thus be removed from the image if a dove prism is placed along the axis and rotated at half the speed and in the same direction as the scanning mirror. This, basically, is the principle of the dove scanning machine.

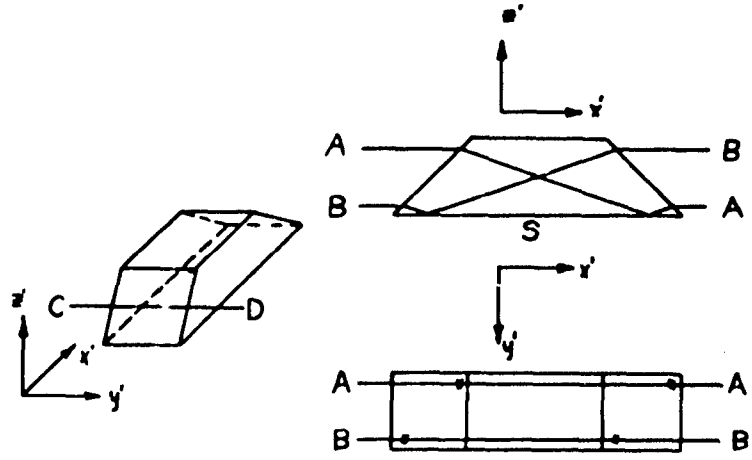

Figure 5-17. Dove Prism

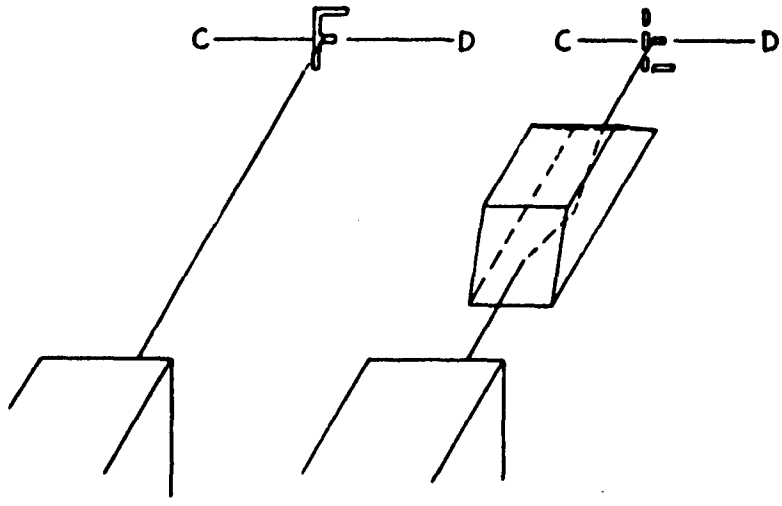

Figure 5-18. Projected Image With and Without Dove Prism

2. Optics

a. Optical Components

Since the dove prism is to be the basis of the proposed apparatus, it shall be investigated first. Figure 5-22 shows a 45° face dove prism, i.e., a prism with the ends at an angle of 45° with respect to the reflecting surface S. Since this is one of the most common angles used, it shall be considered as given.

The prime restriction involved in using a dove prism is that it must operate on parallel or nearly parallel light. To illustrate, one needs only to show that light rays entering at different angles travel different distances through the prism.

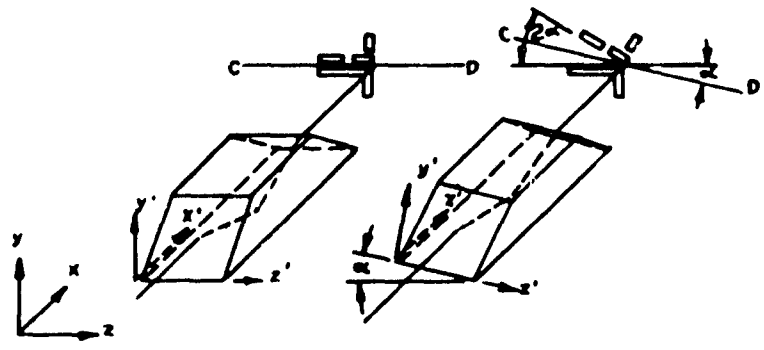

Figure 5-19. Angular Positioning With Dove Prism

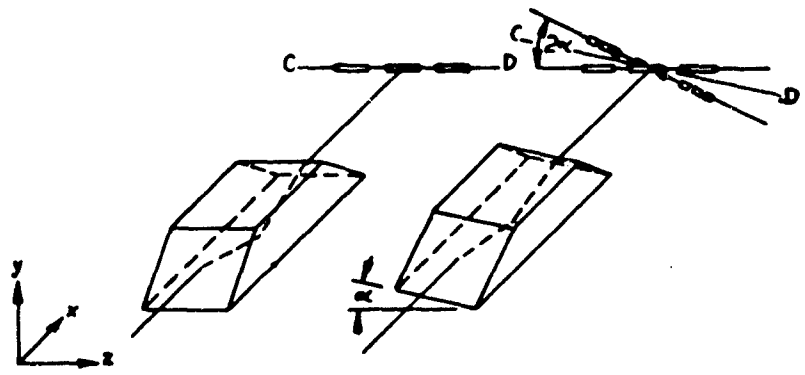

Figure 5-20. Angular Positioning of Symmetric Image With Dove Prism

The following symbols are used for deriving the optical properties of the dove prism:

R = incident light ray

h_1 = height at which the light ray R enters the prism

h_2 = height at which the light ray R leaves the prism

i = incidence angle R made with normal to prism face

r = refraction angle R made with normal to prism face

N = normal to the surface

L = total length of the base of the prism

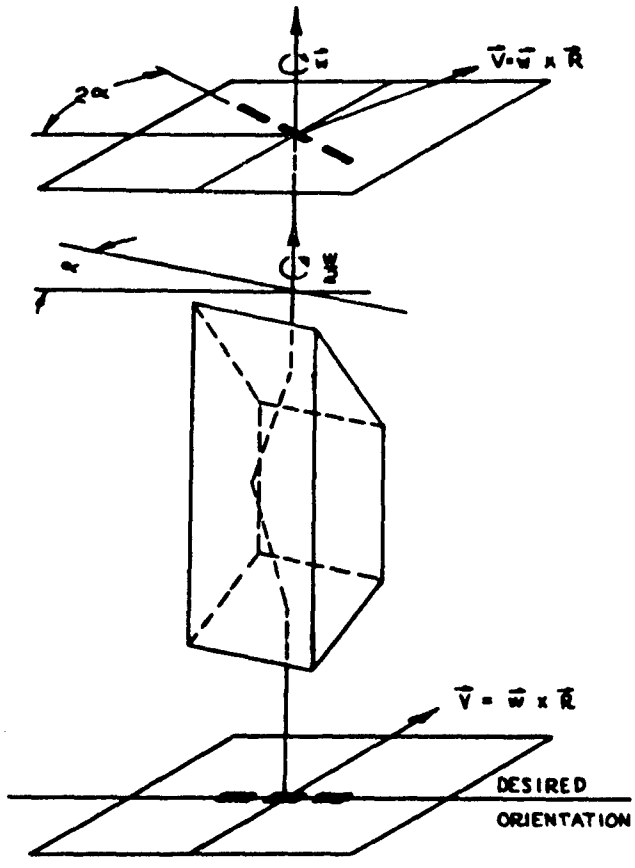

Figure 5-21. Angular Orientation of Image with Dove Prism

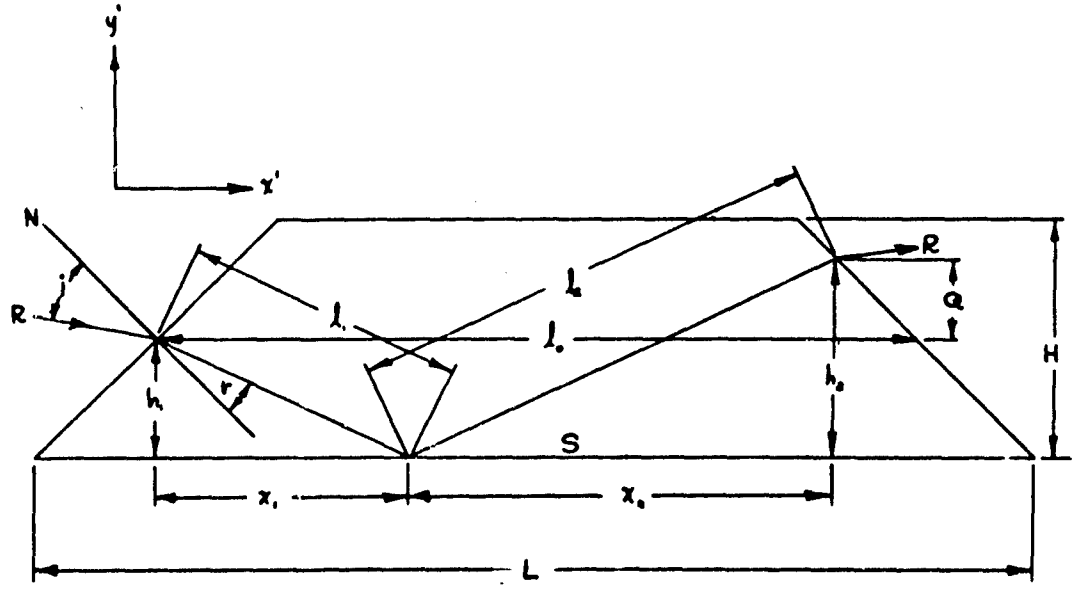

Figure 5-22. Dove Prism

H = total height of the prism

l_o = distance through the prism from where h_1 intersects the prism face to a similar point on the other end and parallel to S

l_1 = distance the refracted light ray travels before it is reflected

l_2 = distance the reflected light travels before it is refracted

X_1 = x direction component of l_1

X_2 = x direction component of l_2

$Q = h_2 - h_1$

$\overline{L} = l_1 + l_2$

An expression relating the total distance travelled by R, $\overline{L}$, to the other parameters will now be derived. Referring to Figure 5-22:

$$l_1 = \frac{h_1}{\sin\left(\frac{\pi}{4} - r\right)} \tag{5-31}$$

$$l_2 = \frac{h_2}{\sin\left(\frac{\pi}{4} - r\right)} \tag{5-32}$$

Combining equations (5-31) and (5-32) gives:

$$l_1 + l_2 = \overline{L} = \frac{1}{\sin\left(\frac{\pi}{4} - r\right)}(h_1 + h_2) \tag{5-33}$$

or, since

$$h_2 = h_1 + Q \tag{5-34}$$

$$\overline{L} = \frac{1}{\sin\left(\frac{\pi}{4} - r\right)}(2h_1 + Q) \tag{5-35}$$

Q is unknown but may be determined in the following manner. Again referring to Figure 5-22:

$$Q = l_o - x_1 - x_2 \tag{5-36}$$

and

$$x_1 = \frac{h_1}{\tan\left(\frac{\pi}{4} - r\right)} \tag{5-37}$$

$$x_2 = \frac{h_2}{\tan\left(\frac{\pi}{4} - r\right)} = \frac{h_1 + Q}{\tan\left(\frac{\pi}{4} - r\right)} \tag{5-38}$$

or

$$x_2 = l_o - x_1 - Q = l_o - \frac{h_1}{\tan\left(\frac{\pi}{4} - r\right)} - Q$$

$$\frac{h_1 + Q}{\tan\left(\frac{\pi}{4} - r\right)} = l_o - \frac{h_1}{\tan\left(\frac{\pi}{4} - r\right)} - Q \tag{5-39}$$

Solving for Q

$$Q = \frac{l_o \tan\left(\frac{\pi}{4} - r - 2h_1\right)}{1 + \tan\left(\frac{\pi}{4} - r\right)} \tag{5-40}$$

Substituting back into equation (5-35) and non-dimensionalizing

$$\frac{\bar{L}}{l_o} = \frac{1}{\sin\left(\frac{\pi}{4} - r\right)} \left[2\frac{h_1}{\ell_o} + \frac{\tan\left(\frac{\pi}{4} - r\right) - 2\frac{h_1}{l_o}}{1 + \tan\left(\frac{\pi}{4} - r\right)} \right] \tag{5-41}$$

Snell's law gives the following relation between incidence angle i and refraction angle r.

$$n_i \sin i = n_r \sin r$$

where n is the index of refraction of the mediae. Hence

$$r = \sin^{-1}\left(\frac{n_i \sin i}{n_r}\right) \tag{5-42}$$

and (5-41) becomes

$$\frac{\bar{L}}{l_o} = \frac{1}{\sin\left[\frac{\pi}{4} - \sin^{-1}\left(\frac{n_i}{n_r}\sin i\right)\right]}\left[2\frac{h_i}{\ell_o} + \frac{\tan\left[\frac{\pi}{4} - \sin^{-1}\left(\frac{n_i}{r_r}\sin i\right)\right] - 2\frac{h_i}{l_o}}{1 + \tan\left[\frac{\pi}{4} - \sin^{-1}\left(\frac{n_i}{r_r}\sin i\right)\right]}\right] \tag{5-43}$$

which is the desired expression.

Once the parameters l_o, n_i, n_r, and h_1 are known, this expression gives the total distance travelled within the prism by a light ray entering at height h_1 and at angle i. One characteristic of a dove prism is that $h_1 = h_2$ for a light ray entering parallel $\left(i = \frac{\pi}{4}\right)$ to the reflecting surface S. Hence, for a known n_r, the ratio $\frac{h_1}{l_o}$ can be determined. Here we shall assume a reasonable n_r

of 1.60. Combining equations (5-37) and (5-42) we get:

$$x_1 = \frac{h_1}{\tan\left[\frac{\pi}{4} - \sin^{-1}\frac{n_i \sin i}{n_r}\right]} \qquad (5\cdot 44)$$

Solving with the given values

$$x_1 = \frac{h_1}{.3218}$$

$$2x_1 = l_o = \frac{2h_1}{.3218}$$

and

$$\frac{h_1}{l_o} = .1609 \qquad (5\text{-}45)$$

This ratio of $\frac{h_1}{l_o}$ determines the x-y dimensions of any dove prism which is made of a material with $n_r = 1.60$ and has 45° refracting surfaces.

With these values, equation (5-43) becomes

$$\frac{\bar{L}}{l_o} = \frac{1}{\sin\left[\frac{\pi}{4} - \sin^{-1}\left(\frac{\sin i}{1.60}\right)\right]}\left[.3218 + \frac{\tan\left[\frac{\pi}{4} - \sin^{-1}\left(\frac{\sin i}{1.60}\right)\right] - .3218}{1 + \tan\left[\frac{\pi}{4} - \sin^{-1}\left(\frac{\sin i}{1.60}\right)\right]}\right] \qquad (5\text{-}46)$$

Figure 5-23 shows this function plotted for $30° \leq i \leq 60°$. This figure illustrates that incident light rays which make the same angle with respect to the prism center line l_o travel different distances through the prism. The import of this fact is apparent from Figure 5-24. The two rays A and B entering the glass plate at the same angle with respect to ℄ see different thicknesses as illustrated. Hence, an image cannot be in focus in any plane parallel to the plane of the lens if a dove prism is added to the system. The defect can be reduced

to a negligible effect if the light rays traversing the prism are parallel or nearly parallel, since by symmetry, they will travel the same distance in the prism.

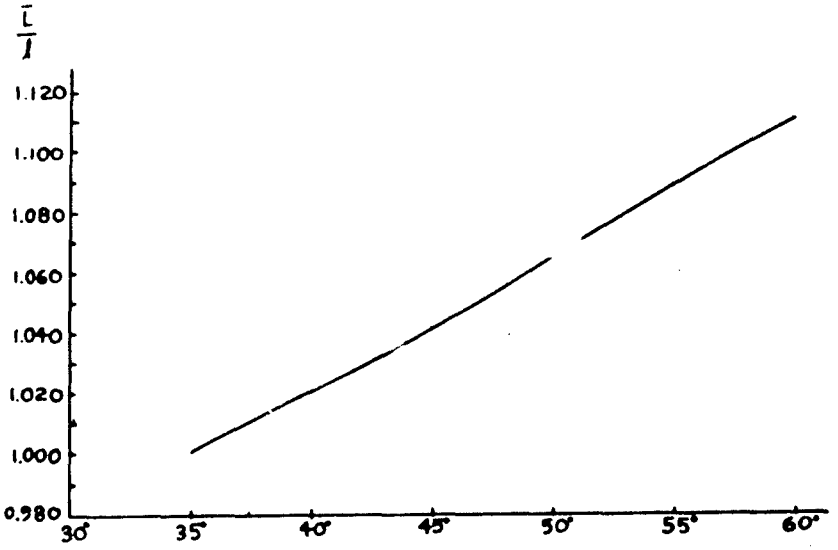

Figure 5-23. Incidence Angle Versus Distance Traveled For A Light Ray Traversing Dove Prism

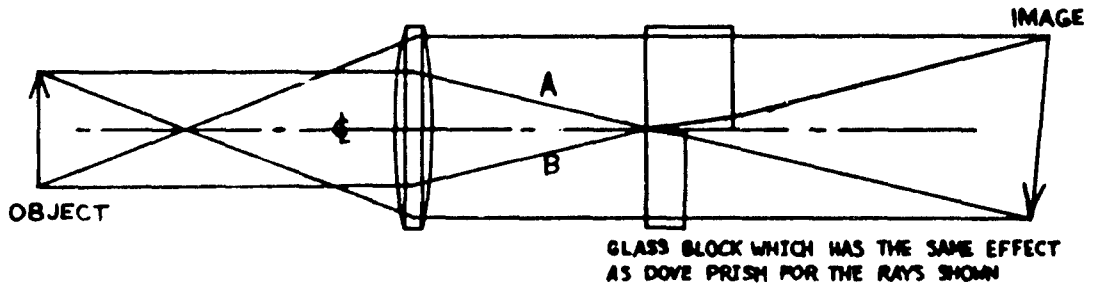

Figure 5-24. Image Distortion Analogy

This fact alone dictates the optical configuration shown in Figure 5-25. The field lens F must have a focal length equal to its effective distance from the field while the projection lens P_1 may have any focal length depending on the desired magnification. The dove prism must be placed between F and P_1.

While it has been necessary to examine the dove prism in detail, other optical components are elementary in nature, requiring only brief mention.

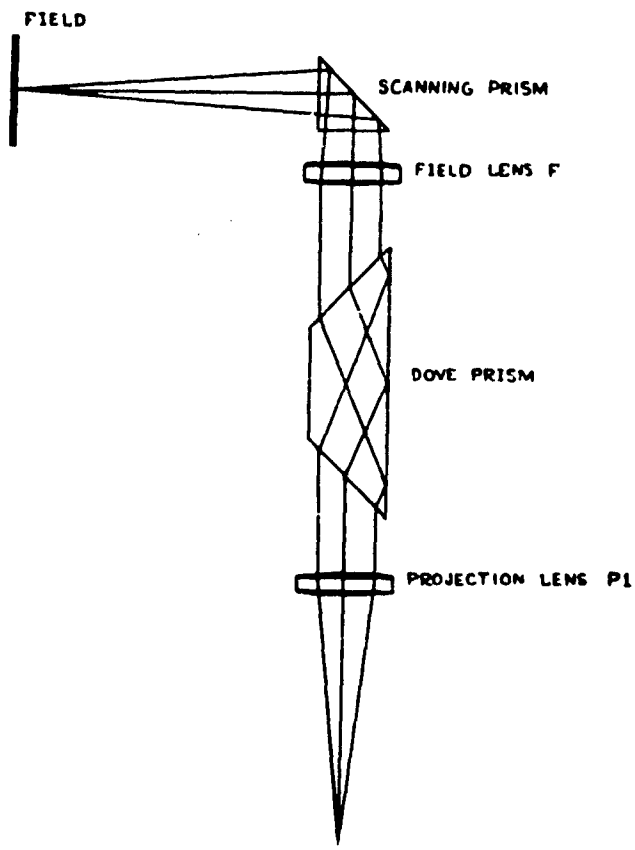

Figure 5-25. Required Component Arrangement, Dove Scanner

All lenses used in the dove scanner are good quality achromats; all mirrors are first surface, both of which contribute to the quality of the images formed while helping to eliminate extraneous images in other than the desired planes. Image and object location were calculated from the thin lens equation since the locations of the nodal planes of the lenses were not known before the lenses were purchased. This discrepancy was accounted for by allowing position adjustment mechanisms where needed. The thin lens equation and sign conventions used in the optical design are as follows:

$$\frac{1}{S} + \frac{1}{S'} = \frac{1}{f} \qquad (5\text{-}47)$$

where S is the object distance, considered positive if lying to the left of the lens; S' is the image distance, considered positive if lying to the right of the lens; and f is the focal length of the lens.

b. Optical Design

Having established the required configuration, it became necessary to design the mechanical and optical systems for optimum performance. As

mentioned at the beginning of Chapter 3, the dove system has as its main objective a storage capacity of 1000 to 2000 bits with scanning rates up to 10,000 times per minute. With a film linear bit density of 60 lines per inch (unreduced film) a field diameter of 5.3 inches would be required. This, of course, is the same diameter as would be required for a 2 to 1 reduction film with a capacity of 2000 bits per track. The decision was thus reached to optimize the scanner geometry around the midpoint between these upper and lower bounds. Normal 35mm film has a usable field height of .935 inch; finding the midpoint between unreduced and film reduced 2 to 1 establishes the optimum field height to be .70 inch. Taking into account the necessity of gripping the film at its ends to secure it in place on a film holder, it was decided to increase the drum diameter to the nominal figure of 6 inches.

The next step was to make sure that the optical components chosen would be capable of scanning the entire field height. Mechanical construction considerations restricted the effective distance from the field lens F to the field to greater than 3.22 inches; likewise, the distance from the leading edge of the dove prism to the field lens was restricted to greater than .84 inch. Since a minimum length optical path is desirable, these two dimensions were taken as given, thereby specifying a field lens focal length of 82 mm.

While it is desirable to have the dove prism as large as possible from an optical point of view, it becomes quite undesirable when designing the gearing system. From available stock, the dove prism illustrated in Figure 5-26 was selected. The choice proved to be a fortunate one from both points of view. The prism, having a 16mm x 16mm cross section, could be fitted into a mounting tube of .935 inch diameter, allowing small gear and bearing components, while at the same time being ideally suited to the .70 inch field.

To show that the prism is suited to the optical requirements we shall refer again to Figure 5-26. In this figure, we let diameter A represent a field aperture placed directly after the field lens F, W the field height, and H the height of the prism. Geometrically similar triangles give the following relation between field height W and other dimensions.

$$W = \frac{1_3}{1_4} (H - A) \qquad (5\text{-}48)$$

where 1_3 and 1_4 are defined in Figure 5-26. Letting A = KH, where K is the aperture variable, and substituting the dimensions given in the figure:

$$W = 1.380 (1 - K) \qquad (5\text{-}49)$$

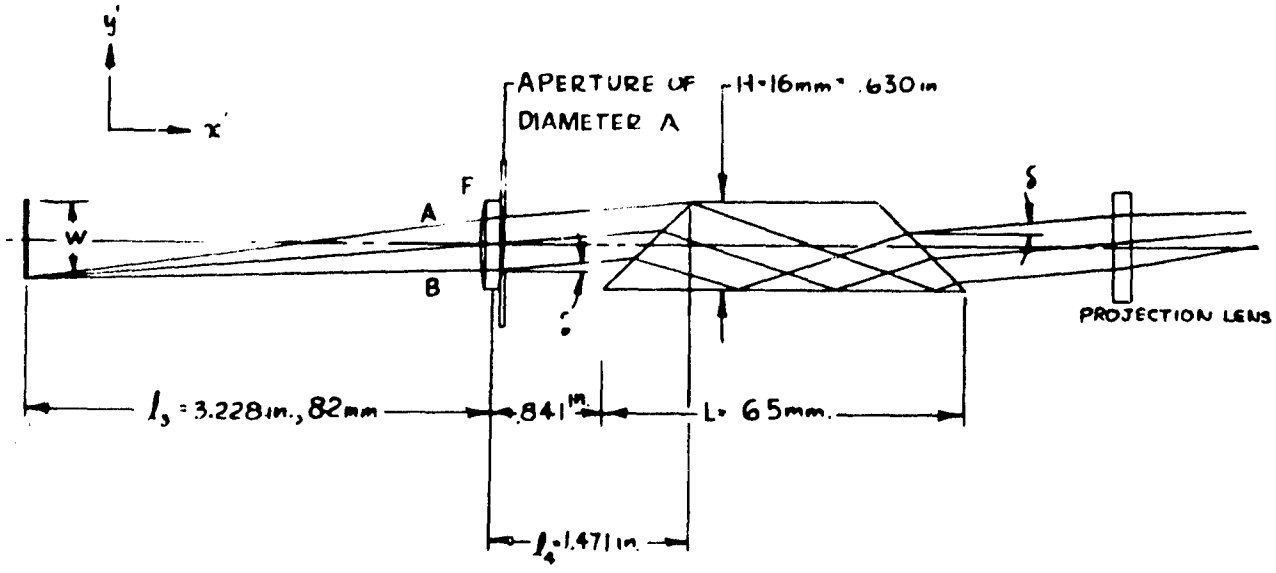

Figure 5-26. Diagram For Calculating Field Height Vs. Aperture

This function was drawn graphically to aid in experimental work and is reproduced in Figure 5-27. Note that the maximum field lens diameter required is .632 inches. A 20mm diameter by 82mm focal length lens was duly selected. The scanning prism, which replaces the scanning mirror of Figure 5-16 could be slightly smaller being closer to the field, and was therefore chosen from stock to have 15mm by 15mm right angle faces.

Borrowing the following expression from heat transfer equation[31] for the radiant energy transferred from one circular area of radius W/2 to another circular area of radius A/2, separated by a distance l_3 where T is the total flux received and E is the radiant energy given off per unit area of the first area.

$$T = E\frac{\pi}{2}\left[\left(\frac{W}{2}\right)^2 + \left(\frac{A}{2}\right)^2 + l_3^2 - \sqrt{\left[\left(\frac{W}{2}\right)^2 + \left(\frac{A}{2}\right)^2 + l_3^2\right]^2 - 4\left(\frac{WA}{4}\right)^2}\right] \tag{5-50}$$

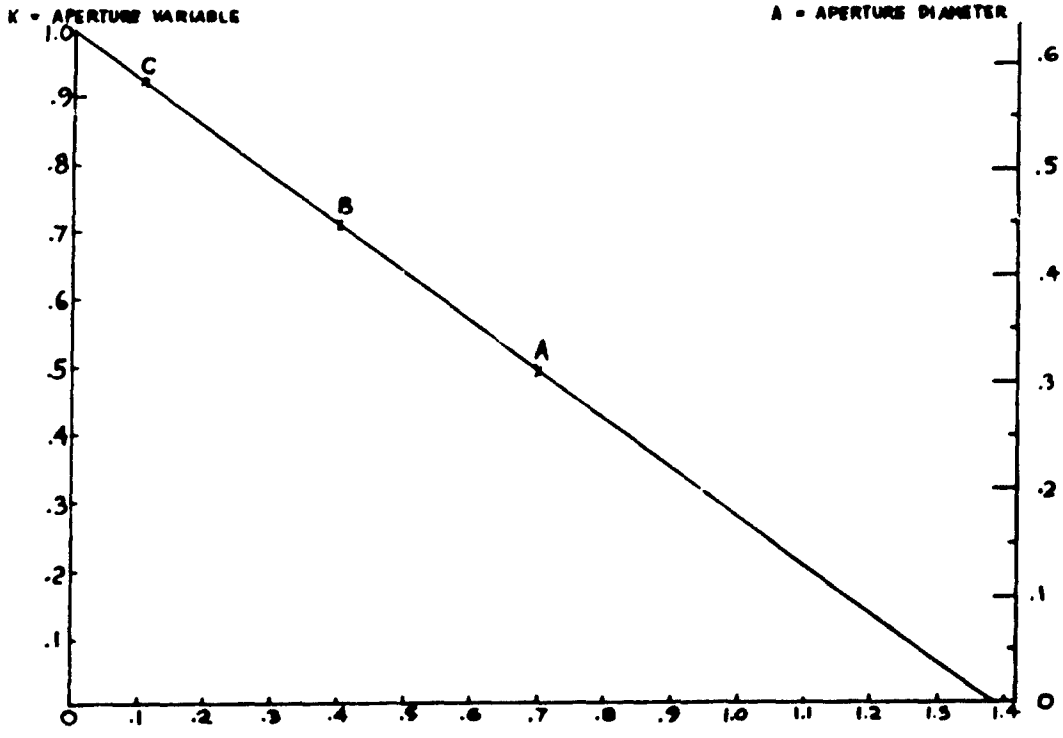

Figure 5-27. Field Height Vs Aperture Variable And Diameter

the total flux received at the second area can be found as a function of its diameter KH. Substituting equation (5-49) into (5-50) and reducing gives:

$$T = \frac{E\pi}{2}\left[10.895 - .950K + .574K^2 - \sqrt{(10.895 - .950K + .574K^2)^2 - .192(K^2 - 2K^3 + K^4)}\right] \quad (5\text{-}51)$$

This expression, solved for all values of K is plotted in Figure 5-28. It should be noted that the maximum flux is received when the system is being operated with an aperture corresponding to a field height of .70 inch.

Once the light is through the prism, it must be reformed into a real image before going to the phototransducer. The diameter of the projection lens P1 can be determined with the aid of Figures 5-26 and 5-27. The maximum field height of .935 inch is found to correspond to a field aperture of .21 inch. The light ray B in Figure 5-26 is the ray with the most extreme geometrical requirements since it is from the last point in the -y direction that need be

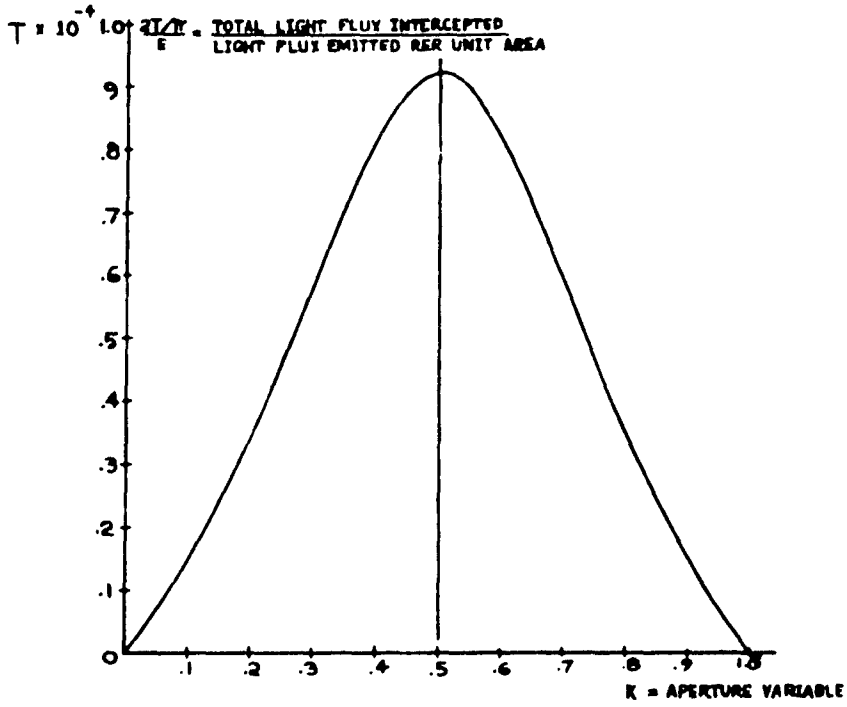

Figure 5-28. Intercepted Light Flux Vs Aperture Variable

projected with full intensity. The angle δ , the angle at which the ray enters the prism, and to a first approximation the angle at which it leaves, has

$$\tan \delta = \frac{H/2 - A/2}{1_4} = .1428 \qquad (5\text{-}52)$$

or the angle has a value of 8.217°. The height of the ray leaving the prism is to a first approximation the same as the entrance height or

$$H/2 - A/2 - .841 \tan \delta = .90 \text{ inches} \qquad (5\text{-}53)$$

Thus, for a lens .866 inch from the end of the dove prism, or effectively 1.271 inches from the point where the ray emerges, the required radius would be

$$1.271 \tan \delta + .090 = .271 \text{ inch} \qquad (5\text{-}54)$$

In a similar manner, for a lens 8.25 inches from the end of the dove prism, a lens radius of

$$8.655 \tan \delta + .090 = 1.325 \text{ inch} \qquad (5\text{-}55)$$

would be required for the .935 inch field film. These two dimensions are used for illustration purposes since two different projection lenses were used, located at these distances from the dove prism.

The selection of the focal length of the lenses following the dove prism was based on two requirements: the image size needed for the phototransducers, and the packaging requirements of the system. We shall simply state that a 25mm diameter by 279mm focal length lens was selected corresponding to the shortest dimension given above, and intended for use with films with field heights smaller than .467 inch; and that a 37mm diameter by 82mm focal length lens was selected for the longer distance, to be used with .467 to .935 inch field height. These lenses are designated as projection lens 1a and 1b respectively. The first lens was deliberately selected oversize since for small films, a larger aperture can be used; for a zero height field the maximum diameter would simply be the effective prism diameter or 16 mm. The second lens does not meet the diameter requirements for uniform projection of the full field thereby causing the two outer tracks on a .935 film to appear dim. The principal reason for selecting the lens despite this fact is that it has the same focal length as the scanning head field lens, thereby giving an object to image size ratio of 1. For experimental purposes, the slight discrepancy is of no importance. The primary image as formed by projection lens 1a has been magnified by

$$M = \frac{\text{f projection lens 1a}}{\text{f field lens}} = \frac{279 \text{ mm}}{82 \text{ mm}} = 3.4 \qquad (5\text{-}56)$$

At this point, we shall jump ahead slightly and state that the RCA 931-A photomultiplier tube was selected for the phototransducer. These tubes were arranged into two rows of three tubes each, the two rows facing each other. The images of each of the six tracks were transmitted to one of the phototubes with a small right angle prism mounted in a 3/8-inch diameter holder, requiring that the final projected image have a field height of at least 2.25 inches. However, the photomultipliers are mounted on 1-3/8 centers, implying that a nominal image height of 3 inches would be more desirable.

Since different size data films were used, a second projection lens, designated as projection lens P2, was installed in the system to enlarge the primary image from the projection lens P1 to the desired image height, this,

of course, requiring that the second projection lens have an adjustable primary image to final image distance. The projection lens P2 selected is identical to projection lens P1b with a focal length $f_2 = 3.228$. A mechanical system was duly designed to provide the correct length optical path (see Figure 5-29) according to the following criterion.

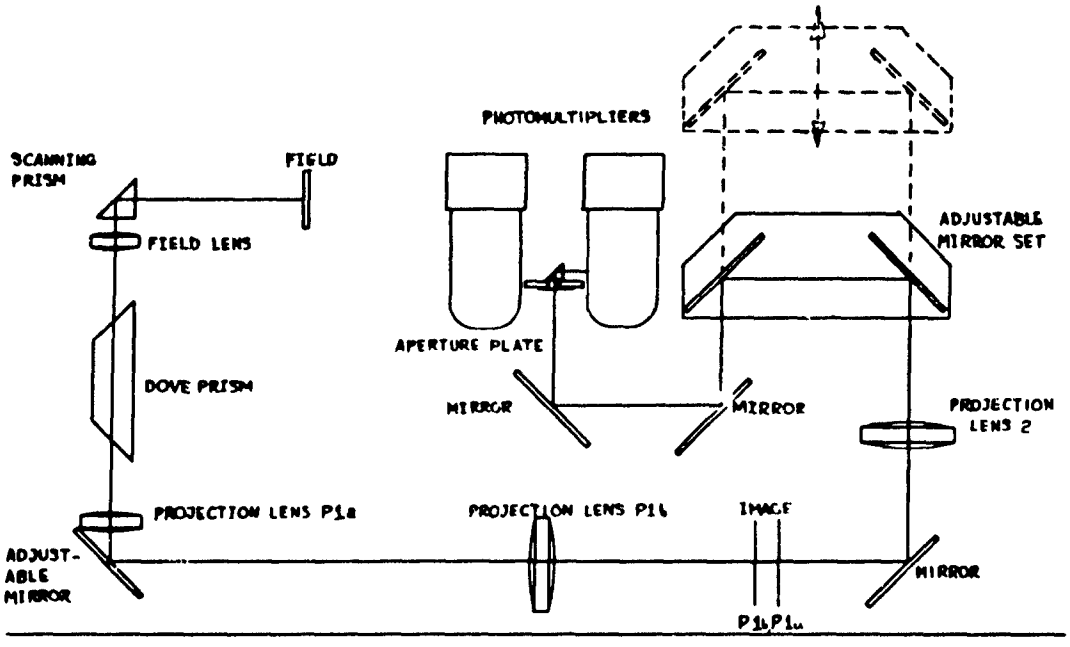

Figure 5-29. Layout Of Optical Components

For the design field film heights, that is, .935 to .467 inch, projection lens P1b is used, giving primary image heights corresponding to the field film heights. To obtain the correct final image height of 3 inches, the primary image must be magnified from 3.21X to 6.42X. Letting $S' = 3.21S$ and $6.44S$ in the thin lens equation (5-47) since the magnifications

$$M = S'/S \tag{5-57}$$

$$\frac{1}{S} + \frac{1}{3.21S} = \frac{1}{f_2} \qquad \frac{1}{S} + \frac{1}{6.42S} = \frac{1}{f_2} \tag{5-58}$$

and solving for S gives the values

$S = 4.23$ inches $\qquad S = 3.73$ inches

$S' = 13.58$ inches $\qquad S' = 23.95$ inches

$S + S' = 17.81$ inches $\qquad S + S' = 27.67$ inches

which are the limits of adjustment necessary for the optical path. The system as designed in Figure 5-29 has an adjustable path of 17.80 inches to 27.70 inches.

When projection lens P1a is installed in the system, (P1b having been removed), the primary image is located .375 inch further away from the dove prism shortening the adjustable path by an equivalent amount, the adjustment limits being 17.42 to 27.32 inches. With this lens in the system, the primary image is 3.4 times the field height (5-56). This image can in turn be magnified by projection lens P2 within limits found as follows from the thin lens equation (5-47) and path length limits

$S + S' = 17.42$ in. $\qquad S + S' = 27.32$ in.

$$\frac{1}{S} + \frac{1}{(17.42-S)} = \frac{1}{f} = \frac{1}{3.23} \tag{5-59}$$

$$\frac{1}{S} + \frac{1}{(27.32-S)} = \frac{1}{f} = \frac{1}{3.23} \tag{5-60}$$

which reduces to

$S^2 - 17.42S + 56.27 = 0 \qquad S^2 - 27.32S + 88.24 = 0$

having the pertinent solutions

$S = 4.29 \qquad S = 3.74$

$S' = 13.13 \qquad S' = 23.58$

The secondary magnifications are therefore

$$M_2 = \frac{13.13}{4.29} = 3.06X \qquad M_2 = \frac{23.58}{3.74} = 6.30X \tag{5-61}$$

making the overall system magnification M

$$M = M_1 M_2 = 10.4X \text{ to } 21.42X \qquad (5\text{-}62)$$

It will be noted that between the projection lenses P1 and projection lens P2 available magnification, there is a gap from 6.64X to 10.4X. This resulted from a decision to attempt to read 300 bit per inch film with the scanner despite its original intended use. The second optical system was fitted into the already constructed apparatus as best as possible. To make it possible to read films with field sizes requiring magnifications in the unavailable region, the receiving prisms in front of the multipliers were made adjustable for image heights of 2.25 to 4.0 inches, although this type of adjustment is rather tedious to accomplish. This completes the optical design from the data film to the photomultipliers.

The problem of field illumination can be solved in one of two ways: 1) Behind the film, a cylindrical ground glass can be mounted, behind which are many small DC filament lamps geometrically arranged so as to provide a more or less uniform field illumination. 2) A small prism can be mounted on the scanning head receiving focused light from a single axis mounted source and projecting it onto two conical mirrors such that the light is transmitted through the film back to the scanning head (see Figure 5-30).

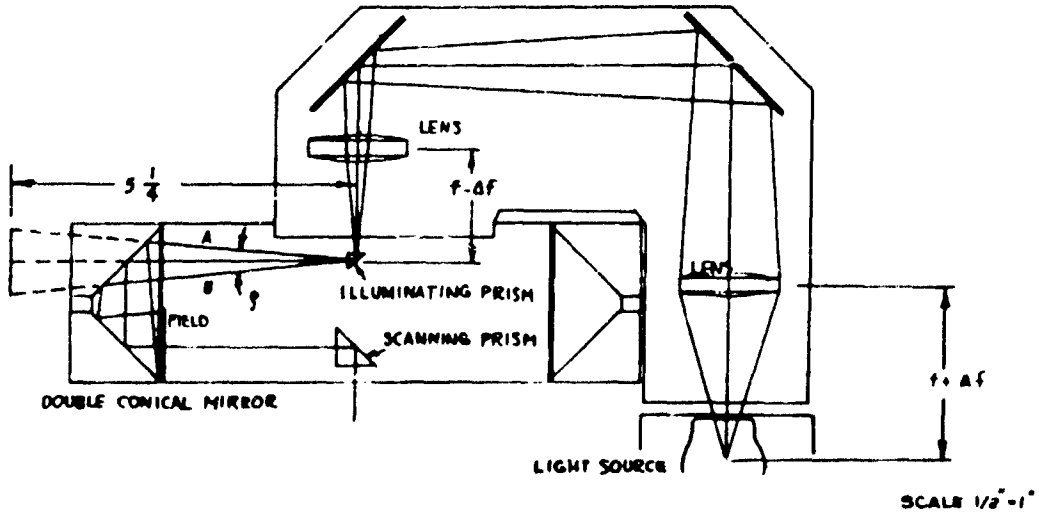

Figure 5-30. Illumination Assembly

Each system has its obvious faults since both cylindrical and conical optical components are not stock items. The first system has the additional disadvantage that the entire field is illuminated regardless of the portion being scanned; the second system having the advantage that only the portion of the field being illuminated is being read. The second system has the additional advantage that one light source instead of many is required, resulting in increased reliability of the system since one burned out small light among many small lights may not be noticed, causing part of the field not to register. It was therefore decided to use the second system.

The methods used to construct the double conical mirror will be discussed later in this chapter; here dimensional considerations will be taken up.

System packaging requirements dictate the light source position shown in Figure 5-30, necessitating the illumination assembly of two mirrors and two lenses. It is desirable to position a large diameter collecting lens as close as possible to the light source since the light power collected is a direct function of the solid angle intercepted. For this lens, and for convenience, the second lens also, a 39mm diameter by 63mm focal length lens was selected. To insure that the entire field will be illuminated, the included angle between light rays A and B should be such that

$$\tan 1/2\ \varphi = \frac{.935}{2(5.25)} \qquad (5\text{-}63)$$

Since the overall path length is known for the system, it is possible to set up a mathematical expression for the lens positions in terms of the required angle; likewise a graphical approach using successive approximations could be used. It should be noted, however, that both lenses are operating with the object or image very near the focal point of the lens. Under these conditions, a very small increment in image or object distance entails a drastic change in the solution obtained by either mathematical or graphic methods.

The best approach to the problem, for this type of design is to simply allow for lens position adjustment around the focal length and experimentally set the lens positions; this is the approach used with the dove scanner with excellent results.

c. Experimental Verification of Design

Before construction of the scanner was begun, the simple mock-up in Figure 5-31 was set up to ascertain the feasibility of the scanner concept. The mock-up was different from the final design, however, in that field illumination was accomplished by allowing the light to pass through the film, be reflected

from a finely polished aluminum cylinder, and then returned through the film to the scanning prism. An additional difference lies in the fact that a drive shaft was used to drive the dove prism and scanning head, this arrangement later being replaced with a planetary system. The setup confirmed within experimental accuracy the field height and aperture considerations discussed in previous section (5C2b) of this chapter, as well as verifying the calculated lens positions and magnifications.

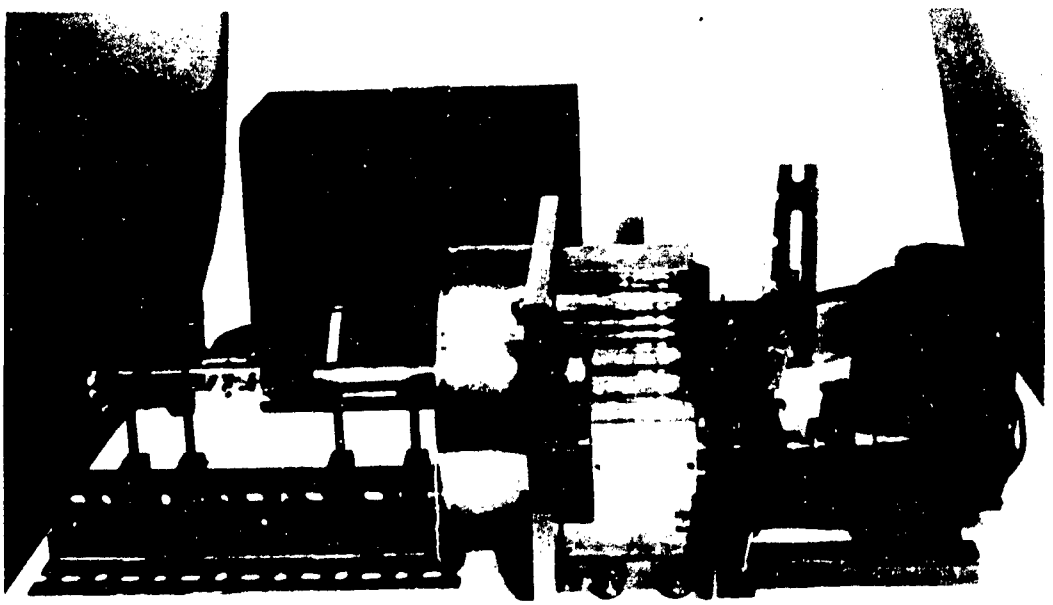

Figure 5-31. Experimental Verification Apparatus

3. Mechanical Design

a. Design Considerations

In addition to being a "production" type design intended for field use, the dove scanner was also intended to serve as an experimental apparatus in which various film formats could be tested. As is usually the case when two divergent goals are sought, the resulting apparatus is a compromise between the two extremes. Thus, the dove scanner has too many adjustments for a commercial device and not enough for true experimental work. Access has been provided to areas rarely requiring work, and no effort has been made to reduce the quite audible sound of the gearing system. It is felt, however, that the resulting design makes considerable inroads into both the design and experimental aspects of dove scanning.

The NOEL I data processing unit is made up of components, panel-mounted on two side-by-side 19-inch racks, the entire assembly contained in a metal cabinet; approximately 15 inches of the lower part of one rack has been left for a memory device. The last two panels above the memory space were extremely thin, allowing access to the top of the memory unit from the rear of the processing unit. It was this area that dictated the configuration of the dove memory unit.

To make the maximum use of the space available and to keep the weight of the scanner as low as possible, thereby facilitating installation and removal, unitized construction was used throughout. For experimental purposes, the assemblies and subassemblies were designed with the modular concept in mind, although the modules were fastened securely together for the sake or rigidity and required some time to remove. Like most optical systems, extreme rigidity is essential to maintain optical alignment. The bottom of the machine was kept clear so that table mounting was possible for experimental work.

Figure 5-32 shows a front view of the machine. The entire machine was panel-mounted on a 19 x 12-1/4 x 1/8-inch aluminum rack panel which also served as a control panel. Each photomultiplier connected to a common power supply input, has its own power input switch so that only those tubes in use need be turned on. Separate inputs are provided for the arc lamp, scanner motor, and fan motor; separate switches are provided for the scanner and fan motors.

Figures 5-33 and 5-34 give end views of the scanners. Visible from the left end are the two conical mirrors (extending through the wall), the illumination assembly (above the wall), the horizontal illumination assembly adjustment (slotted bar with two screws), and the adjustable mirror cover plate (black). Visible from the right end are the projection lens 2 assembly (lower center), the quick release catch to the phototube and mirror assembly hinged top (top center), and the top of the phototube and mirror assembly (uppermost center, black). Both views show the frame assembly.

Figure 5-35 gives the rear view. Visible in the picture are the phototube and mirror assembly (left half) which also contains the arc lamp cooling fan, the arc lamp housing (modern art type panel), the illumination assembly, and the conical mirrors.

Figure 5-36 illustrates best the general layout of the machine. Visible from left to right are the scanning unit (which contains the conical mirrors and drive motor), the illumination assembly, and the phototube and mirror assembly. Also visible are the many pin jacks employed to make the machine more easily disassembled.

Figure 5-32. Dove Scanner, Front View

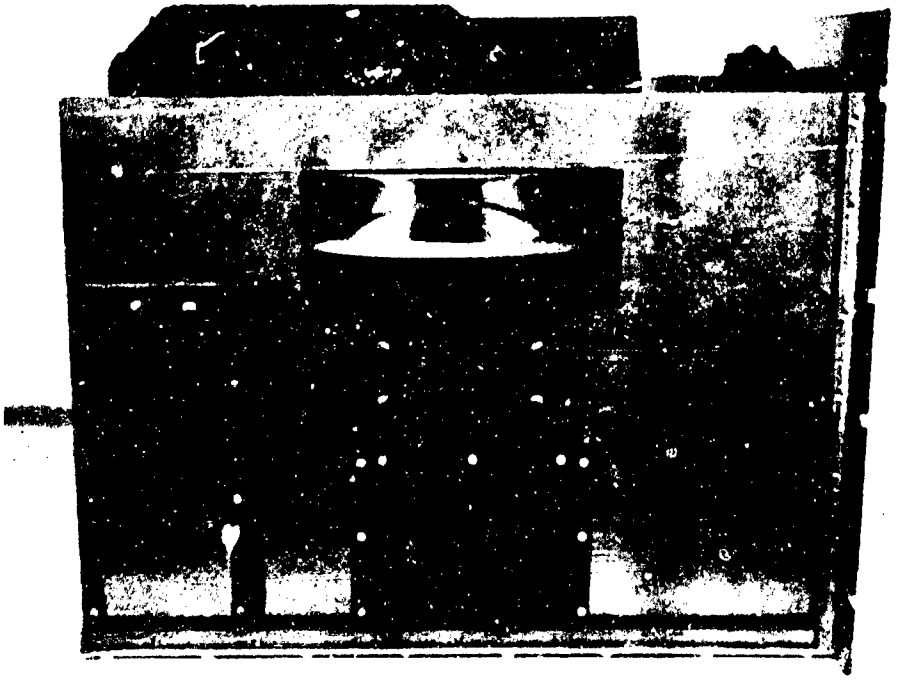

Figure 5-33. Dove Scanner, Left End View

Figure 5-34. Dove Scanner, Right End View

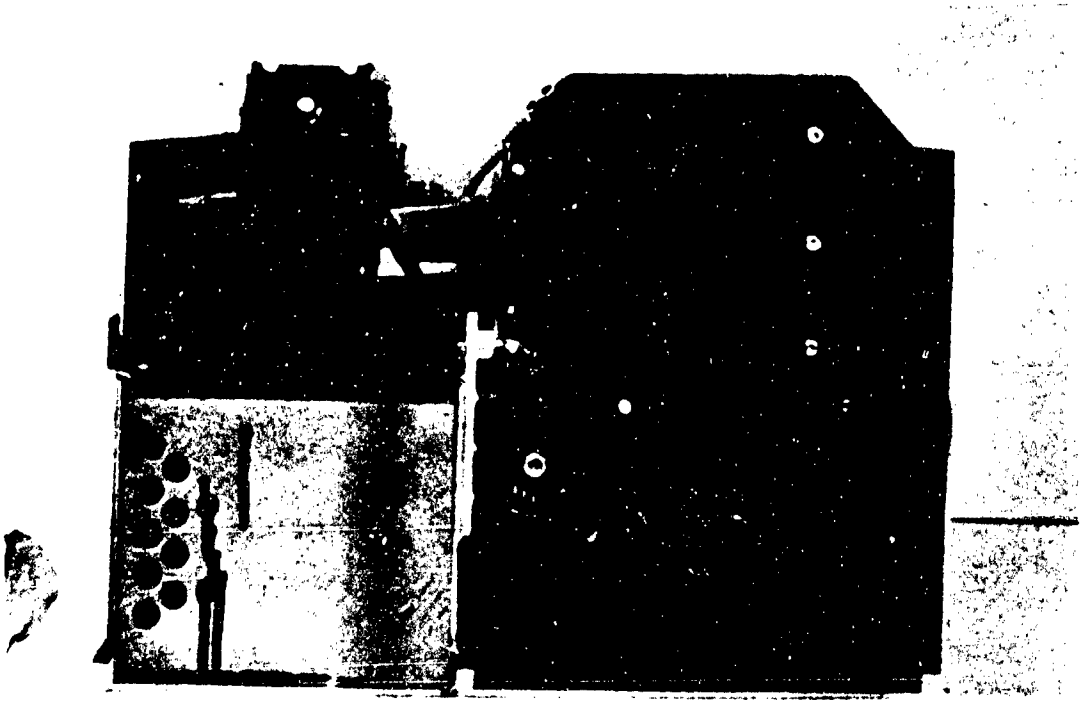

Figure 5-35. Dove Scanner, Rear View

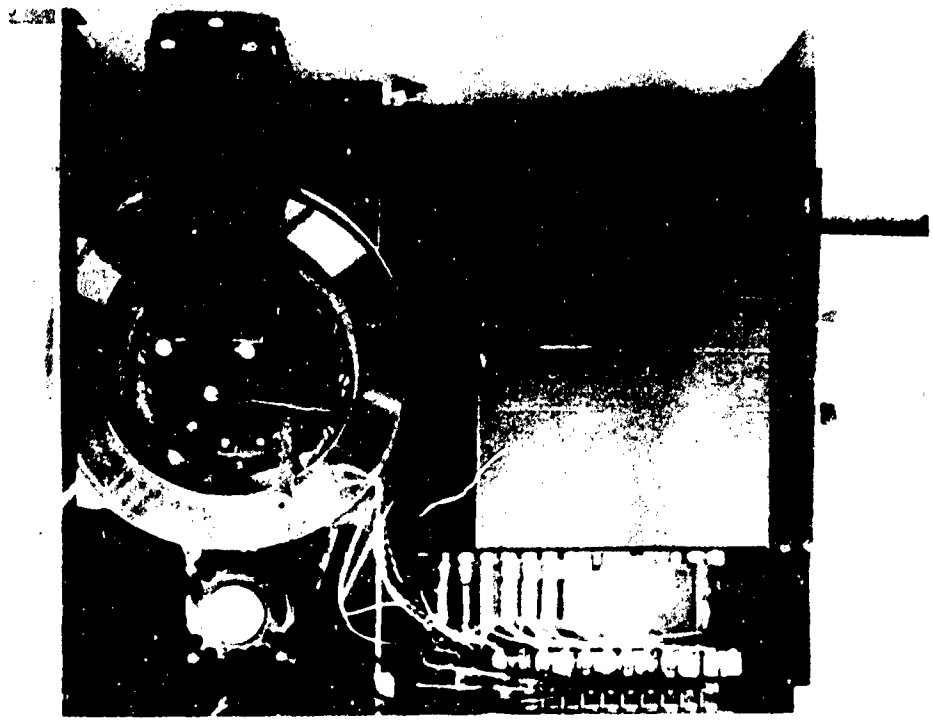

Figure 5-36. Dove Scanner, Top View

Figure 5-37 is an exploded view of the scanner and is for the most part self-explanatory. Missing from the picture are the two projection lneses Pla and Plb. Lens Plb fastens directly to the top of the adjustable mirror assembly (8); projection lens Pla fastens to the floor of the frame assembly (1) in the black area.

In the following sections, the main assemblies and subassemblies will be discussed.

b. Frame Assembly

Figures 5-32 through 5-37 show most views of the frame assembly. The main support for the components is furnished by the end panels which are made of 1/8-inch aluminum sheet fastened to the front panel with 3/8- by 3/8-inch square aluminum gussetbars. This type of construction is also used to fasten the center support panel to the front panel and the bottom to all four vertical panels. With the exception of the front panel, all other structural panels also serve as partitions between components, providing, where necessary, shielding from stray light and dust. The frame assembly also contains the arc lamp housing, formed by the two sheet metal partitions between the left end panel

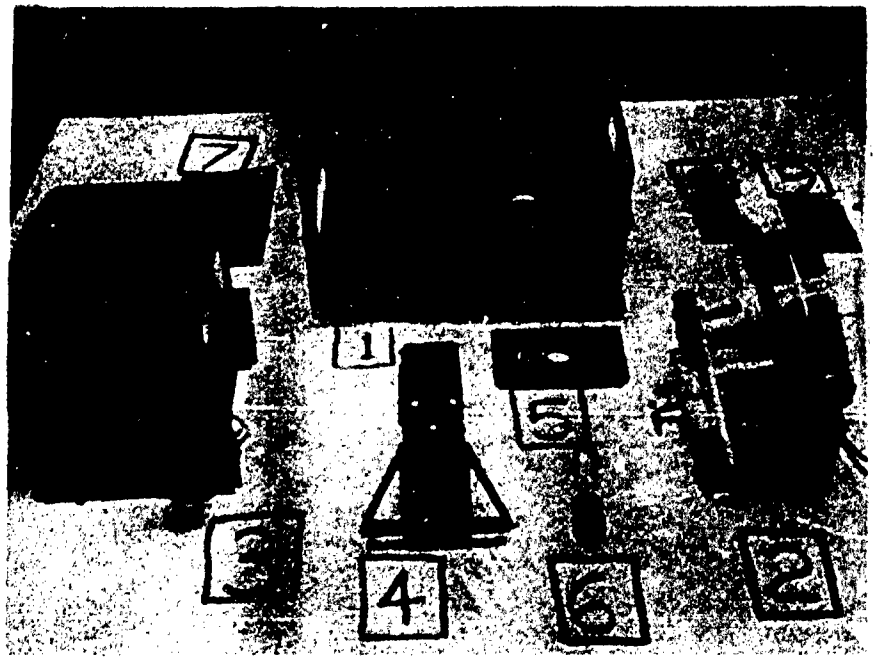

Figure 5-37. Exploded View of Dove Scanner
The Parts and Subassemblies are: 1) Frame Assembly; 2) Scanning Unit; 3) Phototube and Mirror Assembly; 4) Illumination Assembly 5) Arc Lamp Cover Assembly; 6) Arc Lamp; 7) Projection Lens 2 Assembly; 8) Adjustable Mirror Assembly; 9) Cover Plate

and the center support panel (see Figure 5-37). These two partitions add a significant amount to the structural rigidity of the system.

c. Scanning Unit

The general configuration of the scanning unit can be seen from Figure 5-38, the main components of which are:

- double conical mirror,
- motor
- frame assembly
- planetary gear subassembly,
- optical subassemblies (not visible)

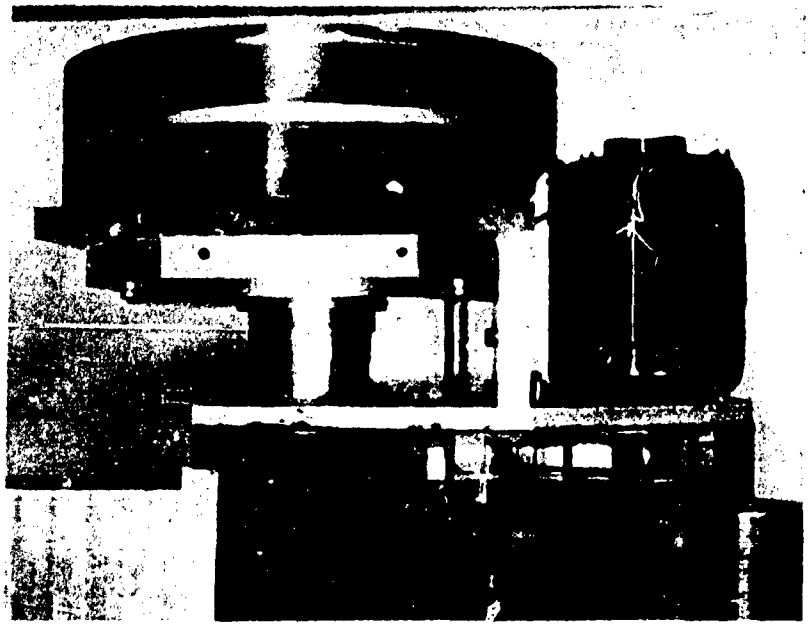

Figure 5-38. Dove Scanner, Scanning Unit

- oil pan
- oil pump (visible through the pan), and
- chain drive.

We shall proceed to discuss each one of these components in turn.

The double conical mirror, the cross section of which is drawn in Figure 5-30, was constructed in the following manner. Two flat Plexiglas blanks 1-1/4-inches thick by 11 inches square were purchased and turned to a uniform thickness of 1-3/32 inches on the face plate of a lathe. The center of each plate was turned out to a diameter of 6-1/16 inches, followed by a beveling cut at 45° until only 3/32 of the 6-1/16-inch diameter remained, forming the basic mirror blank. The outside diameter, approximately that required on the finished mirror, was cut with a bandsaw. The two mirrors were then hand-polished with oil and succeedingly finer abrasives, the last being done with a commercial silver polish. The two polished halves were then glued to a spacer ring (the center ring of three in Figure 5-38) and the entire assembly placed in a lathe and the outside diameter turned to the required dimension. Both mirror surfaces were then aluminized utilizing commercial vacuum deposition techniques, after which a 1/32-inch thick cylindrical liner was cemented into the 6-1/16-inch

diameter mirror ends, protecting the aluminized surfaces and completing the assembly. The entire assembly is held to the scanning unit frame with four 8-32 screws in 1/4-inch diameter frame holes, thereby allowing a centering adjustment.

The motor is the same type as is used on the drum scanner, and is mounted vertically on the frame, the shaft passing through an oil seal into the oil pan. The frame construction is evident from the picture, most of it being 3/8-, 1/2-, and 1-inch plate aluminum. This frame is the heaviest single component in the entire scanner for two main reasons: first, extreme rigidity is required for the high-speed, large diameter instrument bearings in order to minimize vibrations, and second, should the planetary gear system disassemble in mid-flight, it will stay in the scanner. Mounting of the assembly to the frame is accomplished by four screws, two in each side of the 1-inch plate.

The planetary gear assembly shown in Figure 5-39 and shown disassembled in Figure 5-40 provides the 2-to-1 ratio between the dove prism and the scanning head. The planetary system was chosen in preference to other methods since the bearings for the scanning head could be nested in the dove prism tube, thereby reducing the relative race velocity from 10,000 rpm to 5000 rpm. To reduce the bulk of the system, thin section, split race instrument bearings were chosen for both the scanning head and the dove prism tube. Both sets of bearings were provided with a preload adjustment in the planetary system design. To provide the required oil mist lubrication for these bearings, a small oil pump was installed in the bottom of the unit which pumped oil onto the rotating planet gears, the gear movement being of sufficient ferocity to create an oil vapor atmosphere. Excess oil is drained back to the oil pan with a return tube.

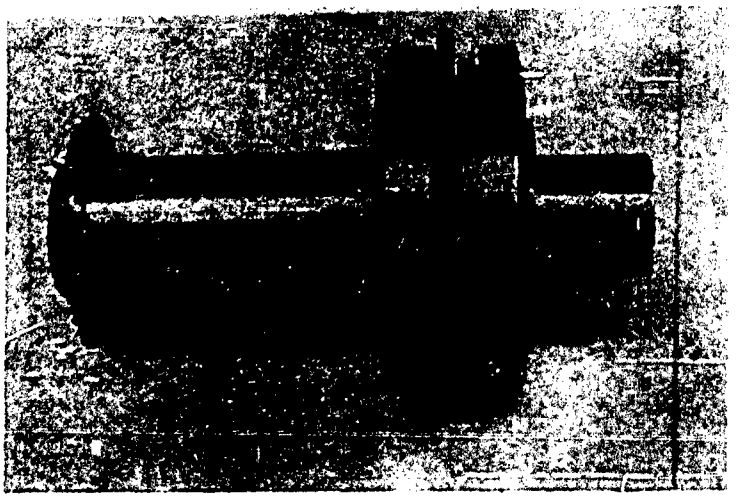

Figure 5-39. Planetary Gear Subassembly

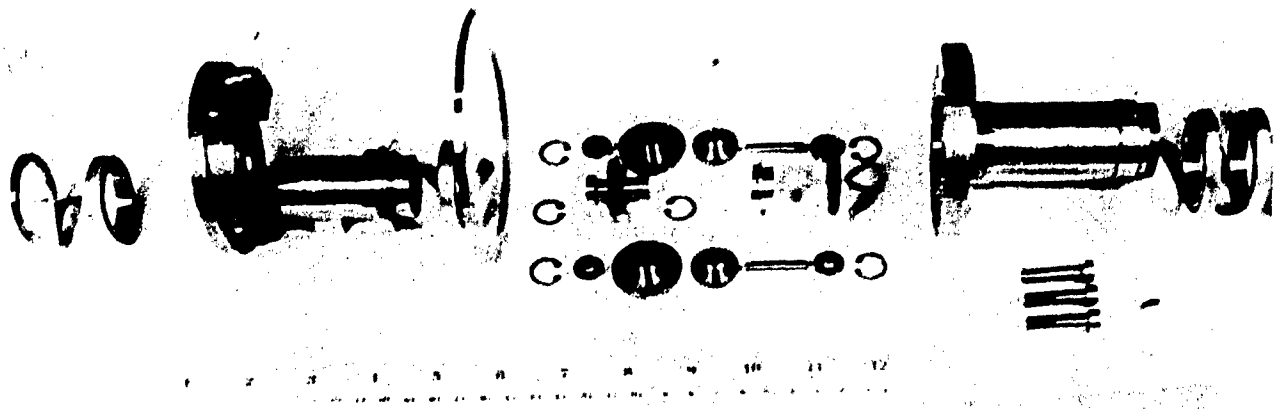

Figure 5-40. Disassembled Planetary Gear System
(Top Cover Missing from Photograph)

The necessity of providing a gear ratio of exactly 2-to-1 is self-evident from the theory of dove scanning. To illustrate the method used to obtain this ratio, we shall refer to Figure 5-41 where

$OP = S_r$ = sun gear radius k P_r

$QP = Q_r$ = planet pinion radius = j P_r

$QS = P_r$ = planet gear radius

$OS = R_r$ = ring gear radius

w_s = angular velocity of sun gear about 0

w_p = angular velocity of point Q about point O

The desired condition for a 2-to-1 ratio is, of course:

$$W_s = 2W_p \qquad (5\text{-}64)$$

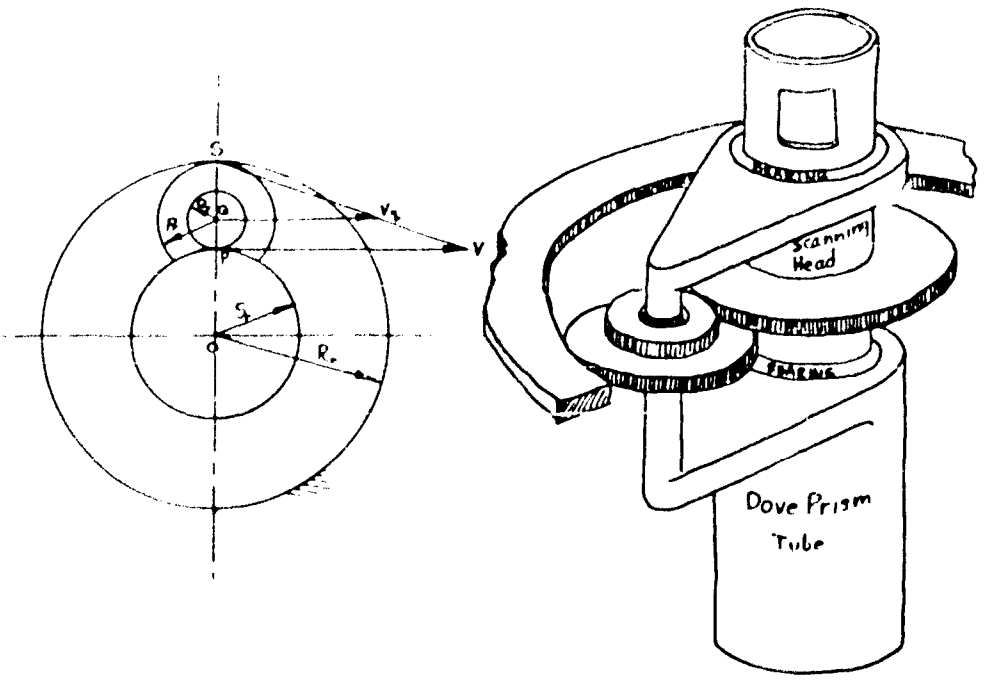

Figure 5-41. Planetary Gear System

From the velocity distribution triangle PSV, the three following relations are taken

$$W_s = V/S_r \tag{5-65}$$

$$W_p = V_q/(S_r + Q_r) \tag{5-66}$$

$$V_q = VP_r/(P_r + Q_r) \tag{5-67}$$

Substituting (5-65) and (5-66) into (5-64), we get

$$V/S_r = 2\,V_q/(S_r + Q_r) \tag{5-68}$$

into which (5-67) is substituted to give

$$\frac{V}{S_r} = \frac{2V\,P_r}{(S_r + Q_r)\,(P_r + Q_r)} \tag{5-69}$$

reducing, with the aid of the definitions, to

$$j^2 + j(k+1) - k = 0 \tag{5-70}$$

having the solution

$$j = -\frac{1}{2}(k+1) \pm \sqrt{(k+1)^2 + 4k}\ /2\ . \tag{5-71}$$

If we are to have gears with an integral number of teeth, both j and k must at least be of the form integer / integer. If the radical in equation (5-41) can be made to be of the form integer / integer by assuming values of k of the same form, then j will also be of that form. It is therefore assumed that

$$(k+1)^2 + 4k = m/n \tag{5-72}$$

where m and n are integers. Solving this expression for k gives

$$k = -3 \pm 1/2 \sqrt{36 + 4\left[(m/n)^2 - 1\right]} \tag{5-73}$$

Integers m and n are tried in the equation until an answer of the right form for ks is found. This occurs at m/n = 7/2 giving k = 3/2, and from (5-41), j = 1/2, the desired answers. Assuming OQ = 1.1250, the pitch diameters of all gears may be readily determined to be:

sun gear - 1.6875 inches

planet pinion - .5625 inches

planet gear - 1.1250 inches

ring gear - 3.3750 inches

Gears of 1/8-inch face were duly selected from 64 pitch precision 3 (up to 10,000 rpm) stock sources.

Further analysis of the planetary system will show the relative race velocities of the planet gear bearings to be 15,000 rpm. Since the planet gear shaft is only 3/16-inch in diameter, as compared to 1-1/16 and 1-5/16-inch diameter for the scanning head and dove prism tube respectively, the velocity requirements are less difficult to satisfy than for the larger bearings.

To provide an image orientation adjustment, the ring gear was mounted in a recess in the frame such that loosening four screws allowed the gear to rotate without translating; once set, this adjustment need not be tampered with since slight adjustments can be made on other parts of the machine.

The maximum stresses in the planetary system occur in the discs which support the planetary gears. For the designed 1.5-inch outside radius, r_o, and .75 inch inside radius, r_i, the stresses can be calculated from the equations:[14]

$$S_r = \rho w^2 \frac{3+\mu}{8}\left(r_o^2 + r_i^2 - \frac{r_o^2 r_i^2}{r^2} - r^2\right)$$

$$S = \rho w^2 \frac{3+\mu}{8}\left(r_o^2 + r_i^2 + \frac{r_o^2 r_i^2}{r^2} - \frac{1+3\mu}{3+\mu} r^2\right)$$

where μ = Poisson's ratio. For a rotating disc with a hole in the center, the maximum stress is tangential and occurs at the inside radius r_i, for the planetary system this figure is 14,000 psi., well below the yield point of the steel used in the discs.

The optical subassemblies which mount in the scanning head and dove prism tube are shown disassembled in Figure 5-42. The dove prism and threaded cylinder (upper part of picture) are clamped into place with the split cylinder and four screws. Once assembled, this entire unit is screwed into the sprocket end of the planetary gear assembly and locked with a locking nut (see Figure 5-43). The scanning prism, two silvered right-angle prisms glued back to back (of which only one is used), is clamped between the split, balanced, and interlocked cylinders shown; the illuminating prism, barely visible in the picture, is fitted into the recess on top of the tapered aluminum cylinder and clamped into place with the small U bracket (lower right). The field lens, F, is clamped into its barrel with the circular threaded nut (lower left) and the entire unit assembled with the two long screws in the picture. Once assembled, the unit can be slid into the scanning head and held in place by further tightening of the screws. Slight adjustments of image orientation can be accomplished by rotation of the scanning prism assembly within the head.

The oil pan (Figure 5-38) serves the function implied as well as providing a mounting for the oil pump flow adjustment; construction is entirely of Plexiglas. A seal is provided for the dove prism tube exit and is mounted on an adjustable plate held to the raised portion of the pan with eight screws.

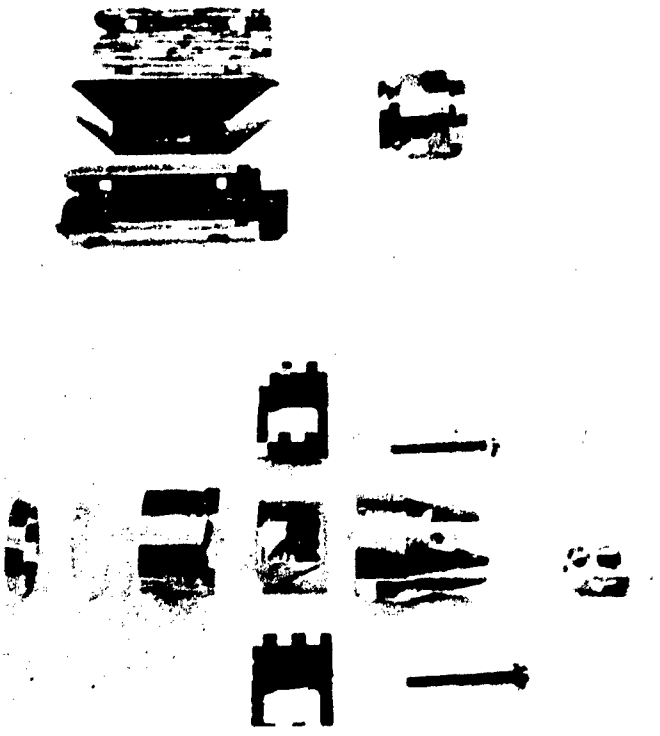

Figure 5-42. Optical Subassemblies, Dove Prism (Top) and Scanning Prism and Field Lens (Bottom)

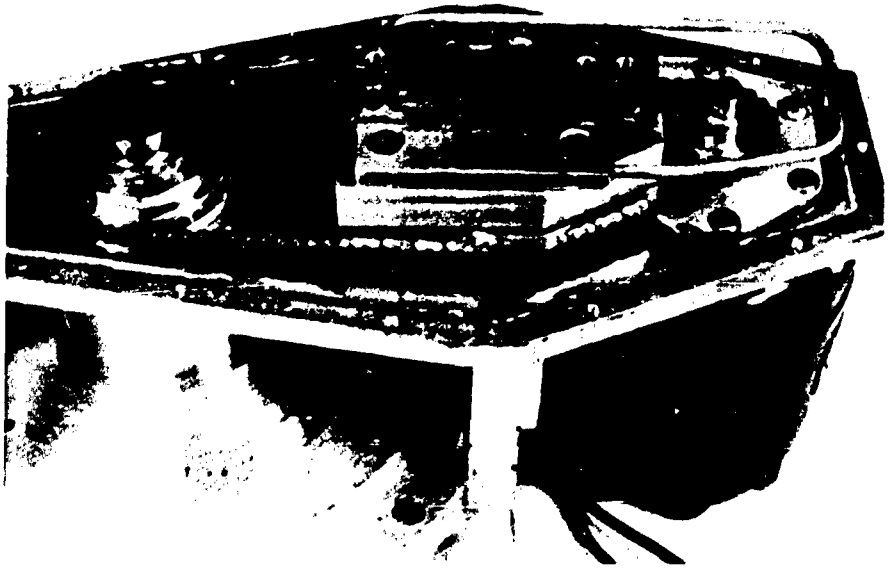

Figure 5-43. Scanning Unit with Oil Pan Removed

The oil pump serves two purposes: to provide the lubrication necessary for the gears and bearings, and to provide the drive chain tension. Sandwich-type construction was used, the two outer plates containing the sleeve bearings for the gear shafts, the center one providing the necessary contoured housing. Dowel pins were used for locating the sandwich decks while the two mounting screws which hold the pump to the frame also serve to hold the pump together. As noted from Figure 5-43, slots are provided for the two mounting screws so that the pump can be slid on its mount to achieve the desired chain tension, the driving sprocket for the pump being mounted directly on one of the gear shafts. To accommodate the pump movement, the flexible supply line arrangement in the picture was necessary. The hole in the output manifold (mounted on the bottom of the pump) is a curtain orifice, the adjustable plate for which is mounted on the oil pan. Maximum flow is eight cubic inches per minute for the maximum pump design speed of 5000 rpm, precisely the capacity of the pan.

A chain drive was chosen for the scanner since it allowed the desired packaging with the least machining. Maximum chain design speed is 10,000 inches per minute, precisely that required for the scanner using the sprockets shown.

d. Phototube and Mirror Assembly

The function of the phototube and mirror assembly is to provide the adjustable length optical path necessary for the projection lens 2 and direct the final image onto the photomultipliers, thereby transforming the image into usable electrical pulses. The unit is composed of basically three subassemblies: the frame, the adjustable mirror set, and the phototube subassembly. The position of the assembly in the scanner can be seen from Figures 5-35 and 5-36; the assembly is held in place with six screws, two each in the center support panel, the right end panel, and the bottom of the frame assembly, thereby providing the added rigidity required of the unit as a whole.

Figure 5-44 shows the construction of the unit; the two flat structural end plates provide the location for all components and are held apart structurally by the adjustable mirror set and individual mirror mounting bars. The two vertical dovetail ways, visible from the top in Figure 5-45, guide the adjustable mirror set, the function of which is evident from Figure 5-29. The two horizontal bars are used to support the photomultiplier subassembly, the aperture plate, and the small right angle prism plate, the latter two being visible in the center of the apparatus in Figure 5-44.

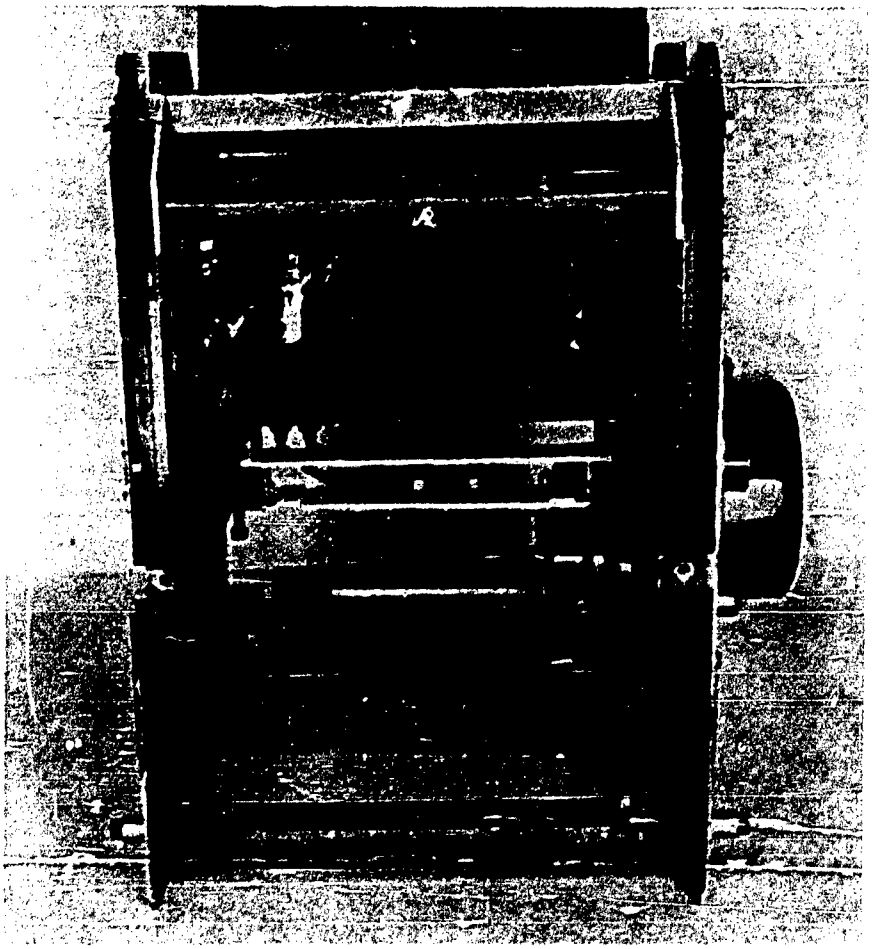

Figure 5-44. Phototube and Mirror Assembly with Phototube Subassembly Removed

Both the prism plate and the aperture plate are individually removable for convenience. When adjusting the orientation and focus of the final image, the prism plate is removed and a ground glass placed on the aperture plate; when adjusting the small right angle prisms to direct the final image onto the photomultipliers, the aperture plate is removed. The prism plate, normally held in place by the phototube subassembly is merely lifted out; the aperture plate, held in place by four leaf springs, can be slid out by depressing two of them.

The photomultiplier subassembly, shown in Figure 5-46, can be slipped into place with the prism and aperture plates already in position. Since the prism plate is narrower than the aperture plate, the photomultiplier light shields bottom directly on the aperture plate, thereby cutting off all parts of the final image not desired. The six multiplier tubes can be detached from the base, if so desired, by removing the four screws which secure the tube mounting plate to the four support posts.

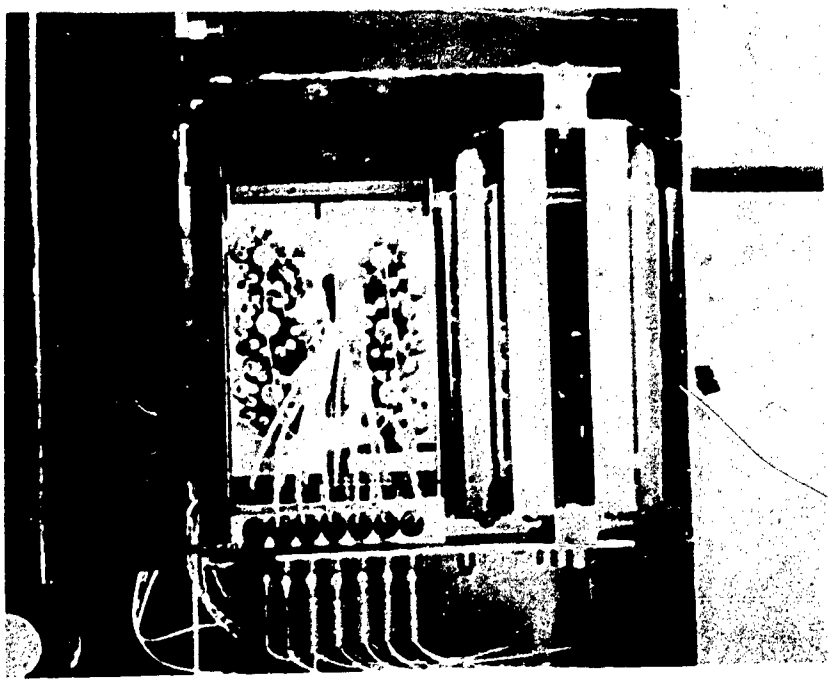

Figure 5-45. Phototube and Mirror Assembly, Top View

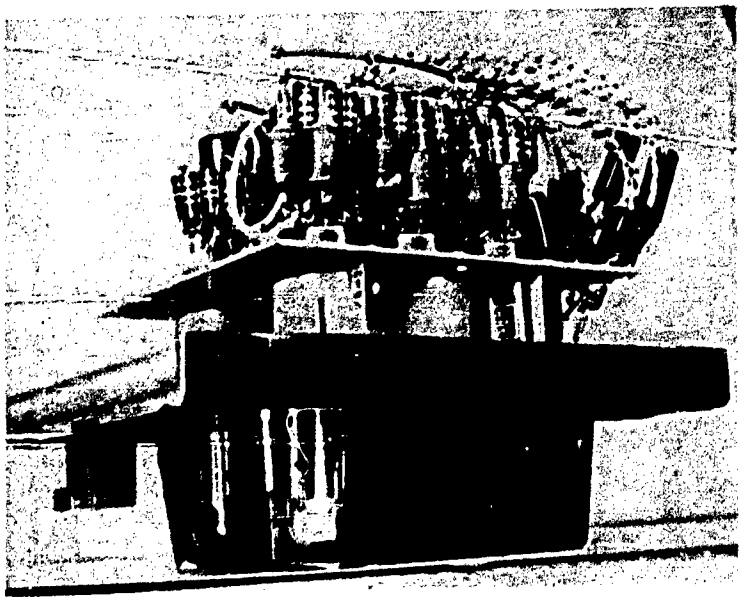

Figure 5-46. Phototube Subassembly

The fan in Figure 5-44 mounted on one of the horizontal bars, is used to cool the 100-watt arc lamp, and is identical to the one used on the drum scanner. Cooling requirements were calculated from equation (5-3) despite the increase in light size, the same fan could be used since the lamp operates at a higher temperature and has a larger surface area.

The double pin jacks (Figure 5-45) should be noted; these jacks allow quick removal of the photomultiplier subassembly from the phototube and mirror assembly, and the phototube and mirror assembly from the scanner frame.

e. Illumination Assembly

The illumination assembly, shown in Figure 5-47, transfers the arc lamp output to the top of the scanning head from whence it is projected onto the field. The entire assembly is pivot-mounted on the rod in the lower left-hand portion of the picture so that the assembly can be raised, via the handle (far right), to insert the memory film into the double conical mirror assembly. Unitized construction is used, the sides being made of 1/8-inch aluminum plate; the removable top and end panels are made of sheet metal. Both lenses are provided with vertical adjustments; both mirrors are provided with angular adjustments. The assembly can be slid sideways on the pivot rod; the pivot rod can be adjusted horizontally in the frame, providing all adjustments necessary for correct field illumination.

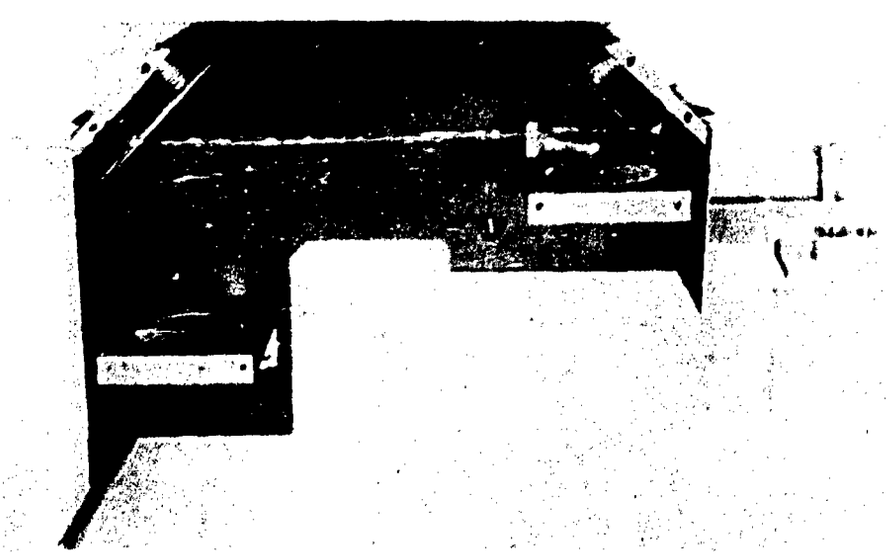

Figure 5-47. Illumination Assembly
With One Side Removed

f. Arc Lamp Cover Assembly

The arc lamp cover assembly, shown in Figure 5-39, is made of two parts - the main cover, which fits over the arc lamp housing, and a lamp positioning sheet, attached to the cover with four sheet metal screws. The necessity of holding the position of the arc lamp fixed is evident from the design of the illumination system. Refer to Chapter 5 (paragraph D2) for the arc lamp data.

g. Projection Lens 2 Assembly

The projection lens 2 assembly shown in Figure 5-48 provides the necessary lens position adjustments for different size data films. Once assembled the unit merely allows the lens position to be adjusted from outside the scanner without allowing light to leak into the system.

h. Adjustable Mirror Assembly

The adjustable mirror assembly shown in Figure 5-37, (not to be confused with the adjustable mirror set) is located directly below the dove prism and deflects the light towards the phototube and mirror assembly. The first surface mirror is mounted on a spring-loaded tilting plate, allowing correct positioning of the light.

This concludes the dove scanning machine design.

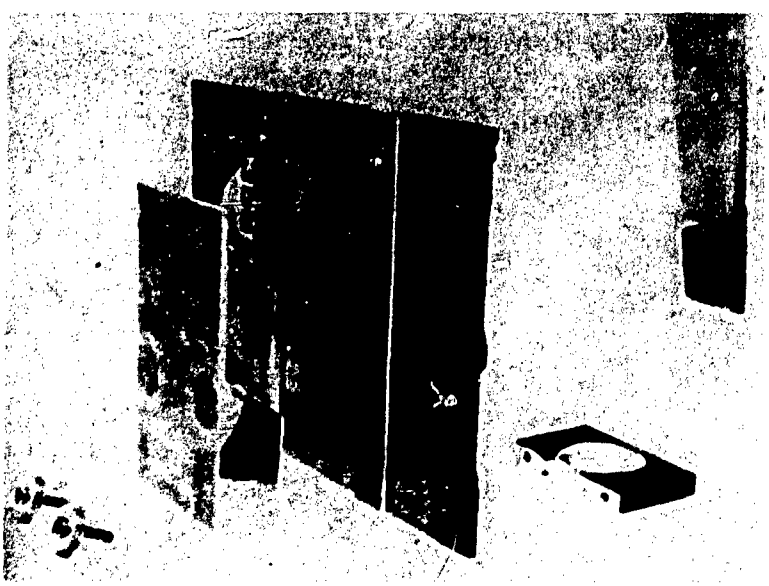

Figure 5-48. Dove Scanner, Projection Lens 2 Assembly

D. ELECTRICAL SYSTEMS FOR DOVE PRISM AND CYLINDER SCANNERS

1. Introduction

In both optical data retrieval systems, electronic components play a prominent role inasmuch as they are the instruments by which an optical image is converted to signals suitable for NOEL I circuitry. In a manner similar to other information transfer devices, a sending unit produces the media into which the stored data is encoded for transmission to the receiver unit, the receiver unit in turn decoding and transforming it to some desired output form. For both data retrieval systems, this process can be represented by the block diagram in Figure 5-49. Since both data retrieval systems use identical or conceptually similar electronic components, the following descriptions apply to both scanners.

2. Concentrated Arc-Lamp and Power Supply

The concentrated arc-lamp used in our work is a new type of light source produced by Sylvania Electric Products, Inc. In contrast with conventional arc lamps, the Sylvania lamp is provided with permanent long-life electrodes. The two electrodes, a metallic anode and a specially prepared refractory oxide cathode, are sealed into a glass shell filled with argon. When a high voltage is applied, an arc is established, raising the oxide surface of the cathode to its melting temperature, thereby liberating molten zirconium and emitting an intense light. Since an arc is established only at one point on the surface, the size of the light-emitting spot is very small and the emitted light has a cosine type spatial distribution as illustrated in Figure 5-50. Even though the spot size is small, the brightness is several times that of a standard 2870 tungsten filament lamp. The type C lamp is furnished with a ground and polished optically flat glass so that any bubbles or striae which could cause heavy shadows are eliminated.

The spectral energy distribution of the arc-lamp is shown in Figure 5-51. Referring this curve to the curve for a standard 2870° K tungsten source will show that most of the energy is associated within a small band centered on the visible-infrared border line. Other pertinent technical data for the two lamps used, the C-25 and the C-100 for the drum and dove scanners respectively, is given in Figure 5-52.

As noted from the table, these lamps require special power supplies which will provide a high starting voltage followed by a relatively low maintenance voltage and current. General specifications of the power supplies used are given in Figure 5-53.

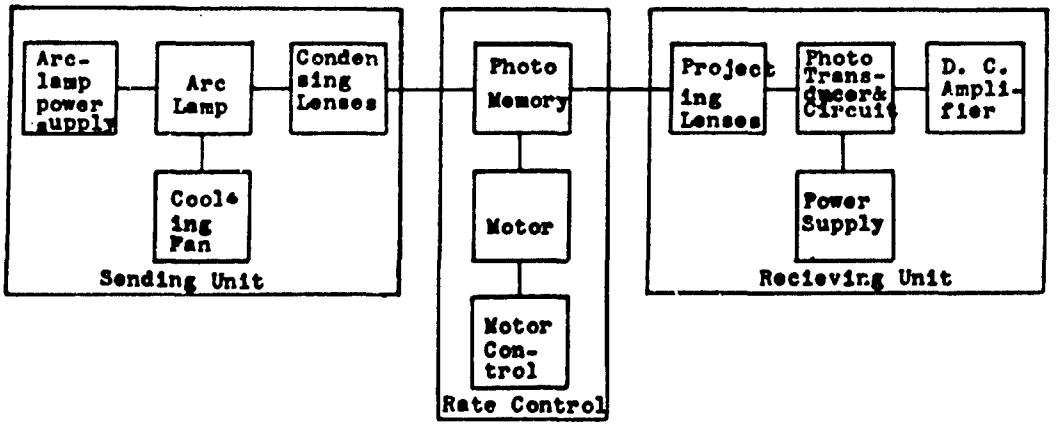

Figure 5-49. Block Diagram of NOEL Scanner

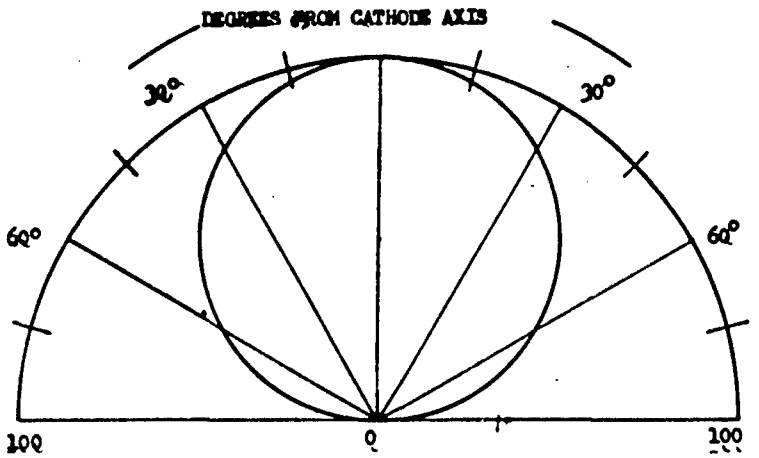

Figure 5-50. Spatial Distribution of Candlepower

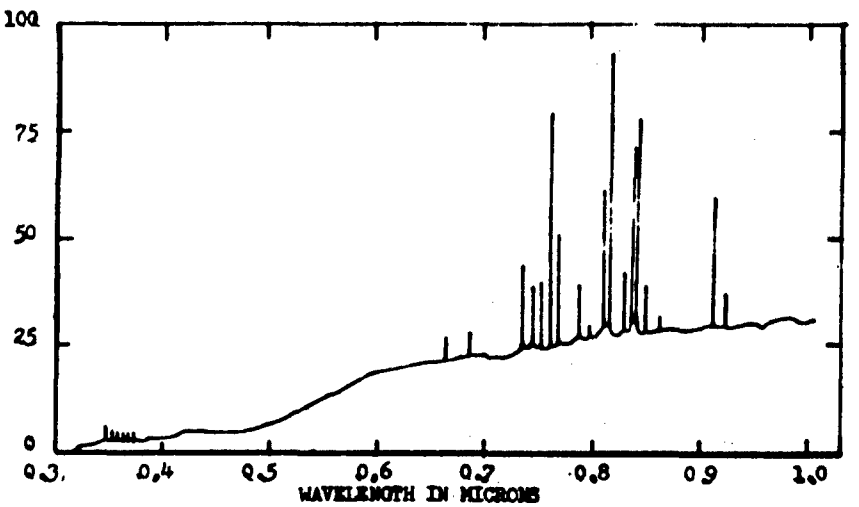

Figure 5-51. Spectral Energy Distribution

Watts	Lamp Volts	Lamp Amps	Supply Volts Min.	Min. Volts Starting	Mean Light Source Dia.
25	20	1.25	50	1000	0.030 in
100	16	6.25	50	2000	0.072 in

Ave. Brightness Candles per Square mm	Ave. Brightness Candles per Square inch	Ave. Axial Candle Power	Mean Candle Power per Watt	Ave. Lumens in 90° Angle
36	22,500	16.0	0.64	25.0
39	24,500	100.0	1.0	157.0

Bulb Type	Base	Max. Temp. F° Bulb	Base	Ave. Life Hrs.
T19	Octal 8 Pin	355	145	600
ST19	Med. 4 Pin	470	160	375

Figure 5-52. Technical Data of Arc Lamp

Model	Watts	Ripple	Dimensions in	Weight	Input
C25	25	13%	6x61/[illegible]x81/2	12 lbs 24 lbs	117vAC 117vAc
C100	100	14%	5x9x10		

Figure 5-53. Technical Specifications of Power Supply

3. Photo-Transducers

Selection of a Suitable Photo-Transducer

The main component of the receiving unit is the photosensitive device used to convert modulated light into electrical pulses for computer use. The frequency limitation of this device is singularly important since it determines the maximum information output of any possible foregoing scanning system. The sensitivity determines the amount of power which must be pushed through the preceding systems and is therefore an additional important consideration. In some cases, the size of the device is a determining factor.

To date, there are three different kinds of devices for high-frequency light demodulation. They are: multiplier phototubes, semiconductor phototubes, and microwave phototubes. Mr. R. G. E. Hutter of Sylvania Electric Products has drawn a comparison of these three devices. Such a comparison is, of course, useful to the designer when selecting components; hence, an abbreviated form follows for reference.

A. MULTIPLIER PHOTOTUBES

Advantages	Disadvantages
1. High sensitivity; fair quantum efficiency; low dark current (cooling reg'd) 2. Internal amplification (by election multiplication)	1. Limited frequency response and bandwidth: max=1,000Mc at present, due to transit time and other effects; great improvements not likely. 2. Not responsive to frequency modulated light. 3. Not a rugged component: response sensitive to temperature, aging, easily damaged by overload, mechanically complex, multiple electron multiplication stages make fabrication complicated. 4. Infrared response limited (with present day photosurfaces)

A. MULTIPLIER PHOTOTUBES (Continued)

Advantages	Disadvantages
	5. Not suitable for optical superheterodyne* reception: direct current due to local oscillator would be amplified, causing burnout.

*A device capable of receiving continuous light wave signals; the signals having been formed by impressing on a carrier wave another set of oscillations representing the information to be transmitted.

B. SEMICONDUCTOR PHOTODETECTORS
(pin junction photodiodes)

Advantages	Disadvantages
1. High sensitivity; near unity quantum efficiency: low dark current. 2. Simple rugged device (although it requires auxiliary equipment) 3. Infrared response good (due to small band gap) 4. Suitable for optical superheterodyne reception.	1. Limited bandwidth; response occurs in small lumped element with high capacitance, must be resonated. 2. No internal amplification (auxiliary amplification required) 3. Small detection area (light must be focused onto small junction region) 4. Not responsive to frequency modulated light.

C. MICROWAVE PHOTOTUBES

Advantages	Disadvantages
1. Extremely broad frequency response: up to highest microwave-tube frequencies: bandwidths comparable to traveling wave tubes--at least 3:1. 2. Internal amplification (by traveling-wave interaction or by other methods) 3. Suitable for optical super-heterodyne reception (local oscillator's direct current will assist amplification) 4. Responsive to frequency-modulated light (by use of transverse wave interactions) 5. Good sensitivity (sensitivity depends on photosurface) 6. Rugged (ruggedness, ease of manufacture comparable to or better than other micro-wave tubes)	1. Infrared response limited (with present day photosurfaces)

Obviously superheterodyne requirements are far in excess of NOEL requirements. For this reason, and for the additional fact that microwave phototubes are much too large in physical size, class C was eliminated immediately. However, the basic requirements of high sensitivity, small size, and low cost are met by both classes A and B. Photodiodes, having a good response in the infrared region appeared to be a better match to the light source than would be the photomultiplier, and therefore, was one of the first phototransducers used in the project. Experimental photodiodes provided by Raytheon* proved to have good sensitivity but were exceptionally difficult to keep intact since their mechanical design allowed the junction to separate under

* These diodes are not commercially available and were supplied on an experimental basis.

the slightest provocation. An additional experimental photodiode made by Philco was tried but failed to give any reasonable results. Rather than pursue this form of photo-transducer further, it was decided to use photomultipliers.

The ideal photomultiplier matched to the light source would be the RCA 7102, data for which is given in Figure 5-54. The cost of this tube, ($110.00), however, prohibits its use in any low cost design. Therefore, one tube was purchased but used only for experimental testing. A less responsive tube, the RCA 931-A was tried and found to give satisfactory results despite the mismatch between its characteristics and those of the light source. The cost ($10.00) was agreeable; hence this tube was chosen as the design component. The 931-A characteristics are given in Figure 5-55.

4. The Photomultiplier

A photomultiplier is essentially a vacuum phototube containing the cathode and anode with several dynodes interposed, schematically illustrated in Figure 5-56. Photocathodes are usually made from an alkali metal since these metals have the smallest photo-emission work functions. To liberate an electron, light, with its associated quantum energy $h\,c/\lambda$, must impart to the electron sufficient kinetic energy to enable the electron to overcome the surface bonding force $e\phi$, where:

h = $6.62 \times 10 - 34$ Watt/sec^2
Planck's Constant

c = 3×10^8 m/sec: speed of light

λ = wave length of light

e = charge of electron

ϕ = work function of photocathode surface

Once out of the surface, the electron is accelerated towards the first dynode by the electric field E_{st} (voltage across one stage) where in turn, secondary electrons are released, the process being repeated at each dynode.

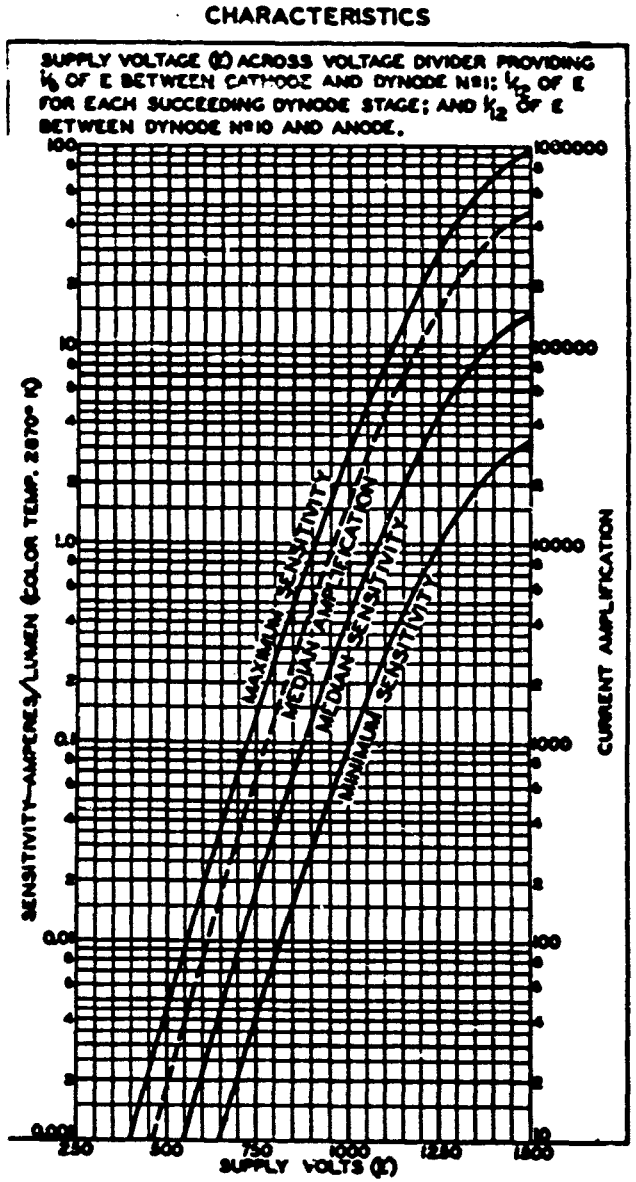

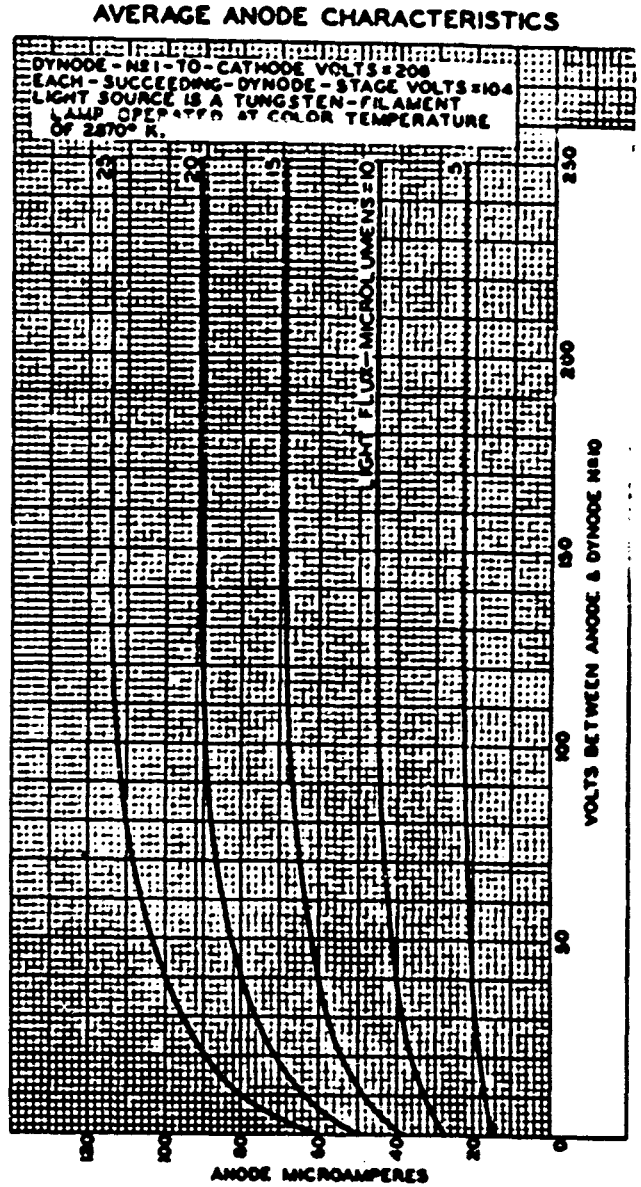

Figure 5-54a. 7102 Photomultiplier Characteristics

MULTIPLIER PHOTOTUBE

♣ For conditions where the light source is a tungsten-filament lamp operated at a color temperature of 2870° K. A light input of 10 microlumens is used. The load resistance has a value of 0.01 megohm.

• An output current of opposite polarity to that obtained at the anode may be provided by using dynode No.10 as the output electrode. With this arrangement, the load is connected in the dynode-No.10 circuit and the anode serves only as collector.

♠ For conditions the same as shown under (♣) except that the value of light flux is 0.01 lumen and 150 volts are applied between cathode and all other electrodes connected together as anode.

♦ Under the following conditions: 2870° K tungsten light source; light flux of 0.01 lumen incident on Corning No.7540 infrared filter (melt 1413, 2.61 mm thick, or equivalent); irradiated area of photocathode is 2.26 inch in diameter.

◊ For spectral characteristic of this source, see sheet SPECTRAL CHARACTERISTIC OF 2870° K LIGHT SOURCE AND SPECTRAL CHARACTERISTIC OF LIGHT FROM 2870° K SOURCE AFTER PASSING THROUGH INDICATED INFRARED FILTER at front of this section.

● Measured at a tube temperature of 25° C and with the supply voltage (E) adjusted to give a luminous sensitivity of 4 amperes per lumen. Dark current caused by thermionic emission and ion feedback may be reduced by the use of a refrigerant.

▲ Under the following conditions: Supply voltage (E) 1250 volts, 25° C tube temperature, dc-amplifier bandwidth of 1 cycle per second, tungsten light source at color temperature of 2870° K interrupted at 7 low audio frequency to produce incident radiation pulses alternating between zero and the value stated. The "on" period of the pulse is equal to the "off" period. The output current is measured through a filter which passes only the fundamental frequency of the pulses.

† Measured at 8000 angstroms.

OPERATING CONSIDERATIONS

The 7102 is capable of very short time-resolution. For an input pulse having a duration of 1 millimicrosecond or less, the time spread of the pulse at the anode is about 5 millimicroseconds measured at 50 per cent of the maximum pulse height. This time spread corresponds to an electron transit-time spread of about 4 millimicroseconds. The transit-time spread can be reduced to about 2 millimicroseconds by irradiating only a small central area of the photocathode.

When stability of operation is important, the use of an average anode current well below the maximum rated value of 10 microamperes is recommended. This maximum rating should never be exceeded because operation at higher average output currents may cause a permanent decrease in infrared sensitivity and a consequent decrease in tube life.

A small temporary loss of infrared sensitivity may be observed after long periods of operation. The sensitivity recovers during idle periods but only very slowly at temperatures below 25° C.

Electrostatic and/or magnetic shielding of the 7102 may be necessary.

SPECTRAL-SENSITIVITY CHARACTERISTIC of Phototube having S-1 Response is shown at front of this Section

MULTIPLIER PHOTOTUBE

Characteristics Range Values for Equipment Design:

Under conditions with supply voltage (E) across voltage divider providing 1/6 of E between cathode and dynode No.1; 1/12 of E for each succeeding dynode stage; and 1/12 of E between dynode No.10 and anode

With E = 1250 volts (except as noted)

	Min.	Medium	Max.	
Sensitivity:				
Radiant, at 8000 angstroms	–	400	–	μa/μw
Cathode radiant, at 8000 angstroms	–	0.0027	–	μa/μw
Luminous:♣				
At 0 cps	1	4.5	30	amp/lumen
With dynode No.10 as output electrode•	–	2.7	–	amp/lumen
Cathode luminous:				
With tungsten light source♠	10	30	–	μa/lumen
With infrared source♠◊	0.012	0.036	–	μa
Current Amplification	–	150000	–	
Equivalent Anode-Dark-Current Input●	–	3×10^{-7}	5×10^{-6}	lumen
	–	3.3×10^{-9}†	5.5×10^{-8}†	watt
Equivalent Noise Input▲	–	1.5×10^{-10}	7.5×10^{-10}	lumen
	–	1.7×10^{-12}†	8.4×10^{-12}†	watt

With E = 1500 volts (except as noted)

	Min.	Medium	Max.	
Sensitivity:				
Radiant, at 8000 angstroms	–	1250	–	μa/μw
Cathode radiant, at 8000 angstroms	–	0.0027	–	μa/μw
Luminous:♣				
At 0 cps	–	14	–	amp/lumen
With dynode No.10 as output electrode•	–	8.4	–	amp/lumen
Cathode Luminous:				
With tungsten light source♠	10	30	–	μa/lumen
With infrared source♠◊	0.012	0.036	–	μa
Current Amplification	–	465000	–	

• Averaged over any interval of 30 seconds maximum.

♣,•,♠,●,◊,▲,†: See next page.

Figure 5-54b. 7102 Photomultiplier Characteristics

MULTIPLIER PHOTOTUBE

	Min.	Bedson	Max.	
Cathode radiant, at 4000 angstroms. . .	-	0.03	-	μamp/μwatt
Luminous:[6]				
At 0 cps.	4.5	24	300	amp/lumen
At 100 kc	-	23	-	amp/lumen
Cathode luminous[6] . .	-	30	-	μamp/lumen
Current Amplification .	-	800,000	-	
Equivalent Anode-Dark-Current Input[6a] . . .	-	-	2.5×10^{-9}	lumen
Equivalent Noise Input[6]	-	3.5×10^{-13}	-	lumen

With E = 750 volts (except as noted)

	Min.	Bedson	Max.	
Sensitivity:				
Radiant, at 4000 angstroms	-	3300	-	μamp/μwatt
Cathode radiant, at 4000 angstroms. . .	-	0.03	-	μamp/μwatt
Luminous:[6]				
At 0 cps.	-	3.3	-	amp/lumen
Cathode luminous[6] . .	-	30	-	μamp/lumen
Current Amplification .	-	110,000	-	

[6] For conditions where the light source is a tungsten-filament lamp operated at a color temperature of 2870°K, a light input of 10 microlumens is used. The load resistor has a value of 0.01 megohm.

[6a] For conditions the same as shown under (6) except that the value of light flux is 0.01 lumen and 200 volts are applied between cathode and all other electrodes connected together as anode.

[6b] Measured at a tube temperature of 20°C and with the supply voltage (E) adjusted to give a luminous sensitivity of 20 amperes per lumen. Dark current caused by thermionic emission and ion feedback may be reduced by the use of a refrigerant.

[7] For maximum signal-to-noise ratio, operation with a supply voltage (E) below 1000 volts is recommended.

[8] Under the following conditions: Supply voltage (E) is 1000 volts, external shield operated at -1000 volts with respect to anode; 25°C tube temperature, ac-amplifier bandwidth of 1 cycle per second, tungsten light source at color temperature of 2870°K interrupted at a low audio frequency to produce incident radiation pulses alternating between zero and the value stated. The "on" period of the pulse is equal to the "off" period. The output current is measured through a filter which passes only the fundamental frequency of the pulses.

OPERATING CONSIDERATIONS

The operating stability of the 931-A is dependent on the magnitude of the anode current and its duration. When the 931-A is operated at high values of anode current, a drop in sensitivity (sometimes called fatigue) may be expected. The extent of the drop below the tabulated sensitivity values depends on the severity of the operating conditions. After a period of idleness, the 931-A usually recovers a substantial percentage of such loss in sensitivity.

AVERAGE ANODE CHARACTERISTICS

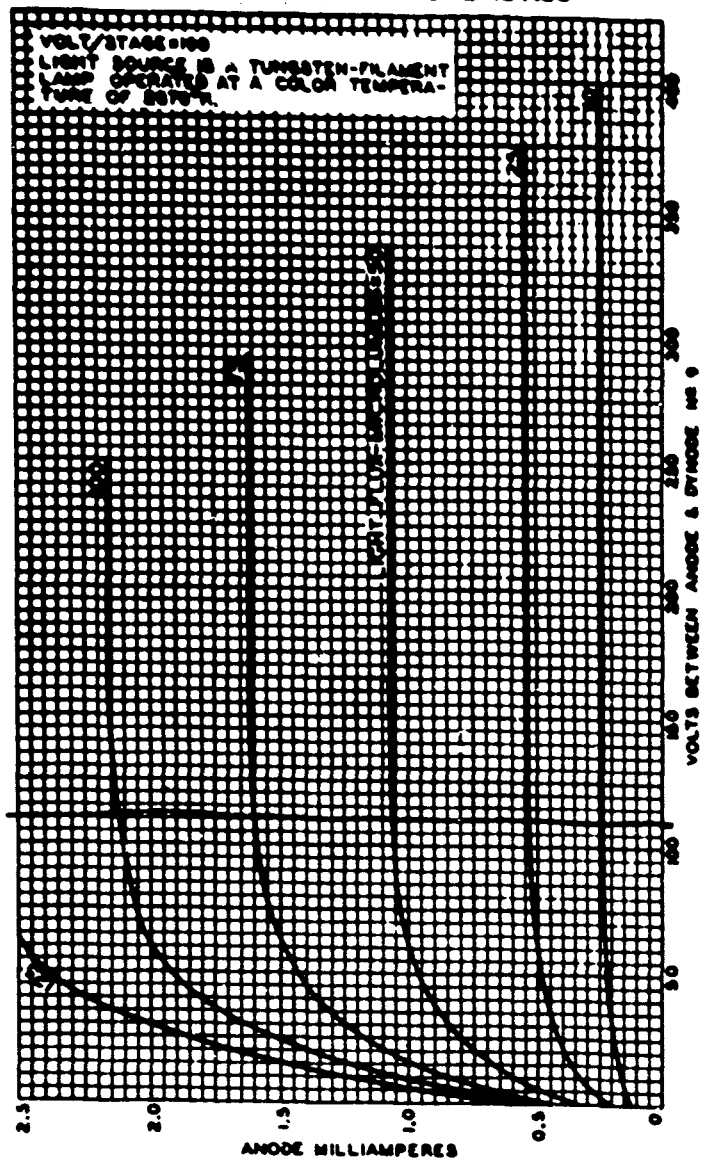

Figure 5-55a. 931-A Photomultiplier Characteristics

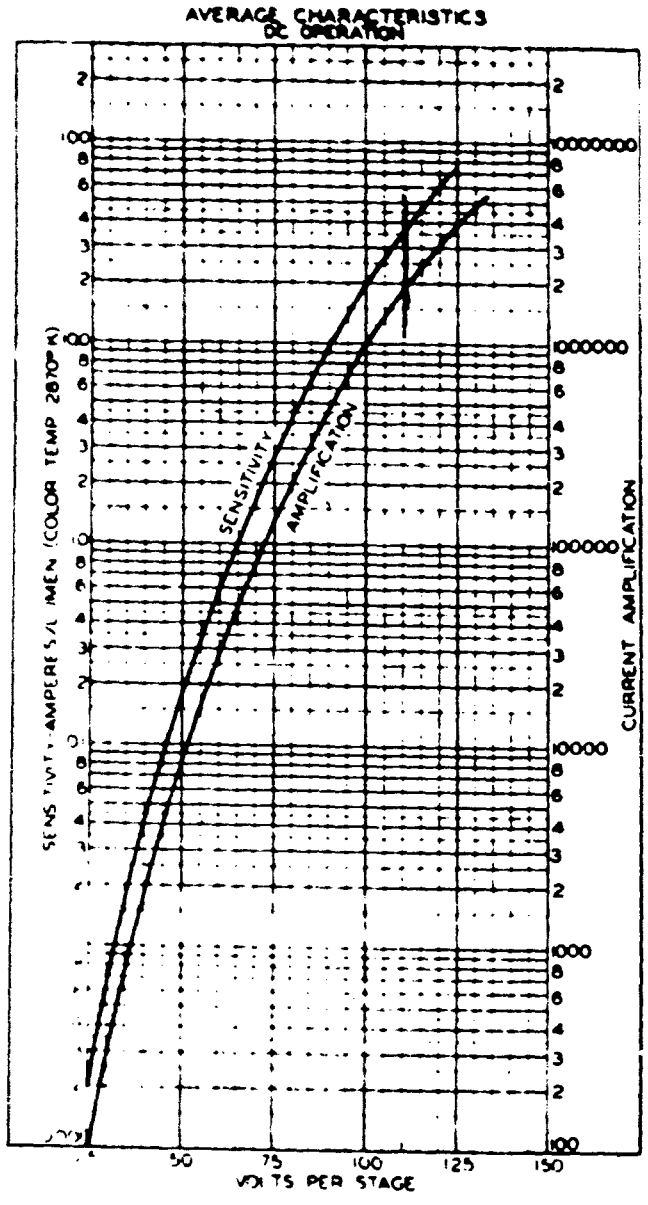

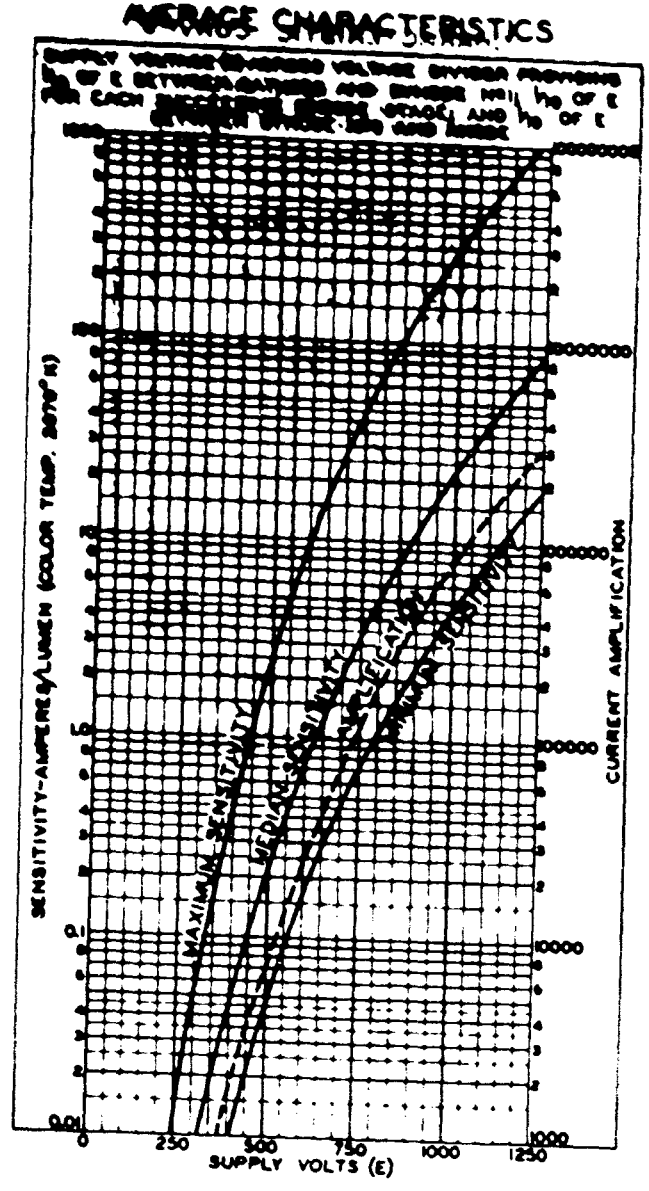

Figure 5-55b. 931-A Photomultiplier Characteristics

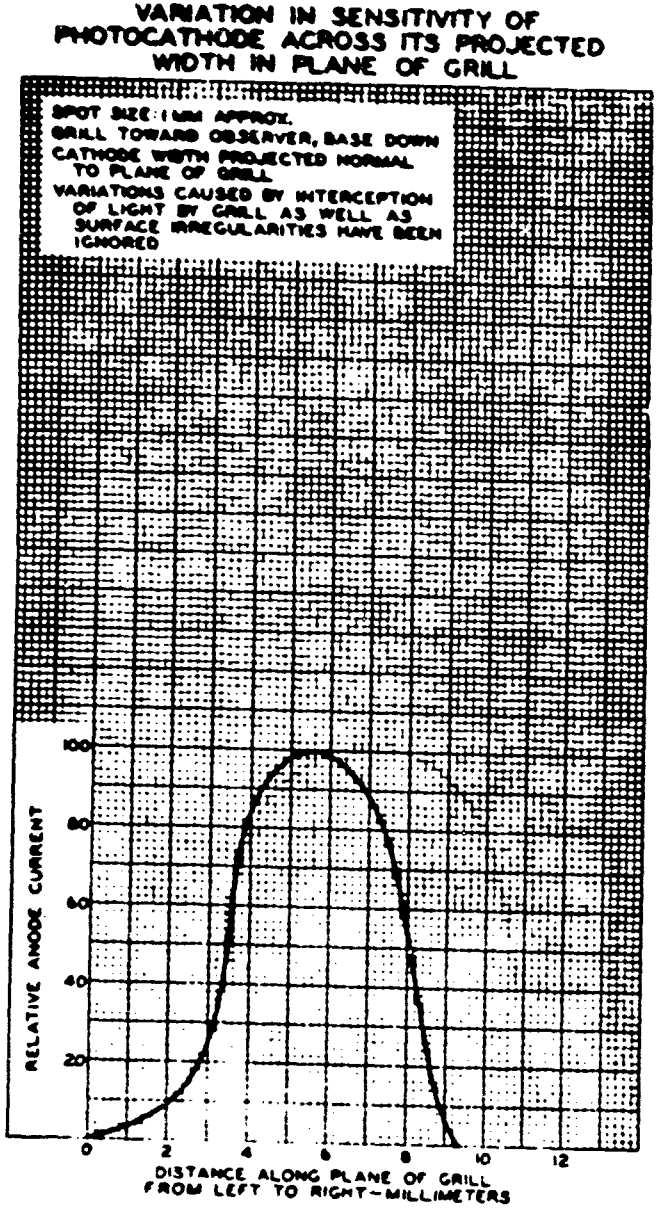

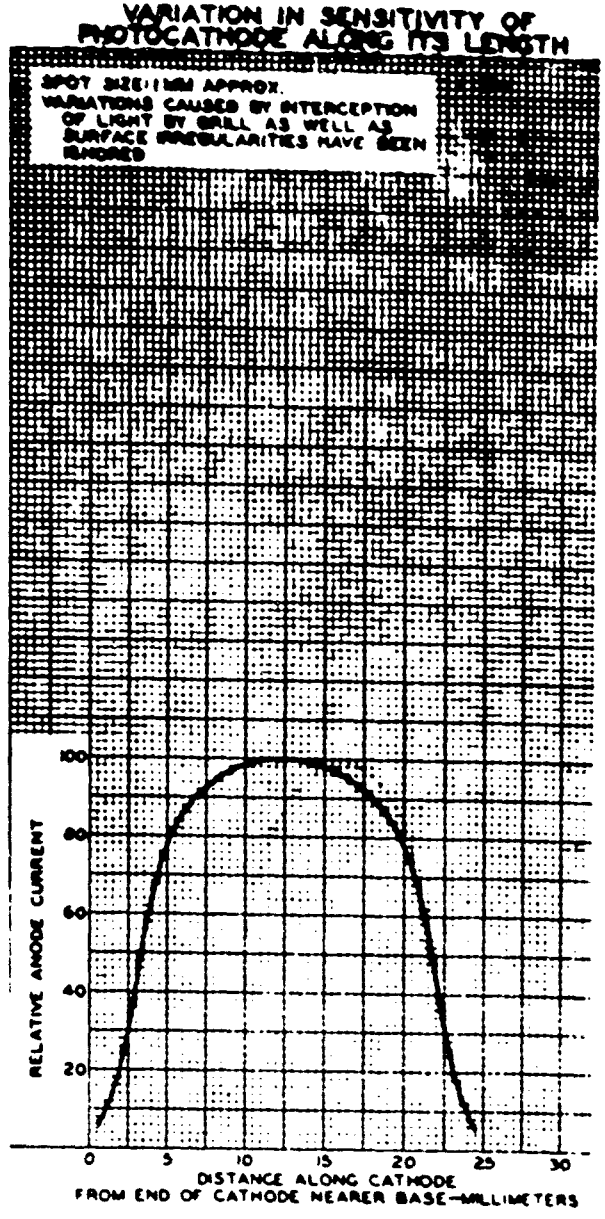

Figure 5-55c. 921-A Photomultiplier Characteristics

The quantum yield, i.e., the number of electrons emitted for a given number of absorbed light quanta, increases monotonically with decreasing wavelength (increasing energy) as illustrated in Figure 5-57. For commercial phototubes, this yield is approximately 5%. The photoelectric cathode to first dynode current, I_c is generally proportional to the illumination, φ, of the cathode.

$$I_c = S\,\varphi \tag{5-74}$$

where S is the sensitivity, the magnitude of which depends upon the composition of the cathode surface, tube construction, and incident light wavelength. Since S can be expressed in either watts or amperes per lumen, the sensitivity can be expressed in amperes per watt (radiant sensitivity) or in amperes per lumen (luminous sensitivity); the variation of sensitivity with wavelength is given in Figure 5-58 for several types of photocathode surfaces; all phototubes are given an S number which indicates the characteristic response of that tube; hence, the current I_c for any illumination can be determined.

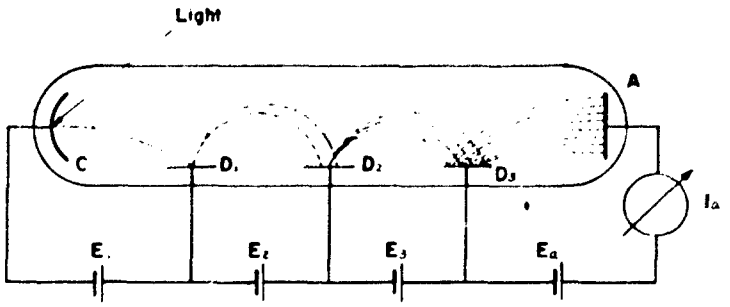

Figure 5-56. Photomultiplier, Schematic Diagram

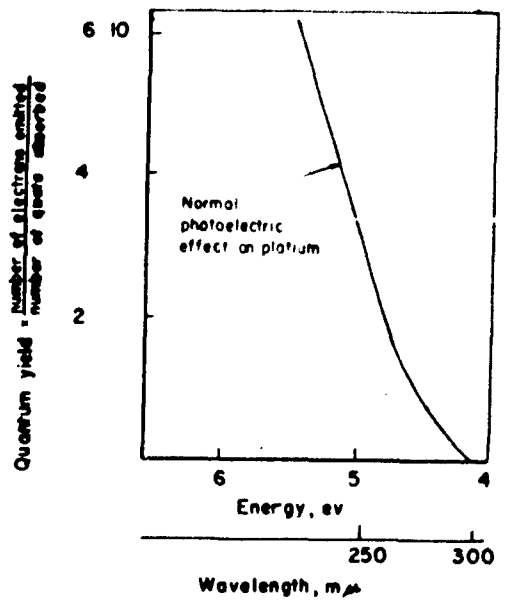

Figure 5-57. Quantum Yield for Photoelectric Emission

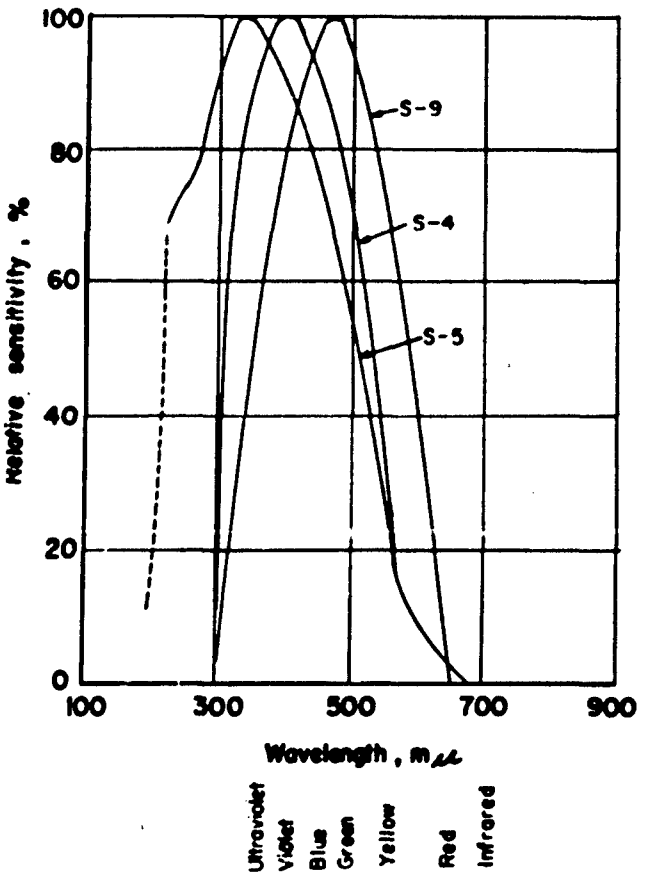

Figure 5-58. Relative Sensitivity of Different Commercial Photocathodes

The current output from the tube is a function of the number of dynode stages. If q is the number of secondary electrons emitted from a dynode per primary incident electron, a current amplification factor for n dynodes can be defined as:

$$A = q^n$$

the factor q depending on the E_{st} field between stages. C. C. Larson and H. Salinger give the gain analytically as:

$$q = k \sqrt{E_{st}}$$

where k is a constant. The relation is quite satisfactory for E_{st} less than 150v. Characteristic sensitivity and current amplification curves are given in Figures 5-54 and 5-55 for the photomultipliers used.

5. Photomultiplier Circuitry, 931-A

For stable operation, the 931-A anode current should be limited to 1.0 ma.; for ultra-stable operation, the anode current should be limited to less than 10 uA, as noted in Figure 5-55a. Hence, for stability, the maximum light flux input is 50 microlumens for any reasonable sensitivity and node to dynode 90 voltage (Figure 5-55b).

The first 931-A circuit used was similar to the circuit used by Baumann and is reproduced in Figure 5-59, the anode to ground resistor being 1M. E in the diagram is left as a variable, but is generally on the order of 1100 v. Experimental results indicated that the megohm resistor was too large when connected with a shunt capacitance of 20 μ farads (the approximate magnitude of an oscilloscope input capacitance). Such a connection gives a frequency response of

$$f_c = \frac{1}{2\pi RC} = 10 \text{ kc}$$

which is insufficient. Therefore, the load resistor was changed to 20 k, resulting in a suitable frequency response of 400 kc. All data taken in Chapter 6 was accomplished with the 20 k resistor.

6. Photomultiplier Output Amplifier

Upon recommendation of Mr. P. J. Parker*, it was decided to limit the anode current to 40 microamps, or in effect, limit the incident light to .2 microlumens, corresponding to a final output voltage of .8 volts which is too small for use with NOEL I circuitry. Accordingly, Mr. Parker also provided a signal amplifier, the schematic of which is given in Figure 5-60. While this arrangement provided a satisfactory frequency response, the problem of a positive voltage over-shoot arose, thus making unavailable to the computer part of the net signal voltage. Despite this defect, the amplifier was invaluable to our experimental work.

An amplifier (Figure 5-61) better matched to the problem has been designed by P. Marcus[30] as a result of his study of the positive voltage over-shoot problem. Figure 5-62 gives the schematic amplifier design used with the scanners to obtain part of the data of Chapter 6.

* D. J. Parker, Manager, Applied Physics of Applied Research, RCA, Camden 2, N. J.

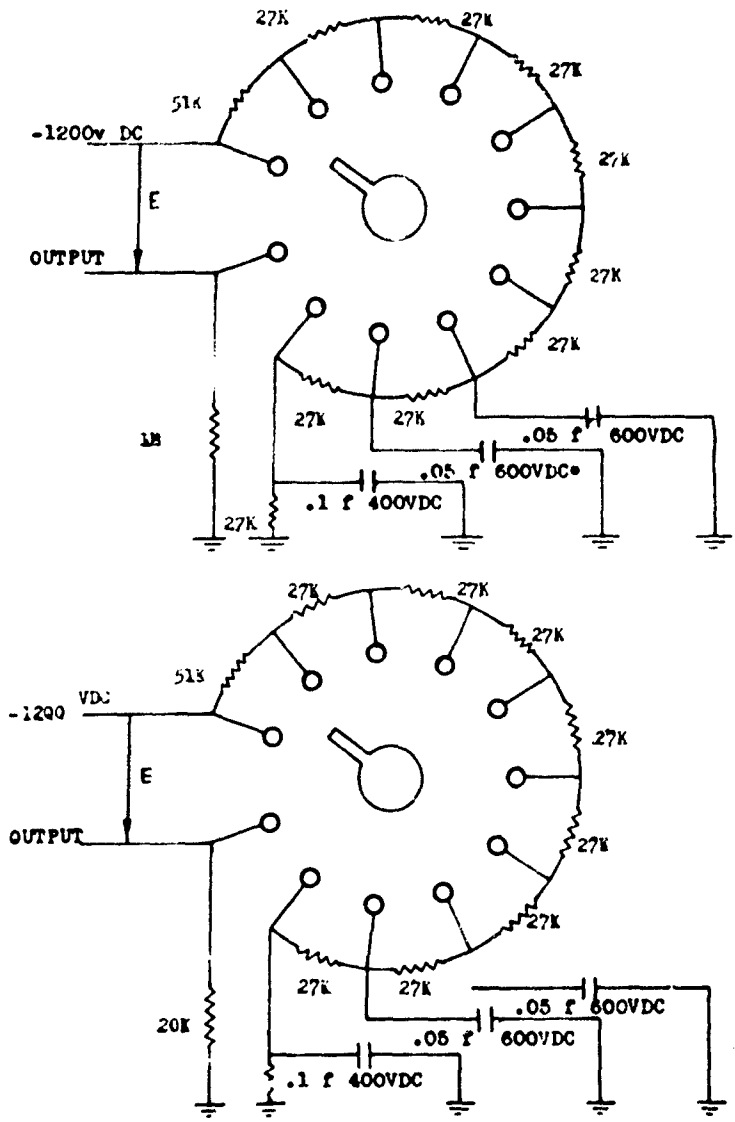

Figure 5-59. RCA 931-A Photomultiplier Tube Circuit

7. Photomultiplier Power Supply

The maximum voltage required for either photomultiplier is 1500 VDC as noted in Figures 5-54 and 5-55. To this end, the power supply diagramed in Figure 5-63 and shown in Figure 5-64 was designed and constructed. The input 117 VAC first passes through a variable output ac transformer before entering the level change and rectifying circuit, thereby providing a means of regulating the supply output voltage, hence the photomultiplier sensitivity. The power supply was attached to a 12 x 19 inch rack panel in such a manner that the assembly could be rack-mounted or table-mounted, as required. Voltage and current meters were also panel-mounted to facilitate experimental data taking. Since the unit served both the dove and the drum systems, connections were with pin-type and standard two prong plugs.

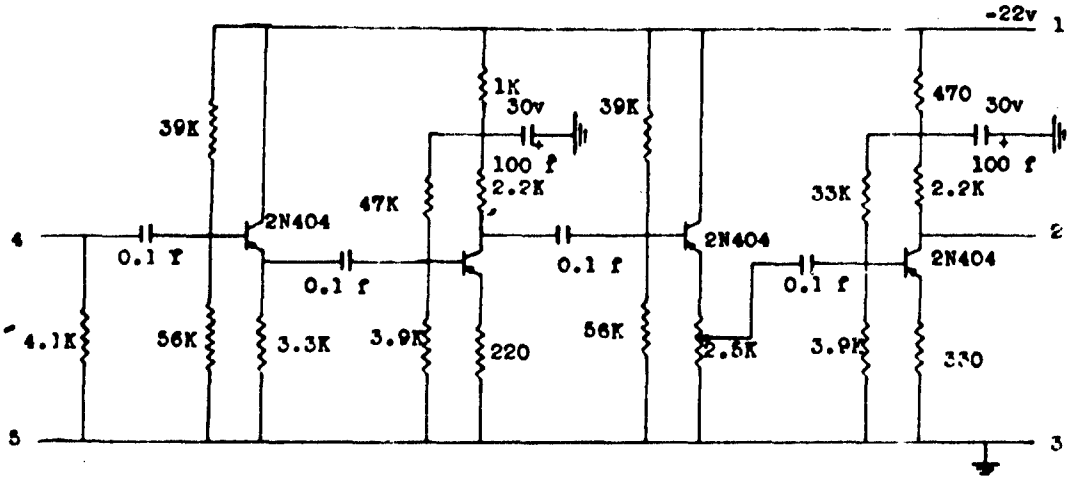

ALL RESISTORS 10%, 1/2W
Potentiometer 1/3W

1-3: POWER INPUT

4-5: SIGNAL INPUT

2-3: SIGNAL OUTPUT

Figure 5-60.

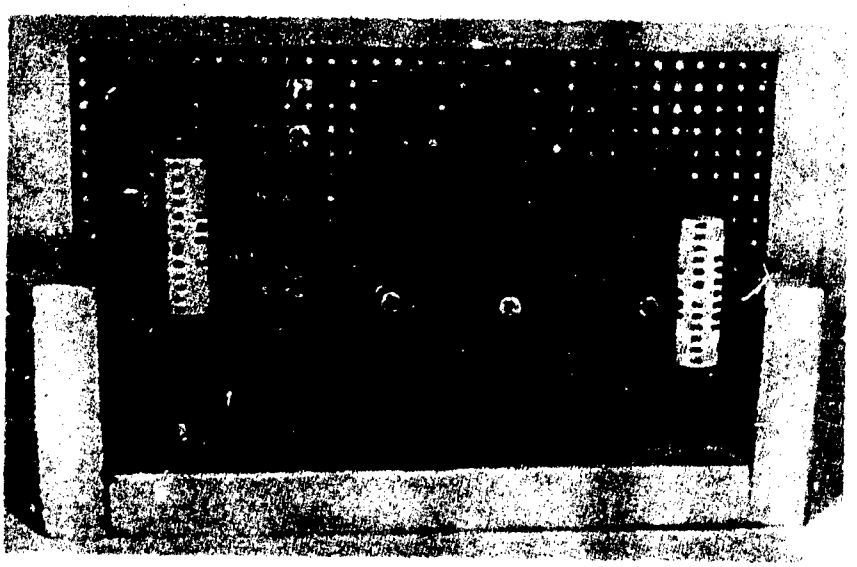

Figure 5-61. Output Amplifier

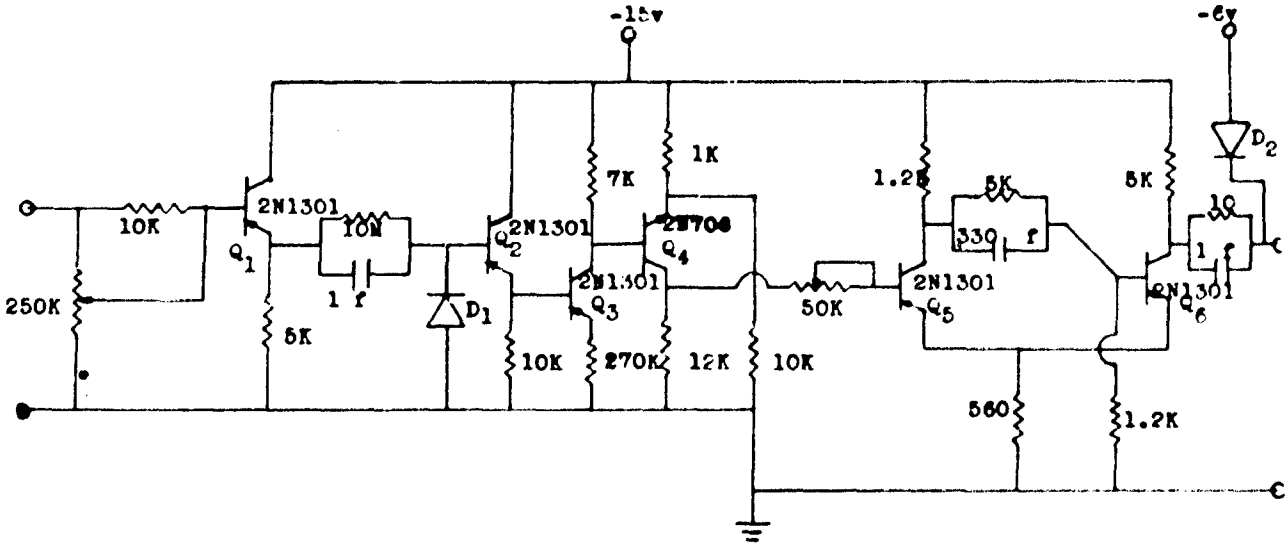

Figure 5-62.

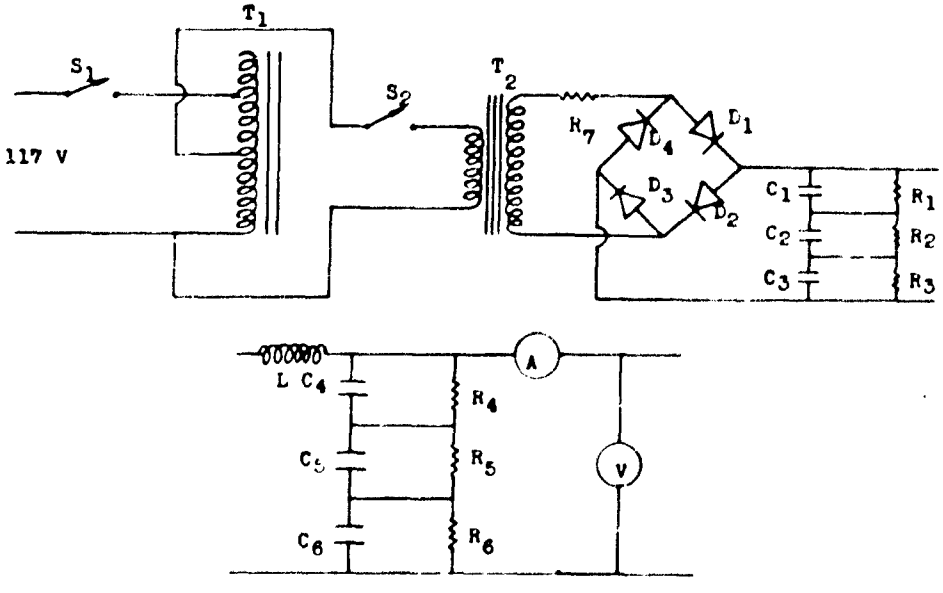

T_1 : VARIAC
T_2 : TRANSFORMER
L_1 : INDUCTANCE 10.5 110ma
D_1, D_2, D_3, D_4: 1N1410

$C_1, C_2, C_3, C_4, C_5, C_6$: 90mf, 500v

$R_1, R_2, R_3, R_4, R_5, R_6$: 100K, 2 Wat ± 10%
R_7 : 100 1/2Watts

Figure 5-63.

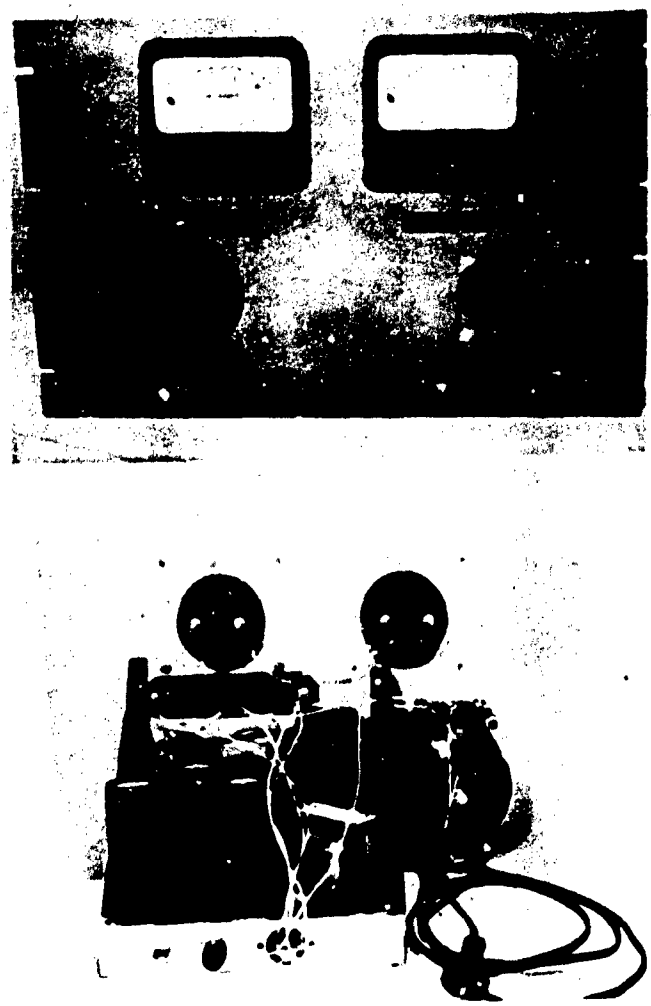

Figure 5-64. Front and Rear Views of the Photomultiplier Tube and Scanner Power Supply Unit

8. Scanner Motor and Controls

The motor used by both the dove and drum scanners is the universal series wound NSE-13 made by Bodine. The motor is self-ventilated, operating at speeds up to 10,000 rpm, and having a rated power output of 1/7 hp; shaft rotation is in the clockwise direction. The physical size is 4 inches in diameter by 4-7/8 inches in length, weight 5 pounds. Under normal operating conditions, continuous operation is allowed; for maximum duty, a duty cycle of 30 minutes on and 30 minutes off is recommended. Motor speed is controlled by a variable output ac transformer mounted on the control panel of the power supply unit (Figure 5-64).

E. EXPERIMENTAL RESULTS

1. Experimental Results of Drum Data Retrieval System

The following results were obtained by using a dual beam Tektronix Type 555 Oscilloscope. Photomultiplier and amplifier output were displayed on upper and lower beams respectively; vertical and horizontal sensitivities for both channels are indicated on the data sheets. Data has been arranged according to increasing bit density as well as increasing drum speed. For instance, A-120 is the first data sheet of 120 bit per inch film at the lowest speed for which data was taken; C-120 is the fastest speed for which data was taken from the same film. Bit density is defined as the number of clear lines per linear inch of film.

Geometrical information concerning the different films used is given in the following table.

FILMS USED TO OBTAIN DATA FROM DRUM SCANNER

Film Density	Bit Size	Spacing
90	.0042 x .073	.0068
120	.0033 x .050	.0049
170	.0020 x .036	.0032
300	.0018 x .016	.0014
600	.0009 x .008	.0007

For experimental purposes, most of the drum perimeter was masked such that only a short block of information was being read. The upper trace of the top picture on each data sheet was used to calculate drum speed since the horizontal distance between the greatly compressed blocks of pulses represents the time required for one revolution, the exception to this procedure being data sheet C-170. Field magnification was constant at 12.0X for films ranging from 90 bits per inch to 300 bits per inch, but was increased to 15.6X for 600 bits per inch. Multiplier operating voltages ranged from 700 to 1300 v.

DRUM DATA RETRIEVAL SYSTEM

DATA SHEET A-90

PHOTOMULTIPLIER OUTPUT

X axis: 10 m sec/cm
Y axis: 10 v/cm
Y axis zero: 4.75 cm

AMPLIFIER OUTPUT

X axis: 50 μ sec/cm
Y axis: 10 v/cm
Y axis zero: 1.75 cm

DRUM RPM:
984

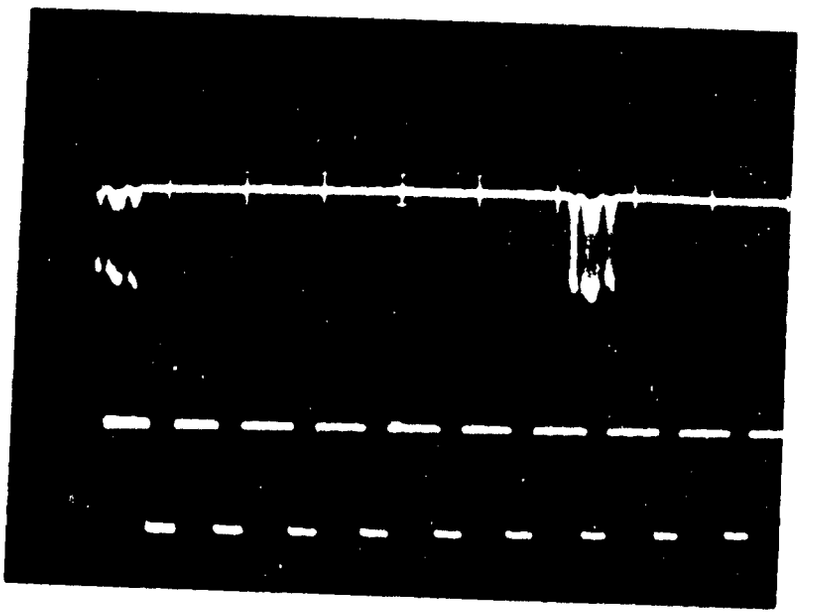

PHOTOMULTIPLIER OUTPUT

X axis: 0.1 m sec/cm
Y axis: 10 v/cm
Y axis zero: 4.75 cm

AMPLIFIER OUTPUT

X axis: 0.1 m sec/cm
Y axis: 10 v/cm
Y axis zero: 1.75 cm

DRUM RPM:

984

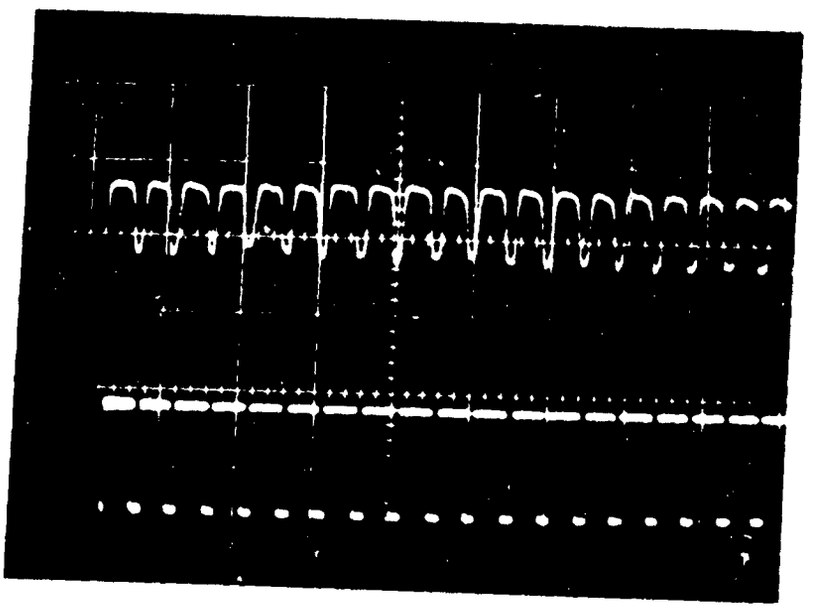

Figure 5-65.

DRUM DATA RETRIEVAL SYSTEM

DATA SHEET B-90

PHOTOMULTIPLIER OUTPUT

X axis: 10 m sec/cm
Y axis: 10 v/cm
Y axis zero: 4.75 cm

AMPLIFIER OUTPUT

X axis: 20 μ sec/cm
Y axis: 10 v/cm
Y axis zero: 1.75 cm

DRUM RPM
1500

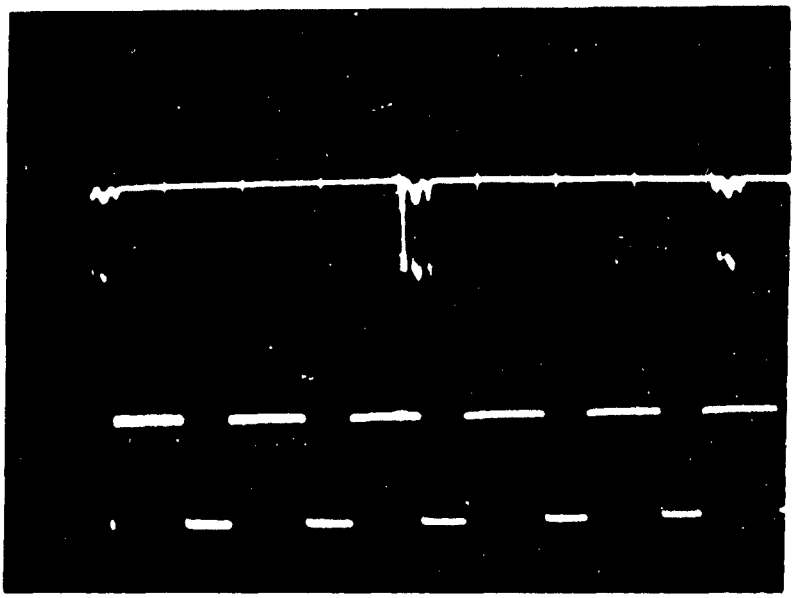

PHOTOMULTIPLIER OUTPUT

X axis: 50 μ sec/cm
Y axis: 10 v/cm
Y axis zero: 4.75 cm

AMPLIFIER OUTPUT

X axis: 50 μ sec/cm
Y axis: 10 v/cm
Y axis zero: 1.75 cm

DRUM RPM
1500

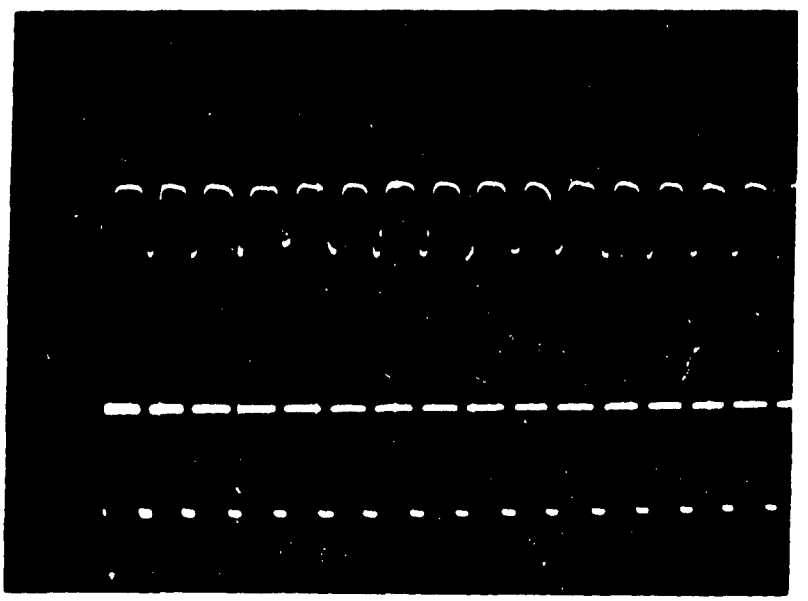

Figure 5-66.

DRUM DATA RETRIEVAL SYSTEM

DATA SHEET C-90

PHOTOMULTIPLIER OUTPUT

X axis: 10 m sec/cm
Y axis: 10 v/cm
Y axis zero: 4.75 cm

AMPLIFIER OUTPUT

X axis: 10 μ sec/cm
Y axis: 10 v/cm
Y axis zero: 1.75 cm

DRUM RPM
2610

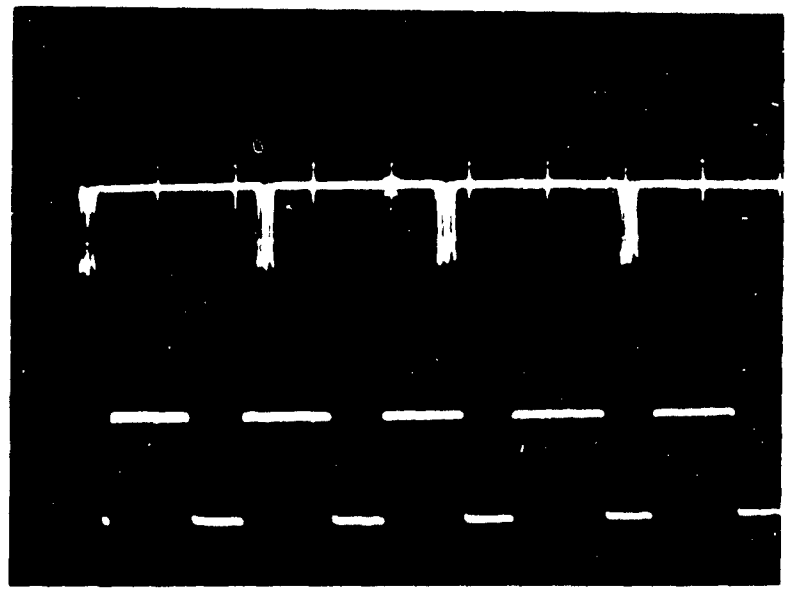

PHOTOMULTIPLIER OUTPUT

X axis: 20 μ sec/cm
Y axis: 10 v/cm
Y axis zero: 4.75 cm

AMPLIFIER OUTPUT

X axis: 20 μ sec/cm
Y axis: 10 v/cm
Y axis zero: 1.75 cm

DRUM RPM
2610

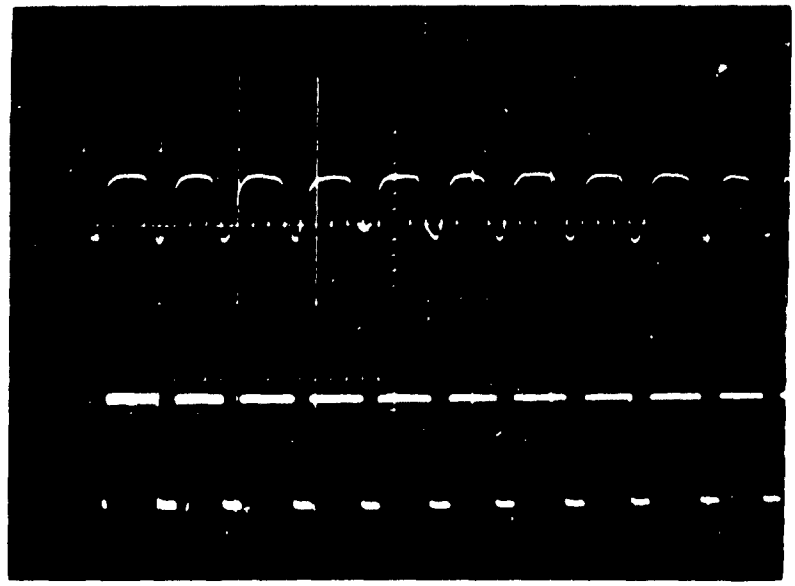

Figure 5-67.

DRUM DATA RETRIEVAL SYSTEM

DATA SHEET A-120

PHOTOMULTIPLIER OUTPUT

X axis: 20 m sec/cm
Y axis: 5 v/cm
Y axis zero: 4.[illegible] cm

AMPLIFIER OUTPUT

X axis: 20 μ sec/cm
Y axis: 10 v/cm
Y axis zero: 2 cm

DRUM REV
1070

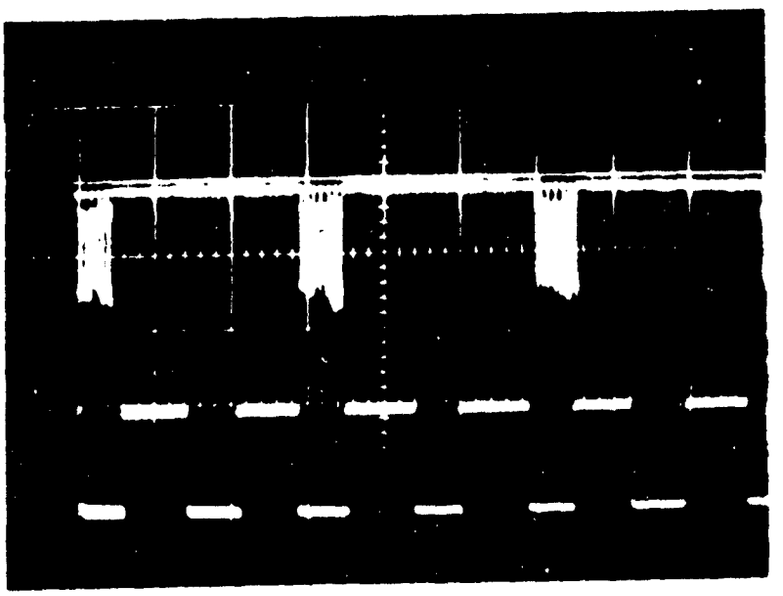

PHOTOMULTIPLIER OUTPUT

X axis: 50 μ sec/cm
Y axis: 10 v/cm
Y axis zero: 4.75 cm

AMPLIFIER OUTPUT

X axis: 50 μ sec/cm
Y axis: 10 v/cm
Y axis zero: 1.[illegible] cm

DRUM REV
[illegible]

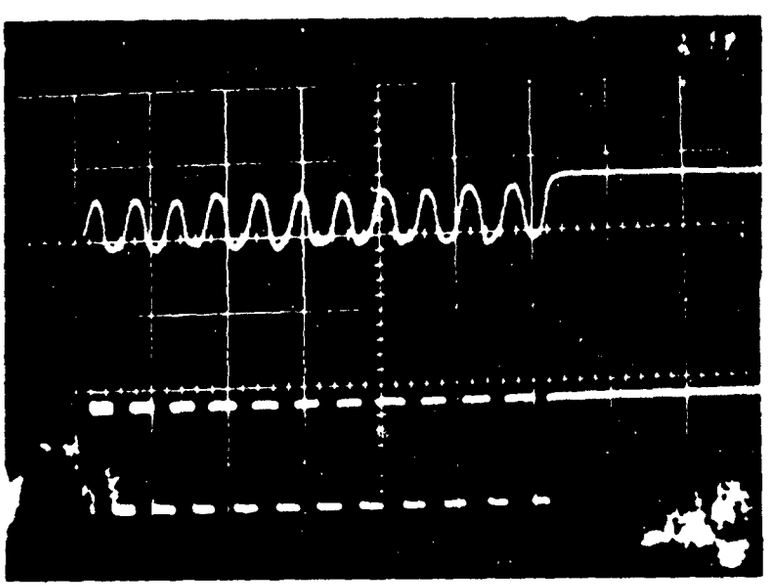

Figure 5-68.

DRUM DATA RETRIEVAL SYSTEM

DATA SHEET B-120

PHOTOMULTIPLIER OUTPUT

X axis: 20 m sec/cm
Y axis: 5 v/cm
Y axis zero: 4.8 cm

AMPLIFIER OUTPUT

X axis: 20 μ sec/cm
Y axis: 10 v/cm
Y axis zero: 2 cm

DRUM RPM
1665

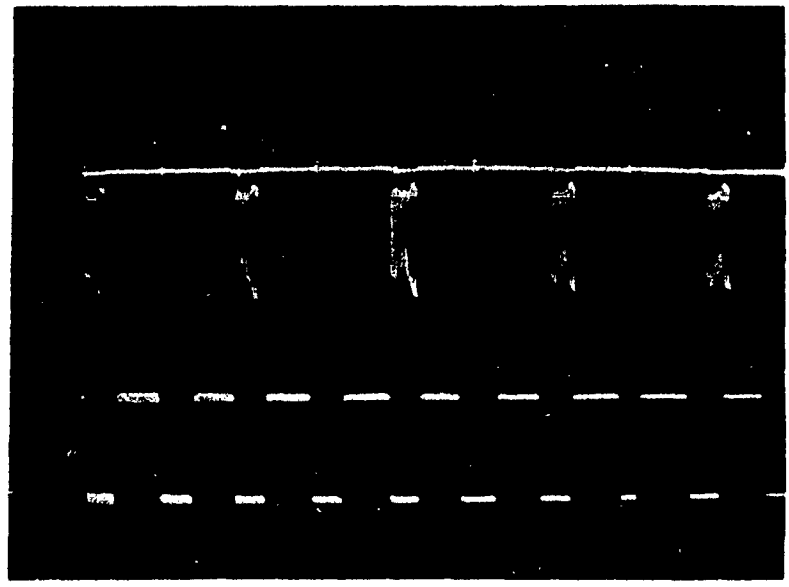

PHOTOMULTIPLIER OUTPUT

X axis: 20 μ sec/cm
Y axis: 10 v/cm
Y axis zero: 4.8 cm

AMPLIFIER OUTPUT

X axis: 20 μ sec/cm
Y axis: 10 v/cm
Y axis zero: 1.8 cm

DRUM RPM
1665

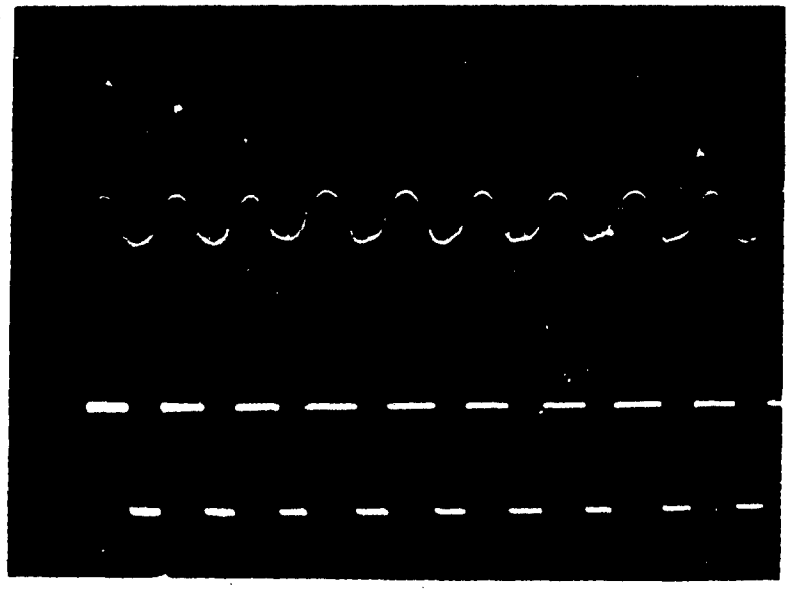

Figure 5-69.

DRUM DATA RETRIEVAL SYSTEM

DATA SHEET C-120

PHOTOMULTIPLIER OUTPUT

X axis: 20 m sec/cm
Y axis: 5 v/cm
Y axis zero: 5 cm

AMPLIFIER OUTPUT

X axis: 10 μ sec/cm
Y axis: 10 v/cm
Y axis zero: 2 cm

DRUM RPM
2625

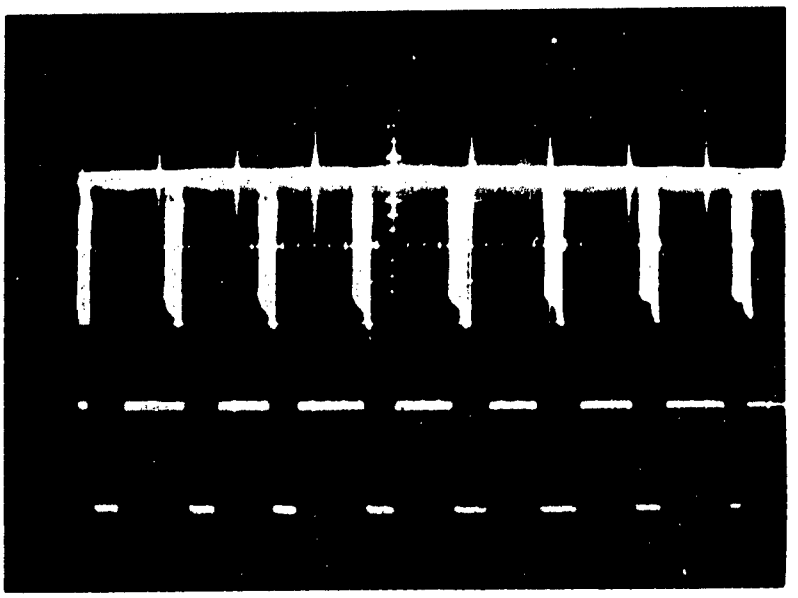

PHOTOMULTIPLIER OUTPUT

X axis: 20 μ sec/cm
Y axis: 10 v/cm
Y axis zero: 4.75 cm

AMPLIFIER OUTPUT

X axis: 20 μ sec/cm
Y axis: 10 v/cm
Y axis zero: 1.8 cm

DRUM RPM
2625

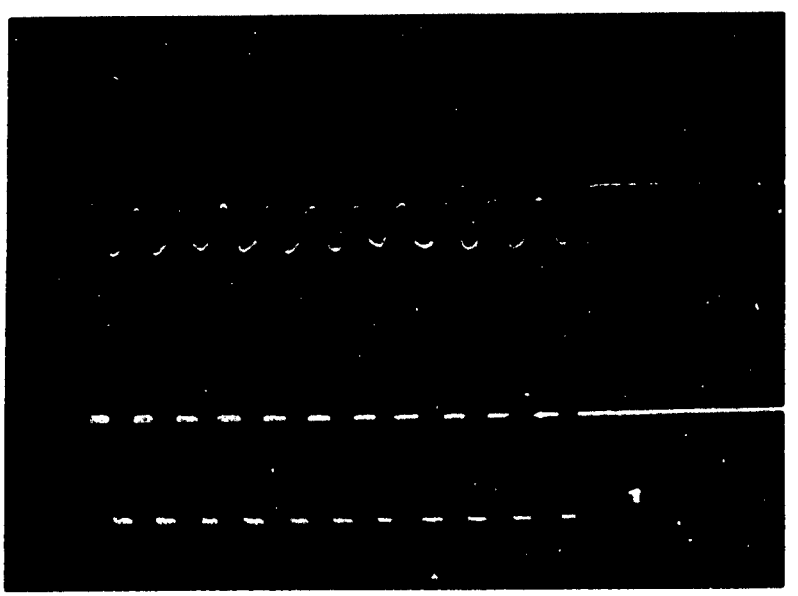

Figure 5-70.

DRUM DATA RETRIEVAL SYSTEM

DATA SHEET A-170

PHOTOMULTIPLIER OUTPUT

X axis: 10 m sec/cm
Y axis: 2 v/cm
Y axis zero: 4.3 cm

AMPLIFIER OUTPUT

X axis: 20 μ sec/cm
Y axis: 10 v/cm
Y axis zero: 1.5 cm

DRUM RPM
968

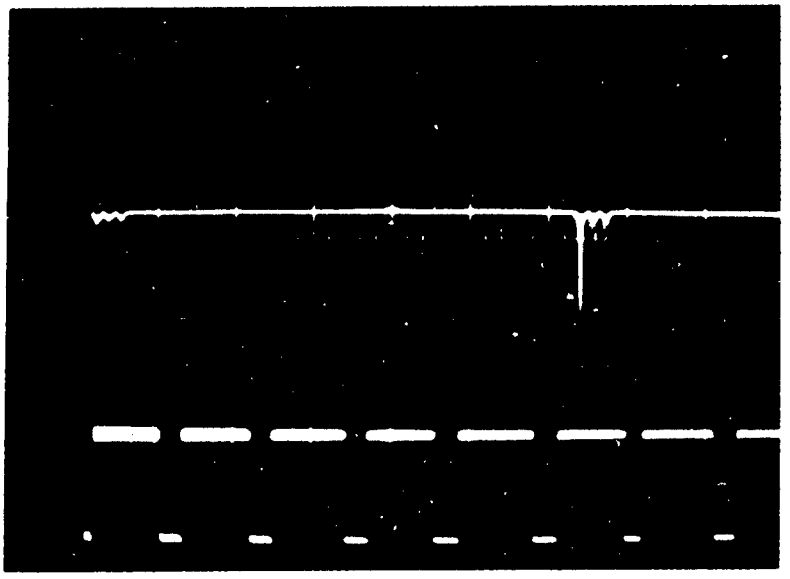

PHOTOMULTIPLIER OUTPUT

X axis: 50 μ sec/cm
Y axis: 10 v/cm
Y axis zero: 4.75 cm

AMPLIFIER OUTPUT

X axis: 50 μ sec/cm
Y axis: 10 v/cm
Y axis zero: 1.8 cm

DRUM RPM
968

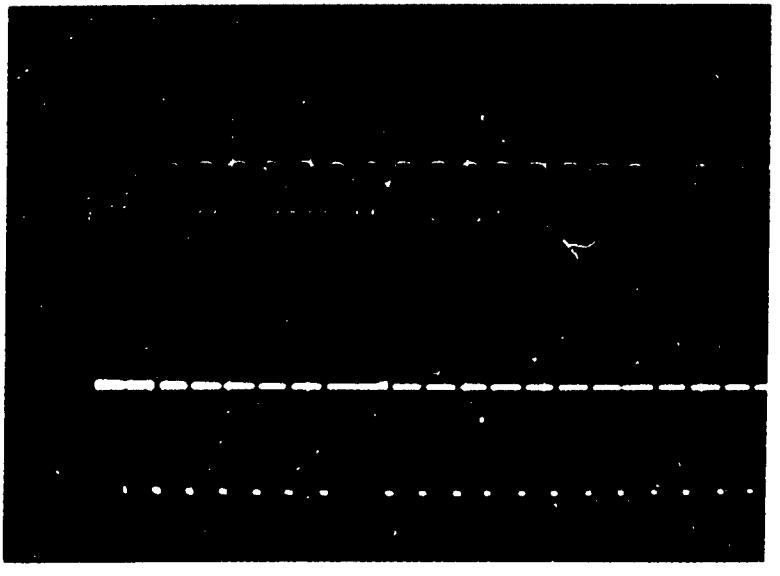

Figure 5-71.

PHOTOMULTIPLIER OUTPUT

X axis: 10 m sec/cm
Y axis: 10 v/cm
Y axis zero: 4.3 cm

AMPLIFIER OUTPUT

X axis: 10 μ sec/cm
Y axis: 10 v/cm
Y axis zero: 1.5 cm

DRUM RPM
1575

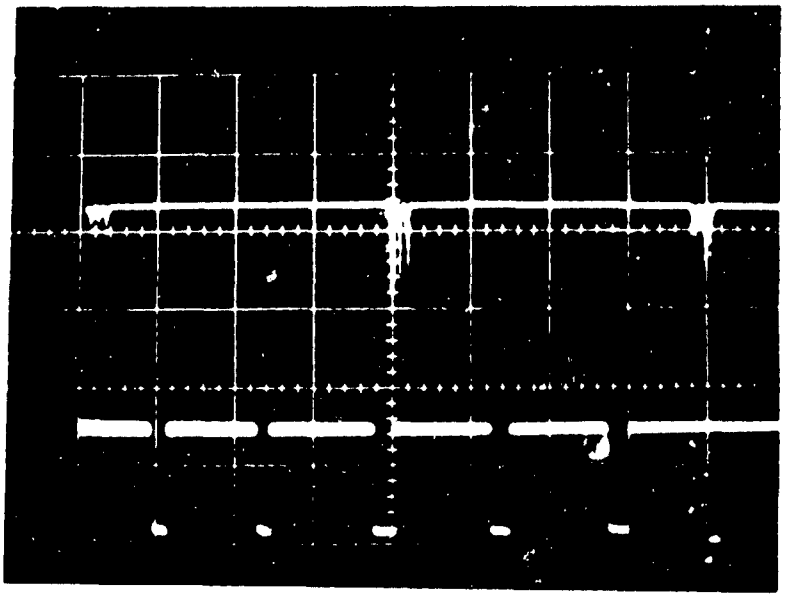

PHOTOMULTIPLIER OUTPUT

X axis: 50 μsec/cm
Y axis: 10 v/cm
Y axis zero: 4.75 cm

AMPLIFIER OUTPUT

X axis: 50 μsec/cm
Y axis: 10 v/cm
Y axis zero: 1.2 cm

DRUM RPM
1575

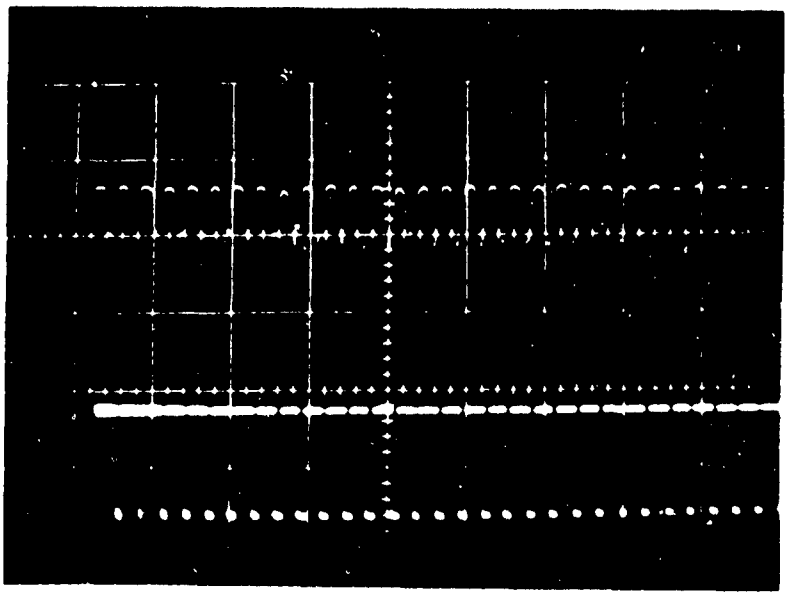

Figure 5-72.

DRUM DATA RETRIEVAL SYSTEM

DATA SHEET C-170

PHOTOMULTIPLIER OUTPUT

X axis: 5 μ sec/cm
Y axis: 10 v/cm
Y axis zero: 4.7 cm

AMPLIFIER OUTPUT

X axis: 5 μ sec/cm
Y axis: 10 v/cm
Y axis zero: 1.5 cm

DRUM RPM
2610

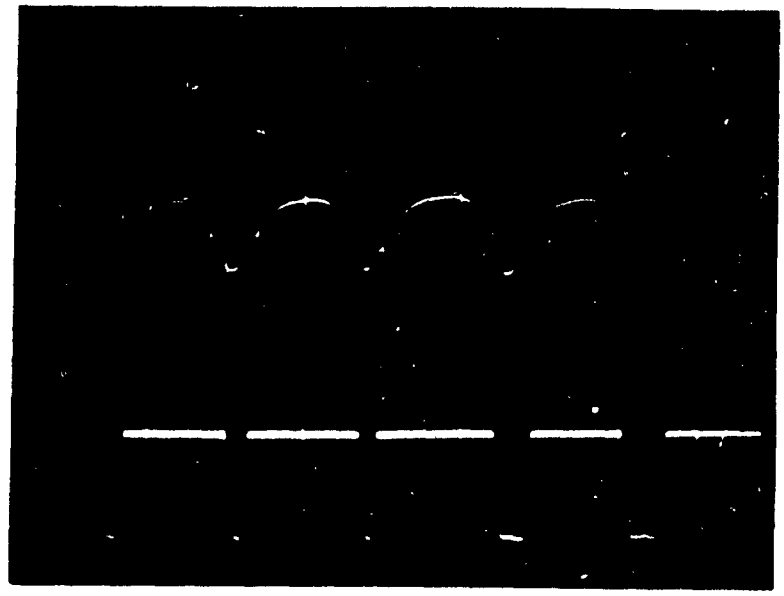

PHOTOMULTIPLIER OUTPUT

X axis: 20 μ sec/cm
Y axis: 10 v/cm
Y axis zero: 4.7 cm

AMPLIFIER OUTPUT

X axis: 20 μ sec/cm
Y axis: 10 v/cm
Y axis zero: 1.8 cm

DRUM RPM
2610

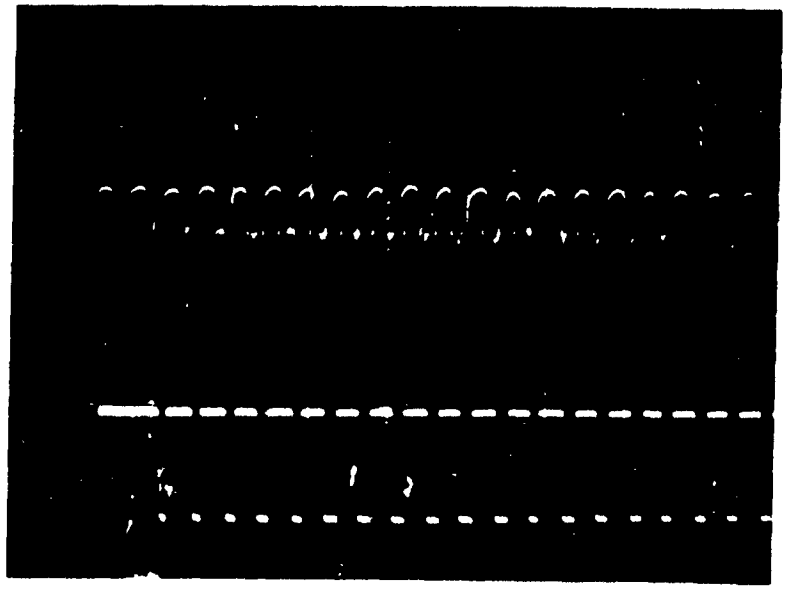

Figure 5-73.

DRUM DATA RETRIEVAL SYSTEM

DATA SHEET A-300

PHOTOMULTIPLIER OUTPUT

X axis: 10 m sec/cm
Y axis: 2 v/cm
Y axis zero: 4.8 cm

AMPLIFIER OUTPUT

X axis: 10 μ sec/cm
Y axis: 10 v/cm
Y axis zero: 1.9 cm

DRUM RPM
1000

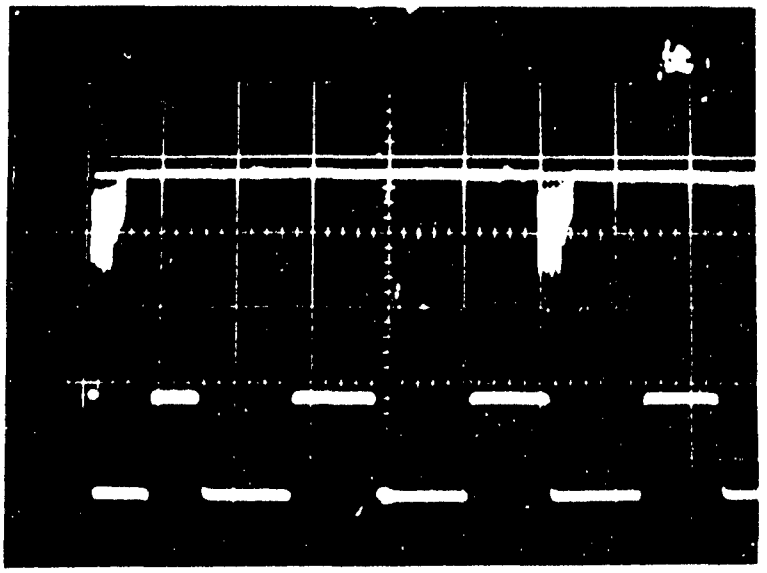

PHOTOMULTIPLIER OUTPUT

X axis: 20 μ sec/cm
Y axis: 10 v/cm
Y axis zero: 4.75 cm

AMPLIFIER OUTPUT

X axis: 20 μ sec/cm
Y axis: 10 v/cm
Y axis zero: 1.8 cm

DRUM RPM
1000

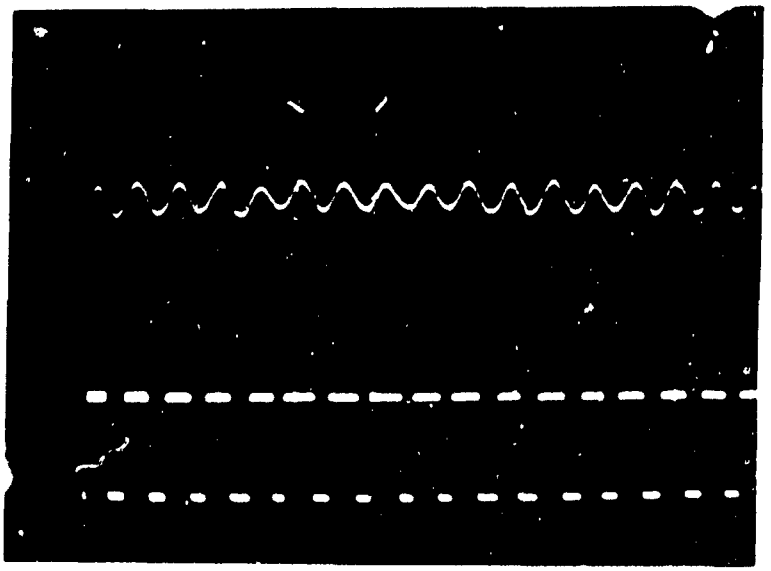

Figure 5-74.

DRUM DATA RETRIEVAL SYSTEM

DATA SHEET B-300

PHOTOMULTIPLIER OUTPUT

X axis: 10 m sec/cm
Y axis: 1 v/cm
Y axis zero: 4.8 cm

AMPLIFIER OUTPUT

X axis: 5 μ sec/cm
Y axis: 1 v/cm
Y axis zero: 1.9 cm

DRUM RPM
1500

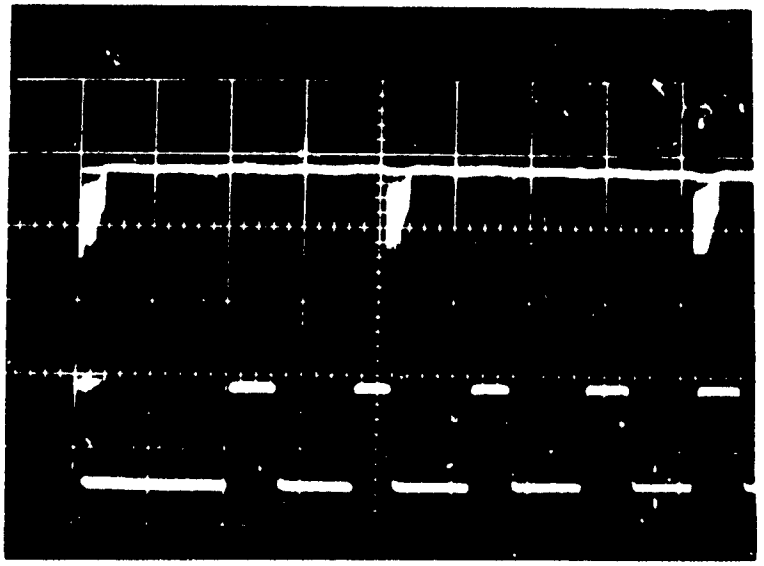

PHOTOMULTIPLIER OUTPUT

X axis: 20 μ sec/cm
Y axis: 5 v/cm
Y axis zero: 4.6 cm

AMPLIFIER OUTPUT

X axis: 20 μ sec/cm
Y axis: 10 v/cm
Y axis zero: 1.8 cm

DRUM RPM
1500

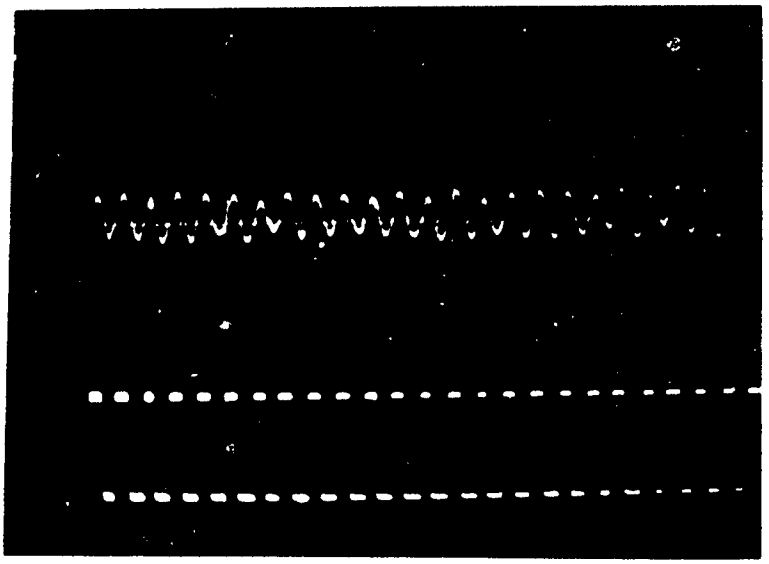

Figure 5-75.

DRUM DATA RETRIEVAL SYSTEM

DATA SHEET C-300

PHOTOMULTIPLIER OUTPUT

X axis: 10 m sec/cm
Y axis: 1 v/cm
Y axis zero: 5.2 cm

AMPLIFIER OUTPUT

X axis: 2 μsec/cm
Y axis: 10 v/cm
Y axis zero: 2.8 cm

DRUM RPM
2500

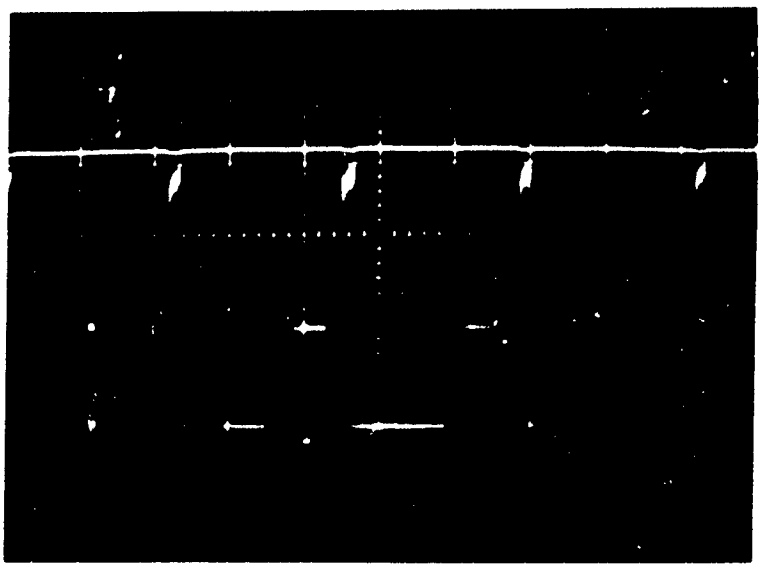

PHOTOMULTIPLIER OUTPUT

X axis: 10 μsec/cm
Y axis: 5 v/cm
Y axis zero: 4.3 cm

AMPLIFIER OUTPUT

X axis: 10 μsec/cm
Y axis: 10 v/cm
Y axis zero: 1.8 cm

DRUM RPM
2500

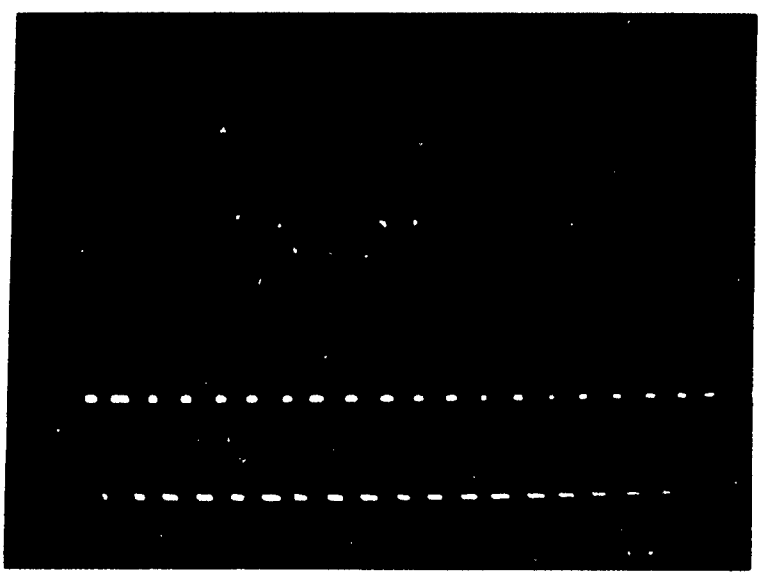

Figure 5-76.

DRUM DATA RETRIEVAL SYSTEM

DATA SHEET A-600

PHOTOMULTIPLIER OUTPUT

X axis: 10 μ sec/cm
Y axis: 1 v/cm
Y axis zero: 4.8 cm

AMPLIFIER OUTPUT

X axis: 10 μ sec/cm
Y axis: 10 v/cm
Y axis zero: 2.8 cm

DRUM RPM
1070

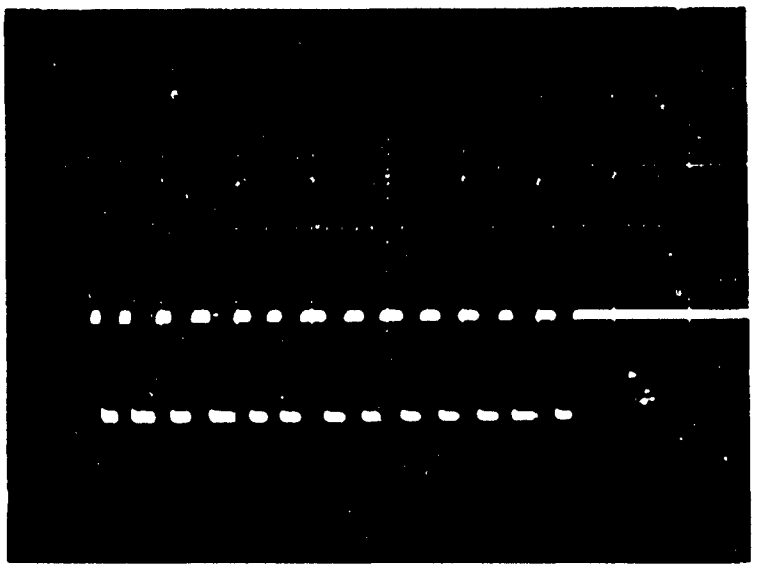

PHOTOMULTIPLIER OUTPUT

X axis: 10 μ sec/cm
Y axis: 1 v/cm
Y axis zero: 4.8 cm

AMPLIFIER OUTPUT

X axis: 10 μ sec/cm
Y axis: 10 v/cm
Y axis zero: 2.8 cm

DRUM RPM
1070

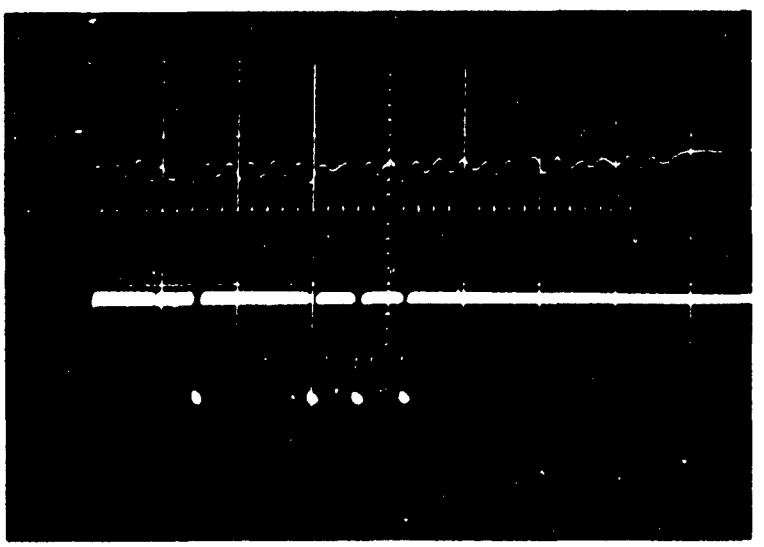

Figure 5-77.

2. Experimental Results of Dove Data Retrieval System

The data in this section was obtained from the dove scanner in a similar manner to that described in the preceding section, the exception being that the multiplier and amplifier output always have the same horizontal sensitivity for any one picture. Data sheets are arranged in sets according to increasing linear bit density each set being arranged according to increasing scanning head rpm. Two exceptions to this procedure are: the last picture on sheet C-90 and the data sheet D-90; and a second rpm series starting with the last picture on sheet C-300. The first exception was made in order to show the effect of photomultiplier aperture on pulse shape; the second to show the improvement in signal output when additional illumination is supplied to small bit patterns. More will be said about these two effects in the next section.

The field aperture used was determined by the field height of the film being scanned. Field height is defined here as the combined length of six bits and five spaces, a space being the distance between rows of bits. In general, the correct aperture, one which permits projection of at least the full field height, was used. However, an oversized field aperture was used for the second rpm series of data sheets 300, thereby simulating an increased arc lamp power output. The films used in this work were not dimensionally proportional, having been made from different 7090 film formats. For this reason the following table is given.

FILMS AND APERTURES USED TO OBTAIN DATA FROM DOVE SCANNER

Film	Field Aperture	Field Height	Bit Size
90	A	.671	.0042 x .073
120	A	.441	.0033 x .050
160	B	.302	.0016 x .036
240	B	.158	.0018 x .016
300	B and C	.151	.0021 x .021

While low density films permitted multiplier operating voltages of 900 to 1200 v for optimum output, higher density films required significantly higher voltages. For instance, a typical voltage of 1500 v was recorded for the data sheet C-240. In taking all data, the output amplifier gain and multiplier voltage were varied to obtain the best results.

DOVE DATA RETRIEVAL SYSTEM

DATA SHEET A-90

PHOTOMULTIPLIER OUTPUT

X axis: 50 μsec/cm
Y axis: 10 v/cm
Y axis zero: 5.8 cm

AMPLIFIER OUTPUT

X axis: 50 μsec/cm
Y axis: 10 v/cm
Y axis zero: 2.0 cm

SCANNING HEAD RPM
1645

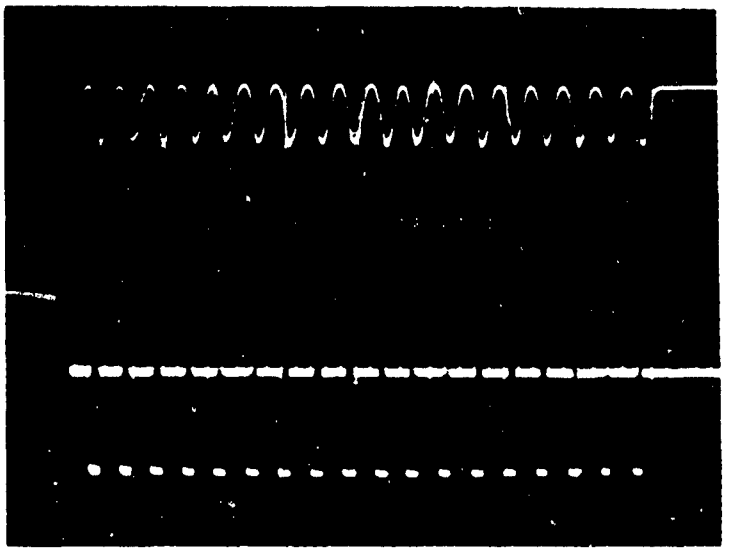

PHOTOMULTIPLIER OUTPUT

X axis: 20 μsec/cm
Y axis: 10 v/cm
Y axis zero: 5.8 cm

AMPLIFIER OUTPUT

X axis: 20 μsec/cm
Y axis: 10 v/cm
Y axis zero: 2.0 cm

SCANNING HEAD RPM
4115

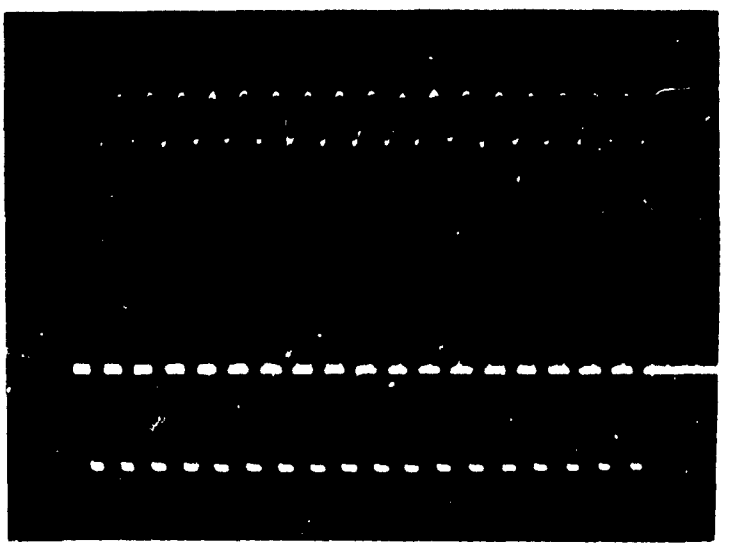

Figure 5-78.

DATA SHEET B-90

PHOTOMULTIPLIER OUTPUT

X axis: 10 μ sec/cm
Y axis: 10 v/cm
Y axis zero: 6.0 cm

AMPLIFIER OUTPUT

X axis: 10 μ sec/cm
Y axis: 10 v/cm
Y axis zero: 2.0 cm

SCANNING HEAD RPM
6180

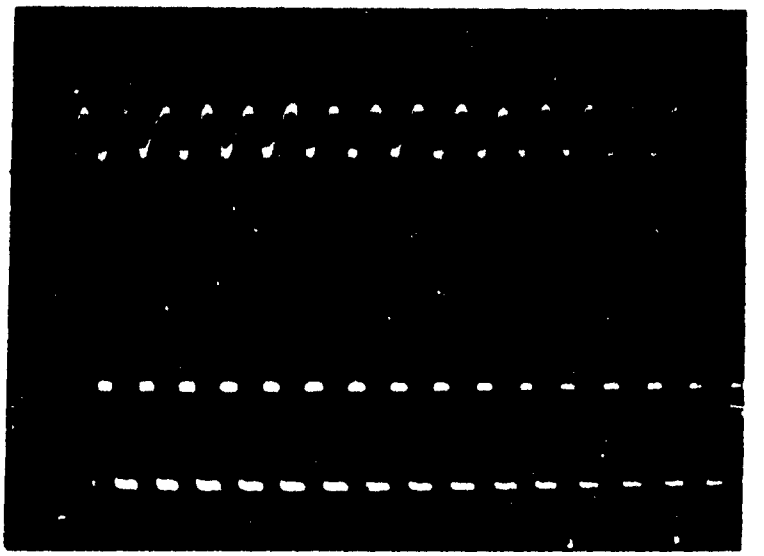

PHOTOMULTIPLIER OUTPUT

X axis: 5 μ sec/cm
Y axis: 10 v/cm
Y axis zero: 6.0 cm

AMPLIFIER OUTPUT

X axis: 5 μ sec/cm
Y axis: 10 v/cm
Y axis zero: 2.0 cm

SCANNING HEAD RPM
8060

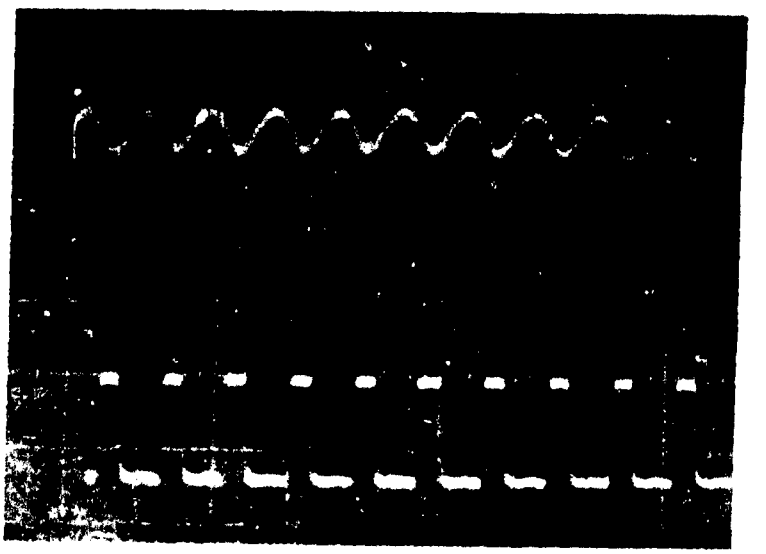

Figure 5-79.

DOVE DATA RETRIEVAL SYSTEM

DATA SHEET C-90

PHOTOMULTIPLIER OUTPUT

X axis: 5 μ sec/cm
Y axis: 10 v/cm
Y axis zero: 6.0 cm

AMPLIFIER OUTPUT

X axis: 5 μ sec/cm
Y axis: 10 v/cm
Y axis zero: 2.0 cm

SCANNING HEAD RPM
10,100

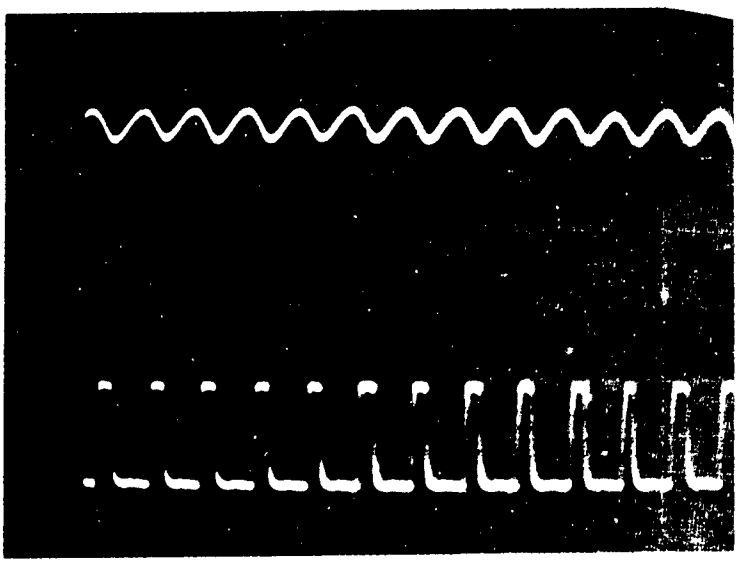

PHOTOMULTIPLIER OUTPUT

X axis: 50 μ sec/cm
Y axis: 5 v/cm
Y axis zero: 6.0 cm

AMPLIFIER OUTPUT

X axis: 50 μ sec/cm
Y axis: 10 v/cm
Y axis zero: 3.0 cm

SCANNING HEAD RPM
740

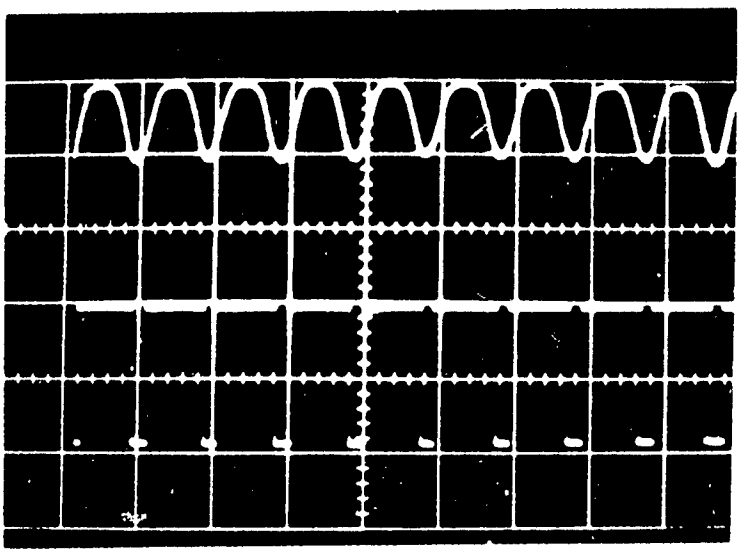

Figure 5-80.

DOVE DATA RETRIEVAL SYSTEM

DATA SHEET D-90

PHOTOMULTIPLIER OUTPUT

X axis: 10 μsec/cm
Y axis: 5 v/cm
Y axis zero: 5.6 cm

AMPLIFIER OUTPUT

X axis: 10 μsec/cm
Y axis: 10 v/cm
Y axis zero: 1.8 cm

SCANNING HEAD RPM
9880

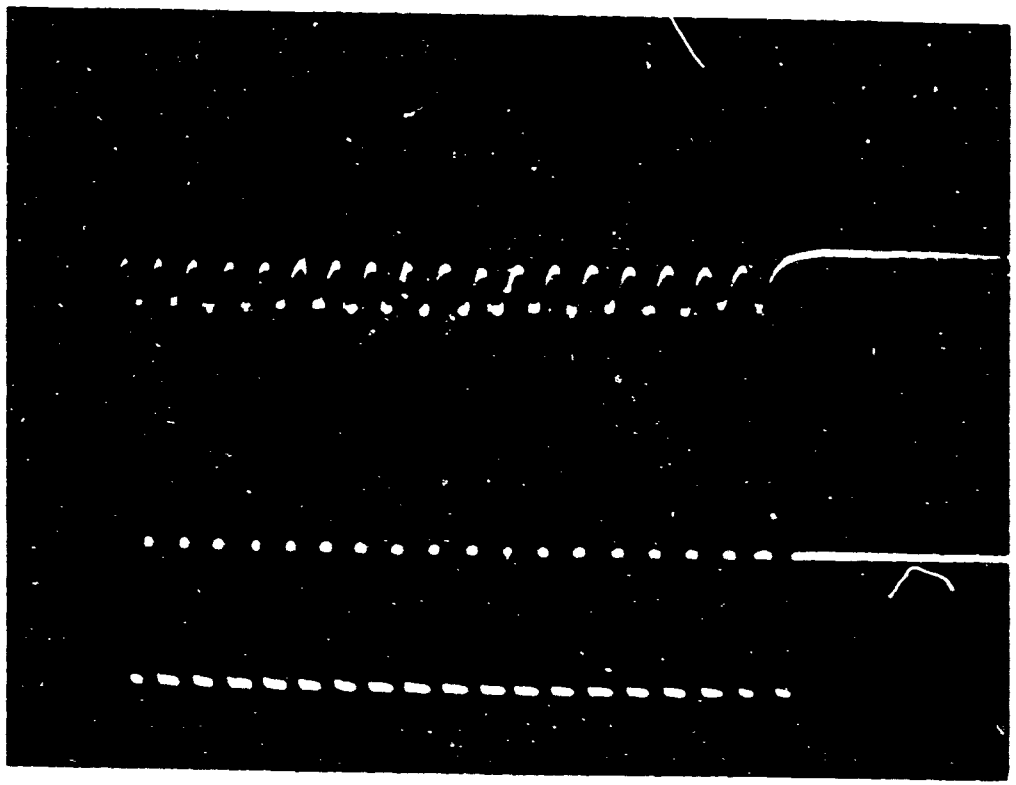

Figure 5-81.

DOVE DATA RETRIEVAL SYSTEM

DATA SHEET A-120

PHOTOMULTIPLIER OUTPUT

X axis: 20 μ sec/cm
Y axis: 10 v/cm
Y axis zero: 6.0 cm

AMPLIFIER OUTPUT

X axis: 20 μ sec/cm
Y axis: 10 v/cm
Y axis zero: 3.0 cm

SCANNING HEAD RPM:
1585

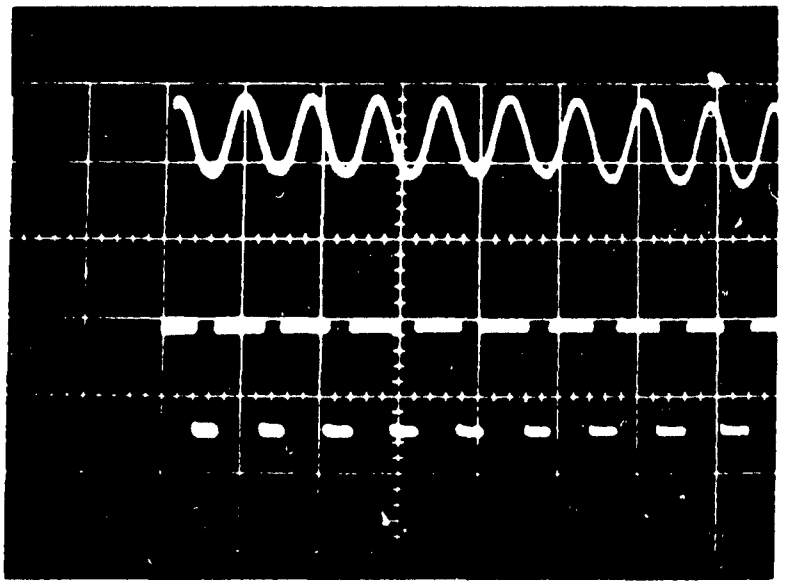

PHOTOMULTIPLIER OUTPUT

X axis: 10 μ sec/cm
Y axis: 10 v/cm
Y axis zero: 6.0 cm

AMPLIFIER OUTPUT

X axis: 10 μ sec/cm
Y axis: 10 v/cm
Y axis zero: 3.0 cm

SCANNING HEAD RPM:
4350

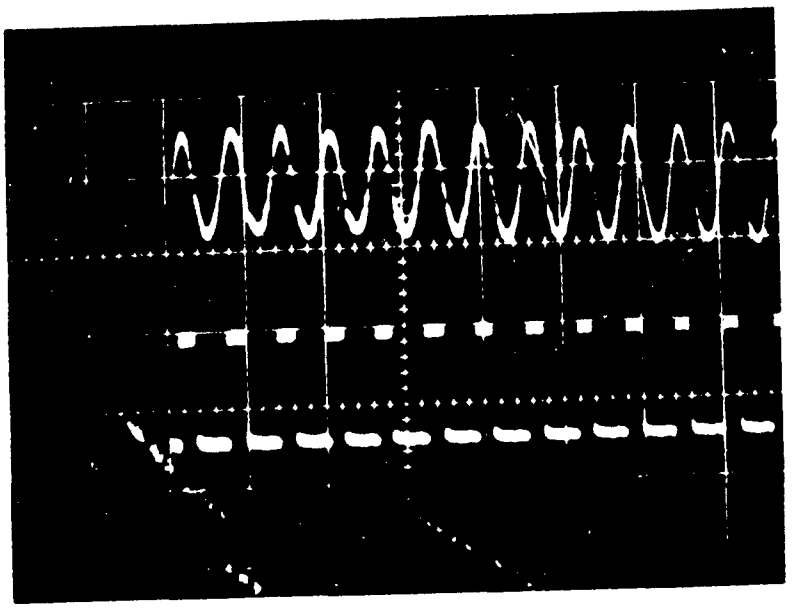

Figure 5-82.

DATA SHEET B-120

PHOTOMULTIPLIER OUTPUT

X axis: 5μ sec/cm
Y axis: 10 v/cm
Y axis zero: 6.0 cm

AMPLIFIER OUTPUT

X axis: 5μ sec/cm
Y axis: 10 v/cm
Y axis zero: 3.0 cm

SCANNING HEAD RPM
6200

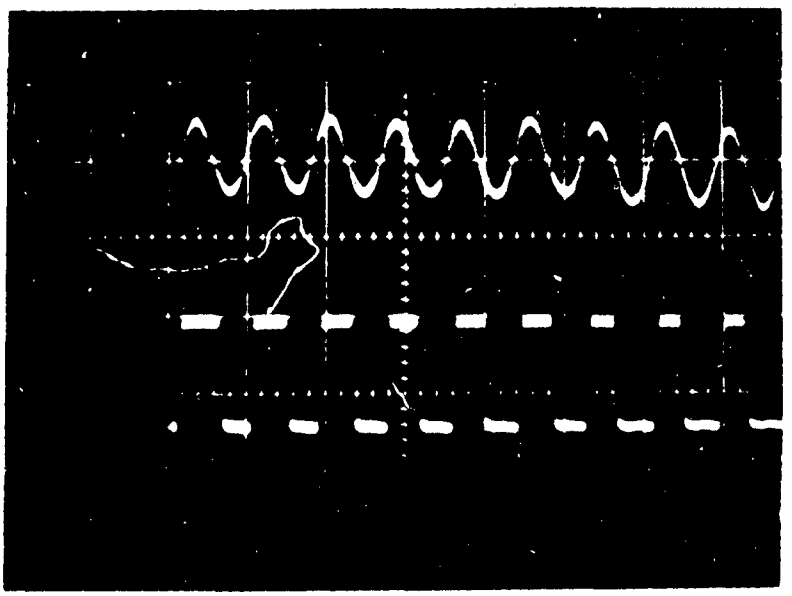

PHOTOMULTIPLIER OUTPUT

X axis: 5μ sec/cm
Y axis: 10 v/cm
Y axis zero: 6.0 cm

AMPLIFIER OUTPUT

X axis: 5μ sec/cm
Y axis: 10 v/cm
Y axis zero: 3.0 cm

SCANNING HEAD RPM
8500

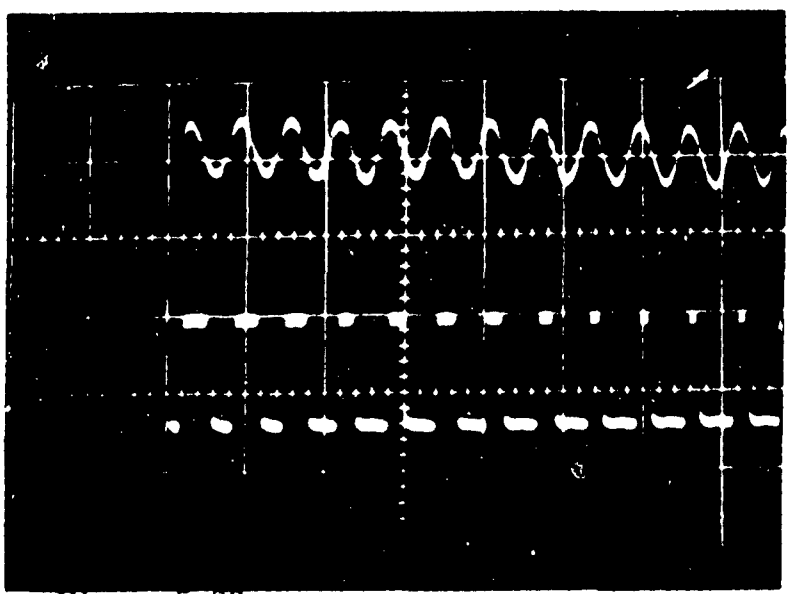

Figure 5-83.

DATA SHEET C-120

PHOTOMULTIPLIER OUTPUT

X axis: 2 μ sec/cm
Y axis: 10 v/cm
Y axis zero: 6.0 cm

AMPLIFIER OUTPUT

X axis: 2 μ sec/cm
Y axis: 10 v/cm
Y axis zero: 3.0 cm

SCANNING HEAD RPM
9830

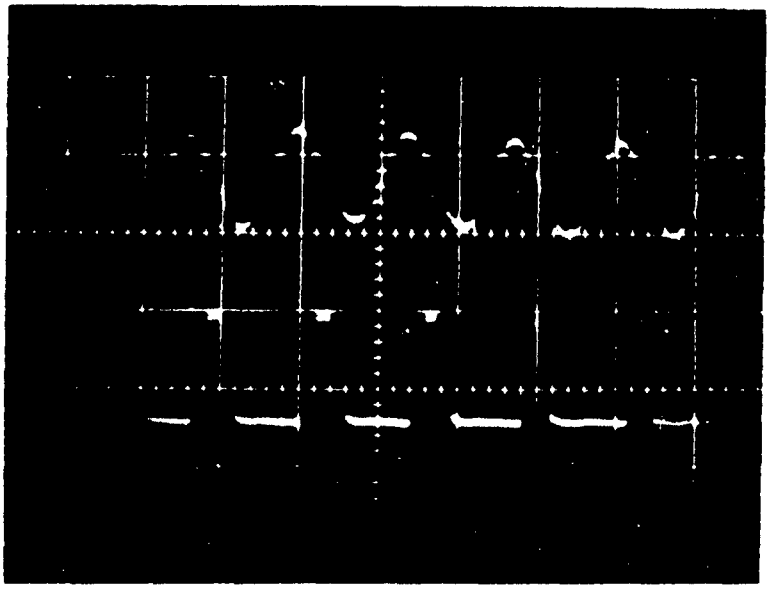

PHOTOMULTIPLIER OUTPUT

X axis: 2 μ sec/cm
Y axis: 10 v/cm
Y axis zero: 6.0 cm

AMPLIFIER OUTPUT

X axis: 2 μ sec/cm
Y axis: 10 v/cm
Y axis zero: 3.0 cm

SCANNING HEAD RPM
11,020

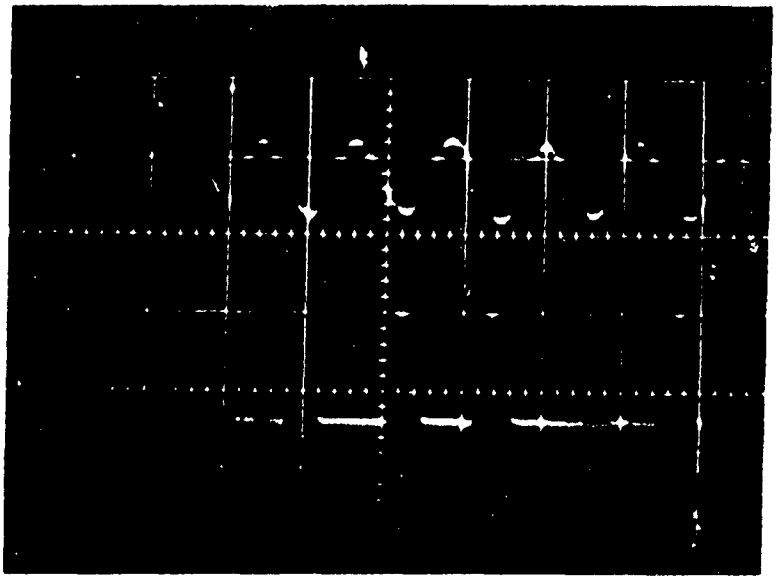

Figure 5-84.

DOVE DATA RETRIEVAL SYSTEM

DATA SHEET A-160

PHOTOMULTIPLIER OUTPUT

X axis: 20 μ sec/cm
Y axis: 5 v/cm
Y axis zero: 5.9 cm

AMPLIFIER OUTPUT

X axis: 20 μ sec/cm
Y axis: 20 v/cm
Y axis zero: 3.1 cm

SCANNING HEAD RPM
1590

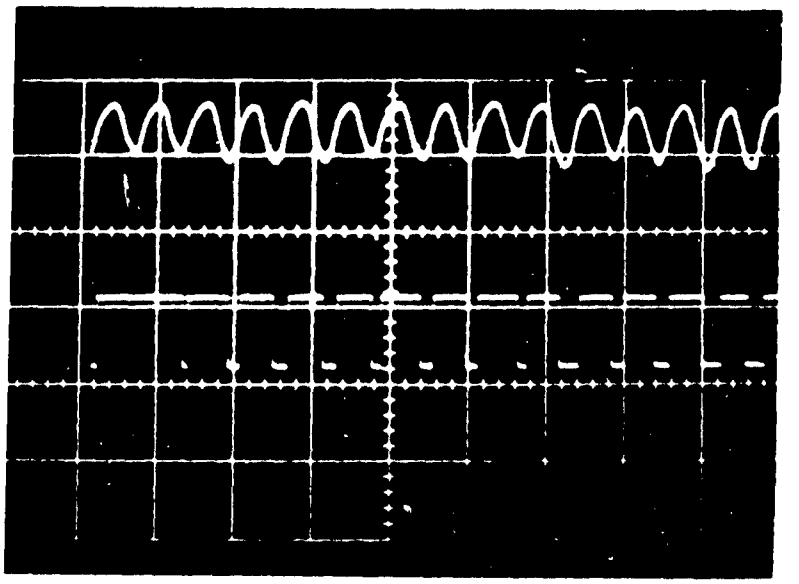

PHOTOMULTIPLIER OUTPUT

X axis: 5 μ sec/cm
Y axis: 5 v/cm
Y axis zero: 6.0 cm

AMPLIFIER OUTPUT

X axis: 5 μ sec/cm
Y axis: 10 v/cm
Y axis zero: 2.0 cm

SCANNING HEAD RPM
1645

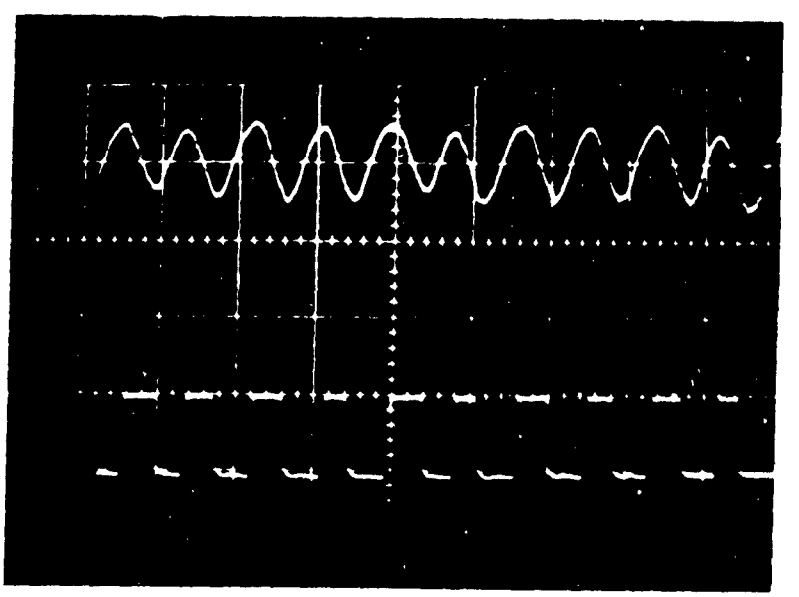

Figure 5-85.

DATA SHEET B-160

PHOTOMULTIPLIER OUTPUT

X axis: 2 μsec/cm
Y axis: 5 v/cm
Y axis zero: 6.0 cm

AMPLIFIER OUTPUT

X axis: 2 μsec/cm
Y axis: 10 v/cm
Y axis zero: 2.0 cm

SCANNING HEAD RPM
6440

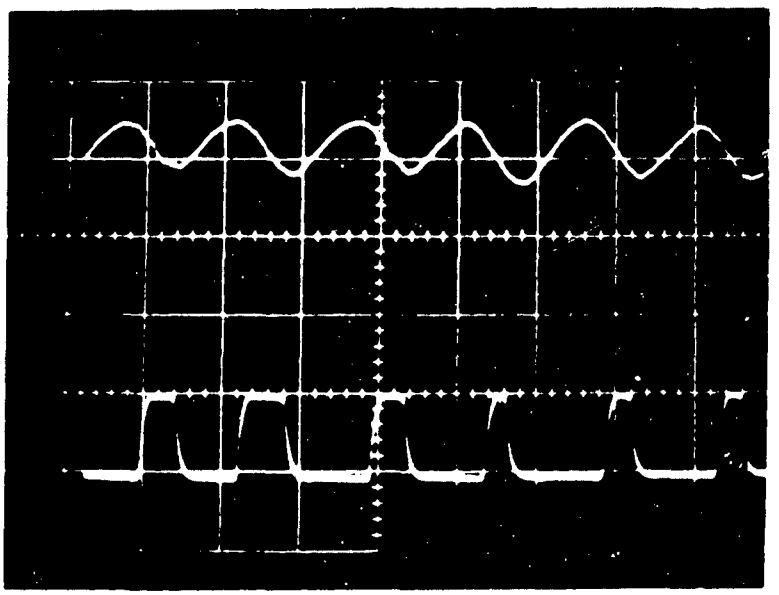

PHOTOMULTIPLIER OUTPUT

X axis: 2 μsec/cm
Y axis: 5 v/cm
Y axis zero: 6.0 cm

AMPLIFIER OUTPUT

X axis: 2 μsec/cm
Y axis: 10 v/cm
Y axis zero: 2 cm

SCANNING HEAD RPM
8825

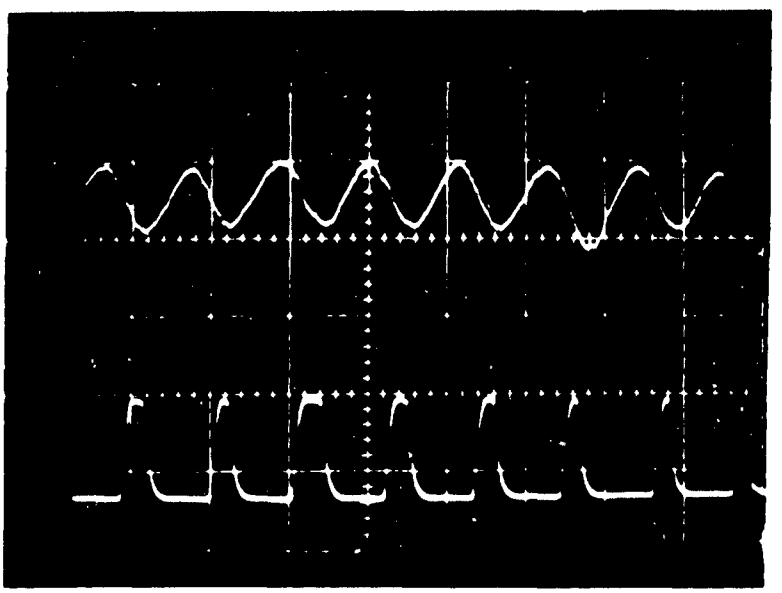

Figure 5-86.

DOVE DATA RETRIEVAL SYSTEM

DATA SHEET C-160

PHOTOMULTIPLIER OUTPUT

X axis: 1 μ sec/cm
Y axis: 5 v/cm
Y axis zero: 6.0 cm

AMPLIFIER OUTPUT

X axis: 1 μ sec/cm
Y axis: [illegible] v/cm
Y axis zero: 2.0 cm

SCANNING HEAD RUN

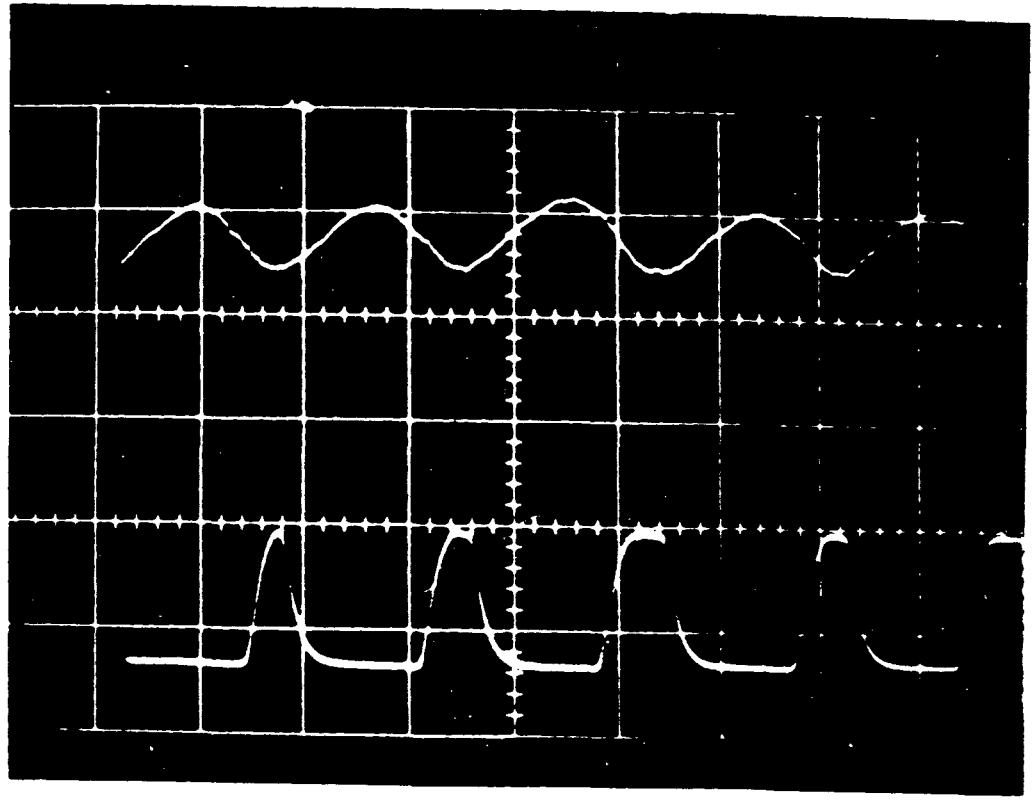

Figure 5-87.

DOVE DATA RETRIEVAL SYSTEM

DATA SHEET A-240

PHOTOMULTIPLIER OUTPUT

X axis: 10 μsec/cm
Y axis: 5 v/cm
Y axis zero: 6.1 cm

AMPLIFIER OUTPUT

X axis: 10 μsec/cm
Y axis: 10 v/cm
Y axis zero: 2.3 cm

SCANNING HEAD RPM
1708

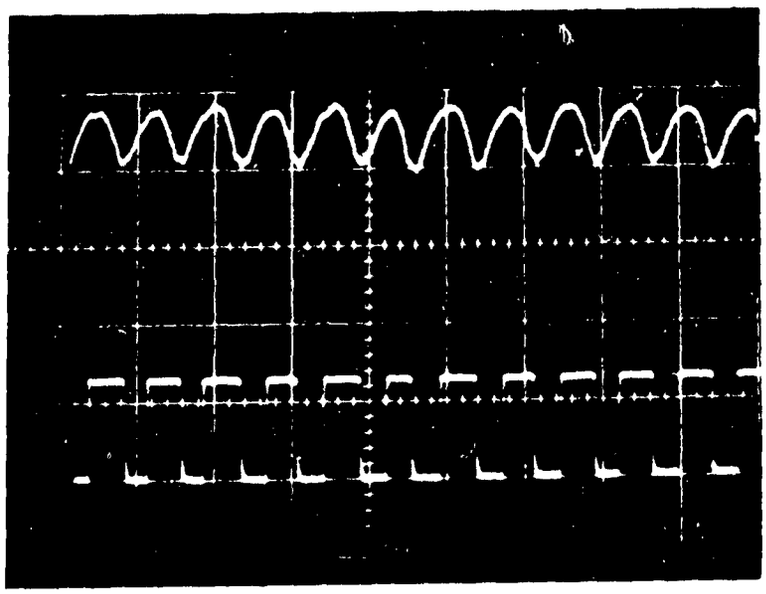

PHOTOMULTIPLIER OUTPUT

X axis: 5 μsec/cm
Y axis: 5 v/cm
Y axis zero: 6.1 cm

AMPLIFIER OUTPUT

X axis: 5 μsec/cm
Y axis: 10 v/cm
Y axis zero: 2.3 cm

SCANNING HEAD RPM
4750

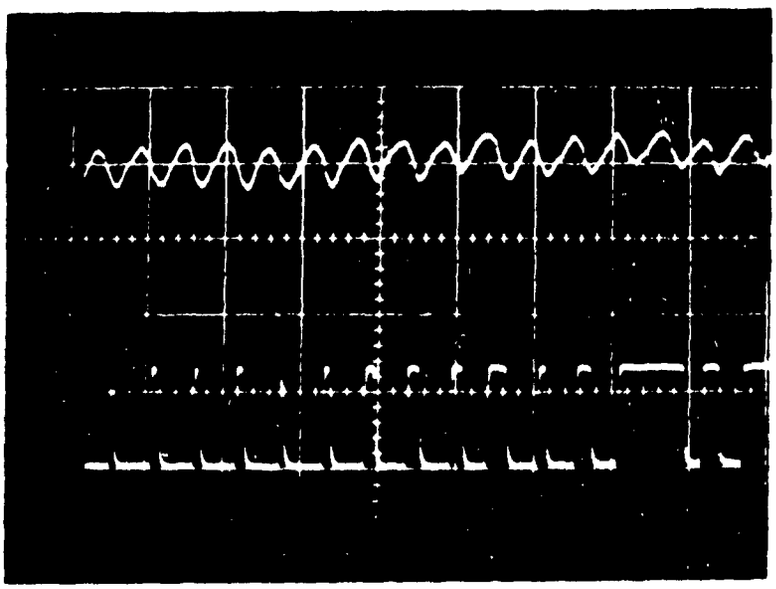

Figure 5-88.

DOVE DATA RETRIEVAL SYSTEM

DATA SHEET B-240

PHOTOMULTIPLIER OUTPUT

X axis: 2 μ sec/cm
Y axis: 5 v/cm
Y axis zero: 6.0 cm

AMPLIFIER OUTPUT

X axis: 2 μ sec/cm
Y axis: 10 v/cm
Y axis zero: 2.3 cm

SCANNING HEAD RPM
6640

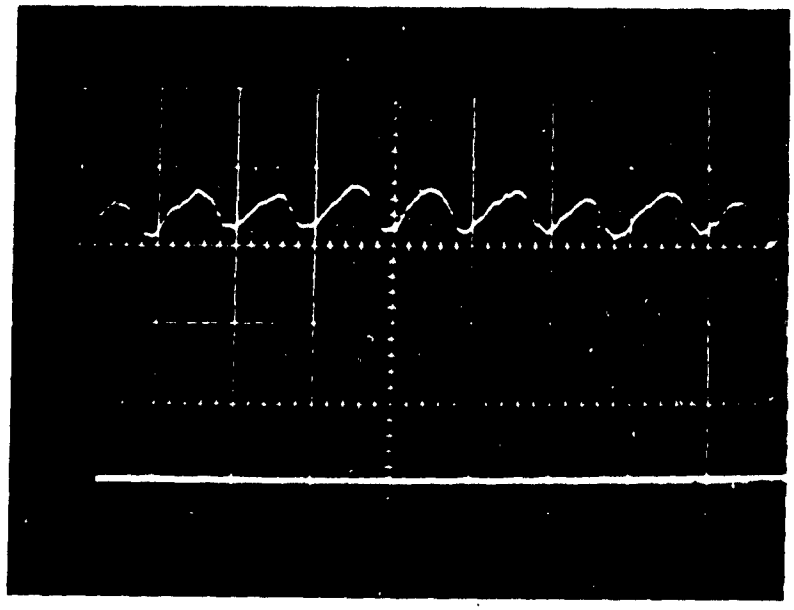

PHOTOMULTIPLIER OUTPUT

X axis: 2 μ sec/cm
Y axis: 5 v/cm
Y axis zero: 5.9 cm

AMPLIFIER OUTPUT

X axis: 2 μ sec/cm
Y axis: 10 v/cm
Y axis zero: 2.3 cm

SCANNING HEAD RPM
6640

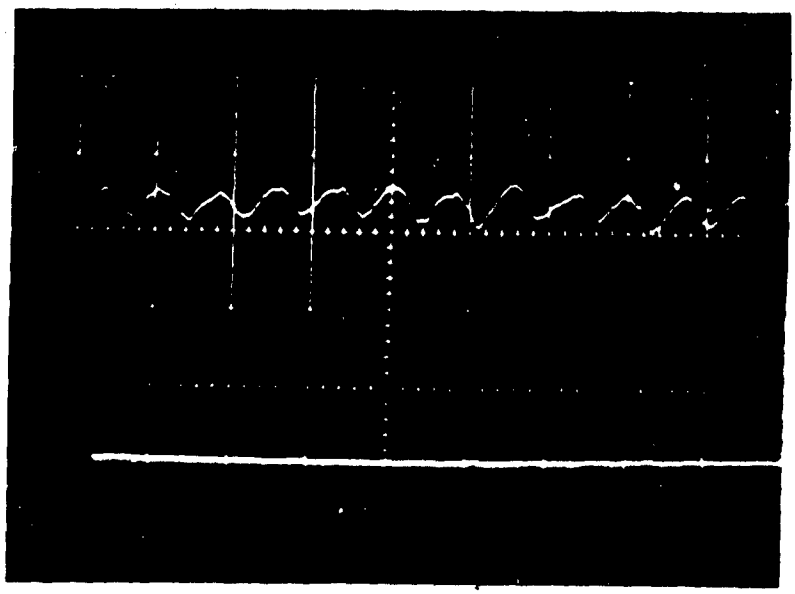

Figure 5-89.

DOVE DATA RETRIEVAL SYSTEM

DATA SHEET C-240

PHOTOMULTIPLIER OUTPUT

X axis: 2 μ sec/cm
Y axis: 5 v/cm
Y axis zero: 5.9 cm

AMPLIFIER OUTPUT

X axis: 2 μ sec/cm
Y axis: 10 v/cm
Y axis zero: 2.3 cm

SCANNING HEAD RPM
11,050

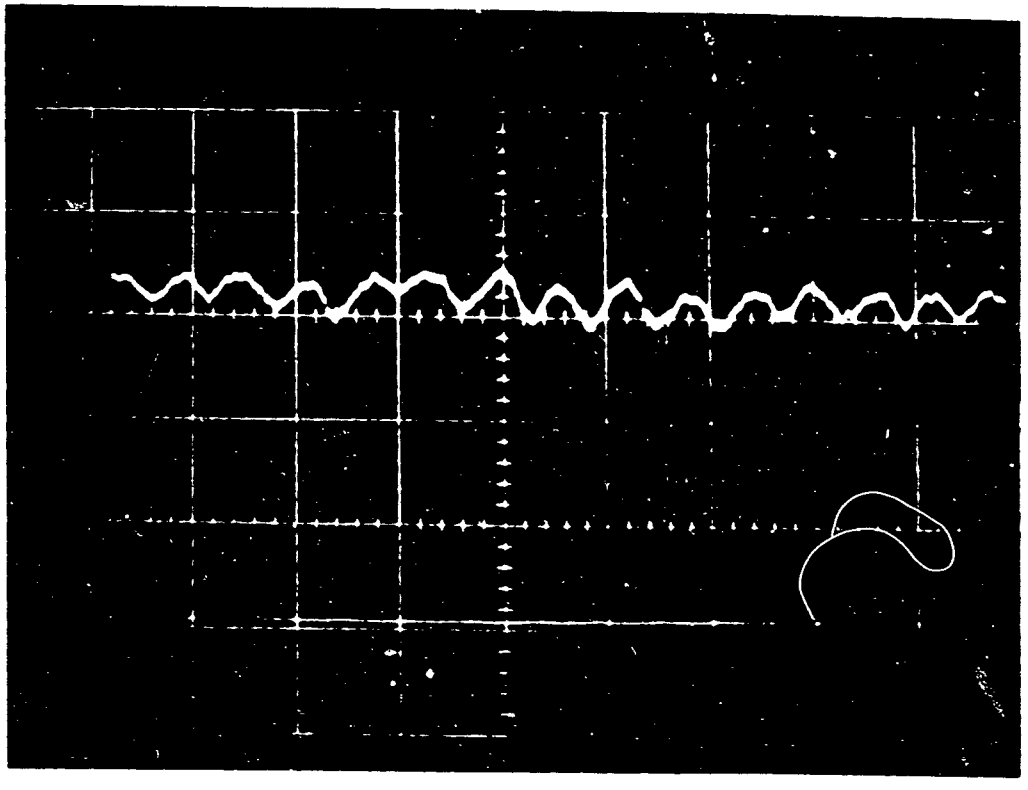

Figure 5-90.

DATA SHEET A-300

PHOTOMULTIPLIER OUTPUT

X axis: 10 μsec/cm
Y axis: 5 v/cm
Y axis zero: 6.6 cm

MULTIPLIER OUTPUT

X axis: 10 μsec/cm
Y axis: 10 v/cm
Y axis zero: 2.0 cm

SPINNING HEAD RPM
1960

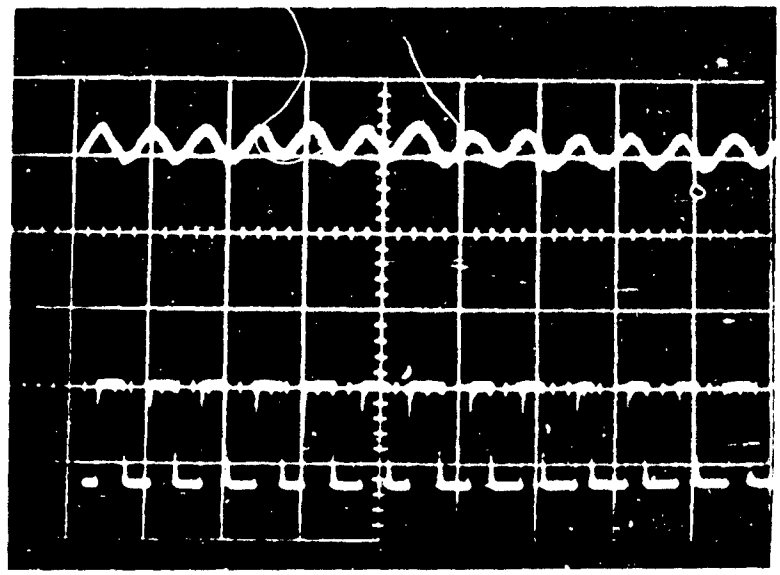

PHOTOMULTIPLIER OUTPUT

X axis: 5 μsec/cm
Y axis: 2 v/cm
Y axis zero: 6.6 cm

MULTIPLIER OUTPUT

X axis: 5 μsec/cm
Y axis: 10 v/cm
Y axis zero: 2.0 cm

SPINNING HEAD RPM

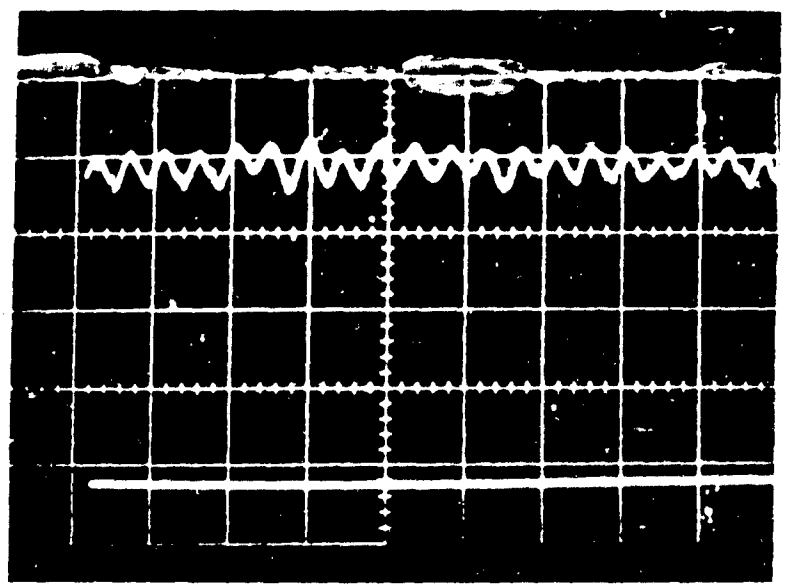

Figure 5-91.

DATA SHEET B-300

PHOTOMULTIPLIER OUTPUT

X axis: 2 μsec/cm
Y axis: 2 v/cm
Y axis zero: 6.0 cm

AMPLIFIER OUTPUT

X axis: 2 μsec/cm
Y axis: 10 v/cm
Y axis zero: 2.0 cm

SCANNING HEAD RPM
6830

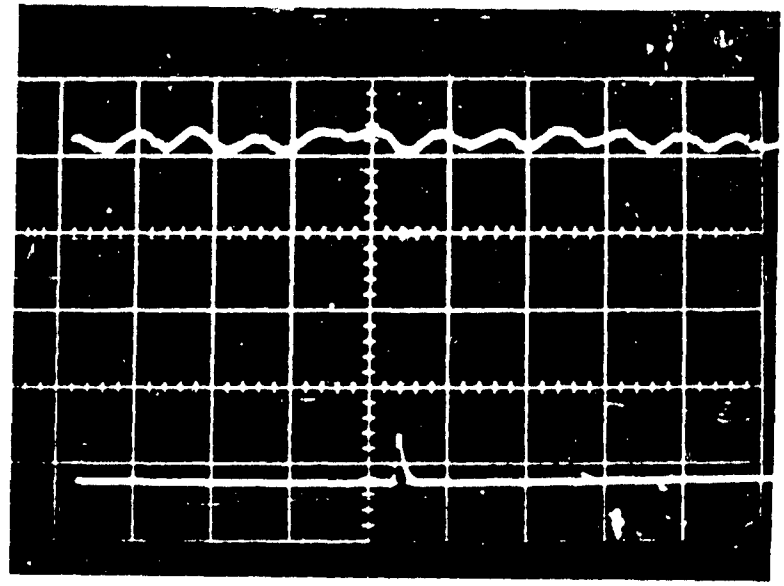

PHOTOMULTIPLIER OUTPUT

X axis: 2 μsec/cm
Y axis: 2 v/cm
Y axis zero: 6.0 cm

AMPLIFIER OUTPUT

X axis: 2 μsec/cm
Y axis: 10 v/cm
Y axis zero: 2.0 cm

SCANNING HEAD RPM
6850

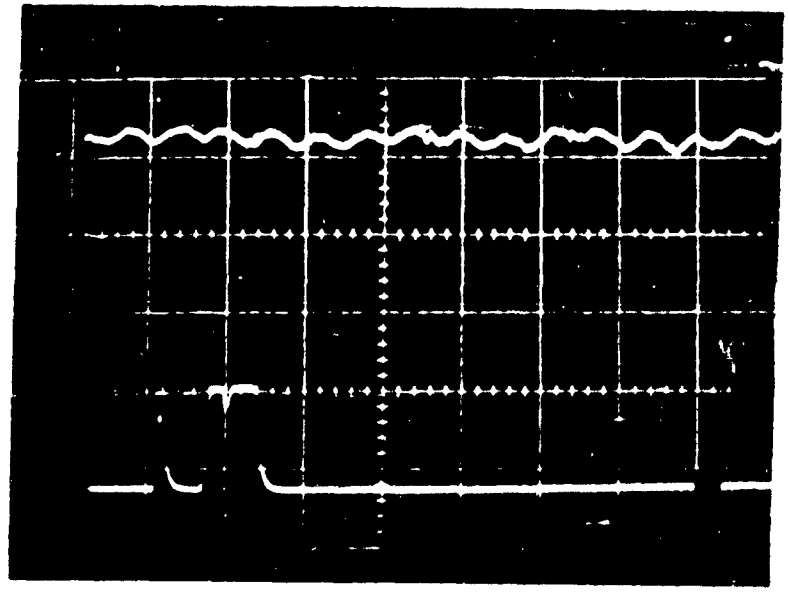

Figure 5-92.

DATA SHEET C-300

PHOTOMULTIPLIER OUTPUT

X axis: 2 μsec/cm
Y axis: 2 v/cm
Y axis zero: 6.0 cm

AMPLIFIER OUTPUT

X axis: 2 μsec/cm
Y axis: 10 v/cm
Y axis zero: 2.0 cm

SCANNING HEAD RPM
11,270

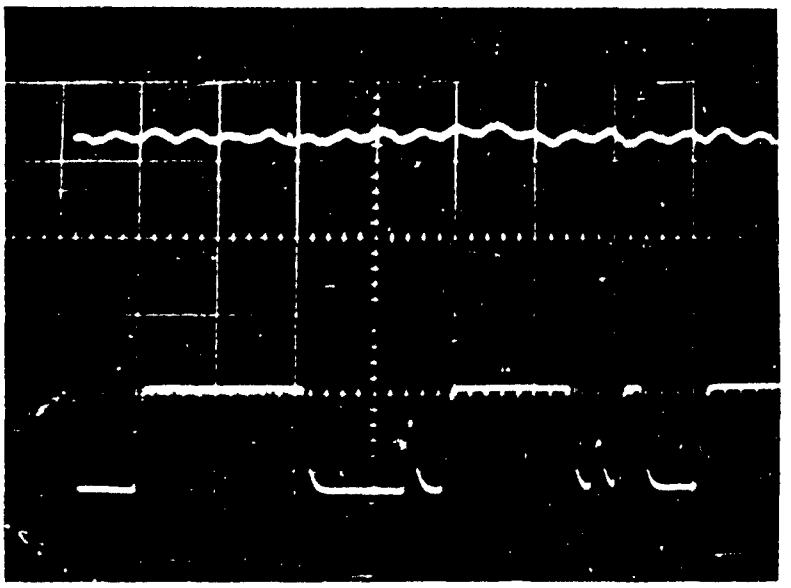

PHOTOMULTIPLIER OUTPUT

X axis: 5 μsec/cm
Y axis: 2 v/cm
Y axis zero: 6.0 cm

AMPLIFIER OUTPUT

X axis: 5 μsec/cm
Y axis: 10 v/cm
Y axis zero: 2.1 cm

SCANNING HEAD RPM
1630

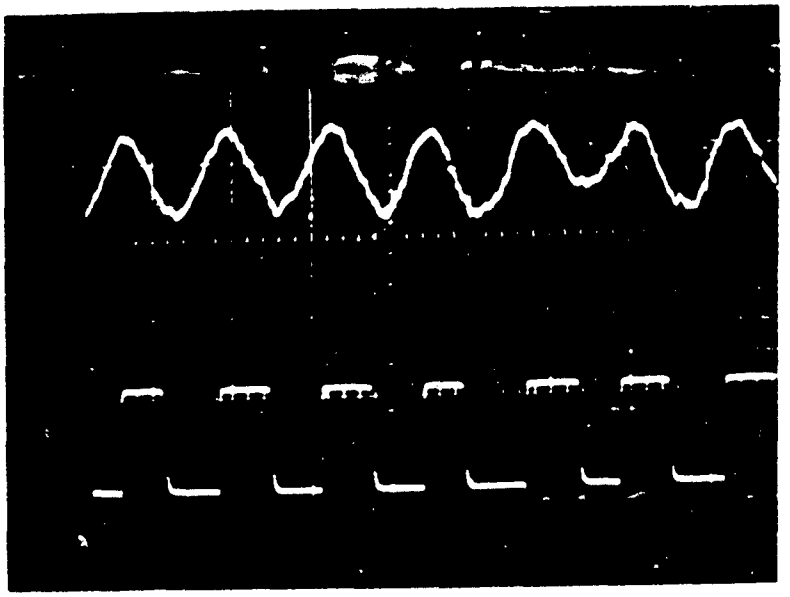

Figure 5-93.

DOVE DATA RETRIEVAL SYSTEM

DATA SHEET D-300

PHOTOMULTIPLIER OUTPUT

X axis: 2 μsec/cm
Y axis: 2 v/cm
Y axis zero: 6.0 cm

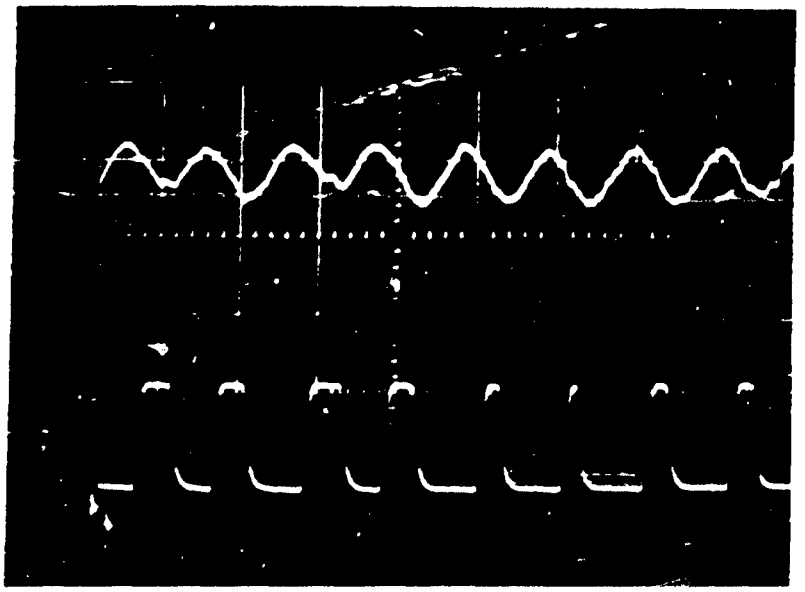

PHOTOMULTIPLIER OUTPUT

X axis: 2 μsec/cm
Y axis: 2 v/cm
Y axis zero: 6.0 cm

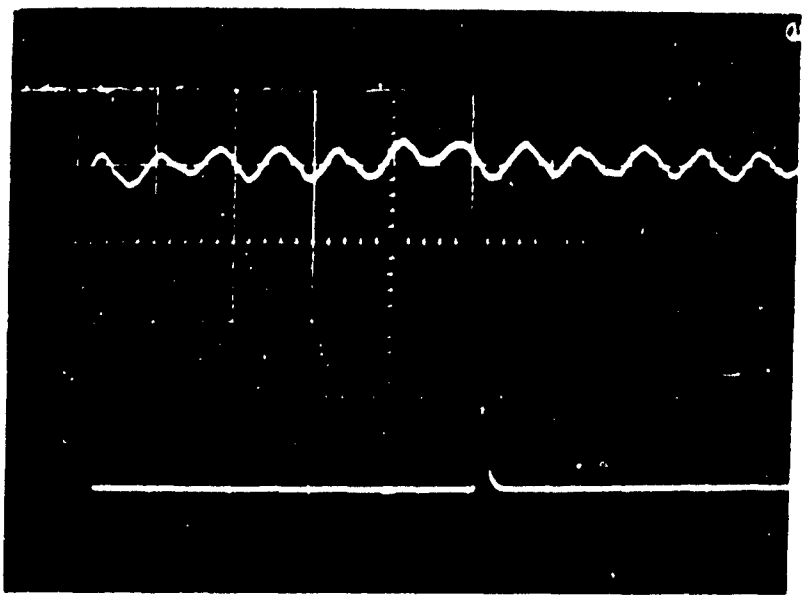

Figure 5-94.

DOVE DATA RETRIEVAL SYSTEM

DATA SHEET E-300

PHOTOMULTIPLIER OUTPUT

X axis: 2 μ sec/cm
Y axis: 2 v/cm
Y axis zero: 6.0 cm

AMPLIFIER OUTPUT

X axis: 2 μ sec/cm
Y axis: 10 v/cm
Y axis zero: 2.0 cm

SCANNING HEAD RPM
9850

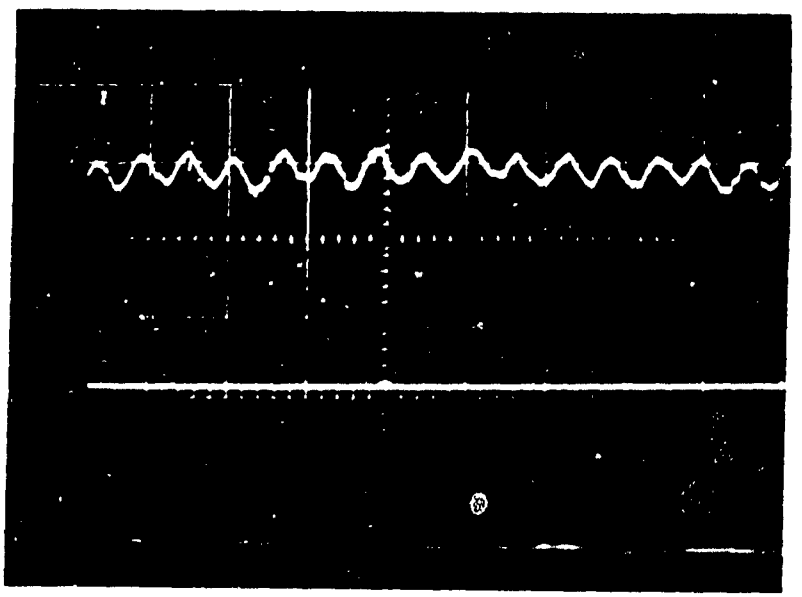

PHOTOMULTIPLIER OUTPUT

X axis: 2 μ sec/cm
Y axis: 2 v/cm
Y axis zero: 6.0 cm

AMPLIFIER OUTPUT

X axis: 2 μ sec/cm
Y axis: 10 v/cm
Y axis zero: 2.0 cm

SCANNING HEAD RPM
[illegible]

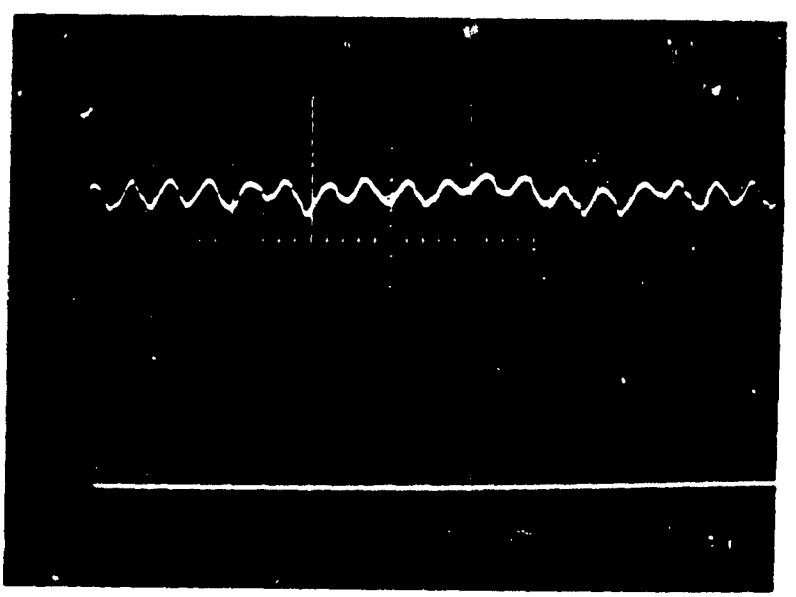

Figure 5-95.

3. Discussion

The authors [28] are gratified with the results of both scanners. As is evident from the data in the preceding section, both of the scanners have exceeded their design specifications. It was originally thought that vibrations at high scanning speeds would cause serious image deterioration, causing the photomultiplier output to become incomprehensible. It will be noted that some photomultiplier output does appear to have degenerated, especially at high film densities with high scanning rates. This appears to be due primarily to two factors: the light per bit reaching the phototube is decreased at higher rates and densities, and the higher density films used are of poor quality.

For the dove scanner, in the design range, the quality of the photomultiplier output at high scanning rates and the quality at low scanning rates are substantially the same, indicating the absence of scanning head vibration. The output deterioration evident at higher densities for both low and high scanning rates can be partially simulated by operating the photomultipliers at 1500v, the voltage required to obtain the data output from the higher density films. A similar phenomenon occurs for the drum scanning system.

A rather extreme example of the film being used is pictured in Figure 4-7. The film shown is a 2.5 to 1 reduction of the 60 line per inch IBM 7090 output film, and illustrates quite clearly one cause of photomultiplier output deterioration. For the most part, only the best portion of the film was used, even that being none too good. With better data films, the performance of both scanners will improve. For operation with the NOEL computer, both scanners must be limited to the speeds and bit densities which allow the output amplifiers to follow; this criterion being indeterminate with the present data films.

It is customary to recommend improvements in the existing apparatus. For the drum scanner, the authors recommend:

- Replace the present gear reduction unit with gears of better quality in order to —
- Increase the drum rpm and make maximum use of the material strength.
- Replace the present film holder, which makes it difficult to change films, to a system which will accept data films which have been laminated between two protecting Plexiglas cylinders, the cylinders attaching to the disc to form the cylinder.

For the dove scanner, the authors recommend:

- Replace or improve the planetary oil seals located between the scanning head and dove prism tube, and the dove prism tube and pan. If possible, eliminate the entire oil system.

- Contour the lower half of the double conical mirror so that the light, after passing through the data film, will tend to focus on the scanning prism in both planes and not simply one plane as it does now.

- Re-aluminize the double conical mirrors which have become contaminated. Apply a protective coating to the surface after aluminizing.

For both systems, replace the photomultiplier tubes with a semiconductor device while at the same time increasing the arc lamp power.

When considering future dove scanner design, two alternative methods should be considered: using synchronous motors to drive both the scanning head and the dove prism tube, these components forming the motor shafts and eliminating the entire drive train; and synchronizing the scanning head and dove prism tubes with air-driven turbines, supporting these components or air bearings, thereby eliminating all but the essential components and raising the scanning rate significantly.

F. SOME READER CIRCUIT PROBLEMS

1. The Variable Delay Circuit

Information is brought into the nomographic computer from six memory tracks. Five of the tracks carry control pulses and information for the computational process, and the sixth acts as a clock track. The design of the computer requires that the pulses from the clock track arrive at the logic circuitry after all the pulses from the other five tracks have arrived. Since the information is read simultaneously from all tracks, the pulses from the clock track are fed into a fixed delay circuit of 0.3 microseconds at the input of the computer. If the pulses from all the tracks arrive simultaneously at the computer input, the delay of 0.3 microseconds is sufficient to delay the clock pulses until the logic circuitry has processed the information from the other tracks and is ready to receive the clock track pulses.

The memory storage and readout devices [37] have characteristics which tend to keep the pulses, which are read from the six tracks, from entering the computer simultaneously. In the paper tape reader, the relays do not all have

the same closing times. In the magnetic memory system, the tracks might not be written simultaneously due to the difference in the inherent delays in the writing amplifiers and the logic circuitry of each track. The output logic circuitry and read amplifiers also add some small delay which will not be exactly the same in each track. In the optical system, the tracks of bit patterns might not be read simultaneously by the optical reader, due to the film not being exactly horizontal. Since the optical scanner reads a narrow vertical strip of the horizontally moving film, it will see the bits of some tracks before others, if the film is not precisely horizontal. To insure proper operation of the computer, an extra delay must be used for the clock track pulses. This chapter describes the design of this delay circuit.

The delay required for the clock track will vary with the memory storage unit being used. The paper tape reader operating at 20 to 30 cps may require a 10 millisecond delay; the magnetic drum operating at 50 kc may require an 8 microsecond delay; and the optical reader operating at 200 kc may require a 2 microsecond delay. Since the delay circuit is to be used with all the memory storage units, the delay must be variable from about one microsecond to forty milliseconds.

The other specifications for the circuit are as follows:

- The input signal amplitude will be between -3 and -10 volts.
- The output signal amplitude should be larger than -4 volts.
- The output pulse duration should be one microsecond or less.
- The circuit should operate reliably over the frequency range of 20 cps to 500 kc.

The final circuit is shown in Figure 5-96. This circuit can be analyzed by dividing it into three parts as shown on the schematic diagram. The first part of the circuit inverts the input pulse and adjusts its amplitude to about six volts. This part of the circuit is simply a common emitter amplifier with a clamped output.

The second part of the circuit provides the variable delay. This part of the circuit is a monostable multivibrator with a variable pulse duration. In its stable state, transistor Q2 is on and transistor Q3 is off. When a positive pulse is applied at point A, transistor Q2 is turned off, and transistor Q3 is turned on. After a time interval determined by the time constant RC, which is adjustable, the circuit will return to its original state.

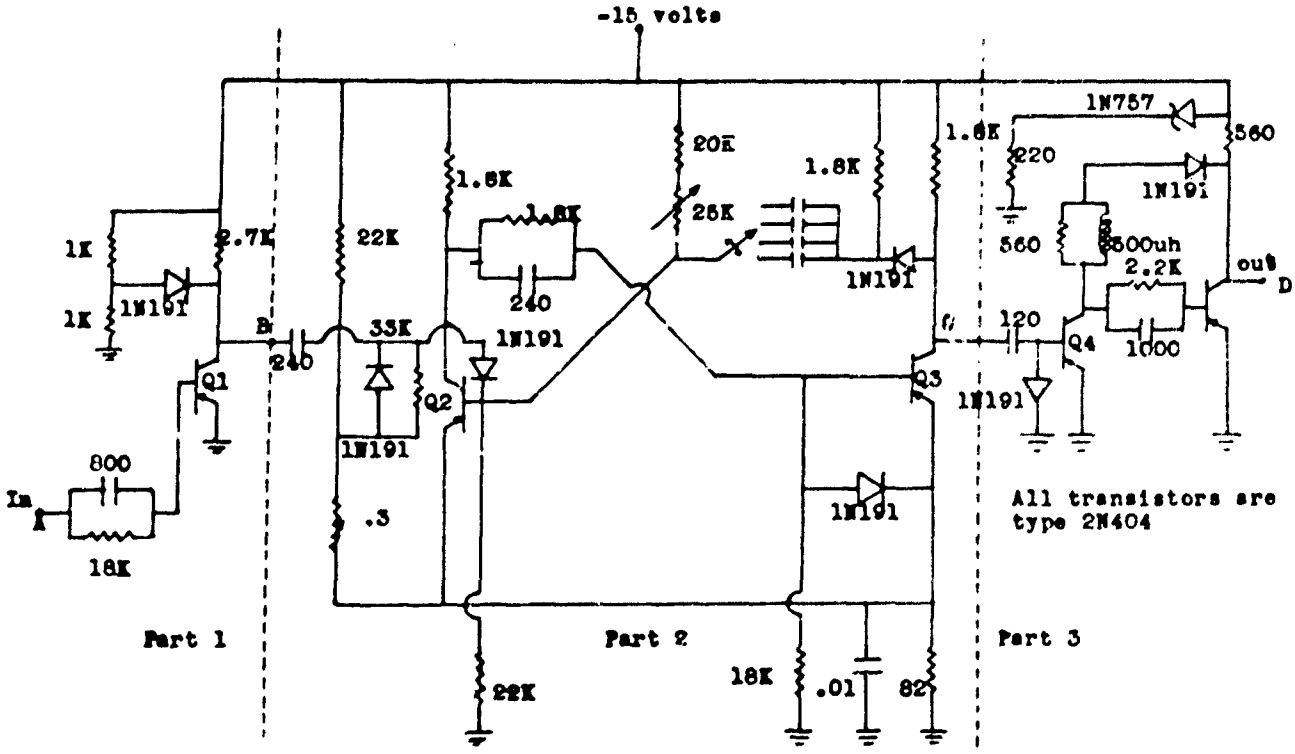

Figure 5-96. Variable Delay Circuit

The third part of the circuit is another monostable multivibrator. In its stable state, transistor Q4 is off and transistor Q5 is on. When the monostable multivibrator in the second part of the circuit returns to its stable state, transistor Q3 goes from its on state to its off state, and its collector voltage goes from about -4 volts to -15 volts. This negative going voltage turns transistor Q4 on and Q5 off. The circuit parameters are adjusted so that the circuit remains in this unstable state for slightly less than one microsecond. The output at the collecter of Q5, a negative pulse, is suitable as input to the computer.

This delay circuit has been built and tested, and its operation is satisfactory in all respects. Typical waveforms of the circuit are shown in Figure 5-97.

2. The Amplifier and Pulse Shaper

The signals coming from the photomultiplier of the optical readers must be amplified and shaped before going into the computer. These signals consist of negative pulses. This chapter describes the design of a circuit to convert the output from the photomultiplier tubes into a form suitable as input to the computer.

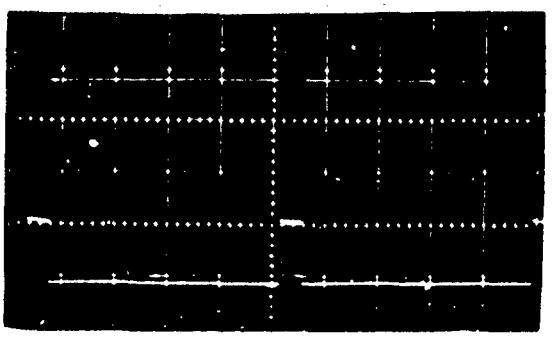

Upper: input
5 volts/cm.
20 usec./cm.

Lower: waveform at B
5 volts/cm.
20 usec./cm.

Upper: input
5 volts/cm.
20 usec./cm.

Lower: waveform at C
5 volts/cm.
20 usec./cm.

Figure 5-97. Typical Waveforms of Delay Circuit

The amplifier and shaper must work reliably for changes in supply voltages and variations in the form of the input signal. One important source of variation in the input signal will be the use of different bit density films. As the bit density of the film is increased. the accuracy and/or the range of the nomogram can be increased. Although this circuit was designed using film having a density of 300 bits per inch, one requirement of the circuit is that it operate with a higher density film when this film becomes available. A final requirement of the circuit is that its input impedance be high enough to prevent drawing excessive current from the photomultiplier tube.

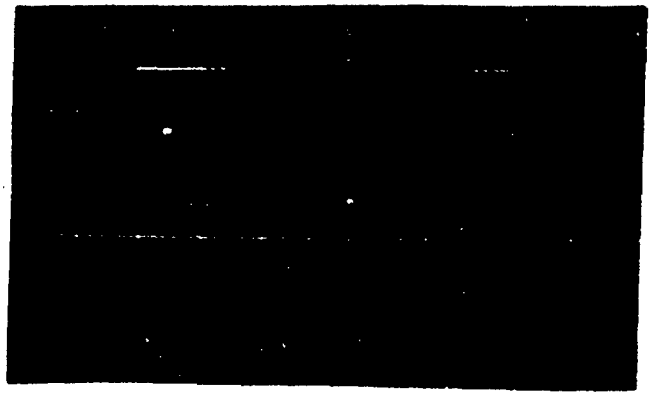

Figure 5-98. Typical Waveforms of Delay Circuit

To design a circuit to amplify and shape the pulses from the optical readers, one must examine the characteristics of the pulses. Some photographs of the output of the optical readers are shown in Figures 5-100 and 5-101. One characteristic is that when the pulses are consecutive, the voltage does not return all the way to ground between pulses. The voltage between pulses is also dependent on the amplitude of the pulses. The reason for these effects is that the light bits cannot be focused on the photomultiplier tube without a small amount of light leaking to the tube between bits. This effect of light leakage is important since it will probably increase as the bit density of the film increases. A signal amplitude of 0.5 volts can be easily obtained from the optical reader. One final characteristic of the signal from the optical readers is that a very small percentage of the pulses are much smaller than the rest of the pulses. This effect is due to imperfections in the film.

Although some of the pulses from the photomultiplier may be smaller than the others. the circuit must be able to detect and shape these pulses reliably. If a pulse from one of the five tracks carrying information about the nomogram is lost. the result is an error in the final answer. If a clock pulse is lost, the result of the entire computation becomes meaningless. For this reason, the r ability of the circuit is of extreme importance.

The final circuit is shown in Figure 5-99. The first stage of this circuit is an emitter follower which provides a high input impedance for the circuit. This high impedance prevents loading of the photomultiplier tube. The output from the first stage goes into a clamping circuit which clamps the most negative part of the waveform at about -0.5 volts. The clamping voltage is obtained by using the voltage developed across the silicon diode D1. Transister Q2 is used as an emitter follower to give a high impedance for the clamping circuit. This high impedance is necessary for good clamping since it prevents the capacitor from discharging between pulses.

The purpose of the clamp is to get the input pulses in a form which can be easily amplified. It standardizes the input so that the rest of the circuit sees approximately the same waveform, even though the input waveform may vary in amplitude. The waveform that the circuit (after the clamp) receives has a constant reference level, between pulses, which is independent of both the time interval between pulses and of the amplitude of the pulses. The reference level between pulses of the waveform from the photomultiplier tube, however, is very dependent upon both the time interval between pulses and the amplitude of the pulses.

The clamp insures a constant reference level between pulses in the following way. Since the most negative part of the waveform is clamped at 0.5 volts, if the signal amplitude is 0.5 volts or greater, the most positive part of the waveform will be at ground potential or higher. When the voltage at the output of the clamp, the base of transistor Q2, goes above ground, transistor Q2 is turned off and the voltage at its emitter will not go above ground. Thus the signal at the emitter of Q2 is always at ground potential between pulses whenever the input signal is 0.5 volts or greater.

Transistor Q3 is used as a common emitter amplifier. Its output goes to transistor Q4, another common emitter amplifier. The circuit parameters have been chosen so that Q4 saturates when the voltage at the base of Q3 is about -0.5 volts. If the amplitude of the input waveform is larger than -0.5 volts, the clamping circuit insures that the voltage between pulses goes back to ground at the emitter of Q2 and the base of Q3. When the base of Q3 is at ground, Q3 is cut off and its collector is at -15 volts. This -15 volts at the base of Q4 cuts off this transistor, and sets its collector voltage at ground between pulses.

If the input voltage is less than -0.5 volts, the voltage at the base of Q2 might not come all the way back to ground. To insure that the voltage at the collector of Q4 will come back to ground between pulses under these conditions, transistor Q4 is biased such that it will cut off whenever the input signal returns to approximately -0.15 volts. This biasing is accomplished by connecting a resistor from the emitter of Q4 to ground.

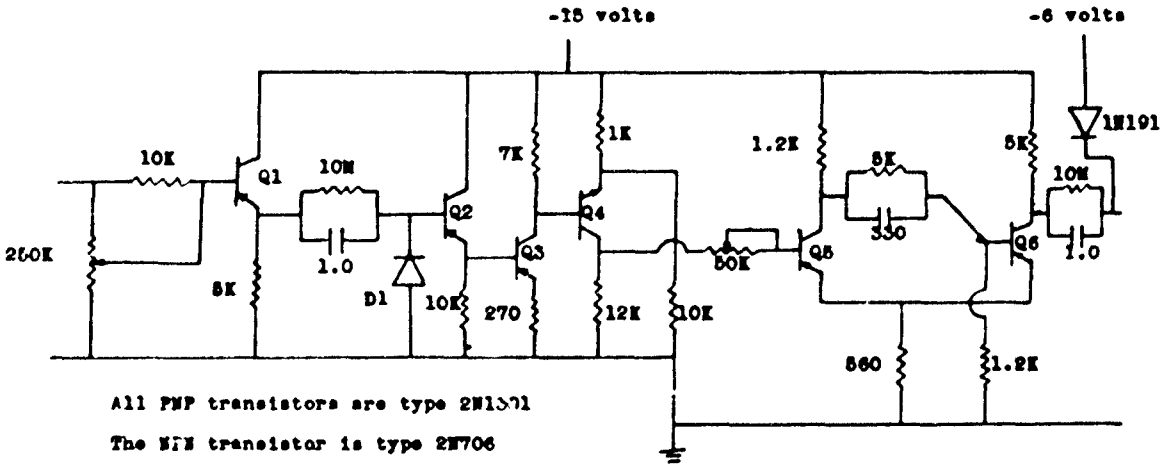

Figure 5-99. Amplifier and Pulse Shaper

Transistors Q5 and Q6 form a Schmitt Trigger, which is a circuit having two stable states. The state of the circuit is determined by the input voltage. When the input voltage goes more negative than some critical voltage, Q5 turns on and Q6 turns off. If the input voltage goes less negative than some other critical voltage, the circuit returns to its original state in which Q5 is cutoff and Q6 is on. Since the transition time between states is very small, the circuit effectively squares off the waveform as shown in Figures 5-100 and 5-101. The circuit parameters have been adjusted so that the output transistor Q6 will turn off as the input voltage at Q5 goes below -1.6 volts, and will turn on as the input voltage at Q5 rises above -1.0 volts.

If the input signal amplitude from the photomultiplier tubes is -0.5 volts, the voltage at the collector of transistor Q4 goes from ground to about -10 volts. The "input signal amplitude" refers only to the amplitude of most of the pulses. Due to imperfections in the film, a few pulses might be much smaller than the rest of the pulses. When one of these small pulses is amplified, the voltage at the collector of transistor Q4 will go from ground to less than -10 volts. With the film used to test the circuit, the small pulses were always at least -4 volts at the collector of Q4. This voltage is more than enough to activate the Schmitt Trigger reliably.

The output voltage of the Schmitt Trigger goes from about -3 volts to -15 volts. Since the computer input must be negative pulses from ground to about -6 volts, the output of the Schmitt Trigger goes to a clamping circuit which clamps the most negative part of the waveform at -6 volts. Because the input to the computer is the base of a PNP transistor, the positive part of the output pulse will be eliminated, and the effective waveform will consist of negative pulses going from ground to -6 volts.

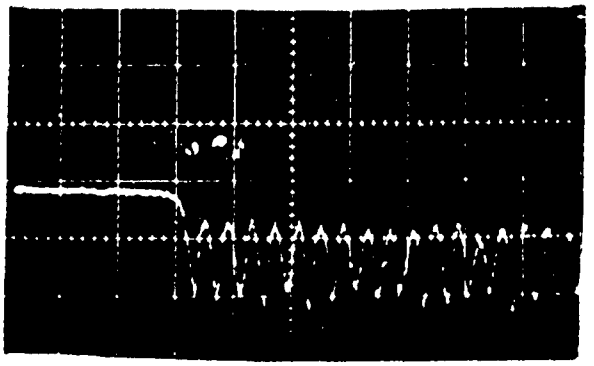

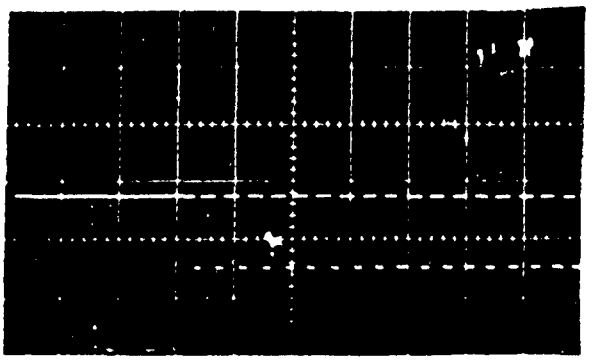

Figure 5-100. Typical Waveforms of Amplifier

This circuit has been built and tested with two different optical readers. The circuit has operated satisfactorily with both readers. Typical waveforms are shown in Figures 5-100 and 5-101. The circuit could be tested at frequencies only up to 300 kilocycles with the optical readers, because of the mechanical speed limitation of the readers. The circuit was tested using a signal generator at frequencies up to five megacycles, which is the maximum frequency of the computer logic circuitry. At five megacycles, the output pulses are more triangular than square, and the voltage swing at the output of the Schmitt Trigger is only about 6 volts. These pulses, however, are still suitable for use as input to the computer.

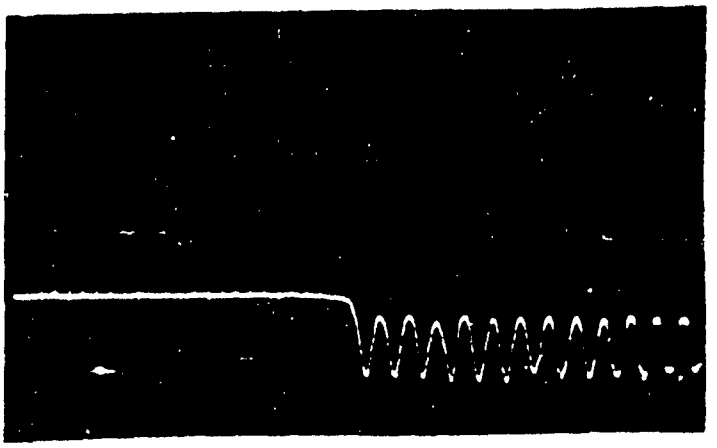

Input waveform

0.5 volts/cm.

50 usec./cm.

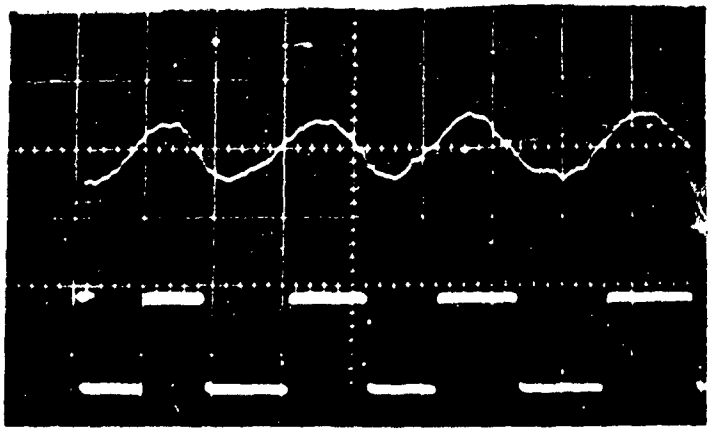

Figure 5-101. Typical Waveforms of Amplifier

G. MAGNETIC DRUM MEMORY. WRITING AND READING

1. Magnetic Drum Memory

a. The Physics of the Drum

The physical structure of the drum will be discussed first. A drum basically consists of a cylinder of aluminum, about 10 inches in diameter and from 5 to 20 inches in height. This cylinder is rotated around its axis of symmetry, and is attached to a motor for the purpose, suspended by bearings at both the top and bottom of the casing. Rotation is around the vertical axis. The speed of rotation is on the order of 3600 revolutions per minute, but could conceivably be slower, or up to ten times as fast, or maybe even faster. Our particular drum, loaned for the project by the Bryant Chuck and Grinder Corp. of Springfield, Vermont, is about ten inches in diameter, five inches in height, and is driven by an induction motor at 1800 rpm.

The outside of the cylinder is coated with a magnetic oxide of iron (chemical formula Fe_3O_4) and recording heads as in a tape recorder are placed along the coating. The orientation of the heads is such that the gaps are transverse to the direction of motion of the coating. In a tape recorder for audio use, because the speed of motion of the tape and hence the coating is a maximum of 30 inches per second, it is practical in terms of head and coating wear to place the heads directly on the coating. However, in a magnetic drum, where the rotation speed of even a slow drum is at least 30 revolutions per second, and the circumference is approximately 30 inches (31.4 to be more exact), we have a linear speed of about 900 inches per second. To minimize wear, the heads are separated from the coating by a small distance, about 1 mil. The gap between the two pole pieces of the head is about one-quarter of a mil. It should be noted that physically a magnetic recording or playback head is a horseshoe electromagnet, but with a very small gap between the pole pieces. The particular heads on our drum have center-tapped windings, the reason for this to be mentioned later.

The nature of magnetic recording will be discussed not from the physics of the hysteresis loop, but what this physics boils down to, for an approximate engineering analysis. Using such an approximation, the level of magnetization of the coating retained after the head has passed is roughly proportional to the instantaneous current flowing through the head until the coating reaches a saturation value, in which case the magnetization is at maximum. In practice the curve of retained magnetization versus record-head current is smooth, and as the magnetization reaches saturation, a linear approximation becomes increasingly poorer. It should be noted that the magnetizations property is anti-symmetric around zero. The playback voltage across the head is, however, proportional to the time derivative of the magnetization. For digital recording,

the current in the head is such as to saturate the coating in either one direction or the other. Because of high-frequency losses, perfect square waves are not obtained. Consequently only a finite height pulse comes out, with about 10 to 15 millivolts being adequate to drive the amplifiers. It should be noted that the amplifiers change the digital levels to currents for writing and the playback voltages to digital levels. Our amplifiers function on a symmetric basis, i.e., to write magnetization in one direction, -4 volts being applied to one of the inputs and 0 to the other. This reverses for writing in the other direction. As mentioned before, the head is center-tapped. Only one-half of the winding is used at any instant for writing.

b. Possible Schemes of Magnetic Recording

There are three schemes relating the digital input or output to the magnetization of the coating. They are non-return to bias (NRB), return to bias (RB), and phase modulation (PM). The form of the non-return to bias used by IBM for their magnetic tapes is as follows: writing a "one" reverses the direction of the magnetization of the coating; writing a "zero" retains the same direction The logic necessary for obtaining this modulation is rather simple. It should be noted that any digital recording, whether magnetic or on film, is synchronous, i.e., only a finite number of places, or bits, for binary information, which is assumed to be constant throughout the bit. The output of a flip-flop is used to control the direction of magnetization. If a "one" is written, a pulse is present (or generated) at the beginning of the bit, such that the flip-flop changes its state. A zero results in the absence of pulses, hence the flip-flop remains in its present state. Detection is also rather simple. As the output of the head is proportional to the change in magnetization, "zeros" on the tape or drum will produce nothing, yet "ones" will produce pulses, alternately positive and negative. If these pulses were rectified (all positive, for example) and fed into circuitry that produces a "one" electrically for the duration of the bit period, we will have recovered our original information.

The return to bias scheme is simpler conceptually. Here, the time of the bit is broken down into two, the bit itself and the space between bits. To electrically record a "one" the coating is magnetized in one direction in the area of the bit itself. A "zero" results in the opposite magnetization in this area. The area between the bits is always magnetized in the "zero" direction. No logic, so to speak, is necessary for recording, only the write amplifier. A read amplifier, that amplifies the positive and negative pulses separately, and uses one set of pulses to set a flip-flop, and the other to clear the flip-flop, is all that is needed. The read and write amplifiers so described and constructed symmetrically constitute the Harvey-Wells units. It should be noted that with either of the two preceding systems, signal levels had to be very carefully controlled and some sort of threshhold element included to prevent noise pickup

from interfering. These problems with interference were the very reasons why the "return to bias" scheme of modulation was abandoned in favor of the phase modulation scheme.

Phase modulation, although considerably more complicated to produce and detect than the other two schemes of recording, is a lot less susceptible to noise problems, and hence poses less stringent requirements on the amplifiers and signal levels. If we again start with our concept of bits, each following right on the heels of its predecessor, and again break the bit into two, a "zero" is represented by negative magnetization for the first part, and positive for the remainder of the bit, a "one" by just the reverse, (in other words, positive magnetization for the first part of the bit, and negative for the remainder). This can be seen easily by examination of three illustrative patterns: continuous "ones", continuous "zeros", and alternate "ones" and "zeros". There is a change in the magnetization at least once each bit and at most twice each bit. The circuitry for production and detection of said bit pattern will be discussed with the rest of the circuitry.

2. Information Transfer Route Using The Drum

Faced with the problem of getting the information in the computer onto the drum, and not wishing, at first, to explore the possibilities of connecting a drum directly to the IBM 709 or 7090, the thought came almost immediately of getting the information from the IBM 709 or 7090 on magnetic tape in exactly the same format as is used on the film, and then transferring this information directly to the drum. As mentioned previously, it was decided to use the same format for information on the magnetic drum as is used on the film. Since just about anything in terms of data format is possible as an output from a large general-purpose computer such as the IBM 709 or 7090, this portion of the problem was then considered solved, or easily solvable, and then left to be returned to later and finished. (The next section of this chapter is devoted to the description of the program that produces the desired magnetic tape format.) The other portion of the problem, transferring the information from the tape to the drum, was then examined.

Being somewhat familiar with tape recorders for audio use, and having observed the duplication of a tape by playing back one with information, most frequently music, recorded on it, and simultaneously recording said information on a second tape, it was believed that the same procedure could probably be used for transfer of information from tape to drum. This would have been the case had the tape and drum utilized a common information rate in terms of pulses per second. "Information rate" refers to the number of bits per second, expressed as a frequency. Their speeds did not necessarily have to be the same, however. It might be noted that the information rate of two audio tapes, both

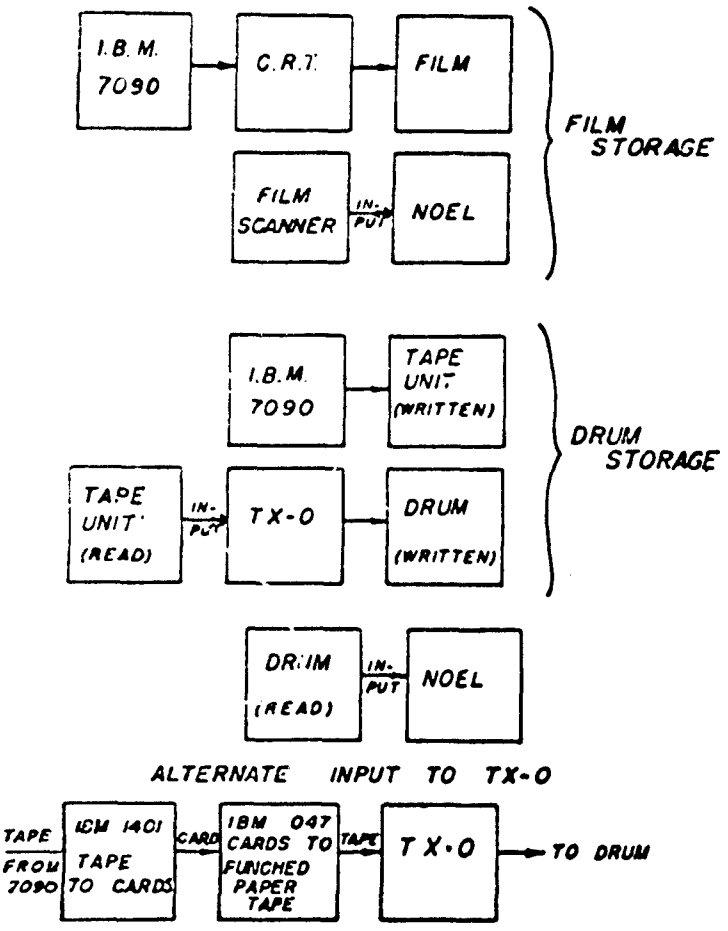

Figure 5-102. Block Diagram for Information Transfer

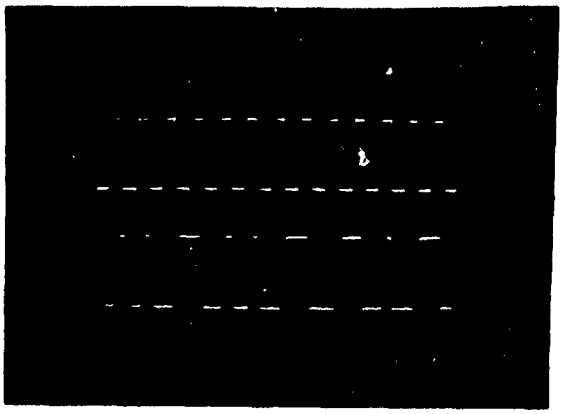

Figure 5-103. Drum Signals. Upper Track Is The Clock. Lower Track Is The Recorded Phase-Modulated Bit Pattern

machine is not without problems. At the beginning of the summer the only working input was paper tape. A magnetic tape unit which was compatible with IBM magnetic tapes was in the process of being installed and debugged. When it would be operating satisfactorily, no one knew. A route was found, using several off-line pieces of computer hardware, of converting the magnetic tape to punched paper tape. This method will be discussed later. At the end of the summer the tape unit was pronounced working, and was placed into regular service. A more serious problem was that the TX-0 was too slow for the magnetic drum. The obvious answer was to slow the drum down. This introduced two other problems, circuitry (amplifier) trouble and how to operate the drum slowly with an induction motor. The circuitry problems, being the most perplexing, will be discussed later. The slow-speed operation was first obtained by driving the motor with an audio power amplifier bed from the signal generator at 20 cycles per second. Later it was found that the speed of the drum could be easily monitored with an oscilloscope and could be slowed down by turning it off after running at full speed, and letting it slow down by itself, monitoring the speed with the oscilloscope. As the TX-0 can be, and is, synchronized to the drum, the exact speed of the drum is not critical, as an information rate of about 20 to 25 kilocycles per second is fine. The speed decrement occurring during the interval of recording, less than one-fifth of a second, is negligible.

3. Obtaining the Magnetic Tape

The computer subroutines that produce the film and the tape write three 6-bit "words," hereafter referred to as a word group, on film or tape at a time, where a word consists of the bits in all six tracks, at any position. The nature of the word written is determined by where or at what address the subroutine is entered. This address is called an entry point. For example, if the subroutine is entered at D 3, a specific address in the subroutine, "ones"* are written in track 3, in the first two words of the word group we are considering, while if the entry is at T 2, a second specific address, "ones" are written in track 2, in all three words of the group. Other bit routines are similar, and are shown in the diagram. In any word group several of these routines are combined to produce the desired information, and all information is combined in a "logical or" method.

The other entry points that control the writing of words are ADV (advance) and RESET. RESET is called only once in the running of any nomographic program, and merely sets all counters to zero, so that the film is started at the beginning. ADV has two functions, that of writing bits in all three words of track 6, and preparing the computer to put the next set of accumulated data into the next group of three words.

* In the binary language, each bit (or digit) can contain either a "zero" or a "one". We assume all bits start off as, and are reset to, zero.

The tape routine does not write on the tape for each entry but rather formulates the data in core storage, and then prepares a tape, after a sufficient quantity of data has been assembled in core storage. Inasmuch as each register of core storage contains 36 bits (in the IBM 709 or 7090) and each word on film or tape contains 6 bits, 6 words of film or tape go into, or are generated from, 1 register of core storage. Two word groups, consisting of 3 words of tape each, fit into 1 register, consequently.

The tape subroutine generates the word group in the rightmost (least significant) 18 bits of 36 bit register used only for temporary storage and word generation. It does this by logically adding (the "logical or" operation) various binary number constants, 1 each corresponding to D 3, T 2, etc. The ADV entry alternates between shifting the information to the leftmost 18 bits of the temporary storage register and transferring the contents of temporary storage to permanent storage followed by clearing the temporary storage register.

The permanent core storage is filled consecutively by a programming technique called indirect addressing. This technique means that the address designated by the instruction contains the address that the instruction will use. "One" is added to this address each time this portion of the program is run through.

After 330 registers of core storage have been filled, the information is then put onto magnetic tape. As each register of core storage occupies 6 words on tape, a total of 1980 words of tape are written. Inasmuch as the magnetic drum we are using has a capacity of only 2048 words, there is little margin as is, and I would be very hesitant to decrease the margin further.

4. Information Through the TX-0

There are now two methods of loading the TX-0[46] from magnetic tape: one is to use the tape unit on the TX-0, the other is to convert it to punched paper tape. A description of the magnetic tape-loading program will comprise the discussion of the direct loading. The method of conversion to paper tape will be presented by first discussing the route and apparatus for conversion, and then describing the operation of the paper tape loader.

The magnetic tape loader program is, in essence, composed of three parts. The first part of the program loads the 6-bit words, three at at time, into consecutive TX-0 registers, by an indexing process. The reader is sufficiently familiar with programming a computer, in general, to be familiar with an index register. Most of the instructions of the program are more or less standard instructions and their functions are rather obvious from the manual. A brief explanation of the functioning of these follows.

The instruction read select 1 (rds 1) begins the reading or unit 1. As there are no other units, the number doesn't matter. (Note—the current tape manual lists the instruction read tape binary 1, or rtb 1, as the instruction to use. It turns out that they are both equal to the same numerical constant in the vocabulary of the assembler, MIDAS, and are hence equivalent.) The instructor copy (cpy) actually results in the reading of a computer word from the tape (18 bits, or three tape words, each of six-bits).

The second portion of the program is an "unpacking" routine, designed to separate the three tape words into three different computer registers. It does this by blocking out the undesired words using logical "and" instructions, and shift, or cycle left (cyl) instructions. Note the reader is referred to manuals for the TX-0 computer for the exact operations of the various instructions. It might be added here, however, that an address of .+1, for example, means the address of the register following the one in which the .+1 appears; reasoning by analogy is valid for .-2 and other possible combinations, like tem +1.

A routine for loading the now obtained "unpacked" data onto the drum now follows the "unpacking" routine, separated by a halt (hlt). The repeat 5, ex 2 is equivalent to writing ex 2, as an instruction, five times, ex 2 being the synchronizing instruction causing the computer to wait for a pulse from external equipment. Other instructions are simple, common ones. The meaning of decimal and octal should be quite clear; how to interpret constants that follow.

The procedure to produce a punched paper tape from the magnetic tape starts with obtaining column binary cards with the same formats as the magnetic tape in the lower six holes. This done either directly from the computer, or using the 1401 as an off-line device. As there is no useful information in any columns except 7 through 72, duplicate cards will be made with only these columns punched. These duplicate cards also get a punch in the seventh hole from the bottom, again in columns 7 through 72.

Using an IBM 047 paper-tape-to-card Unit modified to also do the reverse, we get an eight-channel paper tape with the data in channels 1 through 6, a hole in 7, and 8 being blank. There are blank spots separating sections of data due to the fact that the 047 as modified duplicates columns 2 through 72 of the cards; however, this does not cause difficulty. It shall be noted that eight-channel paper tape is interchangeable with the seven-channel tape, if some of the left-hand tape guides are adjusted or bypassed. A seven-channel tape is now obtained from the eight-channel tape, using this method on a seven-channel flexowriter. The mode of operation of the flexowriter is such as to duplicate the tape exactly, including the blank spots. The TX-0 however, accepts only data in channels 1 through 6 if there is a punch in channel 7, and hence, the blank spots have no adverse effect.

The paper tape loading program is very simple compared to the magnetic tape loader.

5. Circuitry

By far the biggest, and most under-estimated problem with the drum has been with the associated circuitry. A discussion of the general circuitry in use or planned at present will ensue, to be followed by a brief discussion of the problems.

As mentioned previously, the TX-0 has rather easy input-output access. The contents of a central register, the Live Register (LR) is brought out on a jack panel. The logic levels are 0 volts and -3 volts. There are two pins for each of the eighteen bits in the register such that when a "one" is in that bit, we have either 0 volts ("0" side output) or -3 volts ("1" side output). The opposite levels would be present if a zero were in that bit. There is also a set of eight jacks for applying external pulses to the TX-0 for external control, and a corresponding number of control instructions. (EX0 through EX7.) Normally these jacks have repetitive pulses going in via jumper wires, and therefore will not stop the computer if one of these instructions is executed inadvertently. If external pulses are to be used, the jumper wire is removed from the appropriate jack, and a source of external pulses is used. To play safe, the pulse standardizers of the temporary logic are used between an external pulse source and the TX-0. The pulse source in our case is the clock track of the drum.

The output of the TX-0 live register is fed into a phase modulation circuit, to record using phase modulation on the drum. Operation at slow speed is accomplished by applying power to the drum motor, to bring it up to full speed, connecting an oscilloscope to the amplifier output on the clock track, then turning the motor off, letting the drum slow down sufficiently to produce a 40 microsecond bit length. The computer program has halted meanwhile, but is restarted when the 40 microsecond bit length is reached. Inasmuch as all data is written on the drum in less than one-fifth of a second, any further slowdown during the writing is negligible. Connecting the drum output to the NOEL computer through, of course, the amplifiers and a detection circuit, and operating the motor at full speed, is the final step. As previously mentioned, we do not have as yet six tracks working in connecting the drum to the TX-0; therefore we do not have a nomogram on the drum. Test pulses from the drum have gone into the computer, and we have a test signal correctly on the drum, using phase modulation.

The phase modulation circuit is based around a flip-flop. Pulses for control of the flip-flop, derived from the clock track, are available at the beginning and in the middle of each bit. The pulse in the middle of the bit always complements

the flip-flop. The other pulse is gated to either set or clear the flip-flop, depending on whether a "zero" or "one" is to be written (the gates are controlled by the applied logic level).

Detection is also rather simple, Due to some still undetermined phenomena there is a phase shift in recording even from one track to another. This comes in rather handy. to have the pulses always occurring at steady portions of the signal. If the correct pulse is gated with the correct phase of signal, pulses will result where a "one" has been written, and no pulses when there was a "zero".

Some quite unusual trouble was with the power supply to the amplifiers. Mechanically, the drum and peripheral equipment are on a separate rack from the computer, and, therefore, require a comparatively long power supply line to the computer power supply. Two of the read-write amplifiers caused no difficulty whatsoever. The remaining five caused the -15 volt line to change to -22. These cards all had a 1 microfarad capacitor between their +10 volt input and ground. A representative of the Harvey-Wells Electronics firm found that removing the capacitor cleared up the trouble. Eventually it appeared that 25 microfarad electrolytic capacitors across the -15 volt and +10 volt lines corrected the difficulty also.

CHAPTER 6

COMPUTER CIRCUITRY

A. THE COMPUTER ROLE

In Chapter 1 we broached the notion of establishing a correlation between a variable and a pair of functions of that variable whereby, when feasible for three variables of the equation $F(U, V, W) = 0$, a new simpler relationship common to all three pairs might result between pair members. If pairs were given the role of Cartesian coordinates and plotted for values of their respective variables, an answer set U_o. V_o, W_o implied three pairs U_1, U_2; V_1, V_2; W_1, W_2; that lay on an answer locus having an analytical form simpler or less obdurate than the original equation. Knowledge of values of two variables, U_o and V_o, (input values) yielded the values of these correlated pairs, (U_1, U_2), (V_1, V_2), and hence the particular member of the locus family satisfied by all three variables. We identify that nomographic technique for dealing with an equation as congruent to this procedure and can then think in nomographic terms. An example was given where the relationship between pair members was linear, (see Chapters 1 and 2A), and the constants of the correlation were furnished from knowledge of two input values which yielded the value of the third pair.

> WE MUST CONFINE OURSELVES IN MOST OF THIS ARTICLE TO THE ELEMENTARY CASE WHERE, EXPRESSING THE FACE THAT $F(U, V, W) = 0$, THERE IS A COMMON LINEAR RELATIONSHIP BETWEEN THE TWO ELEMENTS OF EACH OF THE THREE PAIRS OF FUNCTIONS OF VARIABLES U, V, W. NOMOGRAPHICALLY SPEAKING, WE NEED A COMPUTING ELEMENT CAPABLE OF EVALUATING (OR IDENTIFYING) THE THIRD PAIR W_1, W_2, WHERE U_o AND V_o, AND HENCE (U_1, U_2), (V_1, V_2) ARE KNOWN. THIS WILL SERVE AS THE COMPUTING ELEMENT TO SOLVE (2) FOR (W_1, W_2). THE ANSWER W_o, WILL THEN BE KNOWN BY THE INVERSE CORRELATION.

B. AN ACCEPTABLE SOLUTION FOR CIRCUIT PURPOSES. NOEL I

In Figure 6-1, a difference of slopes between the U_O-V_O answer line and a line thru U_O scanning up the W curve will have a numerator

$$S = (Y_{Vo} - Y_{Uo})(X_W - X_{Uo}) - (Y_W - Y_{Uo})(X_{Vo} - X_{Uo}) \qquad (6\text{-}1)$$

whose vanishing will be considered as the criterion for solution in the computer because the scanning line and the answer line will then coincide and the difference between their slopes will be zero.

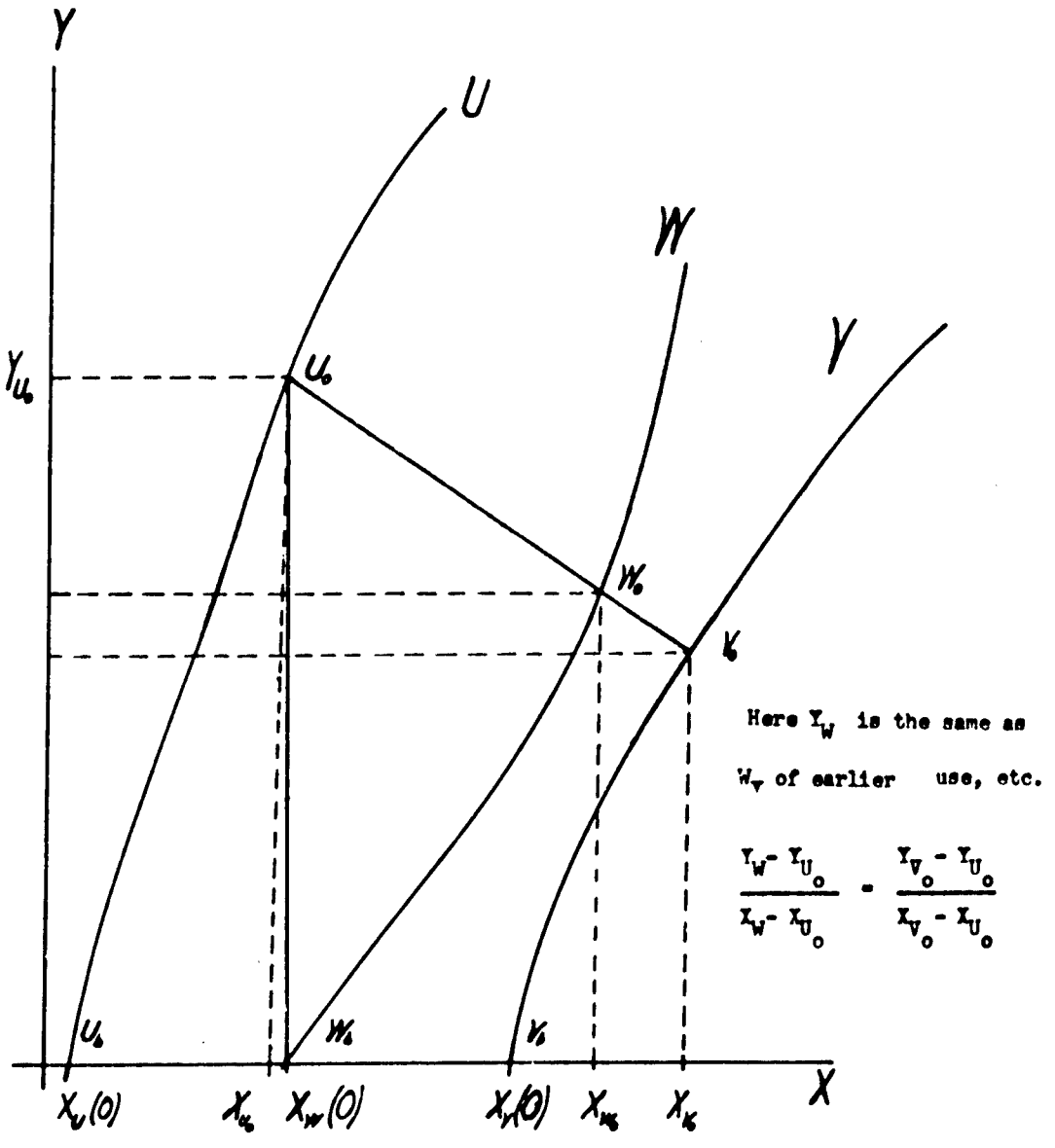

Figure 6-1. Three-Variable Alignment Chart

The position and orientation of the curves of the nomogram, taken as an aggregate, are purely arbitrary. By placing the lower ends of the curves on the X axis, the X coordinates of the curves at the X axis, $X_U(0)$, $X_W(0)$, $X_V(0)$, are determined.

We now write S in two parts:

$$S_1 = (Y_{Vo} - Y_{Uo})\ (-X_{Uo}) + (Y_{Uo})\ (X_{Vo} - X_{Uo}) \tag{6-2}$$

$$S_2 = (Y_{Vo} - Y_{Uo})\ (X_W) \quad - (Y_W)\ (X_{Vo} - X_{Uo}) \tag{6-3}$$

$$S = S_1 + S_2$$

where S_1 is the constant part of S, corresponding to the difference in slopes between the fixed line through U_o and V_o and the fixed line through U_o and W_b, and S_2 is the incremental portion which occurs as the latter line is pivoted about the point U_o until it passes through the point W_o. By performing two successive computations or passes, the computer can obtain a solution for W. Having decided to have the computer operate on equation (6-1) to determine the solution, and having designed the machine to handle this equation in the simplest manner, the machine must always consider W as the dependent variable. This is not a serious handicap since in the uses envisioned for the computer, one of the variables should always appear as the dependent one.

In the first pass the machine must accumulate the quantities in both parentheses of equation (6-2), each in a separate register, and then perform the indicated multiplication. During the second pass, the S_2 is added to S_1. When the sum S changes sign, the operation stops.

C. THE MEMORY SECTION

For NOEL I, the computer to do this job, the strip of information is being divided into five sections, each of which will be made up of six tracks. In the first portion occur the control pulses which are used to clear the computer, preset initial values of various functions into the proper registers, and set up the machine for the operations to be performed in pass I. The second segment of the information contains all of the data needed for the first pass, these being increments in U, V, X_U, X_V, and Y; the last of which has been chosen as the reference function. The sixth track contains a train of pulses which are used to synchronize all operations.

After pass I is completed, in which the terms of equation (6-2) are acquired, the third portion of the information strip contains more control pulses which perform the multiplication indicated above and then prepare the computer for the second pass, the data for which follows in the fourth segment of the information strip. This consists of increments in W, X_W, and Y, the latter again serving as the reference. The fifth portion is used to translate the answer in the machine into the correct form in which it must appear at the output.

D. OPERATION OF THE ELECTRONIC CIRCUITRY

Figure 6-2 shows the information passing through NOEL I. The first step is the computation of the coordinates of the input variables. To do this, counter #1, an n-bit binary counter, is preset to the value $2^n - U_o$ and counter #2 is preset to $2^n - V_o$. Increments in the U function are then passed through gate G2, which is open only during the first pass, through the scale factor unit to weight the pulses accordingly, into counter #1 where they are counted positively.

When a total of U_o increments have been counted, the contents of counter #1 will be 2^n which appears as zero. This then closes gates G4 and G6. During this counting interval, increments in X_U have been flowing through gate G4 so that when this gate is shut a total value of X_{Uo} has passed through. Similarly, gate G6 will be held open long enough to admit Y_{Uo} increments.

In a like fashion counter #2, which sums the increments in the V function which come by way of gate G3 and the V scale factor unit to be counted positively, holds gates G5 and G7 open until a total of V_o increments causes the counter to overflow. The pulses which are passed by gate G5 will total X_{Vo} while those through gate G7 will have a total value of Y_{Vo}.

Counter #3, which was initially cleared to zero, counts the Y_V increments positively and the Y_U increments negatively, the Y_V pulses being delayed so that two pulses do <u>not</u> arrive on different lines to be counted simultaneously. At the end of pass I, $Y_{Vo} - Y_{Uo}$ will be stored in that counter. Counter #4, preset before pass I to a value of $- X_U(0)$, then sums the X_U pulses negatively so that the final number is $- X_{Uo}$. Counter #5 adds the X_V pulses positively and the X_U pulses negatively to the initial value of $X_V(0) - X_U(0)$ which was set into the counter, attaining a final value of $X_{Vo} - X_{Uo}$. Counter #6, cleared to zero at the beginning of the pass, counts the Y_U pulses positively, until the total of Y_{Uo} is reached.

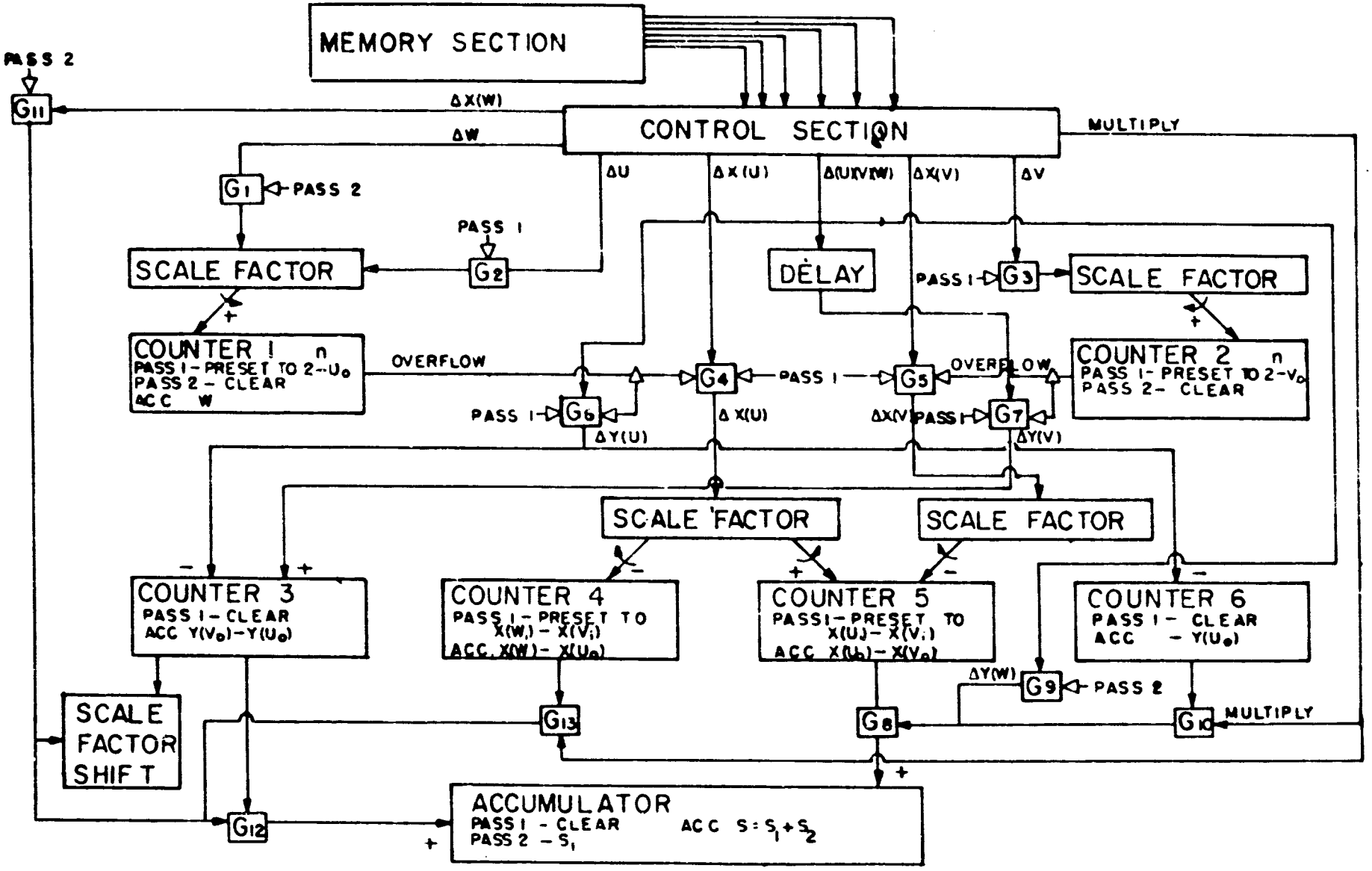

Figure 6-2. Block Diagram for NOEL I

After pass I has been completed, the control pulses multiply the contents of Counter #3 by the number in Counter #4 through gates G12 and G13, the answer being stored in the accumulator. At the same time, the pulses through gates G8 and G10 perform the same operation on the contents of Counters #5 and #6. The delay is added so that the two numbers do not enter the accumulator simultaneously. Before pass II occurs, the number in Counter #5, $X_{Vo} - X_{Uo}$, is changed to $X_{Uo} - X_{Vo}$, and Counter #1 is preset to the value W_b.

For pass II the increments in the W function are sent through gate G1 and the scale factor unit to be summed in Counter #1. Each increment in X_W adds the contents of Counter #3 to the accumulator via gates G11 and G12, this number being shifted to account for the scale factor setting of X_W. The Y_W increments perform a similar operation in the contents of counter #5 by way of gates G8 and G9, except that no scale factor is needed here because Y is the reference function. When the sign of the number in the accumulator changes from positive to negative, gate G1 is closed, shutting off the flow of W pulses. The number in Counter #1 is now W_o.

As mentioned above in the nomographic theory, there may be a need to perform a transformation of coordinates. This arises because perhaps not all scales on the variable curves increase in the direction of increasing Y coordinates. In order to allow the machine to work only on nomograms in which all scales do increase in the positive Y direction, the information strip has one set of control pulses at the beginning and another at the end, the purpose of which is to transform the variables in the actual nomogram into a dummy set which does always increase. The machine does all its operation on this internal, pseudo-nomogram and then returns the answer back to the scale of the original nomogram. This has permitted a considerable saving in circuitry.

It has been assumed in the foregoing discussion that the curves of the variables do not curve back on themselves, that is, as one moves up along a curve, the X coordinate either increases or remains constant. If this were not the case, the increments in X_U, X_W, and X_V would have to have both positive and negative values. In order to simplify NOEL I, it was decided never to allow the increments in the X coordinate to decrease. At the same time, to assure that contents of Counters #4 and #5 will be positive, the latter only during pass I, the criterion

$$X_V \geq X_W \geq X_U$$

for any X_V, X_W, X_U must be met. Both of these requirements are met by means of a graphical technique known as central projection, in which the nomogram is projected onto another plane at some arbitrary orientation to,

and an arbitrary distance from, the plane of the nomogram. Although the new curves may no longer casually resemble those of the original nomogram the alignment property is still present.

E. SCALE FACTOR SETTINGS

The purpose of the variable scale factor settings has already been discussed. Implementation of the method has been accomplished in the following manner. Each unit can be thought of as a movable 'funnel' which 'pours' the increments entering it into the proper bit of the counter. Pulses so 'poured' into the 2^0 bit are weighted by 2^0, those going into the 2^1 bit are weighted 2^1, etc.

In order to shift the location in the counter into which the increments are 'poured', codes are included on the information strip to indicate both the occurrence and the direction of a shift. The initial plan was to use a form of pulse-width-modulation, recording a pulse of unit width for data, one of twice the width to indicate a shift to a higher order bit, and one of triple the width to shift the scale factor unit in the opposite direction.

However, this scheme did not prove feasible with any of the memory units presently being used due to the sharp restrictions on the pulse widths which were required by the electronic circuitry. To circumvent this, a type of pulse-mode-modulation has been introduced. Instead of having a single bit carry several types of information, three bits are grouped together to form a 'word'. The presence of a bit in the first position indicates an increment in the function of the track. A bit in the second position is used in place of the double-width pulse of the other method and the triple-width pulse is replaced by a bit in the third position.

Because three bits are now used in place of one on the information strip, the use of this coding scheme requires three times the total number of bits that were required with the pulse width modulation method. Consequently, one third the information can be stored, reducing the accuracy to one-third of that possible before. At the same time, the effective operating speed, determined by the intervals between data bits, would also be cut to one-third of the previous running speed if the old accuracy is to be maintained. Although these side effects are undesirable, they appear to be unavoidable if a reliable scale factor system is to be used.

F. THE BINARY POINT

The last of the 'special-effects' that have been built into the computer to minimize the circuitry of NOEL I is in connection with fractions of integers. No provision has been made within the system to account for the position of the binary point in Counters #1 and #2. However, since input variables may take on values less than unity, and increments in variable functions may also have fractional values, it is necessary to know beforehand the position of the binary point, and to take this into consideration both in reading in the input variables and in reading out the answer. This position will be given to the operator for each nomogram. The deficiency will be eliminated from later computers. The first NOEL has been described. It represents a plateau of achievement worth working for even though a number of its techniques were obsolete when it was begun. It has proven an excellent medium for learning about many of the entirely new elements and problems of this approach to computing, such as bit reading and circuit performance. It shows good promise of living up to the expectations that were held for it in most ways. In particular, it has supported and renewed confidence in the graphical method as a tool capable of making an important contribution to modern engineering and science.

In this single, limited application of Graphics the most startling fact is the broad association of this field with many other technical fields. Clearly Graphics is useful and may be essential to the design of many skillful arrangements and devices.

CHAPTER 7

SOLUTION OF DIFFERENTIAL EQUATION WITH THE AID OF A NOMOGRAPHIC COMPUTER

A. INTRODUCTION

Numerical methods of solution for differential equations, both ordinary and partial, often require large numbers of time-consuming numerical calculations. A careful analysis of the techniques available for solving differential equations will indicate many of the difficult calculations are of a standard form and might be handled by a special purpose computer. This paper will attempt to show that a nomographic computer is well-suited to the type of computations which are required.

Methods for the solution of ordinary differential equations (o.d.e.s.) by numerical means are fairly well-developed. Any good book on numerical analysis such as reference (22) or (45) will give a variety of possible techniques. The methods which have proven to be useful on today's high-speed digital computers are discussed in reference (38). These methods are of two general types: first, step-by-step formulas in which Y_{n+1} is calculated but once from X_i, Y_i and Y_i'; and second, iterative methods in which Y_{n+1} is computed more than once until the true value is found. In general X_i, Y_i and Y_i' should be considered to be column vectors. Different choices of these vectors will define different methods of solution. Of these methods, the Runge-Kutta formulas are probably the easiest to implement with the nomographic computer. At any rate, the use of iterative methods does not seem to be well-suited to nomographic methods. The so-called "step-by-step" methods such as the Euler method and the Runge-Kutta methods will probably be of most interest with the proposed equipment. In nearly all of the step methods, as contrasted with iterative methods, the value of one or more of the derivatives of the dependent variables must be calculated at each step in the integration. For example, in the classical Runge-Kutta formula, the equation

$$F(Y', Y, X) = 0 \tag{7-1}$$

must be solved for the value of Y' four times, as indicated by equation (7-4), at each step in the integration. This fact points out some of the complexities involved in the numerical integration of differential equations. Any device used in numerical integration should be able to perform fairly complex calculations at a reasonable rate. Although a general purpose machine may be able to handle the given differential equation with sufficient ease, it is possible that introducing a special purpose computer to handle the routine calculations would

provide more efficient use of both time and equipment. In this connection, the nomographic computer's solution time will be shown frequently to be independent of the algebraic complexity of the equation to be solved.

In contrast to the present situation with o.d.e.s., adequate methods for the solution of partial differential equations (p.d.e.s.) by numerical means have been slow in developing. Even with the latest computing machines available, the solution of p.d.e.s. tends to be a long, time-consuming process with only moderate accuracy being obtained. The whole field of nonlinear p.d.e.s. is relatively unexplored. The Runge-Kutta method can be expanded to the solution of partial differential equations (see 7E), but this method, in the past, has been considered too slow and laborious to be of any value. The advent of a fast nomographic computer may justify employment of this method.

The Nomographic Electronic Computer (NOEL) now being developed at M.I.T.'s Engineering Projects Laboratory has characteristics which are useful in the two areas indicated, namely p.d.e.s. and o.d.e.s. The main problems in the application of NOEL to these areas lie in the limited accuracy of NOEL. It will be necessary to use a method of integration which is relatively unaffected by lack of accuracy in the computation. For the sake of argument, an accuracy of 0.1% will be assumed for the nomographic computer.

B. ORDINARY DIFFERENTIAL EQUATIONS

The role that a nomographic computer can play in the solution of o.d.e.s. (33) becomes readily apparent from a consideration of the simplest possible method, i.e., the Euler method. If equation (7-1) is solved for $Y' = F(X, Y)$, the basic equation of the Euler method is

$$Y_{n+1} = Y_n + hF(X_n, Y_n). \qquad (7\text{-}2)$$

In this expression Y_n is the value Y at the given value X and h is the size of the increment in X. The solution of this difference equation gives an approximation to the actual curve Y(X) at each of the points $X_1, X_2 \ldots X_n$. The error involved in this process is $Y(X_n) - Y_n = \epsilon$, where ϵ is a small number. In order to find the value Y_n, the function F(X, Y) must be evaluated n times. Since the function F(X, Y) may require a large computing time, special considerations should be made for its efficient solution. Since the solution time on a nomographic computer is essentially independent of the solution complexity, this device might be used to a great advantage. The only restriction that the nomographic device places on the solution process is in terms of accuracy. In general the best a nomographic computer can do at present is in the order of 1000 solutions per second with an accuracy of 0.1%.

The Euler method is in itself too inaccurate for most problems. More accurate one-step methods are available in the form of the Runge-Kutta formulas. These formulas are obtained by matching the terms of a proposed solution with the terms of a Taylor series expansion of $Y(X + h)$ to an order of h^k. These methods avoid the evaluation of derivatives of order higher than the first. The simplified Runge-Kutta formula [22] is of the form

$$Y_{n+1} = Y_n + hF(X_n + 1/2h,\ Y_n + 1/2\ k) \qquad (7\text{-}3.0)$$

$$K = hF(X_n, Y_n) \qquad (7\text{-}3.1)$$

The truncation error involved with this method is in the order of h^3. In view of the fact that a nomographic computer introduces a large round-off error, this method may prove to be the most effective for use in the system to be developed. In the interest of speed it should be noted that, if h is a known constant, it would be advantageous to compute $hF(X_n, Y_n)$ on the nomographic computer.

If even greater accuracy is required the classical Runge-Kutta method could be used to reduce the truncation error to the order of h^5. If the round-off due to the nomographic computer is greater than this the use of this method may not be justified.

The classical Runge-Kutta formula is given by the following set of equations:

$$Y_{n+1} = Y_n + 1/6\ (K_1 + 2K_2 + 2K_3 + K_4) \qquad (7\text{-}4.0)$$

$$K_1 = hF(X_n, Y_n) \qquad (7\text{-}4.1)$$

$$K_2 = hF(X_n + h/2,\ Y_n + K\ 1/2) \qquad (7\text{-}4.2)$$

$$K_3 = hF(X_n + h/2,\ Y_n + K\ 2/2) \qquad (7\text{-}4.3)$$

$$K_4 = hF(X_n + h,\ Y_n + K_3) \qquad (7\text{-}4.4)$$

These formulas require considerable bookkeeping which can best be handled by a general purpose (G. P.) digital computer. In most of the suggested uses of NOEL (the nomographic computer on which this report is based) control by a G. P. machine is a desirable feature. It can probably be safely assumed that a G. P. machine will control any future nomographic computer. Therefore, the bookkeeping task can be taken care of in the G. P. machine.

The sole purpose of the nomographic computer will be to efficiently calculate the function $Y' = F(X_n, Y_n)$. To illustrate this point, the numerical solution of the following equation will be attempted:

$$50e^{-Y'} + (X - Y)\, e^{Y'} = 10X. \qquad (7\text{-}5)$$

This equation illustrates an important point. Although it is complicated algebraically, it has a simple nomographic form which is shown in equation (7-6).

$$\begin{vmatrix} X/5 & 0 & 1 \\ Y/5 & 1 & 1 \\ e^{-Y'} & 0.1e^{Y'} & 1 \end{vmatrix} = 0 \qquad (7\text{-}6)$$

With an equation of this type, a nomographic computer can apparently compete with even the best digital machines. To solve equation (7-5), the classical Runge-Kutta method will be used with $h = 0.5$ and with initial conditions of $X_n = 1.5$ and $Y_n = 2.0$. The calculations are to be made on the nomograph shown in Figure 7-1, and are probably self-explanatory. Using equation (7-4),

Part 1: $K_1 = 0.5 \times F(1.5, 2)$

From the nomograph in Figure 7-1, $F(1.5, 2) = 1.11$

$$K_1 = 0.555$$

Part 2: $K_2 = 0.5 \times F(1.5 + 0.25, 2 + 0.2775)$

$$K_2 = 0.5 \times F(1.75, 2.278) = 0.490$$

Part 3: $K_3 = 0.5 \times F(1.75, 2.245) = 0.490$

Part 4: $K_4 = 0.5 \times F(2.00, 2.490) = 0.430$

Part 5: $Y_{n+1} = Y_n + 1/6\,(K_1 + 2K_2 + 2K_3 + K_4)$

$$Y_{n+1} = 2.491$$

$$Y_o = 2.00\ ;\ Y_1 = 2.491$$

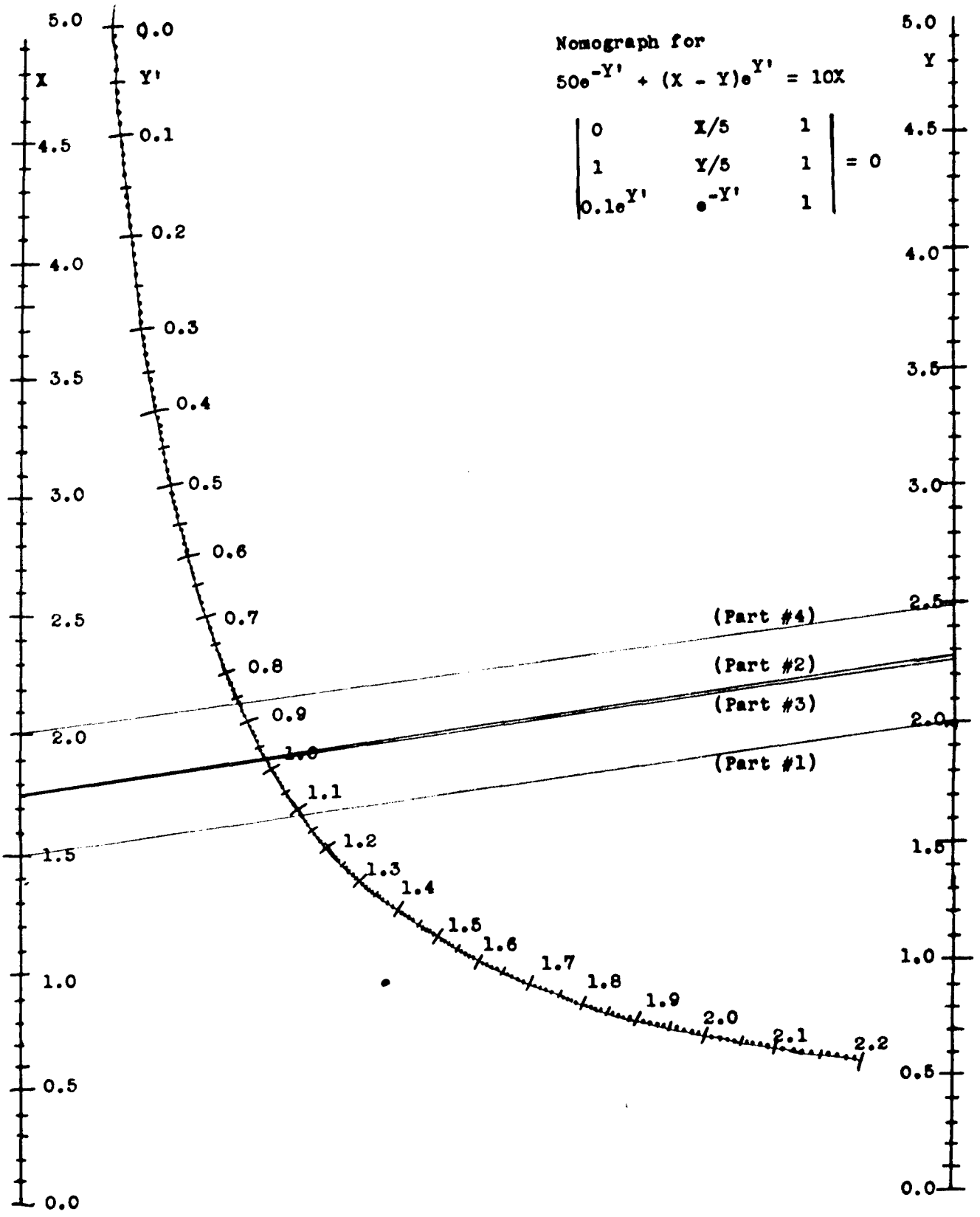
Nomograph for
$50e^{-Y'} + (X - Y)e^{Y'} = 10X$
$\begin{vmatrix} 0 & X/5 & 1 \\ 1 & Y/5 & 1 \\ 0.1e^{Y'} & e^{-Y'} & 1 \end{vmatrix} = 0$
X
Y'
Y
(Part #4)
(Part #2)
(Part #3)
(Part #1)

Figure 7-1.

This process can be repeated n times to find Y_n even though an explicit solution is not available. A second example appears in Figure 7-2.

These examples indicate that the nomograph is potentially quite useful in the solution of differential equations. One of the readily apparent disadvantages is that the ranges of the variables are limited and must be known before the nomograph is constructed.

Ordinary differential equations of order greater than one may be reduced to a system of first order equations or they may be integrated directly by the Runge-Kutta method(33). Both approaches are worth investigation, but more attention will be placed on the approach using systems of equations. The solution of systems of equations is of sufficient interest in itself to justify spending time to develop an efficient method of solution. The Runge-Kutta formula for systems of equations is expressed by equation 4 if K_1, K_2, K_3, K_4, F, and Y_n are interpreted to be vectors. The situation is complicated by the fact that M^2 nomographs are required to solve M functions in M + 1 variables. Although the solution time is increased, a nomographic solution is still possible.

C. DISCUSSION OF ERRORS IN NOEL

At the present level of development, the nomographic computer should obtain an accuracy of 0.1%. This order of accuracy may well be the limiting factor in the numerical process. The error involved in the nomographic computer arises from the fact that the machine determines its answer by counting bits. Since the machine cannot contain an infinite number of bits, the answer is, of necessity, rounded off. If the round-off error is considered to be approximately random, the error can be estimated in some cases.(5) In the NOEL system, the result cannot be more accurate than 0.001 h, where h is the size of the integration step. Any method used should be relatively insensitive to an error of this order so that the error does not cause the solution to diverge.

D. ESTIMATED RUNNING TIME AND STORAGE REQUIREMENTS

For a system of equations in P dependent variables and an independent variable, it is shown in 7-F that the total computation time required by the classical Runge-Kutta for n increments in the independent is

$$T = n(p\,ap + 12\,mp + 4\,p^2 J)$$

where J is the basic solution time for the nomographic computer, "M" is the multiplication time on the general purpose machine which is used in connection

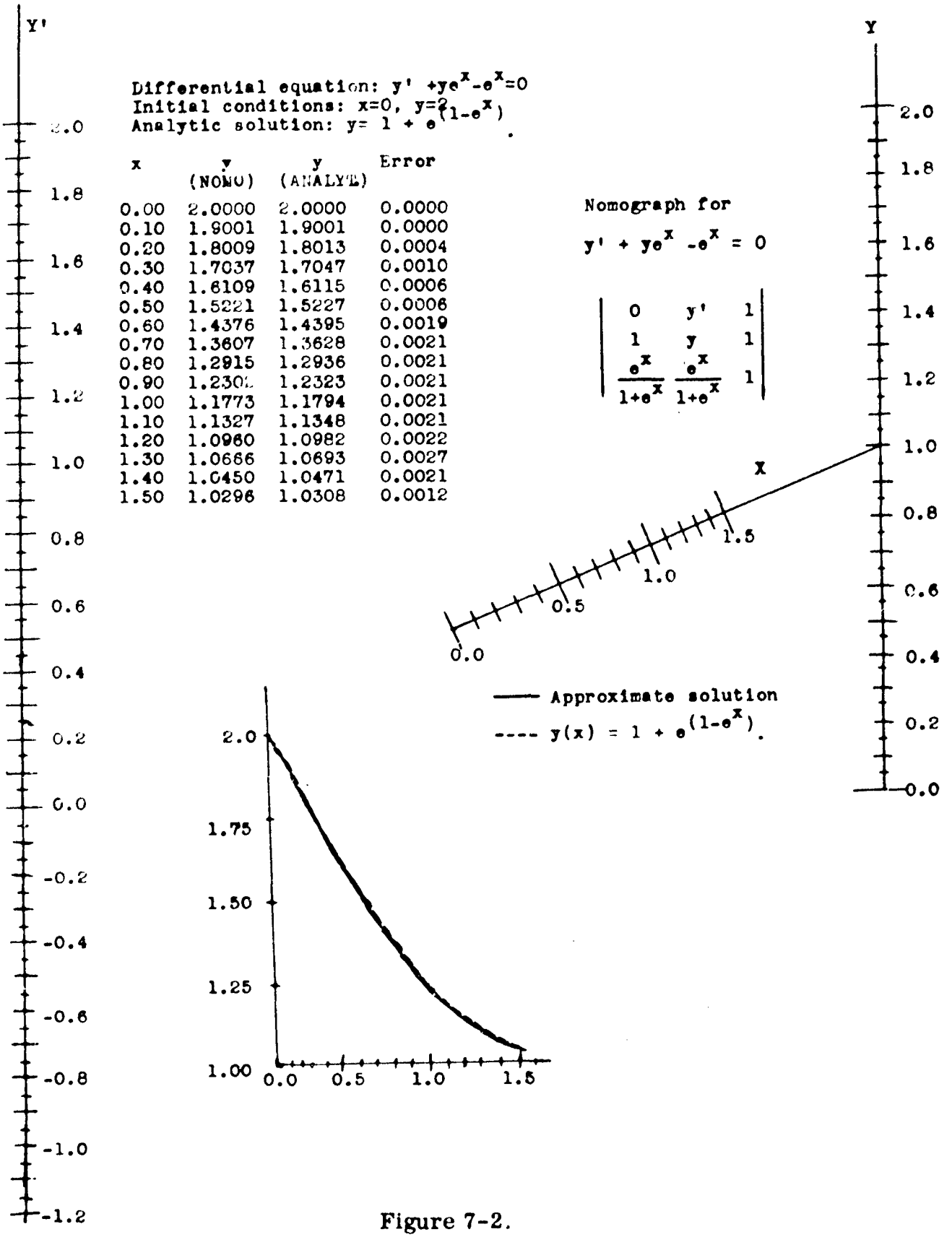
Y'
2.0
1.8
1.6
1.4
1.2
1.0
0.8
0.6
0.4
0.2
0.0
-0.2
-0.4
-0.6
-0.8
-1.0
-1.2
Differential equation: y' +ye^x-e^x=0
Initial conditions: x=0, y=2
Analytic solution: y= 1 + e^(1-e^x)
x y (NOMO) y (ANALYT) Error
0.00 2.0000 2.0000 0.0000
0.10 1.9001 1.9001 0.0000
0.20 1.8009 1.8013 0.0004
0.30 1.7037 1.7047 0.0010
0.40 1.6109 1.6115 0.0006
0.50 1.5221 1.5227 0.0006
0.60 1.4376 1.4395 0.0019
0.70 1.3607 1.3628 0.0021
0.80 1.2915 1.2936 0.0021
0.90 1.2302 1.2323 0.0021
1.00 1.1773 1.1794 0.0021
1.10 1.1327 1.1348 0.0021
1.20 1.0960 1.0982 0.0022
1.30 1.0666 1.0693 0.0027
1.40 1.0450 1.0471 0.0021
1.50 1.0296 1.0308 0.0012
Nomograph for
y' + ye^x -e^x = 0
0 y' 1
1 y 1
e^x/(1+e^x) e^x/(1+e^x) 1
X
0.0
0.5
1.0
1.5
Y
2.0
1.8
1.6
1.4
1.2
1.0
0.8
0.6
0.4
0.2
0.0
Approximate solution
y(x) = 1 + e^(1-e^x)
2.0
1.75
1.50
1.25
1.00
0.0
0.5
1.0
1.5

Figure 7-2.

with the nomographic computer, "a" is the addition time of the G. P. machine, "P" is the number of equations in the system, and "n" is the number of increments performed. For a system of 20 equations it is possible, but very unlikely, that 400 nomographs would be required and that 1600 nomographic solutions would be required per step. Assuming J = 1 millisecond, a total time of more than 1.6 seconds per step might be required. Fortunately this "worst case" is rarely encountered in physical systems. For the simplified Runge-Kutta method, the "worst case" solution time is

$$T = n(3\,pa + 3\,pm + 2\,p^2 J).$$

If all the values of the dependent variables are to be saved at each step, approximately n x p storage spaces will be required. However, if the problem is to be solved in "real-time" only the present values of the dependent variables will be necessary.

E. SOLUTION OF PARTIAL DIFFERENTIAL EQUATIONS

A survey of the methods presently used to solve partial differential equations will indicate that most of these methods are based on the use of difference equations. Due to the large number of difference equations involved and the method used to solve them, i.e. iteration, the solution time required even on a general purpose computer may become quite large. In view of the simple form of the resulting difference equations, a nomographic computer cannot efficiently be used to solve these equations. However, the use of nomographic organization of the entire solution technique may allow a more direct approach to the problem.

An attempt is now under way to find methods which make full use of the nomographic computing system. One possible method is to extend the more powerful methods used in o.d.e.s. to the solution of p.d.e.s. Gans [18] showed that the Runge-Kutta formulas could be extended to two dimensions. It has been thought that this extended Runge-Kutta formula might easily be used on a nomographic computer, but results obtained thus far have not been sufficiently convergent.

Another possible method is to reduce the partial differential equation to a system of ordinary differential equations. This is possibly accomplished by replacing the derivatives in one space direction by a set of difference equations while retaining the differential expressions in the other space direction. Work upon this approach is being carried forward.

F. SOLUTION TIME FOR ORDINARY DIFFERENTIAL EQUATIONS

The system to be solved is

$$Y_{n+1} = Y_n + 1/6\,(K_1 + 1K_2 + 2K_3 + K_4)$$

$$K_1 = hF(X_n, Y_n)$$

$$K_2 = hF(X_n + h/2, Y_n + K\,1/2)$$

$$K_3 = hF(X_n + h/2, Y_n + K\,2/2)$$

$$K_4 = hF(X_n + h, Y_n + K_3)$$

Let J be the average solution time for the nomographic computer; M and a are defined as the multiply and add times for the controlling general purpose machine. Let $T(K_1)$ denote the time required to compute K_1

$$T(K_1) = M + J$$

$$T(K_2) = M + J + 2(a + M)$$

$$T(K_3) = M + J + 2(a + M)$$

$$T(K_4) = M + J + (a + M)$$

$$T(K_1 + 2K_2 + 2K_3 + K_4) = 3a + 2M + T(K_1) = T(K_2) + T(K_3) + T(K_4)$$

$$T(Y_{n+1}) = T(Y_n) + a + M + T(K_1 + 2K_2 + 2K_3 + K_4)$$

$$T(Y_{n+1}) = T(Y_n) + 9a + 12M + 4J$$

finally

$$T(Y_{n+1}) = n(9a + 12M + 4J)$$

This derivation gives the total elapsed time for the numerical computation; bookkeeping this is not included in the analysis.

In order to handle a system of equations, K_1, K_2, K_3, K_4, Y_n and F must be considered to be vectors of order P. To solve an equation in P + 2 variables by nomographic means, a total of P nomograms must be solved. The solution of the system requires that P such equations be solved to find the column vector K_1. To account for this $J(K_1)$ is

$$T(K_1) = PM + P^2J$$

By similar reasoning

$$T(K_2) = PM + P^2J + 2P(a + M)$$

$$T(K_3) = PM + P^2J + 2P(a + M)$$

$$T(K_4) = PM + P^2J + P(a + M)$$

$$T(K_1 + 2K_2 + 2K_3 + K_4) = (3a + 2M)P + T(K_1) + T(K_2) + T(K_3) + T(K_4)$$

$$T(Y_{n+1}) = T(Y_n) + (a + M)P + T(K_1 + 2K_2 + 2K_3 + K_4)$$

$$T(Y_{n+1}) = T(Y_n) + 4P^2J + 9aP + (8P + 4P)M$$

$$T(Y_{n+1}) = n(9aP + 12P)M + 4P^2J)$$

This result should be interpreted as an upper bound on the time involved since the number of computations in an actual system can be reduced. This is the maximum time required to increment the solution n times for a system of M first order ordinary differential equations in M unknowns.

For the simplified Runge-Kutta equations a similar result may be found. The system to be solved is

$$Y_{n+1} = Y_n + hF(X_n + h/2,\ Y_n + K\ 1/2)$$

$$\frac{K_1}{2} = \frac{h}{2} F(X_n,\ Y_n)$$

for simplicity it will be assumed that h/2 is known.

$$T\left(\frac{K_1}{2}\right) = PM + P^2J$$

$$T(hF(X_n + h/2,\ Y_n + K\ 1/2)) = PM + P^2J + P(M + 2a) + T\left(\frac{K_1}{2}\right)$$

$$T(Y_{n+1}) = T(Y_n) + Pa + T(hF(X_n + h/2,\ Y_n + K\ 1/2))$$

$$T(Y_{n+1}) = T(Y_n) + Pa + 2(PM + P^2J) + P(M + 2a)$$

$$T(Y_{n+1}) = T(Y_n) + 3Pa + 2PM + 2P^2J$$

$$T(Y_{n+1}) = n(3Pa + 3PM + 2P^2J)$$

CHAPTER 8

SYSTEMS DESIGN FOR NOEL

A. INTRODUCTION

1. Some Observations

The advantages of the NOEL system as a multi-specific-purpose computer have been discussed in various places in previous chapters from the point of view of a high rate of repetitive computation with respect to random inputs and the efficient use of table storage space. However, no quantitative comparison between the NOEL system and other computers has been made. This chapter reviews and systematizes several characteristics of the NOEL system as a usable and effective special-purpose digital computer on the basis of a quantitative comparison between the expected computing speed of NOEL and the computing speed of the IBM 7090 computer for three given equations and specified accuracy.

Photographic storage and optical reading techniques have been stressed for information storage and retrieval because of high resolving power (density), short access time and cheapness of the production. We note that thermoplastic storage and magnetic storage, possibly with optical reading, have some advantages but cannot rival the advantages of photographic storage and optical reading as long as erasability of memory is not important in the design. Optical parameters [25] involved in the photographic storage and optical retrieval have been dualized (below) on the assumption of a Seidel optical field. Mechanical parameters of the system's operation have resulted from using a simple scanning model of disc and drum. The upper limit of the speed of solution is found to depend on mechanical properties of the storage medium, the density of the memory, the accuracy required of the computation (which determines the total required number of bits per solution) and the arithmetic element response time. A unified equation for the speed of solution as a function of the several parameters is derived and evaluated at the end of this chapter.

2. General Description of the NOEL System

The NOEL system consists of four subsystems as follows:

- Computation organization
- Memory
- Control
- Arithmetic unit

Relationships between parameters of these elements are suggested by the flow diagram of Figure 8-1.

The structure of each unit is discussed in previous chapters. Chapters 1, 2, and 3 describe the computation organization, Chapter 4 explains the memory, Chapter 5 discusses reading and modulating of the information, and Chapter 6 deals with the arithmetic unit. This chapter, therefore, will not deal in detail with the subsystems but will discuss parameters important for obtaining optimum conditions.

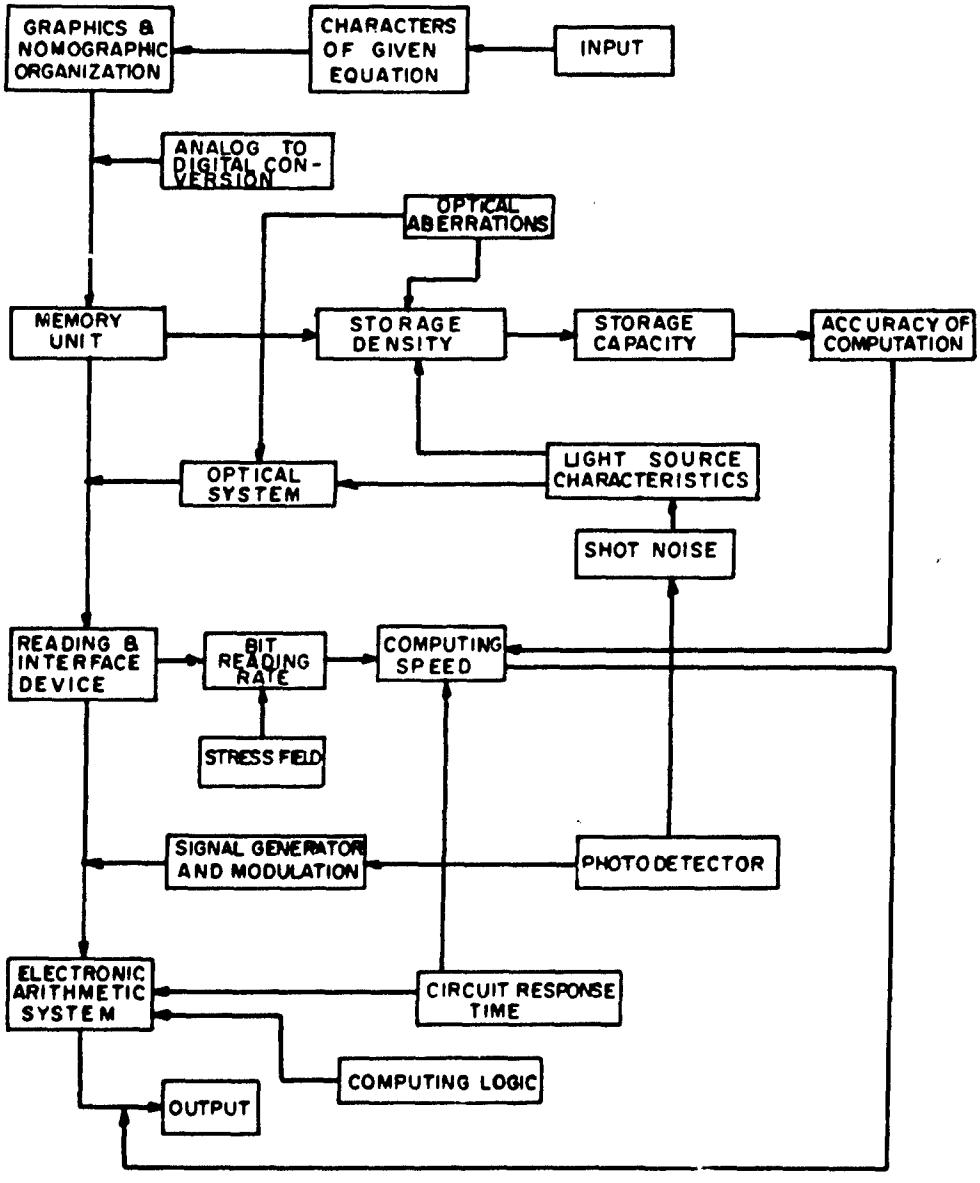

Figure 8-1.

B. SYSTEM COMPARISON

To get a numerical feel for the computing speed of NOEL, the computing speed of the IBM 7090 and the expected computing speed of NOEL are presently compared for three equations for accuracy of 0.1%. The equations are:

1. The heat-exchanger equation to compute the optimum coolant flow rate for given costs and inlet and outlet temperature differences;

2. A velocity computing equation; and

3. A probability density equation, all of which are good nomographic functions.

To get the value of Y for given X and Z, the Newton-Raphson iteration technique is used in the heat exchanger equation. For the dependent variables V and Y in the velocity and the probability-density equation respectively, a successive iteration technique is adopted. The 7090 solved those problems at the rate of 257-880 solutions/second.

With Kodak Estar film [11] 870 solutions/second will result at the desired accuracy of .1%, on the basis of 500 bits/inch as shown in the following table. The table shows that the NOEL system will not only compute the given equations faster than the IBM 7090 but also furnish accuracy beyond that of the analog computer for which accuracy is 3%, in general. Another advantage not mentioned so far pertains especially to implicit functions, as quoted in the examples. Using the IBM 7090, the iterative procedure is only stable when the initial value is properly determined. The NOEL computer is always stable as long as the input and the output data are in the specified range. The above-mentioned computing speed of the IBM 7090 is the speed when they are executed with properly chosen initial values, prechecked by the computation of the programmer. The 7090 is less effective when the computation is required with respect to certain random input data. The 7090 usage may be lost when such a random computation is required to be executed at certain high speeds. NOEL, however, maintains accuracy and computing speed regardless of the fashion of the input data - whether random or regular. To overcome this disadvantage of the 7090, a table look-up technique may be used after one series of computations, but then the IBM 7090 with $2^{15} = 32,768$ words of storage is able to hold an accuracy of only .55% for three variables.

COMPARISON OF COMPUTING RATES BETWEEN IBM 7090 AND NOEL

1) $X = \left[\frac{Z + 1 - Y}{Y - 1}\right]^2 \left[\log_e Y - (1 - \frac{1}{Y})\right]$ Heat Exchanger

Newton-Raphson Techniques

Find Y, given X and Z

2) $V = 52.8\ A\left(1 - \frac{B}{3V}\right)^{\frac{1}{3}}$ Velocity Equation

Successive Iteration Technique

Find V, given A and B

3) $Y = \frac{1}{2\pi(\delta)^2}\ e^{-1/2\left(\frac{r}{\delta}\right)^2}$ Probability Density Equation

Successive Iteration Technique

Compute δ , given Y and r

Equation Number	IBM 7090 Net Computing Rate Excluding Any Recording Time (Solutions per sec.)	NOEL Density of Stored Information		
		500 bits/in.	1000 bits/in.	2000 bits/in.
		(Solutions per second)		
1	320	870	1740	3480
2	880	870	1740	3480
3	260	870	1740	3480
The Accuracy of Computation is 0.1% Relative Error				

C. PARAMETERS

1. A Natural Upper Limit of Storage Density

Optical parameters which determine storage capacity resulting from the rectangular-shaped information bit are important system variables of the memory unit. For our theoretical analysis, a wave model using light in a Seidel field was used. The natural upper limit of storage density (number of bits/unit length or number of bits/unit area) is defined on the basis that the maximum readable storage density arises when no optical imperfections occur such as optical aberration, etc.

The theory of image formation of an extended object as developed by Duffieu [9] concludes that the spatial frequencies, exceeding a certain value, generated by the object in an image forming system are not transmitted by the system. If the aperture of the optical system is circular, the upper limit will be obtained for an object of rectangular shape, $\underline{a}$ by $\underline{b}$, with b = ma and for a partially coherent and quasimonochromatic light source.[4]

$$R = \frac{m}{1 + m^2} \left(\frac{N_o}{\bar{\lambda}_o} \right)^2 \text{ bits/unit area} \qquad (8\text{-}1)$$

for two-dimensional storage.

$$R = \frac{m}{\sqrt{m^2 + 1}} \left(\frac{N_o}{\bar{\lambda}_o} \right) \text{bits/unit length} \qquad (8\text{-}2)$$

for one-dimensional storage.

where

N_o : numerical aperture of the optical system

$\bar{\lambda}_o$: average wave length of the light source in vacuum

The maximum storage density[25] is obtainable when the bit forms are square for two dimensional storage, and when they are lines for one dimensional storage. These conclusions can be drawn by differentiating the equations with respect to m, putting them equal to 0 and solving for m.

Then

$$R_{\text{two dimen.}} = \frac{1}{2}\left(\frac{N_o}{\bar{\lambda}_o}\right)^2 \quad \text{bits/unit area} \tag{8-3}$$

$$R_{\text{one dimen.}} = \left(\frac{N_o}{\bar{\lambda}_o}\right) \quad \text{bits/unit length} \tag{8-4}$$

2. The Effect of Primary Aberrations on Storage Density

When a system[25] contains aberrations of such an amount that the width of the blurred part of the image is less than one quarter of the width of the Gaussian image, the aberrations can be tolerated in the system. According to this criterion under the Seidel Theory of aberrations, the following results are obtained for the aberration coefficients under which the aberration defects on the density of the storage are eliminated.[4]

$$B \leq \frac{M \cdot a \cdot \bar{\lambda}_o}{4\rho^3 \cdot D_1} \tag{8-5}$$

$$F \leq \frac{M \cdot a}{4\rho^2\left(2a_2 + \sqrt{a_2^2 + b_2^2}\right)} \tag{8-6}$$

$$C \leq \frac{M \cdot a \cdot D_1}{8\rho\, b_2 \sqrt{a_2^2 + b_2^2} \cdot \bar{\lambda}_o} \tag{8-7}$$

$$D \leq \frac{M \cdot a \cdot D_1}{4\left(a_2^2 + b_2^2\right)\rho\ \bar{\lambda}_o} \tag{8-8}$$

$$E \geq 0 \tag{8-9}$$

where

a : the width of the bit object

ρ : optical zonal radius of the object

D_1 : the distance between the image plane and the exit pupil plane

(a_2, b_2) : X-Y co-ordinate of the bit where the aberrational effect is investigated

M : Gaussian magnification factor of image

B : the coefficient of spherical aberration

F : the coefficient of comatic aberration

C : the coefficient of astigmatism

D : the coefficient of curvature of field

E : the coefficient of distortion

It has been seen that spherical aberration, coma, astigmatism, and curvature of field are chiefly responsible for lack of sharpness of the image. The other defects are related to the shape of the image. Generally, it is impossible to design a system which is free from all the primary as well as higher order aberrations. A suitable compromise as to their relative magnitude has, therefore, to be made. In some cases the effect of the aberrations is reduced by balancing aberrations of higher orders and in other cases one has to eliminate certain aberrations completely even at the price of introducing aberrations of other types. In NOEL computation, the chief concern is not the actual shape of the image but image formation which can be recognized as "plus" or "zero" information by the system. The correction of distortion, therefore, is not necessarily important as long as the coefficient of the distortion is positive in value. The other coefficients should be within the above mentioned limits.

3. Information Reading Rate

To realize the maximum reading rate of bits, the system should be mechanically and electrically stable. A free rotating ring for the rotating drum memory and a free rotating thin disc for the rotating disc memory are used to demonstrate the effect of material properties on the reading rate. The errors involved in the simplified model used below are not excessive although stress predictions will be a little on the low side.

The maximum reading rate can be expressed as follows:

$$T_{max} = \frac{\pi DNR}{60} = \omega rR = R\sqrt{\frac{\sigma_{max}}{\rho}} \quad \text{for the drum} \qquad (8\text{-}10)$$

$$T_{max} = \frac{\pi DNR}{60} = \omega rR = R\sqrt{\frac{8}{3+\mu} \cdot \frac{\sigma_{max}}{\rho}} \quad \text{for the disc} \qquad (8\text{-}11)$$

where

D : diameter of the drum or disc $r = \frac{D}{2}$

σ : tangential stress

ρ : density of the material

R : linear storage density of the information

μ : Poisson ratio

ω : angular velocity

N : r.p.m.

The reading rate of the disc memory is higher than the drum memory by the factor $\sqrt{\frac{8}{3+\mu}}$.

The Poisson ratios of transparent materials are usually from .3 to .5. Therefore, the disc reading rate is approximately 50% higher than the drum memory reading rate.

By substituting Equation (8-2) into (8-11) which describes the linear storage density,

$$T_{max} = \frac{m}{\sqrt{m^2+1}} \left(\frac{N_o}{\lambda_o}\right) \sqrt{\frac{8}{3+\mu} \cdot \frac{\sigma_{max}}{\rho}} \quad \text{for disc memory} \qquad (8\text{-}12)$$

4. Light Source Intensity

The occurrence of errors in the signal transducing process from light to electric current is mainly due to the occurrence of shot noise which is generated by the dark current. The rate of the shot noise maximum occurrence above a discriminating level of current signal can be controlled by adjusting the strength of the light intensity for a given geometrical arrangement of the optical system. With the assumption of the point light source, noise free amplification of the electrons in the photodetectors and steady state dark current generation, the following expression for the light source intensity is deduced.

$$I = \frac{4\left[2I_d q \int_0^{\infty} H^2(T)\,DT\, \ell n\, \frac{1}{n} \frac{\int_0^{\infty} T^2 H^2(T)\,dT}{\int_0^{\infty} H^2(T)\,dT}\right]^{1/2} R^2}{S \cdot \eta} \text{ watts/unit area} \qquad (8\text{-}13)$$

where

I : light intensity

R : storage density

n : the rate, in events per second, at which the shot noise maxima exceeds the value of I_1 (the level of discrimination)

I_d : the dark current : Amperes

q : electronic change in coulomb : 1.602×10^{-19} : coulomb

T : bit reading rate

S : the photocathode radiant sensitivity : Amperes/watt

η : the efficiency of the photomultiplier tube

d : the distance between the light source to entrance pupil of condensing lens

This equation can be simplified further by assuming an ideal band pass system and by consideration of the shot noise tolerance[25].

$$I = \frac{4\left[2I_d q\, T\left(\ell_n \frac{10^4}{3e}\right)\right]^{1/2} R^2}{S \cdot \eta} \quad \text{watts/unit area} \qquad (8\text{-}14)$$

e : the relative error tolerated in the computation.

The light source intensity, therefore, is determined by the function of the dark current, bit reading rate, storage density, the efficiency and sensitivity of the photomultiplier, and e. Higher light intensity is required for a higher reading rate and resolution power.

5. Solution Rate

The computing speed of the NOEL system can be written

$$S = \frac{T}{P} \qquad (8\text{-}15)$$

where

S : solutions/second

P : total number of bits per track for one computation.

The maximum computing speed can be expressed by substituting those equations derived for R_{max} and T_{max} into equation (8-15).

$$S = \frac{m}{\sqrt{m^2+1}}\left(\frac{N_o}{\lambda_o}\right)\frac{1}{P}\sqrt{\frac{8}{3+\mu}\cdot\frac{\sigma_{max}}{\rho}} \qquad \text{for the disc memory} \quad (8\text{-}16)$$

$$S = \frac{m}{\sqrt{m^2+1}}\left(\frac{N_o}{\lambda_o}\right)\frac{1}{P}\sqrt{\frac{\sigma_{max}}{\rho}} \qquad \text{for the drum memory} \quad (8\text{-}17)$$

The major parameters for the maximum solution rate are the numerical aperture of the lens, the wavelength of the light source, the Poisson ratio, the maximum stress of the rotating materials used for the information storage, and the storage density as long as the light source intensity is high enough and the lens system is properly designed.

For an example, .9 numerical aperture, 9000 Å wavelength, and $\frac{\sigma_{max}}{\rho} = 10^4 \frac{in^2}{sec}$ (Estar film) for square bit storage will allow NOEL to compute with the drum memory approximately 52,000 solutions/second with the use of 2000 words consisting of three bit words for one computation.

D. CONCLUSION

The use of NOEL as a relatively inexpensive adjunct machine to a fast digital computer appears to be practicable. In this connection, its usefulness in solving differential equations both ordinary and partial is currently being explored. Its efficiency in turning out repeated calculations, though these be highly detailed, warrants its inclusion among newly-developed tools ancillary to powerful digital computers which are not as relatively efficient for these purposes because of their wonderful adaptability to more general ones.

REFERENCES AND BIBLIOGRAPHY

1. Adams, D. P., Advanced Nomography, Technical Documentary Report, No. RADC-TDR-62-274, Vol. I, Sept. 1962, Information Processing Laboratory Rome Air Development Center, Griffiss Air Force Base, Rome, New York.

2. Adams, D. P., "Computer in a Shoebox", MACHINE DESIGN, September 14, 1961.

3. Adams, D. P., "Countable-Bit, Nomographic Electronic Computation", Technical Seminar Series, Report No. 5, Princeton University, Dept. of Graphics and Engineering Drawing, February 11, 1963.

4. Adams, D. P., DSR 8728, Quarterly Report, QR 8728-1, Engineering Projects Laboratory, M. I. T., 1961.

5. Adams, D. P., DSR 8728, Quarterly Report, QR 8728-2, Engineering Projects Laboratory, M. I. T., 1961.

6. Barnum, A. A. and Knapp, M. A., Workshop on Computer Organization, Spartan Books, Inc., Washington, 1963, p. 1-65, D. P. Adams, "Countable-Bit Nomographic Computation—NOEL".

7. Baumann, Dwight, "Photographic Devices for Semipermanent Digital Storage Requiring High Scanning Rates", S. M. Thesis, Department of Mechanical Engineering, Massachusetts Institute of Technology, Cambridge, Mass., September 1958.

8. Blake, E. B., "A Photographic Binary Data Recorder for Business Machine Applications", S. B. Thesis, Department of Mechanical Engineering, Massachusetts Institute of Technology, Cambridge, Mass., September, 1960.

9. Born, Max and Wolf, Emil, Principles of Optics, Pergamon Press Book, The Macmillian Company, 1959.

10. Brettler, B. J., "Photogrammetry", Sc. D. Thesis, Department of Mechanical Engineering, Massachusetts Institute of Technology, 1953.

11. Calhoun, J. M., "Physical Properties of Estar Polyester Base Aerial Films for Topographic Mapping", Eastman Kodak Co., 1961.

12. Cohen, John B., "Nomag: Computation and Simulation for the MSP Nomographic Computing System", Preliminary Report, Dynamic Analysis and Control Laboratory, M.I.T., October, 1961.

13. Dancis, Douglas E., "Magnetic Drum Memory Unit for the Nomographic Electronic (NOEL) Computer," B.S. Thesis, Department of Electrical Engineering, M.I.T., June, 1963.

14. Den Hartog, J.P., Advanced Strength of Materials, McGraw-Hill, 1952.

15. Dossé, W.G., "Storage of Binary Data on Photographic Plates", S.M. Thesis, Department of Mechanical Engineering, Massachusetts Institute of Technology, February, 1960.

16. Elliott, A. and Dickson, J.H., Laboratory Instruments Their Design and Application, Chapman and Hall Ltd., London, 1954.

17. Frank, Nathaniel H., Introduction to Electricity and Optics, McGraw-Hill Book Company, Inc.

18. Gans, R., Zeitschrift fur Mathematik und Physik, Vol. 48, 1902, pp 394-99.

19. G.E. Research Laboratory, "Thermoplastic Recording", Research Information Services of General Electric Company, January 1960.

20. Halliday, David and Resnick, Robert, Physics, For Students of Science and Engineering, John Wiley and Sons, Inc., 1960.

21. Henrici, Peter, Discrete Variable Methods in Ordinary Differential Equations, John Wiley & Sons, Inc., New York, 1962, pp. 87-99.

22. Hildebrand, F.B., Introduction to Numerical Analysis, McGraw-Hill Book Co., Inc., New York, 1956.

23. King, G.W., "A New Approach to Information Storage", Control Engineering, Vol. 2, No. 8, August 1955, pp. 48-53.

24. King, G.W., Brown, W.G., & Ridenour, L.N., Photographic Technique for Information Storage, Proc. IRE, Vol. 41, No. 1, Oct. 1953.

25. Lee, C.J., "Analysis of Some Critical Parameters in Nomographic Electronic Computation", Sc.D. Thesis, Department of Mechanical Engineering, M.I.T., 1964.

26. Lever, A.E., & Rhyes, J., The Properties and Testing of Plastic Materials, Temple Press, 1957.

27. Lohan, F.J., "Introduction to Pulse Magnetic Recording", (Pamphlet, Bryant Computer Products).

28. Lou, Yeong-Suei and McRay, Richard Ferris, "Optical Data Retrieval Systems for Project NOEL", M.S. Thesis, Department of Mechanical Engineering, M.I.T., June 1963.

29. Manual of Operation, IBM 46-47 Tape-to-Card Punch.

30. Marcus, P.D. "Transmission of Information from Transducers to Nomographic Computer", B.S. Thesis, Electrical Engineering Department, M.I.T., 1963.

31. McAdams, W.H., Heat Transmission, McGraw-Hill, 1942, pp. 54.

32. Miyata, J.J., "Optical Read-Out of Digital Magnetic Recording", Communication and Electronics, March 1961.

33. Morita, K. and Simokawa, Y., "Nomographic Solutions of Ordinary Differential Equations of the First and Second Orders", Memoirs of the Faculty of Technology, Kanazawa University, Vol. 1, No. 2, Japan, 1953.

34. "New Eyes for Modern Industry", Reprint No. E-111 of the General Radio Experimeter, Vol. 34, No. 9, September, 1960.

35. O'Neal, R.D., "Photographic Method for Handling Input and Output Data", Annals of the Computation Laboratory of Harvard Univ., Vol. XVI, 1948, pp 260-266.

36. Orr, R.S. "An Extension of Nomographic Digital Computation to the Solution of Equations of Non-Canonical Form", Department of Electrical Engineering, M.S. Thesis, M.I.T., June 1963.

37. Pollack, H.E., "Special Purpose Digital Computer for the Solution of Three Variables Nomogram", S.M. Thesis, Electrical Engineering Department, M.I.T., 1962.

38. Ralston, A., and Wilf, H.S., Mathematical Methods for Digital Computers, John Wiley & Sons, Inc., New York, 1960, pp. 95-132.

39. Reference Manual, 1620 Data Processing System, IBM.

40. Reference Manual, 7090 Data Processing System, IBM.

41. Ridenour, L.N., "Storage and Retrieval Information", Proc. of the Eastern Joint Computer Conference, Nov. 7-9, 1955, pp. 79-82.

42. Roberts, F., & Young, J.Z., "The Flying Spot Microscope", Proc. IEE, Part IIIA, Vol. 99, 1952, p. 750.

43. Rohsenow, W.M. & Choi, H.Y., Heat, Mass and Momentum Transfer, Prentice Hall, 1961, p. 206.

44. Ryan, R.D., "A Permanent High Speed Store for Use With Digital Computers", IRE Transactions on Electronic Computers, Vol. EC-3, No. 3, Sept. 1954.

45. Scarborough, James B., Numerical Mathematical Analysis, The Johns Hopkins Press, Baltimore, 1958.

46. Set of Manuals for the TX-O Computer.

47. Special Systems Features Bulletin, Direct Data Connection for the IBM 709, RPO 80979, IBM.

48. Spencer, R.H. "Digital Encoding Object Position in an Optical Field Using Scan Techniques", E.E. Thesis, 1959, Electrical Engineering Department, M.I.T.

49. Systems Bulletin, FORTRAN ASSEMBLY PROGRAM (FAP) For the IBM 709/7090, and Supplement, IBM.

50. Thumin, A.D., "High Angular Speed Design for Electronic-Nomographic Computer", S.M. Thesis, Mechanical Engineering Department, M.I.T., 1962.

51. Tyler, A.W., "Optical-Photographic Storage Technique", Annals of the Computation Laboratory of Harvard Univ., Vol. XVI, 1948, pp. 146-150.

52. Wasserlein, John H., "Design and Construction of a Printer Unit to Print an Intermediate Binary Memory for Nomographic Electronic Computation", S.B. Thesis, Department of Mechanical Engineering, M.I.T., June 1963.

53. Weiss-Bara, Harold, "An Electronic Reader for the Nomographic-Electronic "NOEL" Computer", M.S. Thesis, Department of Electrical Engineering, M.I.T., June 1963.